frontiers | Research Topics

Case reports in cardio-oncology 2023

Edited by
Reto Asmis

Published in
Frontiers in Cardiovascular Medicine
Frontiers in Oncology

ISSN 1664-8714
ISBN 978-2-8325-5716-7
DOI 10.3389/978-2-8325-5716-7

About Frontiers

Frontiers is more than just an open access publisher of scholarly articles: it is a pioneering approach to the world of academia, radically improving the way scholarly research is managed. The grand vision of Frontiers is a world where all people have an equal opportunity to seek, share and generate knowledge. Frontiers provides immediate and permanent online open access to all its publications, but this alone is not enough to realize our grand goals.

Frontiers journal series

The Frontiers journal series is a multi-tier and interdisciplinary set of open-access, online journals, promising a paradigm shift from the current review, selection and dissemination processes in academic publishing. All Frontiers journals are driven by researchers for researchers; therefore, they constitute a service to the scholarly community. At the same time, the *Frontiers journal series* operates on a revolutionary invention, the tiered publishing system, initially addressing specific communities of scholars, and gradually climbing up to broader public understanding, thus serving the interests of the lay society, too.

Dedication to quality

Each Frontiers article is a landmark of the highest quality, thanks to genuinely collaborative interactions between authors and review editors, who include some of the world's best academicians. Research must be certified by peers before entering a stream of knowledge that may eventually reach the public - and shape society; therefore, Frontiers only applies the most rigorous and unbiased reviews. Frontiers revolutionizes research publishing by freely delivering the most outstanding research, evaluated with no bias from both the academic and social point of view. By applying the most advanced information technologies, Frontiers is catapulting scholarly publishing into a new generation.

What are Frontiers Research Topics?

Frontiers Research Topics are very popular trademarks of the *Frontiers journals series*: they are collections of at least ten articles, all centered on a particular subject. With their unique mix of varied contributions from Original Research to Review Articles, Frontiers Research Topics unify the most influential researchers, the latest key findings and historical advances in a hot research area.

Find out more on how to host your own Frontiers Research Topic or contribute to one as an author by contacting the Frontiers editorial office: frontiersin.org/about/contact

Case reports in cardio-oncology: 2023

Topic editor
Reto Asmis — Wake Forest University, United States

Citation
Asmis, R., ed. (2024). *Case reports in cardio-oncology: 2023*. Lausanne: Frontiers Media SA. doi: 10.3389/978-2-8325-5716-7

Table of contents

frontiers | Frontiers in Cardiovascular Medicine

TYPE Case Report
PUBLISHED 12 October 2023
DOI 10.3389/fcvm.2023.1285233

OPEN ACCESS

EDITED BY
Reto Asmis,
Wake Forest University, United States

REVIEWED BY
Silvia Maestroni,
Papa Giovanni XXIII Hospital, Italy
Nahid Rezaeian,
Iran University of Medical Sciences, Iran

*CORRESPONDENCE
Hyukjin Park
hyukjin@gmail.com

†These authors have contributed equally to this work and share first authorship

RECEIVED 29 August 2023
ACCEPTED 27 September 2023
PUBLISHED 12 October 2023

CITATION
Lee N, Bang H, Park H and Shim H-J (2023) Case report: Successful treatment of malignant pericardial effusion with pericardiocentesis, concurrent anti-inflammatory therapy and cancer therapy.
Front. Cardiovasc. Med. 10:1285233.
doi: 10.3389/fcvm.2023.1285233

Case report: Successful treatment of malignant pericardial effusion with pericardiocentesis, concurrent anti-inflammatory therapy and cancer therapy

Nuri Lee[1†], Hyunjin Bang[2†], Hyukjin Park[1*] and Hyun-Jeong Shim[2]

[1]Department of Cardiology, Chonnam National University Hwasun Hospital, Hwasun, Republic of Korea, [2]Department of Hematology and Oncology, Chonnam National University Medical School and Hwasun Hospital, Hwasun, Republic of Korea

Despite significant advancements in systemic anticancer therapies, cardiac tamponade remains a serious and potentially life-threatening complication in metastatic breast cancer (MBC). However, there is a paucity of comprehensive research investigating alternative management approaches, such as pericardiocentesis and anti-inflammatory therapy (AIT), to effectively address cardiac tamponade and mitigate the risk of heart failure arising from constrictive physiology (CP) in patients with MBC when traditional systemic anticancer drugs fail to yield favorable outcomes. Herein, we describe two cases of MBC with cardiac tamponade that occurred despite the administration of effective systemic anticancer drugs. In each case, pericardial effusion was detected in a patient who was undergoing palliative anticancer therapy for human epidermal growth factor receptor 2 (HER2)-positive MBC. The patients in these cases were successfully treated with pericardiocentesis and AIT (prednisolone and colchicine) for subsequent CP without substitution with their systemic anticancer drugs. Cardiac tamponade and CP are regarded as signs of advanced cancer and are associated with a worse clinical outcome in general; however, they can still be treated with an effective anticancer drug, pericardiocentesis, and management of CP by cardiooncology specialists.

KEYWORDS

cardiac tamponade, constrictive pericarditis, pericardial effusion, breast cancer, pericardiocentesis

Introduction

Metastatic breast cancer (MBC) infrequently involves the pericardium, and only a small proportion of patients with pericardial metastases present with cardiac tamponade (1, 2). Approximately half of pericardial effusion (PE) in patients with cancer is caused by the invasion of the primary malignancy into the pericardium; thus, PE is regarded as an independent predictor of poor prognosis (3, 4). Control of the underlying malignancy by systemic chemotherapy is thought to be the only way to improve clinical outcomes (5, 6); however, heart failure arising from constrictive physiology (CP) following pericardiocentesis frequently disturbs the success of chemotherapy. Moreover, recurrent PE requiring repeated pericardiocentesis can occur despite chemotherapy, which is effective against other metastases. This may be considered a progressive disease, that

could permanently lead to discontinuation of current chemotherapy. However, there is a paucity of comprehensive research investigating alternative management approaches, such as pericardiocentesis and anti-inflammatory therapy (AIT), to effectively address cardiac tamponade and mitigate the risk of heart failure arising from CP in patients with MBC when traditional systemic anticancer drugs fail to yield favorable outcomes.

Herein, we present two cases in which overall control of MBC was ultimately achieved through pericardiocentesis and AIT for CP without switching to anticancer drugs despite the occurrence of malignant PE.

Case description

Case 1

A 44-year-old female patient who had been undergoing 65 cycles of palliative chemotherapy with trastuzumab and pertuzumab for human epidermal growth factor receptor 2 (HER2)-positive MBC presented to the emergency department with dyspnea. The patient's blood pressure was 101/69 mmHg, and her pulse rate was slightly high at 105 beats per min (BPM). Initial electrocardiography (ECG) revealed a low-voltage QRS complex (**Figure 1A**), and her *N*-terminal pro-brain natriuretic

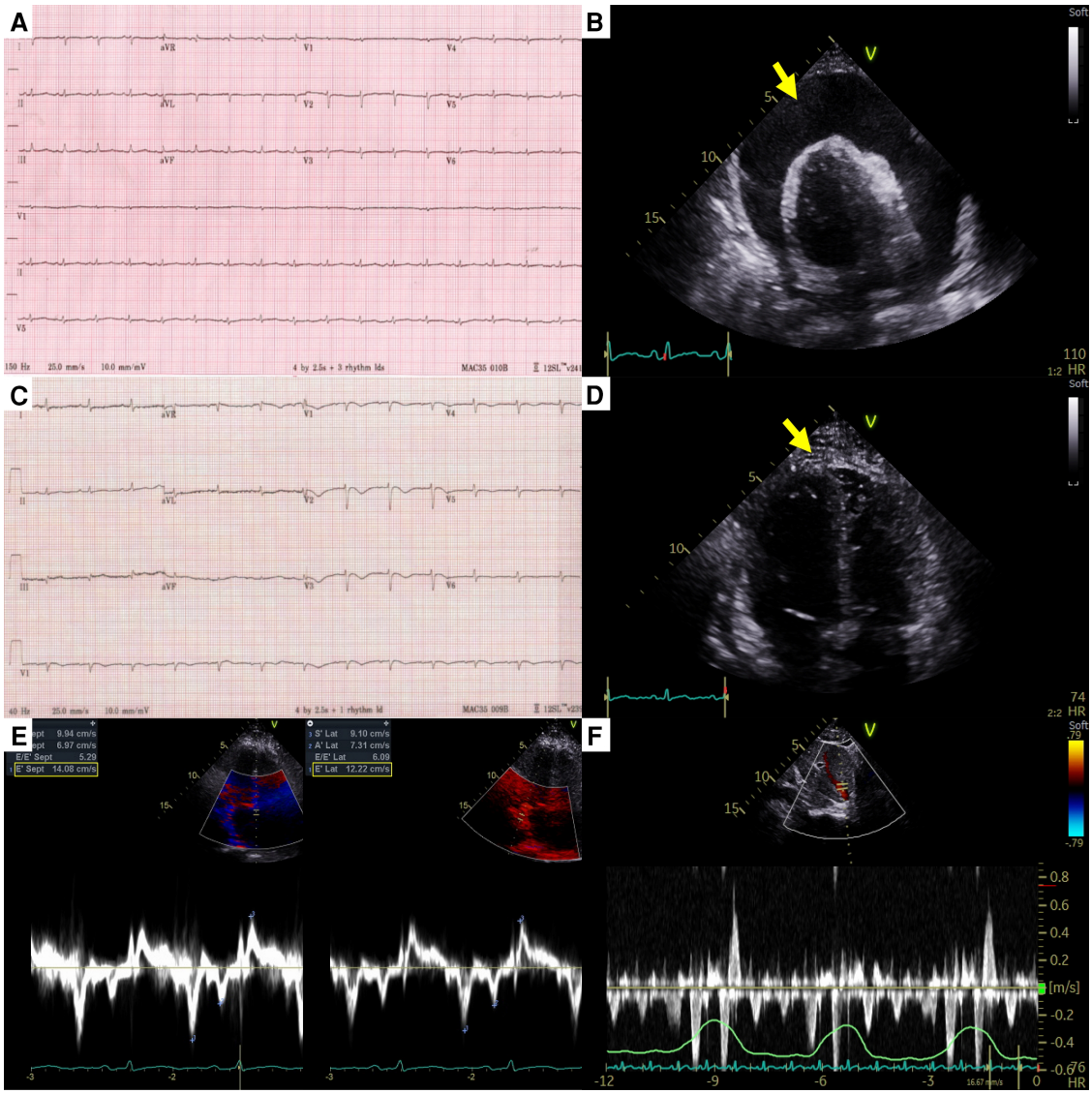

FIGURE 1
Electrocardiography and echocardiography at the first cardiac tamponade episode in case 1. (**A**) Low-voltage QRS complex in initial electrocardiography. (**B**) Large pericardial effusion (arrow) causing cardiac tamponade. (**C**) Newly developed anterior T wave inversion in post-pericardiocentesis electrocardiography. (**D**) Diffuse pericardial adhesions, and thickening (arrow) in post-pericardiocentesis echocardiography. (**E**) The medial early diastolic tissue doppler velocity exceeding the lateral velocity (annulus reversus). (**F**) Prominent expiratory diastolic flow reversal in the hepatic vein. Both (**E**) and (**F**) are suggestive of constrictive physiology.

peptide (NT-proBNP) level was relatively low (424 pg/ml). Therefore, we suspected cardiac tamponade and promptly performed echocardiography. A large PE with definite tamponade physiology was observed (**Figure 1B**, **Supplementary Video 1**), and emergent pericardiocentesis was performed. The next day, the ECG revealed a newly developed anterior T wave inversion (**Figure 1C**). Follow-up echocardiography showed markedly reduced PE, disseminated pericardial adhesions, and thickening with CP, suggesting effusive-constrictive pericarditis (ECP) (**Figures 1D–F**, **Supplementary Video 2**). Two days after pericardiocentesis, her dyspnea and tachycardia did not fully resolve, and the NT-proBNP level was elevated to 1,680 pg/ml, all of which were compatible with ECP. AIT against ECP was initiated using with prednisolone (started with 0.5 mg/kg/day, gradually tapered for 2 months) and colchicine (0.6 mg/day). A metastatic adenocarcinoma was identified on cytopathology in the drained PE, whereas no other possible causes of PE were identified in either serologic or PE analyses. Owing to the positive result of pericardial fluid cytopathology, we judged her breast cancer as a progressive disease and decided to change the cancer therapy to trastuzumab emtansine (T-DM1). However, cardiac tamponade recurred twice (2 and 5 months after initial pericardiocentesis, respectively), even after switching to T-DM1 (**Figures 2A**,**B**, **Supplementary Videos 3** and **4**), while other metastatic sites remained stable. Repeated pericardiocentesis and AIT for ECP were performed for each episode of cardiac tamponade. Despite recurrent cardiac tamponade episodes with T-DM1 therapy, we continued T-DM1 therapy with AIT because the symptoms and signs of heart failure were well controlled after pericardiocentesis and AIT. Furthermore, the oncological response to T-DM1 was thought to be stable, except for recurrent PE. Finally, after three times of pericardiocenteses, AIT, and eight cycles of T-DM1 therapy, cardiac tamponade has not recurred until now. The patient has been on T-DM1 maintenance therapy with an oncologic state of stable disease for two years.

Case 2

A 35-year-old female patient who had been undergoing palliative chemotherapy with gemcitabine and cisplatin for HER2-positive MBC was referred to the Department of Cardiology for New York Heart Association (NYHA) class IV dyspnea. Her blood pressure was within the normal range (110/80 mmHg); however her pulse rate was elevated, reaching 124 BPM. The NT-proBNP level was slightly elevated (249 pg/ml). Echocardiography revealed a large PE with definite tamponade physiology, though only a small PE was detected on the chest computed tomography (CT) one month ago (**Figures 3A**,**B**, **Supplementary Video 5**). Emergent pericardiocentesis was performed on the same day, and a metastatic adenocarcinoma was identified in the PE cytopathology, without other possible causes of PE, similar to Case 1. Two days after the pericardiocentesis, her dyspnea only modestly improved (NYHA class III) and her NT-proBNP level was markedly elevated (4,230 pg/ml). Follow-up echocardiogram showed pericardial adhesions and thickening around the entire cardiac border with CP. Additionally, the right ventricular free wall was captured to the adjacent pericardium, which resulted in right ventricular systolic dysfunction (**Figure 4A**, **Supplementary Video 6**). Both CP and right ventricular systolic dysfunction resulted in plethora of the inferior vena cava (**Figure 4B**). AIT against ECP was also introduced for this patient using prednisolone and colchicine (the same regimen as in Case 1). Despite pericardial metastasis, chemotherapeutic regimen was maintained without changes, simultaneously with AIT because the overall cancer was relatively stable, except for pericardial metastasis. At the 14th day of AIT, her dyspnea completely resolved (NYHA class I), and the NT-proBNP level rapidly decreased to 1,650 pg/ml. After 2 months of AIT, the NT-proBNP level decreased (245 pg/ml), and follow up echocardiogram showed complete resolution of pericardial thickening, adhesion, CP, and right ventricular dysfunction

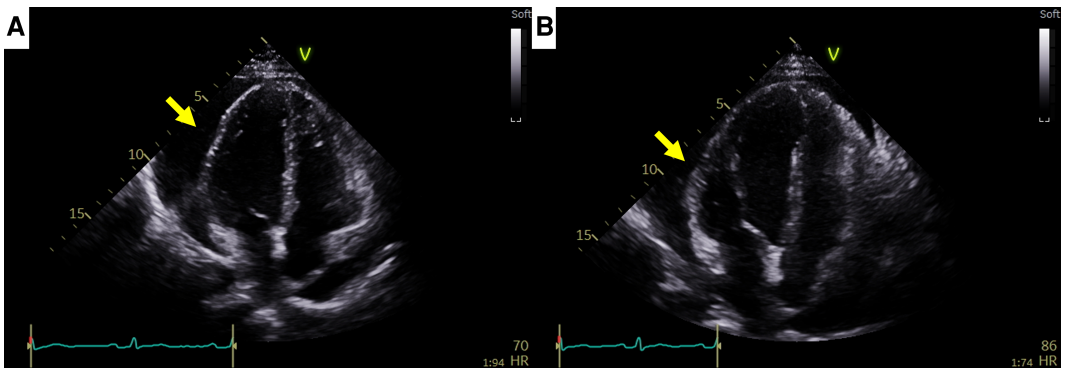

FIGURE 2
Recurrent cardiac tamponade episodes in case 1. (A) Second cardiac tamponade episode with large pericardial effusion (arrow). (B) Third cardiac tamponade episode with large pericardial effusion (arrow).

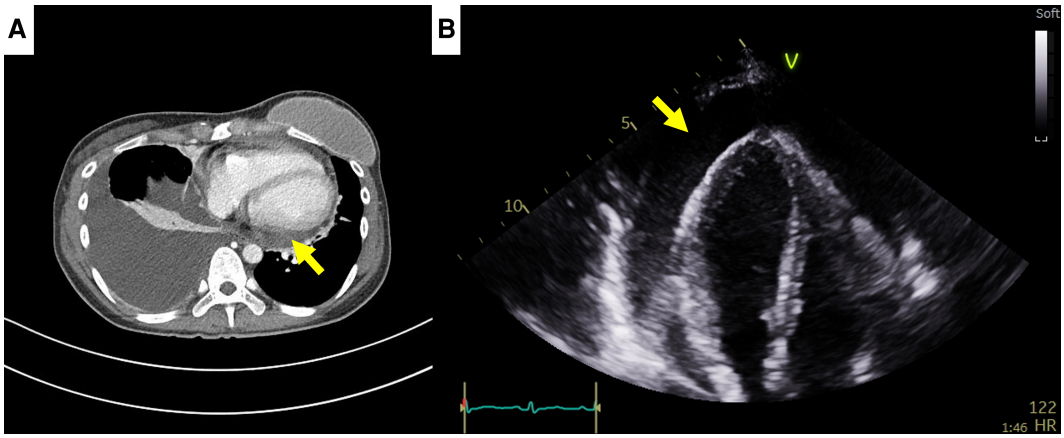

FIGURE 3
Computed tomography (CT) findings of case 2. (A) Small pericardial effusion in chest CT, 1 month prior to cardiac tamponade episode. (B) Large pericardial effusion (arrow) causing cardiac tamponade, 1 month after chest CT.

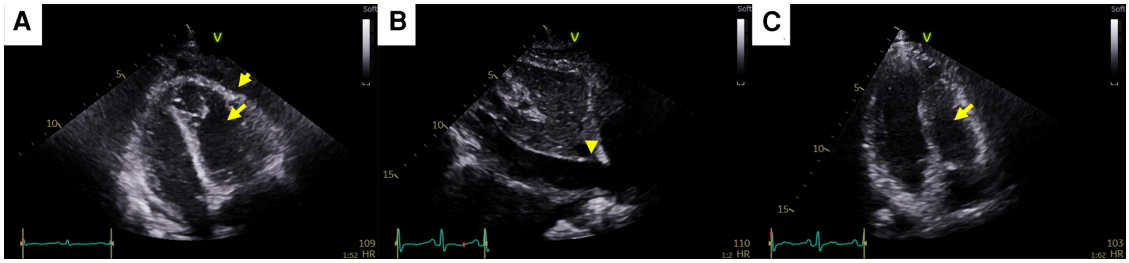

FIGURE 4
Pericardial changes after pericardiocentesis in case 2. (A) Pericardial adhesions and thickening (short arrow) causing constrictive physiology (CP). The right ventricular free wall was captured to the adjacent pericardium, which resulted in right ventricular systolic dysfunction (long arrow). (B) Plethora of the inferior vena cava caused by both CP and right ventricular systolic dysfunction (arrowhead). (C) At the end of anti-inflammatory treatment, pericardial adhesions, thickening, CP, and right ventricular dysfunction (arrow) were completely resolved.

(**Figure 4C**, **Supplementary Video 7**). This patient is still receiving chemotherapy with gemcitabine and cisplatin for 9 months, without recurrence of CP, need for repeated pericardiocentesis, or cancer progression.

Discussion

In these two cases, CP occurred after pericardiocentesis. While managing CP and heart failure with AIT, the current cancer therapy (T-DM1 and gemcitabine/cisplatin, respectively) were maintained. Little is known about adequate oncologic and cardiologic management of CP in patients with malignant PE. Despite ECP with or without recurrent cardiac tamponade events, we continued the current cancer therapy with AIT (and with repeated pericardiocentesis in Case 1) because CT imaging revealed a favorable response in other organs and tumor marker levels were not elevated. Eventually, we achieved an adequate oncologic response including the control of PE and ECP. These two cases give us a clinically important message: even if adverse pericardial events, such as ECP or recurrent cardiac tamponade, occur, proper AIT and/or repetitive pericardiocentesis can lead to the control of pericardial metastasis provided that the current anti-cancer drugs are effective in other organs.

The oncologic prognosis of malignant PE and concomitant cardiac tamponade associated with breast cancer has been known to be poor, with a median survival of 13 months (7). This might be caused not only by the heavy cancer burden represented by pericardial invasion, but also by difficulty in continuing cancer therapy due to heart failure symptoms associated with CP after pericardiocentesis. Patients with positive pericardial fluid cytopathologic results, especially when combined with CP, have lower event-free survival rates than those with negative cytopathological results (4, 5, 8). CP frequently develops after pericardiocentesis, and it is also associated with poor clinical outcomes in the patients by causing heart failure (9). Thus, patients who develop cardiac tamponade are often regarded as being in the terminal stage of cancer, especially when repetitive pericardiocentesis is required or when CP develops.

Several reports have documented successful treatment of MBC and cardiac tamponade, using thoracoscopic pericardial window surgery and chemotherapy (10, 11). However, in most cases,

performing cardiac operations under general anesthesia in patients with advanced cancer is difficult because of their poor general condition and anesthetic risks. The pericardial window operation can cause postpericardiotomy syndrome, resulting in CP. Therefore, the pericardial window operation is not generalizable in real practice.

Recently, several studies have reported inflammatory and reversible CP after pericardiocentesis in patients with cancer (8, 9). From a therapeutic perspective, colchicine use after successful pericardiocentesis is associated with lower composite events (12). These results suggest that some patients may benefit from AIT by reducing pericardial inflammation and the consequent CP. Reduction in this process could relieve heart failure and improve the patient's general condition, enabling further cancer therapy against the primary malignancy.

Conclusion

We report two cases of MBC with recurrent cardiac tamponade that were successfully treated with AIT and systemic anti-cancer therapy, with or without repetitive pericardiocentesis. Adverse pericardial events, such as ECP or recurrent cardiac tamponade, could be successfully managed using this treatment, in patients with malignant pericardial effusion. Long-term outcomes and prognostic indicators in these patients should be investigated, in further research.

Data availability statement

The original contributions presented in the study are included in the article/**Supplementary Material**, further inquiries can be directed to the corresponding author.

Ethics statement

The studies involving humans were approved by Institutional Review Board of Chonnam National University Hospital. The studies were conducted in accordance with the local legislation and institutional requirements. The participants provided their written informed consent to participate in this study. Written informed consent was obtained from the individual(s) for the publication of any potentially identifiable images or data included in this article. Written informed consent was obtained from the participants/patient(s) for the publication of this case report.

Author contributions

NL: Conceptualization, Data curation, Writing – original draft. HB: Writing – original draft. HP: Conceptualization, Funding acquisition, Supervision, Writing – review & editing. HS: Writing – review & editing.

Funding

The author(s) declare financial support was received for the research, authorship, and/or publication of this article.

This study was supported by a grant (HCRI19020) Chonnam National University Hwasun Hospital Biomedical Research Institute. The funders had no role in study design, data collection and analysis, decision to publish, or preparation of the manuscript.

Conflict of interest

The authors declare that the research was conducted in the absence of any commercial or financial relationships that could be construed as a potential conflict of interest.

Publisher's note

Supplementary material

The Supplementary Material for this article can be found online at: https://www.frontiersin.org/articles/10.3389/fcvm.2023.1285233/full#supplementary-material

SUPPLEMENTARY VIDEO 1
Large pericardial effusion causing cardiac tamponade in Case 1.

SUPPLEMENTARY VIDEO 2
Diffuse pericardial adhesions, and thickening in post-pericardiocentesis echocardiography of Case 1.

SUPPLEMENTARY VIDEO 3
Second cardiac tamponade episode with large pericardial effusion in Case 1.

SUPPLEMENTARY VIDEO 4
Third cardiac tamponade episode with large pericardial effusion in Case 1.

SUPPLEMENTARY VIDEO 5
Large pericardial effusion causing cardiac tamponade in Case 2.

SUPPLEMENTARY VIDEO 6
Pericardial adhesions and thickening causing constrictive physiology. The right ventricular free wall was captured to the adjacent pericardium, which resulted in right ventricular systolic dysfunction.

SUPPLEMENTARY VIDEO 7
At the end of anti-inflammatory treatment, pericardial adhesions, thickening, constrictive physiology, and right ventricular dysfunction were completely resolved.

References

1. Hagemeister FB Jr., Buzdar AU, Luna MA, Blumenschein GR. Causes of death in breast cancer: a clinicopathologic study. *Cancer*. (1980) 46(1):162–7. doi: 10.1002/1097-0142(19800701)46:1<162::aid-cncr2820460127>3.0.co;2-b

2. Woll PJ, Knight RK, Rubens RD. Pericardial effusion complicating breast cancer. *J R Soc Med*. (1987) 80(8):490–1. doi: 10.1177/014107688708000811

3. Haddad D E, Iliescu C, Yusuf SW, William WN Jr., Khair TH, Song J, et al. Outcomes of cancer patients undergoing percutaneous pericardiocentesis for pericardial effusion. *J Am Coll Cardiol*. (2015) 66(10):1119–28. doi: 10.1016/j.jacc.2015.06.1332

4. Gornik HL, Gerhard-Herman M, Beckman JA. Abnormal cytology predicts poor prognosis in cancer patients with pericardial effusion. *J Clin Oncol*. (2005) 23 (22):5211–6. doi: 10.1200/jco.2005.00.745

5. Dequanter D, Lothaire P, Berghmans T, Sculier JP. Severe pericardial effusion in patients with concurrent malignancy: a retrospective analysis of prognostic factors influencing survival. *Ann Surg Oncol*. (2008) 15(11):3268–71. doi: 10.1245/s10434-008-0059-z

6. Gross JL, Younes RN, Deheinzelin D, Diniz AL, Silva RA, Haddad FJ. Surgical management of symptomatic pericardial effusion in patients with solid malignancies. *Ann Surg Oncol*. (2006) 13(12):1732–8. doi: 10.1245/s10434-006-9073-1

7. Ilerhunmwuwa N, Sedeta E, Wasifuddin M, Hakobyan N, Aiwuyo HO, Perry JC, et al. Cardiac tamponade in patients with breast cancer: a systematic review. *Cureus*. (2022) 14(12):e33123. doi: 10.7759/cureus.33123

8. Cho IJ, Chang HJ, Chung H, Lee SE, Shim CY, Hong GR, et al. Differential impact of constrictive physiology after pericardiocentesis in malignancy patients with pericardial effusion. *PLoS One*. (2015) 10(12):e0145461. doi: 10.1371/journal.pone.0145461

9. Park H, Yoon HJ, Lee N, Kim JY, Kim HY, Cho JY, et al. Characteristics and clinical outcomes of cancer patients who developed constrictive physiology after pericardiocentesis. *Korean Circ J*. (2022) 52(1):74–83. doi: 10.4070/kcj.2021.0217

10. Ikeda H, Kikawa Y, Nakamoto Y, Takeo M, Yamamoto M. A patient with recurrent breast cancer showing long-term survival after developing pericardial effusion and cardiac tamponade caused by carcinomatous pericarditis. *Breast Care (Basel)*. (2013) 8(1):71–3. doi: 10.1159/000346831

11. Ucche M, Putra A, Gustisiya MAR, Choridah L, Supriatna Y, Dwidanarti SR, et al. Remarkable response to pericardial window procedure and weekly docetaxel treatment in a metastatic breast cancer patient with pericardial effusion and cardiac tamponade. *Clin Case Rep*. (2020) 8(12):3178–83. doi: 10.1002/ccr3.3380

12. Kim SR, Kim EK, Cho J, Chang SA, Park SJ, Lee SC, et al. Effect of anti-inflammatory drugs on clinical outcomes in patients with malignant pericardial effusion. *J Am Coll Cardiol*. (2020) 76(13):1551–61. doi: 10.1016/j.jacc.2020.08.003

frontiers | Frontiers in Cardiovascular Medicine

TYPE Case Report
PUBLISHED 03 November 2023
DOI 10.3389/fcvm.2023.1279177

OPEN ACCESS

EDITED BY
Reto Asmis,
Wake Forest University, United States

REVIEWED BY
George Samanidis,
Onassis Cardiac Surgery Center, Greece
Maruti Haranal,
U N Mehta Institute of Cardiology and Research, India

*CORRESPONDENCE
Chengming Fan
✉ fanchengming@csu.edu.cn

†These authors have contributed equally to this work

RECEIVED 18 August 2023
ACCEPTED 19 October 2023
PUBLISHED 03 November 2023

CITATION
Li Y, Ai Y, Tang W, Liu J, Yang J and Fan C (2023) Case Report: Successful surgical management of a challenging primary cardiac angiosarcoma. Front. Cardiovasc. Med. 10:1279177. doi: 10.3389/fcvm.2023.1279177

Case Report: Successful surgical management of a challenging primary cardiac angiosarcoma

Yichen Li†, Yinze Ai†, Weijie Tang, Jijia Liu, Jinfu Yang and Chengming Fan*

Department of Cardiovascular Surgery, the Second Xiangya Hospital, Central South University, Changsha, China

Primary cardiac tumors are exceptionally rare, with malignant tumor occurrences ranging from 0.0017% to 0.28%. Among these, primary cardiac angiosarcoma (PCA) stands as the most prevalent malignancy, primarily impacting the right cardiac system. In this case report, we present the instance of a 44-year-old woman who recently exhibited acute chest discomfort and was subsequently diagnosed with a microangiosarcoma within the right atrium and superior vena cava. Diagnostic modalities including chest x-rays, CT, MRI, and PET-CT were instrumental in pinpointing the tumor's location and nature. Surgical excision followed by pathological and immunological examinations confirmed the diagnosis. The patient's recovery post-surgery has been encouraging, with successful follow-up chemoradiotherapy administered. Despite advancements, devising optimal strategies for enhancing patient survival and quality of life in angiosarcoma cases remains a pressing research challenge.

KEYWORDS

primary cardiac angiosarcoma, cardiac surgery, malignant, reconstruction, SVC

Introduction

Primary cardiac tumors are infrequently encountered, with a subset manifesting as malignant tumors at an incidence ranging from 0.0017% to 0.28% (1). Among these, benign tumors constitute 75%, encompassing cardiac myxoma, rhabdomyoma, fibroma, hemangioma, and teratoma. Myxoma, for instance, predominantly arises in the left atrium. Conversely, 25% of primary cardiac tumors exhibit malignancy, including sarcoma, lymphoma, and mesothelioma. The spotlight, however, is on primary cardiac angiosarcoma (PCA), the foremost malignant cardiac neoplasm. PCA predominantly affects the right cardiac system and constitutes the majority of malignant cardiac tumors. While radical excision remains the primary therapeutic approach, the unfortunate reality is that a staggering 89% of patients present with metastases at diagnosis (2, 3). Despite multidisciplinary interventions such as radiation, chemotherapy, and targeted therapy, the prognosis remains grim, with surgically treated patients reporting a median survival of merely 14 months (4). As a consequence, these patients often receive chemotherapy and radiation therapy, with the lack of standardized treatment protocols posing a persistent challenge. Notably, the current chemotherapy regimens are extrapolated from extracardiac soft tissue sarcoma data, with doxorubicin and ifosfamide being prevalent choices (5). Even though some similar cases have been reported, in this report, we detail the case of a 44-year-old woman diagnosed with a substantial PCA within the right atrium and superior vena cava and successful surgical management with beating heart technique.

Case report

A 44-year-old woman presented with sudden chest discomfort of unknown origin, prompting a comprehensive medical examination conducted one month prior. This examination revealed the presence of a mass in her right atrium. The patient's chest discomfort occurred without accompanying symptoms such as shortness of breath, coughing, or other pulmonary issues. These symptoms typically subsided after a brief 2-minute rest. Through thorough patient interviews, we established the absence of significant medical history and a lack of familial occurrence of similar medical conditions. Notably, prior to admission, a thorough evaluation had unveiled a substantial pericardial effusion, promptly addressed via pericardiocentesis upon admission. No significant abnormal findings were observed in the cytology of the pericardial fluid. Subsequently, a battery of diagnostic procedures was conducted post-admission, encompassing a chest x-ray, cardiac ultrasound, electrocardiogram, cardiac CT, cardiac MRA, and PET-CT. The patient exhibited a normal electrocardiogram indicative of sinus rhythm. Preoperative echocardiography indicated an enlarged heart shadow, delineating multiple masses of uncertain nature in the right atrium, including a minor pericardial effusion (**Figure 1A**). The cardiac CT highlighted a right atrium lesion with superior vena cava invasion (**Figures 1B–D**). The cardiac MRA was performed and depicted an occupying lesion in the right atrium, signifying a high likelihood of a malignant tumor (**Figure 1E**). This assessment was further confirmed by PET-CT findings of multiple nodules with significantly elevated glucose metabolism in the right atrium and concurrent pericardial effusion.

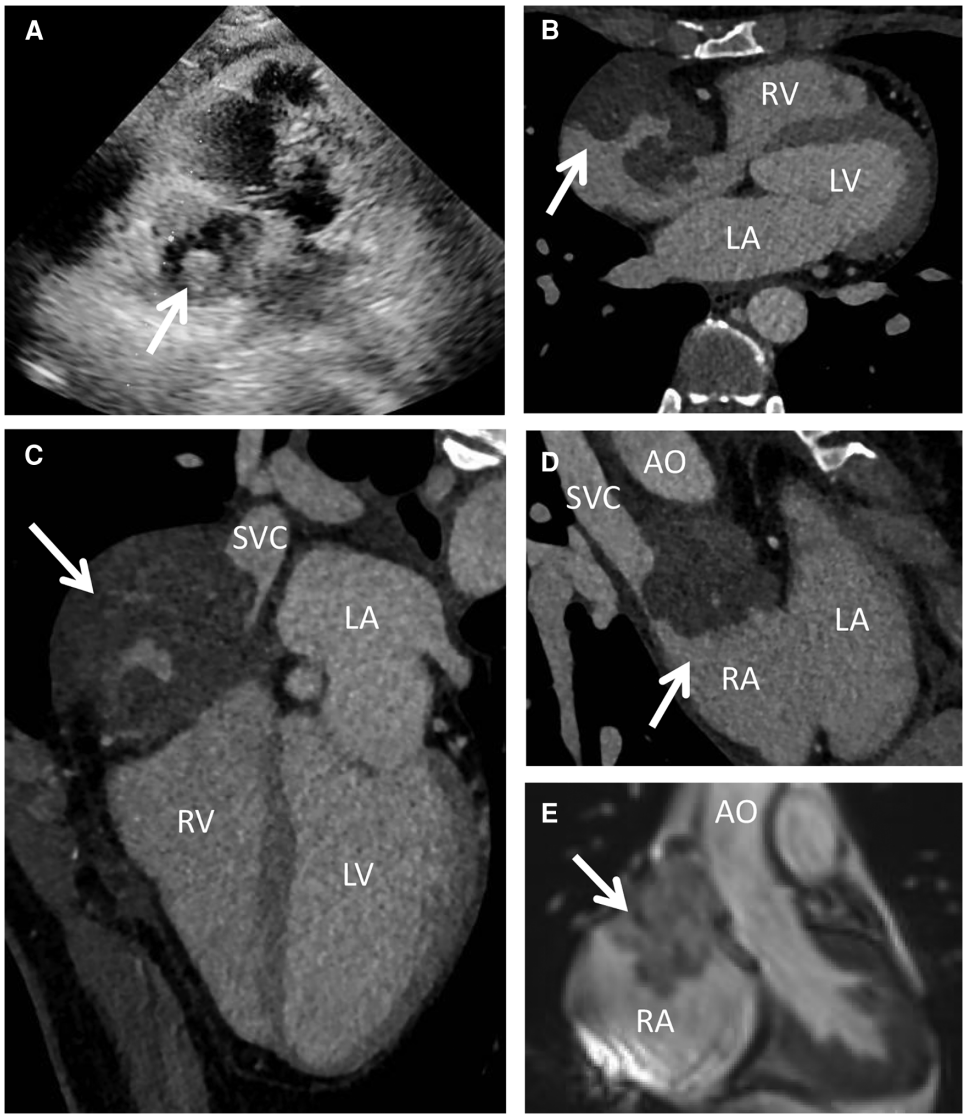

FIGURE 1
Preoperative echocardiography, cardiac CT and MRI. Echocardiography (**A**) showed multiple mixed echogenic masses on the lateral wall of the right atrium; CT scan (**B–D**) showed a giant cardiac mass with the invasion of the RA and SVC; MRI (**E**) indicated that the mass attached to the wall of RA with unclear boundary. AO, ascending aorta; LA, left atrium; LV, left ventricle; RA, right atrium; RV, right ventricle; SVC, superior vena cava.

Following the comprehensive evaluation, immediate surgical resection of the cardiac tumor was performed. A giant mass was observed extent encompassing from the right atrial appendage and the superior vena cava, to the right atrioventricular sulcus, the posterior atrial wall, and approximately 2 cm downward from the inferior vena cava opening (**Figure 2A**, **Supplementary Video S1**). A cluster of three masses, totaling about 3 cm in diameter, was found located on the right side of the aorta. Notably, a pale red coloration marked the pericardial fluid. An incision was made in the right atrium, facilitating the removal of the mass and the invaded right atrial wall (**Figure 2B**, **Supplementary Video S1**). During surgery, the tumor, a small margin (2 cm–3 cm) of the surrounding healthy tissue was removed. Because the procedure was performed with beating heart, tumor excision was performed with great care to avoid damaging the sinus node and causing complete atrioventricular block. The mass, measuring approximately 5 cm × 5 cm × 4 cm, exhibited parenchymal characteristics, a firm consistency, dark red coloration, and an uneven surface (**Figures 2C,D**). The right atrium was finally reconstructed using a bovine pericardium patch of matching size. The pathology postoperatively from both the right atrium and para-aorta were detected similar and revealed that the grayish-red solid mass featured a 2.5 cm × 2 cm × 1.5 cm size portion showcasing pronounced cellular heterogeneity, conspicuous nuclear divisions, extensive hemorrhagic necrosis, and abundant blood vessels (**Figures 3A, B**). Immunohistochemistry findings for the right atrial cardiac adenoma indicated CK (-), S100 (-), TLE1 (-), Ki67 (80%+), P53 (5% weak+, possibly indicative of nonsense mutant type expression), Desmin (-), MyoD1 (-), and Miyogenin (-). Immunophenotypic markers SMA (weak+), CD34 (++), CD31 (++), F8 (++), D2-40 (-), ERG (++), HCAL (-), ER (O), P16 (focal+), and CD10 (-) were documented (**Figures 3C,D**). Post-surgery, the patient's stay in the intensive care unit spanned 18.5 h and discharge on the 12th day with the recommendation of transferred to the oncology department and subsequently underwent conventional and experimental chemoradiotherapy for angiosarcoma [stereotactic radiotherapy and weekly paclitaxel (80–100 mg/m^2) for 6 cycles]. During the ensuing six-month follow-up period, the patient exhibited a favorable recovery trajectory devoid of complications, ultimately experiencing a resumption of normal activities without the recurrence of symptoms. The postoperative echocardiography revealed that the right atrial mass was totally resected, no hemodynamic abnormality and no recurrence signals (**Figures 4A,B**).

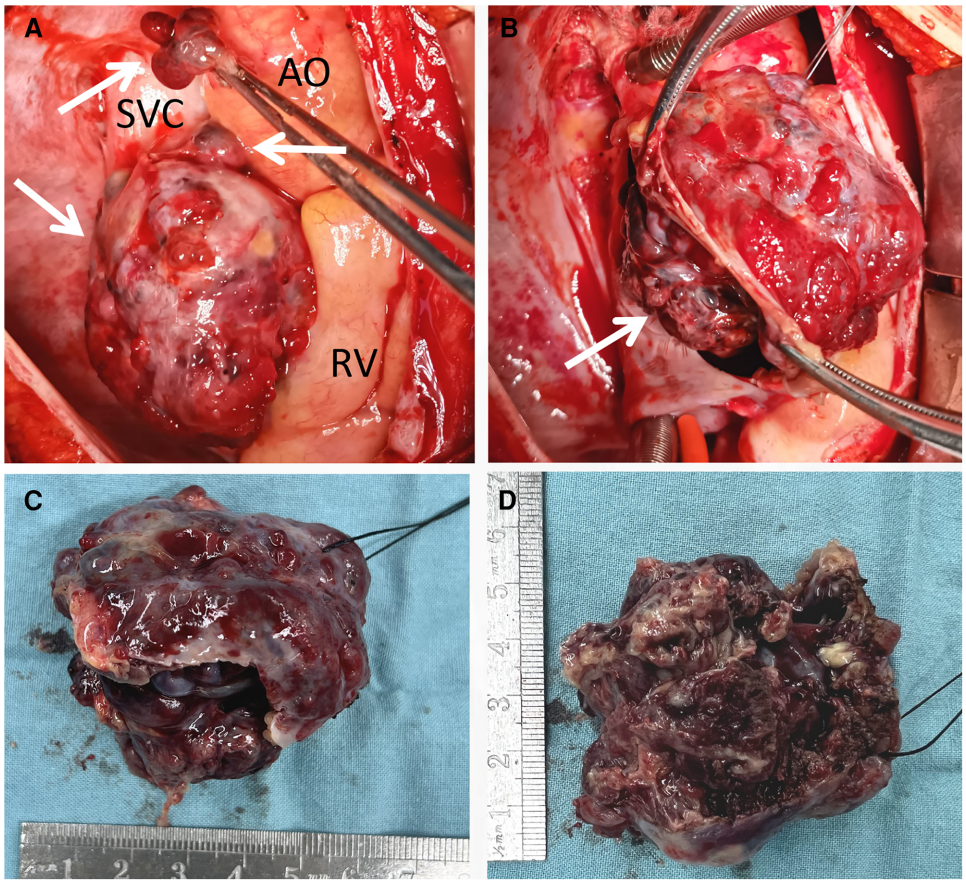

FIGURE 2
Intraoperative view showing a giant mass located in the RA, SVC and pera-AO (**A**), infiltrating the wall of RA and SVC (**B**); after totally removal, the mass was measured approximately 5 cm × 5 cm × 4 cm, exhibited parenchymal characteristics, a firm consistency, dark red coloration, and an uneven surface (**C,D**). AO, ascending aorta; RV, right ventricle; SVC, superior vena cava.

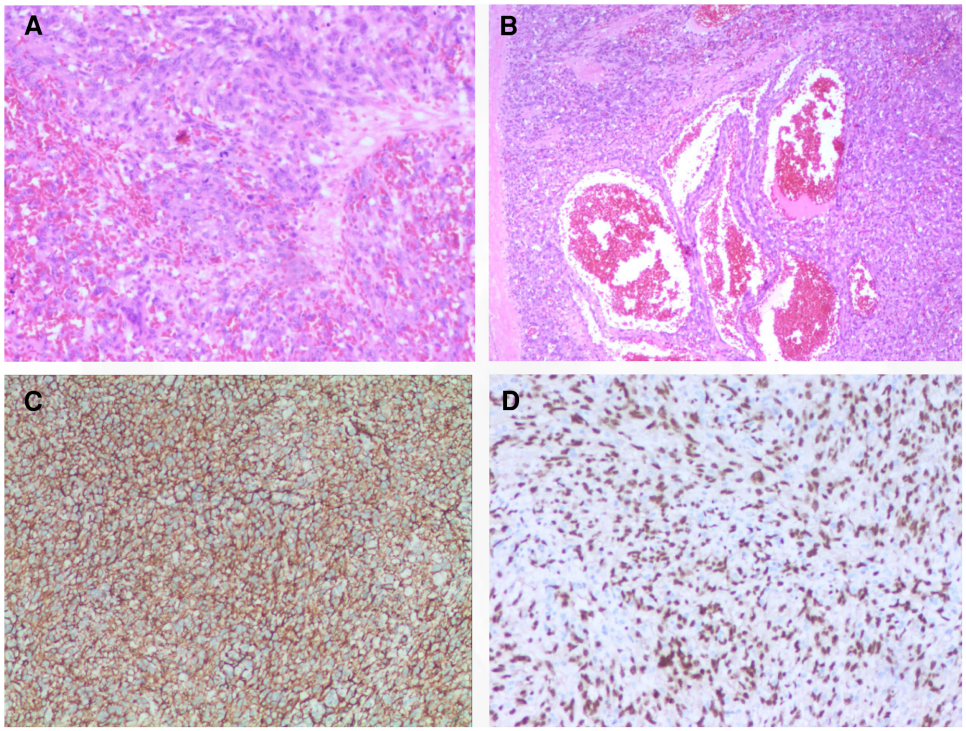

FIGURE 3
Histology and immunohistochemistry of the masses. Malignant tumor derived from mesenchymal tissue, with obvious cell atypia, many mitoses, large areas of hemorrhage and necrosis, rich blood vessels, invasion of surrounding muscle tissue with HE staining (**A**,**B**); immunohistochemical support for angiosarcoma with positive of CD34 (**C**), ERG (**D**), et al. 100× for panel A, C and D; 40× for panel B.

Discussion

Angiosarcoma, a highly malignant endothelial cell tumor, constitutes 1%–2% of soft tissue tumors. It manifests as an exceptionally aggressive cancer with a bleak prognosis, capable of affecting any anatomical region (3). Notably, around 60% of lesions are identified within the epidermis, soft tissues, liver, spleen, bones, and breast. Contrastingly, the heart and kidneys exhibit lower incidence rates (6). PCA stands as a predominant form of primary cardiac malignancy, with 90% of cases arising in the right atrium, while the left atrium or ventricle accounts for less than 5% (4, 7). PCA typically emerges in male patients aged 30–40 (8), and its clinical symptoms are non-specific, contingent upon location and size. The swift infiltrative growth of the tumor results in acute clinical manifestations, including chest pain, constriction, shortness of breath, arrhythmia, pericardial effusion, and right heart failure (9, 10). Given its aggressive nature, the prognosis of PCA is dire, attributed to high local recurrence and early metastasis rates at diagnosis (11, 12).

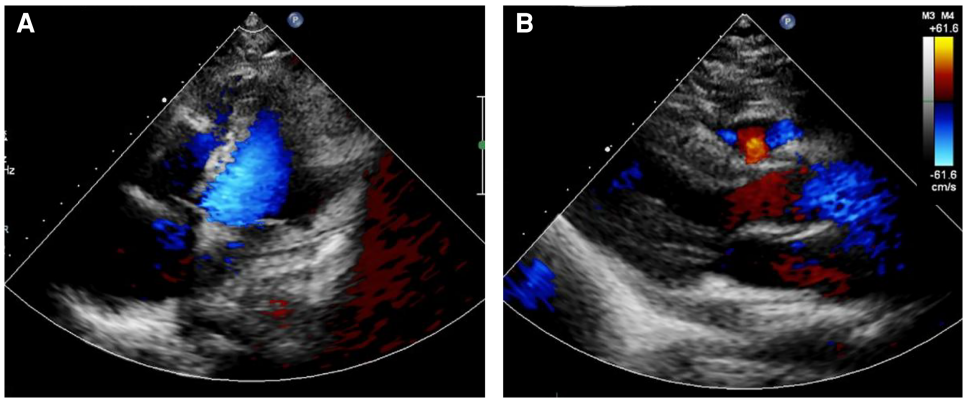

FIGURE 4
Postoperative echocardiography showed that the right atrial mass was totally resected (**A**), no hemodynamic abnormality (**B**) and no recurrence signals.

Imaging techniques and diagnosis

Diagnostic techniques for primary cardiac lesions encompass x-ray, echocardiography, CT, MRI, and PET-CT, with CT and MRI being pivotal for diagnosis (13). Echocardiography has evolved as a primary imaging method due to its precision in tumor size and location assessment, evaluating heart valves, pericardial structures, and its non-invasive, cost-effective nature. However, limitations exist, including operator dependence and constrained visual fields in specific patients (14). CT, especially for lung tissue characterization and systemic metastasis, is more effective. Contrast-enhanced CT scans offer valuable insights into tumor properties, blood vessels, heart walls, and lung parenchyma, minimizing the likelihood of missing lesions (15). On CT scans, PCA showcases uniform or asymmetrical density on unenhanced images, whereas enhanced images exhibit heterogeneous centripetal enhancement (16). Cardiac MRI is regarded as an advanced technique for determining tumor size, location, and signal characteristics, distinguishing between solid, liquid, blood, and fat (17). Additionally, PET-CT aids in discerning benign from malignant tumors, assessing invasiveness, and identifying metastasis. Immunohistochemical markers like CD31, CD34, ERG, and factor VIII confirm PCA's endothelial cell origin (18). The patient's thorough examinations indicated the likelihood of angiosarcoma, requiring essential tissue biopsy for confirmation. Following tumor resection, pathological and immune examinations were conducted, revealing both angiosarcoma and angiomyxfibroma derived from mesenchymal tissue.

Treatment approaches and outlook

Due to the rarity of these tumors, optimal management strategies remain under debate. Presently, available treatments encompass surgery, radiation therapy, and chemotherapy. Surgical excision remains the preferred approach for primary malignant cardiac tumors, yielding the best potential for long-term survival and curative outcomes (19, 20). Median survival for primary cardiac malignancies ranges from 6 to 11 months, while surgical patients experience a median survival of 14 months compared to 3.8 ± 2.5 months for those with inoperable metastases (21, 22). Combining surgical excision and chemoradiotherapy enhances short-term prognosis but lacks discernible effects on long-term outcomes (23). Heart transplantation is an option when resection is unfeasible due to metastases, though prolonged immunosuppressant use post-surgery may induce recurrence and metastasis. Radiation therapy, particularly stereotactic body radiotherapy (SBRT), has yielded positive results with tumor regression and minimal long-term effects (24). Investigation into targeted drugs and immunotherapy shows promise, particularly taxanes as adjuvant chemotherapy for cardiac angiosarcoma (25). Although the optimum chemotherapy regimen is yet to be clearly defined, molecularly targeted medications like amlotinib, imatinib, sorafenib, and bevacizumab hold therapeutic potential (26, 27). The patient's history underscores the significance of swift surgical intervention in cases like a massive right atrial angiosarcoma. The current recovery of the patients is highly encouraging following systematic anti-tumor chemoradiotherapy post-surgery. The present case reveals that the disease had progressed to an advanced stage of angiosarcoma without presenting any discernible symptoms. This serves as a stark reminder of the dangers associated with this condition. The present case underscores the critical importance of swift diagnosis and surgical intervention when dealing with right atrial angiosarcoma. Surgical excision, when combined with subsequent chemoradiotherapy, continues to hold promise as an approach to manage this rare and aggressive cardiac malignancy. Further research and investigation are imperative to optimize diagnostic and therapeutic strategies, ultimately leading to improved patient outcomes.

Conclusion

In conclusion, primary cardiac angiosarcoma, especially within the right atrium, represents an unusual clinical entity. While various imaging modalities aid in diagnosis, treatment strategies for PCA remain elusive, necessitating prompt interventions post-surgical resection. Given the short time follow-up period and rarity of this malignancy, the challenges it poses underscore the imperative of ongoing research to unravel improved diagnostic and therapeutic approaches.

Data availability statement

The raw data supporting the conclusions of this article will be made available by the authors, without undue reservation.

Ethics statement

The studies involving humans were approved by the Ethics Committee of the Second Xiangya Hospital of Central South University. The studies were conducted in accordance with the local legislation and institutional requirements. The participants provided their written informed consent to participate in this study. Written informed consent was obtained from the individual(s) for the publication of any potentially identifiable images or data included in this article.

Author contributions

YL: Data curation, Writing – original draft. YA: Data curation, Writing – original draft. WT: Methodology, Writing – review & editing. JL: Data curation, Writing – review & editing. JY: Methodology, Writing – review & editing. CF: Conceptualization, Formal analysis, Investigation, Supervision, Writing – review & editing.

Funding

The author(s) declare financial support was received for the research, authorship, and/or publication of this article.

This work was financially supported by the Scientific Research Launch Project for new employees of the Second Xiangya Hospital of Central South University (to CF).

Conflict of interest

The authors declare that the research was conducted in the absence of any commercial or financial relationships that could be construed as a potential conflict of interest.

Publisher's note

Supplementary material

The Supplementary Material for this article can be found online at: https://www.frontiersin.org/articles/10.3389/fcvm.2023.1279177/full#supplementary-material

References

1. Look Hong NJ, Pandalai PK, Hornick JL, Shekar PS, Harmon DC, Chen YL, et al. Cardiac angiosarcoma management and outcomes: 20-year single-institution experience. *Ann Surg Oncol*. (2012) 19:2707–15.

2. Bouma W, Lexis CP, Willems TP, Suurmeijer A, van der Horst I, Ebels T, et al. Successful surgical excision of primary right atrial angiosarcoma. *J Cardiothorac Surg*. (2011) 6:47.

3. Fan C, Gao Z, Yin NI, Yang J. Surgical treatment of primary cardiac tumors in children: experience of a single institute. *Oncol Lett*. (2015) 10:2071–74.

4. Patel SD, Peterson A, Bartczak A, Lee S, Chojnowski S, Gajewski P, et al. Primary cardiac angiosarcoma - a review. *Med Sci Monit*. (2014) 20:103–9.

5. Penel N, Bui BN, Bay JO, Cupissol D, Ray-Coquard I, Piperno-Neumann S, et al. Phase II trial of weekly paclitaxel for unresectable angiosarcoma: the ANGIOTAX study. *J Clin Oncol*. (2008) 26:5269–74.

6. Boni A, Cochetti G, Sidoni A, Bellezza G, Lepri E, Giglio A, et al. Primary angiosarcoma of the kidney: case report and comprehensive literature review. *Open Med*. (2019) 14:443–55.

7. Saito M, Saraya T, Oda M, Minamishima T, Kongoji K, Isomura A, et al. Rapidly progressive respiratory failure with multiple halo signs on computed tomography in a patient with primary cardiac angiosarcoma derived from the right atrium: a case report. *BMC Pulm Med*. (2020) 20:321.

8. Xu C, Sun W, Fang L, He L, Yang F, Zhang J, et al. The value of multimodal imaging in the diagnosis of primary cardiac angiosarcoma. *Echocardiography*. (2021) 38:1474–7.

9. Maleszewski JJ, Bois MC, Bois JP, Young PM, Stulak JM, Klarich KW. Neoplasia and the heart: pathological review of effects with clinical and radiological correlation. *J Am Coll Cardiol*. (2018) 72:202–27.

10. Chen Y, Li Y, Zhang N, Shang J, Li X, Liu J, et al. Clinical and imaging features of primary cardiac angiosarcoma. *Diagnostics*. (2020) 10.

11. Jain A, Simon S, Elangovan I. (18)F-fluoro-deoxyglucose positron emission tomography-computed tomography in initial assessment and diagnosis of right atrial angiosarcoma with widespread visceral metastases: a rare case report and review of the literature. *Indian J Nucl Med*. (2015) 30:51–4.

12. Waness A, Batoon AA, Mirza I, Al Mahmeed W. Elusive cardiac angiosarcoma in a young pregnant female: rare presentation with fatal outcome. *Cardiol Res*. (2015) 6:292–6.

13. Elsayad K, Scobioala S, Kriz J, Haverkamp U, Eich HT. Advances in image-guided radiation therapy for primary cardiac angiosarcoma: the role of PET-CT and MRI. *Oncol Res Treat*. (2016) 39:290–4.

14. Chen YC. Localization of angiosarcoma by peri-operative transesophageal echocardiography. *Int J Cardiovasc Imaging*. (2017) 33:1749–51.

15. Do TH, Le XD, Vu TT, Ngo TA, Thi MHN, Tran QT, et al. Primary cardiac epithelioid angiosarcoma: a case report. *Radiol Case Rep*. (2022) 17:3349–54.

16. Yu JF, Cui H, Ji GM, Li SQ, Huang Y, Wang RN, et al. Clinical and imaging manifestations of primary cardiac angiosarcoma. *BMC Med Imaging*. (2019) 19:16.

17. Nijjar PS, Masri SC, Tamene A, Kassahun H, Liao K, Valeti U. Benefits and limitations of multimodality imaging in the diagnosis of a primary cardiac lymphoma. *Tex Heart Inst J*. (2014) 41:657–9.

18. Ge Y, Ro JY, Kim D, Kim CH, Reardon MJ, Blackmon S, et al. Clinicopathologic and immunohistochemical characteristics of adult primary cardiac angiosarcomas: analysis of 10 cases. *Ann Diagn Pathol*. (2011) 15:262–7.

19. Sakaguchi M, Minato N, Katayama Y, Nakashima A. Cardiac angiosarcoma with right atrial perforation and cardiac tamponade. *Ann Thorac Cardiovasc Surg*. (2006) 12:145–8.

20. Fan C, Kong D, Tan C, Yang J. Isolated cardiac peripheral primitive neuroectodermal tumor: a case report. *Cancer Biol Ther*. (2017) 18:4–7.

21. Antonuzzo L, Rotella V, Mazzoni F, Doni L, Bianchini D, Garbini F, et al. Primary cardiac angiosarcoma: a fatal disease. *Case Rep Med*. (2009) 2009:591512.

22. Jang Y, Kim J, Shim JW, Kim EY, Moon J, An J, et al. Primary cardiac angiosarcoma: a prolonged response to surgical resection followed by concurrent chemoradiotherapy with docetaxel. *Springerplus*. (2016) 5:648.

23. Wang JG, Wang B, Hu Y, Liu JH, Liu B, Liu H, et al. Clinicopathologic features and outcomes of primary cardiac tumors: a 16-year-experience with 212 patients at a Chinese medical center. *Cardiovasc Pathol*. (2018) 33:45–54.

24. Stergioula A, Pantelis E. Treatment of a primary cardiac angiosarcoma with stereotactic body radiation therapy. *Hellenic J Cardiol*. (2023) 72:70–1.

25. Kajihara I, Kanemaru H, Miyake T, Aoi J, Masuguchi S, Fukushima S, et al. Combination chemotherapy with S-1 and docetaxel for cutaneous angiosarcoma resistant to paclitaxel. *Drug Discov Ther*. (2015) 9:75–7.

26. Chi Y, Fang Z, Hong X, Yao Y, Sun P, Wang G, et al. Safety and efficacy of anlotinib, a multikinase angiogenesis inhibitor, in patients with refractory metastatic soft-tissue sarcoma. *Clin Cancer Res*. (2018) 24:5233–8.

27. Agulnik M, Yarber JL, Okuno SH, von Mehren M, Jovanovic BD, Brockstein BE, et al. An open-label, multicenter, phase II study of bevacizumab for the treatment of angiosarcoma and epithelioid hemangioendotheliomas. *Ann Oncol*. (2013) 24:257–63.

frontiers | Frontiers in Cardiovascular Medicine

TYPE Case Report
PUBLISHED 08 November 2023
DOI 10.3389/fcvm.2023.1279611

OPEN ACCESS

EDITED BY
Reto Asmis,
Wake Forest University, United States

REVIEWED BY
Yoshihisa Shimada,
Tokyo Medical University, Japan
Paolo Albino Ferrari,
Ospedale Oncologico Armando Businco, Italy

*CORRESPONDENCE
Chloe Ntshaykolo
✉ chloe.ntshaykolo@chu-brest.fr
Thomas Fave
✉ thomas.fave@chu-brest.fr

RECEIVED 18 August 2023
ACCEPTED 11 October 2023
PUBLISHED 08 November 2023

CITATION
Ntshaykolo C, Fave T, Benic C, Boizet A, Geier M, Nicol P-P and Descourt R (2023) Case Report: Coronaro-bronchial fistula vascularizing a squamous cell lung cancer. Front. Cardiovasc. Med. 10:1279611. doi: 10.3389/fcvm.2023.1279611

Case Report: Coronaro-bronchial fistula vascularizing a squamous cell lung cancer

Chloe Ntshaykolo*, Thomas Fave*, Clement Benic, Antoine Boizet, Margaux Geier, Pierre-Philippe Nicol and Renaud Descourt

Centre Hospitalier Universitaire (CHU) de Brest, Hôpital Morvan, Département d'Oncologie Thoracique, Brest, France

Coronary fistulas are rare, having been described for the first time by Krauss in 1865 in postmortem. They are commonly asymptomatic and can be caused by congenital or acquired malformations. We present the case of a 65-year-old patient who was treated for squamous cell lung cancer with chemoimmunotherapy and presented with angina. The coronary angiography showed a coronaro-bronchial fistula that arises from a branch of the right coronary artery and is associated with lung cancer.

KEYWORDS
coronary fistula, coronaro-bronchial fistula, lung neoplasms, coronaropathy, immunotherapy

Introduction

Initially described by Krauss in 1865 in postmortem, a coronary fistula is an abnormal precapillary communication of a coronary artery or one of its branches into a cardiac cavity or other low-pressure vascular structure (1, 2). Coronary fistulas are a rare event with an incidence between 0.2% and 0.6% per year (3). Coronaro-cameral fistulas are more frequent in pediatric populations (congenital), whereas coronary–pulmonary fistulas are more frequent in adults on a process that seems acquired (1).

Squamous cell lung cancer is the second most common type of non-small cell lung cancer, which represents the first cause of cancer death in men and the second in women.

The present case reports a case of a patient with coronaro-bronchial fistula, incidentally discovered during an acute cardiac episode, vascularizing the bronchial tumor in the patient followed up since December 2020 for lung carcinoma.

Case presentation

A 65-year-old Caucasian man, an active smoker of 30 pack-year, was diagnosed with an advanced squamous cell lung cancer cT4N2M1a (contralateral lung nodules). Programmed death-ligand 1 (PDL1) tumor proportion score (TPS) was between 1% and 5% in December 2020. He started chemoimmunotherapy (paclitaxel–carboplatin–pembrolizumab) in January 2021 followed by pembrolizumab maintenance because of a partial tumor response. While on pembrolizumab, he presented to the emergency unit in December 2021 with left chest pain. ECG and troponin assays (initial troponin 1,490 ng/L and then 19,300 ng/L) led to the diagnosis of an ST-troponin + acute coronary syndrome. Further explorations were carried out urgently:

- Cardiac echography showed an apical and apico-septal hypokinesis, overflowing in the middle third of the anteroseptal wall of the left ventricle. Left ventricular ejection

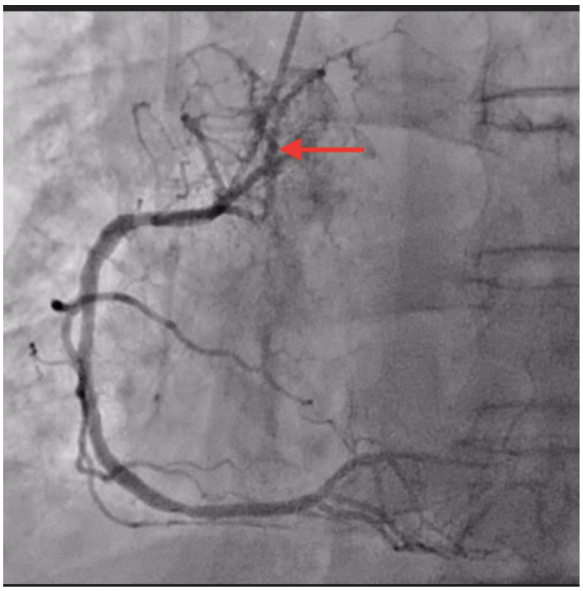

FIGURE 1
Fistula origin (coronary angiography).

fraction (LVEF) and cardiac output were preserved. The right ventricle was normal in size and function.

- Coronary angiography highlighted a right dominance, tandem significant stenosis first segment of left anterior descending artery with ostial significant stenosis diagonal of small caliber with kinetics appearing altered in territory first segment of left anterior descending artery. Significant stenosis bisecting with a poorly developed downstream bed. An atypical coronary fistula was noted, arising from a branch of right coronary artery and perfusing the bronchial tumor (coronaro-bronchial fistula) (**Figure 1**).

Anterior interventricular artery stenting following percutaneous transluminal coronary angioplasty was performed. After discussions with interventional radiologists and the referring oncologist, embolization of the coronaro-bronchial fistula was not performed because this procedure seemed risky for the coronary artery system.

Immunotherapy was continued. The latest tumor assessment in January 2022 showed a stable disease. We asked the radiologists to perform a CT scan to determine the site of the fistula (**Figures 2**, **3**).

Discussion

Coronary fistulas are rare malformations arising more often from the right coronary artery (RCA). Most of them are congenital, but some have been demonstrated to be iatrogenic after cardiac surgery by some case reports (4).

The genesis of a coronary arterial fistula is the result of communication between a coronary artery, a cardiac chamber, a large vessel, or any other vascular structure, initially described by

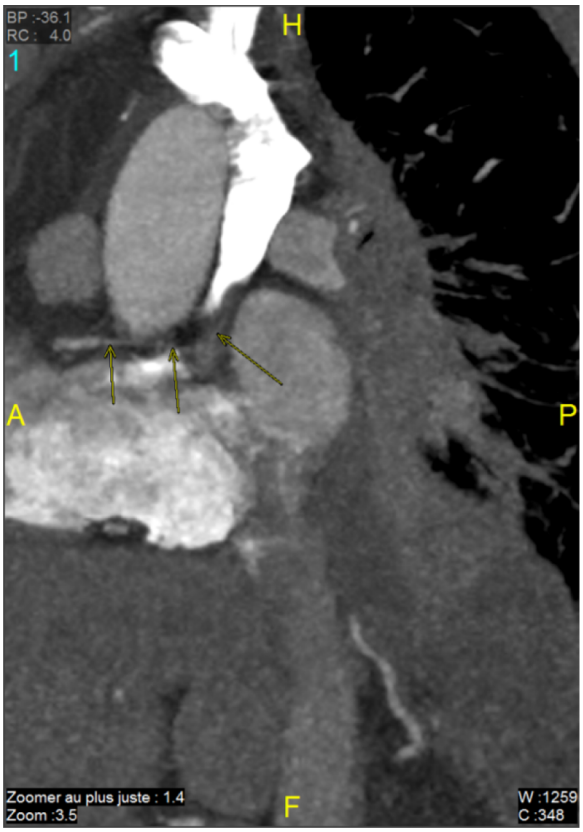

FIGURE 2
Sagittal section: the path of the ectopic bronchial artery (coroscan).

Krauss in 1865 in postmortem (5). It is an abnormal connection between the arteries and a vascular structure of low pressure. In most cases, coronary fistulas are asymptomatic and diagnosed incidentally. In older patients, certain signs can be seen, such as exertional dyspnea, exertional angina, arrhythmia, endocarditis, and stroke (1, 6).

For this patient, the possible causes of this fistula are neoangiogenesis of his cancer and predisposing conditions, age, male sex, and consumption of an estimated 60 packs of weaned tobacco per year.

We consider that this is not a toxicity of immunotherapy, because we have never found similar cases in the literature. However, cardiac toxicities occur, and there is a relationship between immunotherapy and myocardial infarction: 2% of myocardial infarctions are reported with pembrolizumab, and the mechanisms are:

- Associated inflammation may enhance plaque rupture, which is the main mechanism in the case of our patient.
- Systemic inflammatory response providing coronary spasm.
- Direct T cell-mediated.

The reference diagnostic examination remains coronary angiography, which studies the anatomy of the fistula. Cardiac Doppler ultrasound, especially transesophageal, and cardiac CT

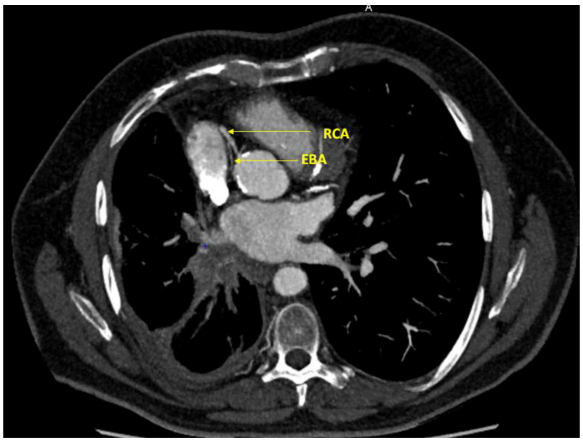

FIGURE 3
Axial section, right coronary artery (RCA) and ectopic bronchial artery (EBA) (coroscan).

scans provide additional morphological information, such as coronary artery affected, diameter of the feeder artery, and diagnosis of complications (1).

The complications of coronary fistulas can be severe including hypoperfusion of the adjacent myocardium, thrombosis, embolism, heart failure, atrial fibrillation, rupture, endocarditis or endarteritis, and arrhythmia (1).

Regarding the different therapeutics, there are two possible approaches, namely, surgical or percutaneous closure (7). Surgical treatment has shown excellent efficacy and long-term safety. Percutaneous closure is also a reliable method with good results (8). In more than 70% of the cases, metallic coils, balloons, and umbrella-type systems rarely covered stents (6, 9).

The emergency intervention would have been embolization (e.g., by a coil) through the fistula to stop bleeding from the tumor.

Given the necrotic nature of the tumor, the risk of fistula rupture is likely, but we did not apply any specific follow-up. The patient underwent frequent CT scans as part of his neoplastic follow-up. We could have realized coroscanner scans, but the cardiologists maintained a standard annual follow-up. Finally, the coronagrophy and the fistula remained unchanged.

Shao et al. (9) reported a case of a coronary fistula and a lung adenocarcinoma, incidentally discovered in a 67-year-old woman admitted to the hospital for a persistent cough. The CT scan found an isolated nodule in the upper lobe of the left lung. Transthoracic echocardiography as part of a preoperative workup showed the coronary fistula confirmed later at angiography but without a link between them. In this case, they adopted a combined operation and surgical treatment of both conditions in a single procedure via sternotomy.

Our case shows a real "coronaro-tumoral" fistula, arising from the RCA and perfusing the lung tumor.

In this patient who was followed up in 2020 and is in good general condition, PS 0-1, the question of treatment arises.

The therapeutic indications remain a predominant question, there is no consensus. In adults, spontaneous closure is rare, and it requires elective surgical or percutaneous closure by "coils" (10).

The patient was eligible for chemotherapy because the benefit–risk ratio was discussed at the multidisciplinary team, and the prognosis was related to neoplasia.

At first, the neoplasia was a locally advanced stage, but radiochemotherapy was not practicable in light of the excessively wide fields of irradiation, so it was considered stage IV. The expected and declared OS, according to KEYNOTE-407, is 18–24 months.

In the neoplastic context, the situation is more complex and will require multidisciplinary consultation, taking into account several elements, disease evolution, oncological prognosis, the pathophysiological impact of the fistula, and the general condition of the patient.

Indeed, no literature review on this case has supported the decision taken.

Conclusion

This is the first case of an active coronary bronchial fistula vascularizing a pulmonary neoplasm in a patient with good general condition. It was decided to perform a simple surveillance without embolization due to the limited experience with this anomaly and its rarity.

Data availability statement

The original contributions presented in the study are included in the article/Supplementary Material, further inquiries can be directed to the corresponding authors.

Ethics statement

Ethical approval was not required for the study involving humans in accordance with the local legislation and institutional requirements. Written informed consent to participate in this study was not required from the participants or the legal guardians/next of kin of the participants in accordance with the national legislation and institutional requirements. Written informed consent was obtained from the individual(s) for the publication of any potentially identifiable images or data included in this article.

Author contributions

CN: Writing – original draft. TF: Investigation, Writing – review & editing. CB: Conceptualization, Writing – review & editing. AB: Conceptualization, Writing – review & editing. MG: Supervision, Writing – review & editing. P-PN: Conceptualization, Writing – review & editing. RD: Supervision, Writing – review & editing.

Funding

The authors declare that no financial support was received for the research, authorship, and/or publication of this article.

Conflict of interest

The authors declare that the research was conducted in the absence of any commercial or financial relationships that could be construed as a potential conflict of interest.

Publisher's note

References

1. Bouzerda A. Les fistules coronaires: à propos d'un cas et revue de la literature. *Pan Afr Med J.* (2015) 21:145. doi: 10.11604/pamj.2015.21.145.7149

2. Leye M, Balde DW, Mbengue A, Gueye K, Manga SJ, Affangl DA, et al. Right coronary artery fistulae draining into right atrium: a Case Report. *World J Cardiovasc Dis.* (2022) 12(2):87–93. doi: 10.4236/wjcd.2022.122009

3. Qureshi SA. Coronary arterial fistulas. *Orphanet J Rare Dis.* (2006) 1:51. doi: 10.1186/1750-1172-1-51

4. Vavuranakis M, Bush CA, Boudoulas H. Coronary artery fistulas in adults: incidence, angiographic characteristics, natural history. *Cathet Cardiovasc Diagn.* (1995) 35(2):116–20. doi: 10.1002/ccd.1810350207

5. Luo L, Kebede S, Wu S, Stouffer GA. Coronary artery fistulae. *Am J Med Sci.* (2006) 332(2):79–84. doi: 10.1097/00000441-200608000-00005

6. Balanescu S, Sangiorgi G, Castelvecchio S, Medda M, Inglese L. Coronary artery fistulas: clinical consequences and methods of closure. A literature review. *Ital Heart J.* (2001) 2(9):669–76.

7. Tirilomis T, Aleksic I, Busch T, Zenker D, Ruschewski W, Dalichau H. Congenital coronary artery fistulas in adults: surgical treatment and outcome. *Int J Cardiol.* (2005) 98(1):57–9. doi: 10.1016/j.ijcard.2002.05.001

8. Perry SB, Rome J, Keane JF, Baim DS, Lock JE. Transcatheter closure of coronary artery fistulas. *J Am Coll Cardiol.* (1992) 20(1):205–9. doi: 10.1016/0735-1097(92)90160-o

9. Shao M, Han T, Chen X, Wang Z, Jiang X, Li W. Coronary artery fistula and lung adenocarcinoma: a case report and literature review. *Ann Palliat Med.* (2021) 10(1):75458–758. doi: 10.21037/apm-20-2015

10. Loukas M, Germain AST, Gabriel A, John A, Tubbs RS, Spicer D. Coronary artery fistula: a review. *Cardiovasc Pathol.* (2015) 24(3):141–8. doi: 10.1016/j.carpath.2014.01.010

frontiers | Frontiers in Cardiovascular Medicine

TYPE Case Report
PUBLISHED 20 December 2023
DOI 10.3389/fcvm.2023.1309613

OPEN ACCESS

EDITED BY
Sai-Ching Jim Yeung,
University of Texas MD Anderson Cancer Center, United States

REVIEWED BY
Tareg Bey,
University of Texas MD Anderson Cancer Center, United States
Agnes S. Kim,
UCONN Health, United States

*CORRESPONDENCE
Aman Wang
✉ wangamandl@126.com
Jiwei Liu
✉ jiweiliudl@126.com

†These authors have contributed equally to this work and share first authorship

RECEIVED 08 October 2023
ACCEPTED 04 December 2023
PUBLISHED 20 December 2023

CITATION
Sun R, Jin C, Qin H, Zhang W, Ning Z, Liu J and Wang A (2023) Case Report: A long-term survival case of diffuse large B-cell lymphoma with left ventricular infiltration and spinal cord compression.
Front. Cardiovasc. Med. 10:1309613.
doi: 10.3389/fcvm.2023.1309613

Case Report: A long-term survival case of diffuse large B-cell lymphoma with left ventricular infiltration and spinal cord compression

Rui Sun[1†], Chenxing Jin[1†], Henan Qin[1], Wenhe Zhang[1], Zhen Ning[2], Jiwei Liu[1*] and Aman Wang[1*]

[1]Department of Oncology, The First Affiliated Hospital of Dalian Medical University, Dalian, China, [2]Department of General Surgery, The First Affiliated Hospital of Dalian Medical University, Dalian, China

Background: Diffuse large B-cell lymphoma (DLBCL) is the most common subtype of non-Hodgkin lymphoma and may occur with lymph node and/or extranodal involvement. However, DLBCL with intracardiac mass is exceedingly rare. In the reported literature, the intracardiac infiltration of DLBCL mostly involves the right ventricle. Lymphoma that invades the heart has an aggressive nature, with symptoms that are easily ignored initially and can lead to multiple complications in severe cases, resulting in a poor prognosis. Early screening and diagnosis may significantly improve the survival rate. Early diagnosis may significantly improve outcomes.

Case summary: We presented a 68-year-old woman with back pain. PET/CT suggested increased FDG metabolism in the left ventricle, right adrenal gland, right erector spinae intramuscularis, multiple bones and multiple lymph nodes. Contrast-enhanced ultrasound showed a left ventricular apical mass with ventricular septum thickening. Cardiac MRI suggested a 1.6*1.1*2.1 cm mass in the apical-central portion of the left ventricle. Biopsy of the right neck mass confirmed the pathologic diagnosis of diffuse large B-cell lymphoma. However, before the pathologic diagnosis was confirmed, the patient was paralyzed due to spinal cord compression caused by the progression of bone metastases. Subsequently, pathology confirmed the diagnosis of diffuse large B-cell lymphoma, and rituximab plus cyclophosphamide, doxorubicin, vincristine, and prednisone (R-CHOP) was treated immediately as first-line therapy. In addition, glucocorticoids and mannitol dehydration were administered to relieve the symptoms of spinal cord compression. After 8 cycles of R-CHOP, the tumor at all sites had almost complete regression. The patient was able to walk normally and had no tumor-related symptoms.

Conclusions: We present a case of DLBCL with a very high tumor load that involved multiple organs, including the left ventricle, but exhibited no cardiac-related symptoms. The combination of various imaging modalities is valuable for the diagnosis of cardiac infiltration. The mass in the left ventricle almost completely regressed after R-CHOP treatment, and no recurrence has occurred in the 5 years of follow-up so far.

KEYWORDS

cardiac lymphoma, cardiac mass, intracardiac mass, lymphoma, large B-cell, diffuse

Introduction

Lymphoma-derived intracardiac masses are more common in two types: primary cardiac lymphoma (PCL) and cardiac invasion by extracardiac lymphoma (1). PCL is an extranodal lymphoma that often involves the right side of the heart. In non-PCL lymphomas, DLBCL has been reported to involve the heart, but left ventricular infiltration is extremely rare. Primary cardiac lymphoma is rare, accounting for less than 2% of all resected primary cardiac tumors in autopsy, and 0.5% of extranodal lymphomas. However, secondary cardiac involvement exists in 25% of patients with disseminated lymphoma (1).

Case presentation

A 62-year-old woman presented to our hospital with lower back pain for 3 months. She had no history of fever, night sweats, weight loss or other symptoms. She had a 9-year history of hypertension, with a maximum blood pressure of 160/100 mmHg, which was controlled at about 120/80 mmHg with amlodipine benzenesulfonate. She had no history of other underlying conditions including coronary artery disease, chronic heart failure, and so on. On admission, her vital signs were stable with a blood pressure of 130/80 mm Hg, a heart rate of 102 beats/min and a temperature of 36.3°C. Because the severe low back pain interfered with sleep, she was mostly confined to bed and was treated with opioid analgesia. A 3.0 cm × 3.0 cm mass was palpable in the right supraclavicular region of the patient, with firm texture, poor mobility, and no tenderness. There was tenderness and percussion pain (+) in the 4, 8, and 11 thoracic regions. Her cardiovascular exam was normal. Laboratory tests revealed moderately elevated lactate dehydrogenase (LDH) at 476 IU/L (100–300 IU/L) and elevated β2 microglobulin (β2MG) at 2.54 mg/L(0–0.3 mg/L). The hematuria and stool routine, liver and kidney function, electrolytes, and tumor markers were normal. The electrocardiogram showed a sinus rhythm with a left axis deviation.

To determine whether the masses were malignant, positron emission tomography (PET) imaging was performed with ^{18}F-fluorodeoxyglucose (FDG). The PET imaging showed multiple masses in the left ventricle, gallbladder, right adrenal gland, and right erector spinae with multiple enlarged lymph nodes and bone destruction throughout the body, all of which had significantly increased FDG uptake. In particular, the maximum standardized uptake value for left ventricular masses was 16.5 and 19.7 after delay, consistent with malignancy (**Figure 1A**). Echocardiography showed a 14 × 17 mm additional echo detectable at the proximal apical segment of the septum in the left ventricle, with irregular morphology, tissue-like echoes, and mobility. Echocardiography of the cardiac chambers showed a detectable contrast-enhanced mass in the septum near the apex, with an irregular morphology, measuring approximately 12 × 22 mm, with a wide base and high mobility at the point of attachment, and with a relatively large amount of contrast filling detectable within it, which was considered to be malignant (**Figure 1B**). The left ventricular ejection fraction (LVEF) was 59%. Axial Fiesta of cardiac magnetic resonance (CMR) showed

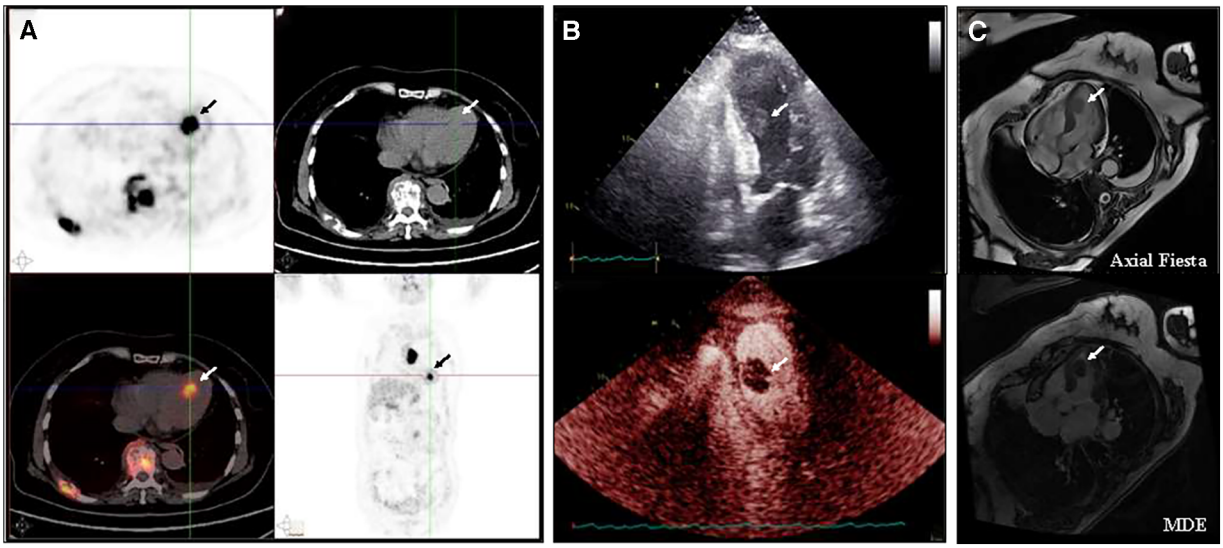

FIGURE 1
Baseline imaging of the left ventricular mass (A) PET/CT indicated multiple masses in the left ventricle, gallbladder, right adrenal gland, and right vertebral column, along with significant lymph node enlargement and widespread bone destruction, all exhibiting markedly increased FDG uptake. (B) Echocardiography showed an additional echogenicity measuring 14 × 17 mm in the proximal segment of the left ventricular septum, with an irregular shape, tissue-like echogenicity, and activity. A detectable filling defect in the septum near the apex is observed, with an irregular shape, approximately 12 × 22 mm in size, broad at the base, highly mobile at the attachment point, and containing a relatively large amount of contrast filling material. (C) CMR showed a mass measuring 1.6 cm × 1.1 cm × 2.1 cm at the left cardiac chamber septum. Long-axis four-chamber myocardial delayed enhancement (MDE) showed that the left ventricular mass appeared non-gadolinium enhancement at baseline.

a mass measuring 1.6 cm × 1.1cm × 2.1 cm at the left cardiac chamber septum. Long-axis four-chamber myocardial delayed enhancement (MDE) showed nodular shadows in the left cardiac chamber, and the mass had no gadolinium enhancement (**Figure 1C**). The patient refused to undergo an endomyocardial biopsy because of concerns about the risks of invasive procedures. Then, the patient underwent a biopsy of the right supraclavicular lymph node.

However, before the pathologic diagnosis was confirmed, the patient experienced spinal cord compression due to bone metastasis. Physical examination indicated that pain and temperature sensation below the level of the fourth thoracic vertebra disappeared, muscle strength of both lower limbs was grade 2, and no pathological reflexes were elicited. Magnetic resonance of the spine suggests bony destruction of vertebrae and appendages of thoracic vertebrae 4, 5, and 12, surrounded by visible soft tissue masses with spinal cord compression and edema. We hypothesized that the patient presented with spinal cord compression due to bone metastases. Glucocorticoids and mannitol dehydration were administered immediately to relieve the symptoms of spinal cord compression. Subsequently, pathology confirmed the diagnosis of diffuse large B-cell lymphoma, with positive immunohistochemical staining for CD20, CD3, CD5, BCL-2, and Ki67 (50%+).

Rituximab plus cyclophosphamide, doxorubicin, vincristine, and prednisone (R-CHOP) was treated immediately as first-line therapy. Almost all sites of tumor lesions were significantly reduced after two cycles of R-CHOP. The left ventricular mass was reduced to 1.1 cm × 0.6 cm, and the pain and temperature sensation below the level of the 4th thoracic vertebra were normalized, and the muscle strength of the left and right lower limbs improved to levels 4 and 5, respectively. After 4 cycles of R-CHOP, the left ventricular mass had almost regressed and the muscle strength of both lower limbs had completely returned to normal. A total of 6 cycles of R-CHOP were completed for first-line treatment, and the efficacy evaluation was complete response and then follow-up. During the treatment period, the LVEF increased from 65% at baseline to 69%, and no cardiovascular-related adverse events were observed. During the 5-year follow-up, all lesions, including the cardiac mass, remained complete regression, and FDG uptake was reduced to normal (**Figure 2**). The patient was able to walk normally and had no tumor-related symptoms. At the time of this manuscript (more than 5 years from follow-up), she is alive and has normal functional capacity. Despite the patient receiving anthracycline-based chemotherapy in first-line treatment, the LVEF remained normal, and no long-term cardiovascular toxicity was observed at 5 years of follow-up.

Discussion

The nature of cardiac masses is mostly attributed to intracardiac thrombi and benign mesenchymal tumors, while malignant tumors are rare, making their differential diagnosis challenging (2). Malignant cardiac tumors can be categorized by tissue type into sarcomas, mesotheliomas, and lymphomas, with sarcomas being the most common (2). Lymphomas presenting as intracardiac masses are exceedingly rare and can either originate within the heart as primary cardiac lymphomas or infiltrate the heart from extracardiac lymphomas. Infiltration of the heart by extracardiac lymphomas is more common, particularly in immunocompromised patients (3). Clinical manifestations of lymphoma-induced intracardiac masses lack specificity but commonly include symptoms such as dyspnea, lower limb edema, signs of right heart failure, intracardiac thrombi, peripheral emboli, valvular heart disease, and pericardial effusion. B-symptoms such as weight loss, night sweats, and fever may also be present (3). Lymphomas most frequently involve the right ventricle and the pericardium, with isolated involvement of the left ventricle being exceptionally rare. The precise mechanism leading to cardiac tropism in lymphomas remains unclear (3). In some cases, when tumors invade the heart, acute signs can precede B-symptoms (occurring in less than 25% of patients), aiding in early lymphoma diagnosis, with a reported incidence of acute heart failure being 20% (4). In our reported case of DLBCL, the intracardiac mass was located in the left ventricular apex-central region and did not manifest cardiac-related symptoms, making it an extremely rare clinical presentation. However, previous studies reported that left ventricular mass may increase the risk of embolization (5, 6). Although the cardiac mass of this patient was asymptomatic, the necessity for prophylactic anticoagulation is worth discussing.

Histopathological biopsy is the gold standard for lymphoma diagnosis. For patients with palpable superficial lymph node enlargement, lymph node biopsy is the preferred and less invasive option. In cases where the nature of intracardiac masses is difficult to determine, some experts suggest considering endocardial biopsy for diagnosis, although this procedure carries significant invasive risks (7). Transthoracic echocardiography is a non-invasive, cost-effective method for cardiac examination. However, it has limitations in specific views, and image quality and tissue resolution depend on the operator's experience (8). Cardiac CT offers advantages of high spatial resolution and three-dimensional volume acquisition, making it valuable for assessing the anatomical morphology and calcification of masses. It is especially useful for evaluating masses or tumors close to or invading the coronary arteries or bypass grafts. However, it has low tissue contrast, making it less suitable for delineating tumor borders (1). MRI provides high temporal resolution and tissue contrast, aiding in qualitative analysis of tumors. Both primary and secondary lymph nodes exhibit equal T1 and long T2 signals on MRI (9). PET/CT, as a sensitive whole-body imaging technique, plays a significant role in differentiating the benign and malignant nature of cardiac masses, assessing overall tumor burden, and predicting prognosis. Previous studies have shown that the majority of cardiac lymphomas are visible on PET/CT (9). Dynamic monitoring with PET/CT after treatment helps evaluate residual tumors and treatment efficacy, optimizing follow-up care. In our case, cardiac ultrasound and cardiac MRI both supported the diagnosis of a malignant tumor, which was confirmed by high-intensity FDG uptake on PET imaging. Due to concomitant superficial lymph node enlargement, a biopsy of the right cervical lymph node confirmed DLBCL, eliminating the need for invasive endocardial biopsy.

DLBCL is an aggressive lymphoma with rapid disease progression, and DLBCL involving the heart carries a poor prognosis. Without treatment, only 10% of patients survive for 9–12 months (10, 11). Clinical aggressiveness is consistent with

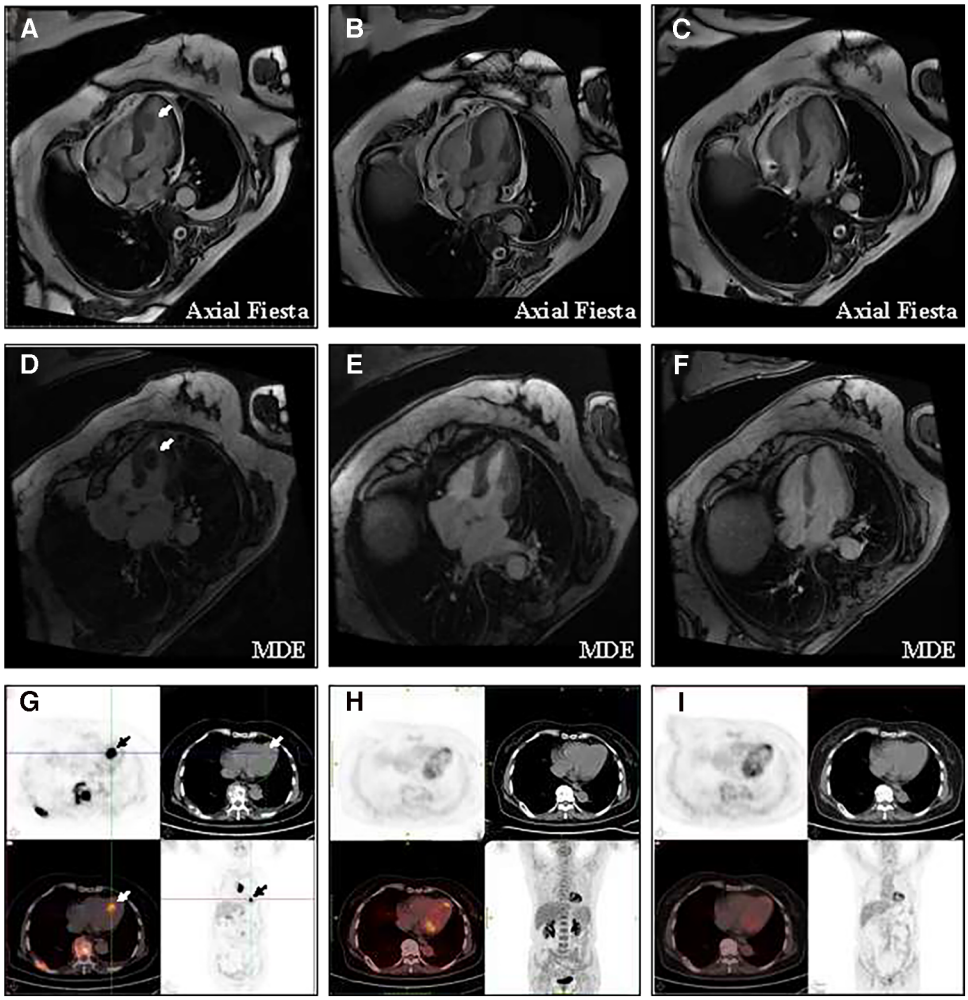

FIGURE 2
Change of the left ventricular mass at baseline and after treatment (**A**) CMR showed that the baseline size of the mass is 1.6 cm × 1.1 cm × 2.1 cm. (**B**) CMR showed that after 4 cycles of R-CHOP, the tumor at all sites had almost complete regression. (**C**) CMR showed no recurrence of cardiac mass in the five years of follow-up. (**D**) Long-axis four-chamber myocardial delayed enhancement (MDE) showed that the left ventricular mass appeared non-gadolinium enhancement at baseline. (**E**) After 4 cycles of R-CHOP treatment, long-axis four-chamber MDE showed the left ventricular mass had almost complete regression. (**F**) MDE showed no recurrence of cardiac mass in the five years of follow-up. (**G**) PET/CT showed that the maximum standardized uptake value for left ventricular masses was 16.5 and 19.7 after delay. (**H**) After 4 cycles of R-CHOP treatment, the left ventricle mass had almost complete regression and the FDG uptake of the left ventricular had returned to normal levels. (**I**) PET/CT showed no recurrence of cardiac mass in the five years of follow-up.

known factors such as high proliferation index, activated B-cell lymphoma phenotype, and expression or rearrangement of MYC, which are associated with extranodal sites and poorer outcomes (12). However, DLBCL is sensitive to treatment. The first-line R-CHOP regimen has shown favorable response rates, with standardized chemotherapy regimens achieving response rates of up to 79%–87% (4). The heart may not be considered a sanctuary for systemic drugs. Currently, there is no evidence to suggest that lymphomas in the cardiac location increase the risk of cardiotoxicity from chemotherapy, especially anthracyclines or rituximab, and this remains inconclusive. Early relapse or refractory disease may be managed with additional chemotherapy and allogeneic stem cell transplantation. In our patient, after R-CHOP chemotherapy, nearly complete regression of systemic masses was achieved, which is expected for diffuse large B-cell lymphoma.

Current guidelines recommend routine follow-up every 3–6 months for effectively treated patients, including medical history review, physical examination, and laboratory tests for 5 years. Imaging follow-up should not exceed every 6 months for 2 years unless clinically indicated (13). Our patient, after 5 years of follow-up post-treatment, has shown no tumor recurrence and remains free of any tumor-related symptoms, leading a normal daily life.

Our case represents a rare occurrence of diffuse large B-cell lymphoma involving the left ventricular apex-central region without cardiac-related symptoms, making it an exceptionally rare clinical presentation. The patient underwent multiple cardiac imaging modalities, highlighting the importance of a multidisciplinary approach in the differential diagnosis of cardiac tumors. The patient demonstrated significant efficacy following chemotherapy combined with targeted therapy, resulting in nearly

complete tumor regression and over 5 years of tumor-free follow-up. Early diagnosis and treatment are key to achieving favorable outcomes in lymphoma. However, our case has many inadequacies and limitations. First, there was no pathologic biopsy of the cardiac mass to further confirm the diagnosis of lymphoma cardiac infiltrate. In addition, as a case report, its conclusions remain to be confirmed by a large-sample clinical study.

Data availability statement

The original contributions presented in the study are included in the article/Supplementary Material, further inquiries can be directed to the corresponding author.

Ethics statement

Written informed consent was obtained from the individual(s) for the publication of any potentially identifiable images or data included in this article.

Author contributions

RS: Writing, collecting medical records and charting – original draft. CJ: Writing and collecting medical records – original draft. HQ: Collecting medical records – original draft. WZ: Charting – original draft. ZN: Writing – review & editing. JL: Writing – review & editing. AW: Writing – review & editing.

Funding

The author(s) declare that no financial support was received for the research, authorship, and/or publication of this article.

Conflict of interest

The authors declare that the research was conducted in the absence of any commercial or financial relationships that could be construed as a potential conflict of interest.

Publisher's note

All claims expressed in this article are solely those of the authors and do not necessarily represent those of their affiliated organizations, or those of the publisher, the editors and the reviewers. Any product that may be evaluated in this article, or claim that may be made by its manufacturer, is not guaranteed or endorsed by the publisher.

References

1. Jeudy J, Burke AP, Frazier AA. Cardiac lymphoma. *Radiol Clin North Am*. (2016) 54(4):689–710. doi: 10.1016/j.rcl.2016.03.006

2. Basso C, Rizzo S, Valente M, Thiene G. Cardiac masses and tumours. *Heart*. (2016) 102(15):1230–45. doi: 10.1136/heartjnl-2014-306364

3. Petrich A, Cho SI, Billett H. Primary cardiac lymphoma. *Cancer*. (2011) 117 (3):581–9. doi: 10.1002/cncr.25444

4. Yin K, Brydges H, Lawrence KW, Wei Y, Karlson KJ, McAneny DB, et al. Primary cardiac lymphoma. *J Thorac Cardiovasc Surg*. (2022) 164(2):573–80.e1. doi: 10.1016/j.jtcvs.2020.09.102

5. Redzek A, Preveden A, Kaloci SR, Samardzija G, Preveden M, Golubovic M, et al. Unusual non-valvular left ventricular endocarditis presenting as multiple brain embolism. *Acta Clin Belg*. (2022) 77(1):142–6. doi: 10.1080/17843286.2020.1789273

6. Spiliopoulos K, Anyfantakis ZA, Diminikos I, Xanthopoulos A, Magouliotis DE, Skoularigis J, et al. Acute myocardial infarction not attributed to coronary artery disease: a seldom initial presentation of a left ventricular myxoma. *Clin Case Rep*. (2021) 9(5):e04029. doi: 10.1002/ccr3.4029

7. Jurkovich D, de Marchena E, Bilsker M, Fierro-Renoy C, Temple D, Garcia H. Primary cardiac lymphoma diagnosed by percutaneous intracardiac biopsy with combined fluoroscopic and transesophageal echocardiographic imaging. *Catheter Cardiovasc Interv*. (2000) 50(2):226–33. doi: 10.1002/(sici)1522-726x(200006)50:2<226::aid-ccd19>3.0.co;2-a

8. Palaskas N, Thompson K, Gladish G, Agha AM, Hassan S, Iliescu C, et al. Evaluation and management of cardiac tumors. *Curr Treat Options Cardiovasc Med*. (2018) 20(4):29. doi: 10.1007/s11936-018-0625-z

9. Carter BW, Wu CC, Khorashadi L, Godoy MC, de Groot PM, Abbott GF, et al. Multimodality imaging of cardiothoracic lymphoma. *Eur J Radiol*. (2014) 83 (8):1470–82. doi: 10.1016/j.ejrad.2014.05.018

10. Chim CS, Chan AC, Kwong YL, Liang R. Primary cardiac lymphoma. *Am J Hematol*. (1997) 54(1):79–83. doi: 10.1002/(sici)1096-8652(199701)54:1<79::aid-ajh13>3.0.co;2-5

11. Habertheuer A, Ehrlich M, Wiedemann D, Mora B, Rath C, Kocher A. A rare case of primary cardiac B cell lymphoma. *J Cardiothorac Surg*. (2014) 9:14. doi: 10.1186/1749-8090-9-14

12. Carras S, Berger F, Chalabreysse L, Callet-Bauchut E, Cordier JF, Salles G, et al. Primary cardiac lymphoma: diagnosis, treatment and outcome in a modern series. *Hematol Oncol*. (2017) 35(4):510–9. doi: 10.1002/hon.2301

13. Tilly H, Gomes da Silva M, Vitolo U, Jack A, Meignan M, Lopez-Guillermo A, et al. Diffuse large B-cell lymphoma (DLBCL): eSMO clinical practice guidelines for diagnosis, treatment and follow-up. *Ann Oncol*. (2015) 26(Suppl 5):v116–25. doi: 10.1093/annonc/mdv304

frontiers | Frontiers in Cardiovascular Medicine

TYPE Case Report
PUBLISHED 11 January 2024
DOI 10.3389/fcvm.2023.1333484

OPEN ACCESS

EDITED BY
Reto Asmis,
Wake Forest University, United States

REVIEWED BY
Francisco José Bermúdez-Jiménez,
Hospital Universitario Virgen de las Nieves, Spain
Jiangang Zou,
Nanjing Medical University, China

*CORRESPONDENCE
Deyan Yang
✉ swallow_sums@aliyun.com
Kang'an Cheng
✉ chengkangan@hotmail.com

†These authors share first authorship

RECEIVED 05 November 2023
ACCEPTED 26 December 2023
PUBLISHED 11 January 2024

CITATION
Yu J, Kong F, Gao P, Chen T, Liu Y, Cheng Z, Deng H, Lai J, Zhang L, Fan J, Wang J, Qin X, Sun K, Li J, Fang Q, Yang D and Cheng K (2024) Case Report: Left bundle branch pacing in an amyloid light-chain cardiac amyloidosis patient with atrioventricular block. Front. Cardiovasc. Med. 10:1333484. doi: 10.3389/fcvm.2023.1333484

Case Report: Left bundle branch pacing in an amyloid light-chain cardiac amyloidosis patient with atrioventricular block

Jiaqi Yu[1†], Fanyi Kong[2†], Peng Gao[3], Taibo Chen[3], Yongtai Liu[3], Zhongwei Cheng[3], Hua Deng[3], Jinzhi Lai[3], Lihua Zhang[3], Jingbo Fan[3], Jiaqi Wang[1], Xiaohan Qin[1], Keyue Sun[1], Jian Li[4], Quan Fang[3], Deyan Yang[3*] and Kang'an Cheng[3*]

[1]Department of Internal Medicine, Peking Union Medical College Hospital, Chinese Academy of Medical Sciences & Peking Union Medical College, Beijing, China, [2]Department of Gastroenterology, Peking Union Medical College Hospital, Chinese Academy of Medical Sciences & Peking Union Medical College, Beijing, China, [3]Department of Cardiology, Peking Union Medical College Hospital, Chinese Academy of Medical Sciences & Peking Union Medical College, Beijing, China, [4]Department of Hematology, Peking Union Medical College Hospital, Chinese Academy of Medical Sciences & Peking Union Medical College, Beijing, China

Introduction: Amyloid light-chain cardiac amyloidosis is a progressive infiltrative disease characterized by the deposition of amyloid fibrils in the cardiac tissue, which can cause serious atrioventricular block requiring pacemaker implantation. Left bundle branch pacing has emerged as an alternative method for delivering physiological pacing to achieve electrical synchrony of the left ventricle. However, left bundle branch pacing in patients with amyloid light-chain cardiac amyloidosis has not been studied in detail. Therefore, in this study, we present a case of left bundle branch pacing in a patient with amyloid light-chain cardiac amyloidosis.

Case summary: A 66-year-old male patient with amyloid light-chain cardiac amyloidosis presented with syncope for 1 month. Holter monitoring revealed intermittent third-degree atrioventricular block. Left bundle branch pacing was performed successfully. During the 1-year follow-up, it was observed that the left bundle branch capture threshold remained stable without any pacemaker-related complications or left ventricle systolic dysfunction, and there was no recurrence of syncope.

Conclusion: Left bundle branch pacing appears to be a safe and feasible option for patients with amyloid light-chain cardiac amyloidosis experiencing atrioventricular block.

KEYWORDS

cardiac amyloidosis, conduction system disease, atrioventricular block, left bundle branch pacing, case report

Abbreviations

AL-CA, amyloid light-chain cardiac amyloidosis; ATTR-CA, amyloid transthyretin cardiac amyloidosis; AVB, atrioventricular block; CMR: cardiac magnetic resonance; cTnI, cardiac troponin I; ECG, electrocardiogram; EHRA, European Heart Rhythm Association; FLC ratio, ratio of serum kappa:lambda free light chain; FLC-diff, difference between involved and uninvolved free light chains; LAFB, left anterior fascicular block; LBBB, left bundle branch block; LBBP, left bundle branch pacing; LVEF, left ventricular ejection fraction; NT-proBNP, N-terminal pro-B-type natriuretic peptide; RBBB, right bundle branch block; SND, sinus node dysfunction; VGPR, very good partial response; V6RWPT, V6 R-wave peak time.

Introduction

Amyloid light-chain cardiac amyloidosis (AL-CA) is a progressive infiltrative disease characterized by the extracellular deposition of misfolded proteins in the cardiac tissue (1, 2). In addition to the most common manifestation of heart failure with preserved ejection fraction, various tachy- and bradyarrhythmias and conduction system diseases, such as atrial fibrillation, ventricular tachycardia, sinus node dysfunction (SND), atrioventricular block (AVB), and bundle branch block (3, 4), can be seen in AL-CA patients. A pacemaker should be implanted to correct serious SND and AVB (5). Pacemaker implantation is a common intervention among patients with cardiac amyloidosis (6). Conventional right ventricular apex pacing may result in left ventricular dysfunctions because of electrical dyssynchronization (7–9). Conduction system pacing, including left bundle branch pacing (LBBP), has been persuasively adopted in clinical practice to achieve electrical and mechanical synchrony of the left ventricle (10, 11). Nevertheless, there is limited evidence regarding the feasibility and safety of LBBP in AL-CA patients and whether the deposition of amyloid fibrils in cardiac tissue might cause pacemaker-related complications, such as an increase in the capture threshold leading to a loss of conduction system capture or ventricular undersensing, remains largely unknown. In the present study, we report a case of LBBP application in an AL-CA patient.

Case presentation

A 66-year-old man presented to our hospital on 13 May 2022 with recurrent syncope for 1 month. He was diagnosed with AL-CA 16 months previously, on 4 January 2021, when he presented with dyspnea on exertion. His blood pressure was recorded at 85/55 mmHg, and a physical examination revealed skin bruising and macroglossia. There was no evidence of polyneuropathy, dysautonomia, or carpal tunnel syndrome. Serum and urine protein electrophoresis with immunofixation revealed a positive result for monoclonal light-chain kappa, and the ratio of serum kappa:lambda free light chain (FLC ratio) was 79.46 (serum free light-chain kappa: 530.00 mg/L, and serum free light-chain lambda: 6.67 mg/L). The difference between involved and uninvolved free light chains (FLC-diff) was 52.33 mg/dl. The presence of amyloid deposits was confirmed by Congo red staining in the bone marrow biopsy tissue. Echocardiography revealed symmetry hypertrophy and diastolic dysfunction of the left ventricle (interventricular septum thickness: 12 mm, posterior wall of left ventricle thickness: 12 mm, left ventricular end-diastolic diameter: 42 mm, e′: 6.1 cm/s, and E/e′: 15.6) without pericardial effusion or aortic stenosis, and the left ventricular ejection fraction (LVEF) was 57%. Cardiac magnetic resonance (CMR) imaging indicated diffuse late gadolinium enhancement in the subendocardial regions and the involvement of the bilateral atrium, bilateral ventricle, and interventricular septum. Holter monitoring revealed an intermittent sinus pause and AVB, suggesting SND and conduction disease (Figure 1A). Per the result of the bone marrow biopsy, the presence of monoclonal light chains, and an abnormal FLC ratio, the diagnosis of light-chain amyloidosis was made. The confirmation of cardiac amyloidosis was based on the unexplained left ventricular thickness ≥12 mm and the diffuse late gadolinium enhancement in CMR (2). Based on the results of FLC-diff, cardiac troponin I (cTnI), and N-terminal pro-B-type natriuretic peptide (NT-proBNP) (FLC-diff: 52.33 mg/dl, cTnI: 0.04 μg/L, NT-proBNP: 1,021 pg/ml), the patient was classified as Mayo Stage Ⅱ (12), and BCD protocol chemotherapy, which included bortezomib, cyclophosphamide, and dexamethasone, was initiated on 8 January 2021.

After undergoing the ninth cycle of chemotherapy in September 2021, the patient achieved a very good partial response (VGPR) at the hematologic level, with a significant reduction in FLC-diff and FLC ratio from 52.33 to 1.55 mg/dl and from 79.46 to 2.24, respectively (13). In addition, cTnI and NT-proBNP decreased from 0.04 to <0.017 μg/L and from 1,021 to 541 pg/ml, respectively. Dyspnea was also relieved. Chemotherapy was suspended by his hematologist.

On 6 April 2022, the patient experienced his first syncope episode. Holter monitoring revealed an intermittent third-degree AVB with and without ventricular escapes (Figures 1B,C). During complete AVB, the heart rate was 38 bpm, and the morphology of ventricular escape exhibited a left bundle branch block (LBBB) pattern (QRS duration: 132 ms), indicating right bundle branch origination (Figure 1B). However, during atrioventricular 1:1 conduction, the PR interval was 220 ms, and the morphology of the QRS complex exhibited a right bundle branch block (RBBB) pattern, indicating conduction through the left bundle branch (Figure 1D). The results of repeated laboratory tests of FLC-diff showed stability without amyloidosis relapse, and the echocardiography results were similar to those of the previous one. On 13 May 2022, the patient was admitted to our hospital for further therapy. Because of the new-onset syncope and the worsening of atrioventricular conduction without reversible etiologies, a permanent dual-chamber pacemaker was planned to be implanted, and to achieve electrical and mechanical synchrony, an LBBP was attempted. Before the implantation procedure, the patient's intrinsic electrocardiogram (ECG) showed a sinus rhythm with 1:1 atrioventricular conduction, and the QRS complex exhibited an RBBB pattern with a duration of 125 ms and without decreased voltage. Because the PR interval was 250 ms and the frontal plane axis showed a left deviation of −43°, consistent with a left anterior fascicular block (LAFB), a diagnosis of first-degree AVB and LAFB was confirmed, and supraventricular excitation was presumed to be conducted through the left posterior fascicle (Figure 2A).

The LBBP procedure was performed as previously described (14). The pacing lead (Model 3830; SelectSecure, Medtronic Inc., Minneapolis, MN, USA) was supported by the delivery sheath (C315His; Medtronic Inc.) via the left axillary vein. The paced ECG and the intracardiac electrogram were collected using an ECG recording system (LEAD-7000 C EP Recording System, Jinjiang Electronic Medical Device Technology Co., Ltd., Sichuan, China). The delivery sheath was advanced across the tricuspid valve summit in the right anterior oblique (RAO) view at 30° and was further advanced to approximately 20 mm toward the right ventricular apex. A counterclockwise torque was applied so that the sheath could reach the right ventricular base to the mid-

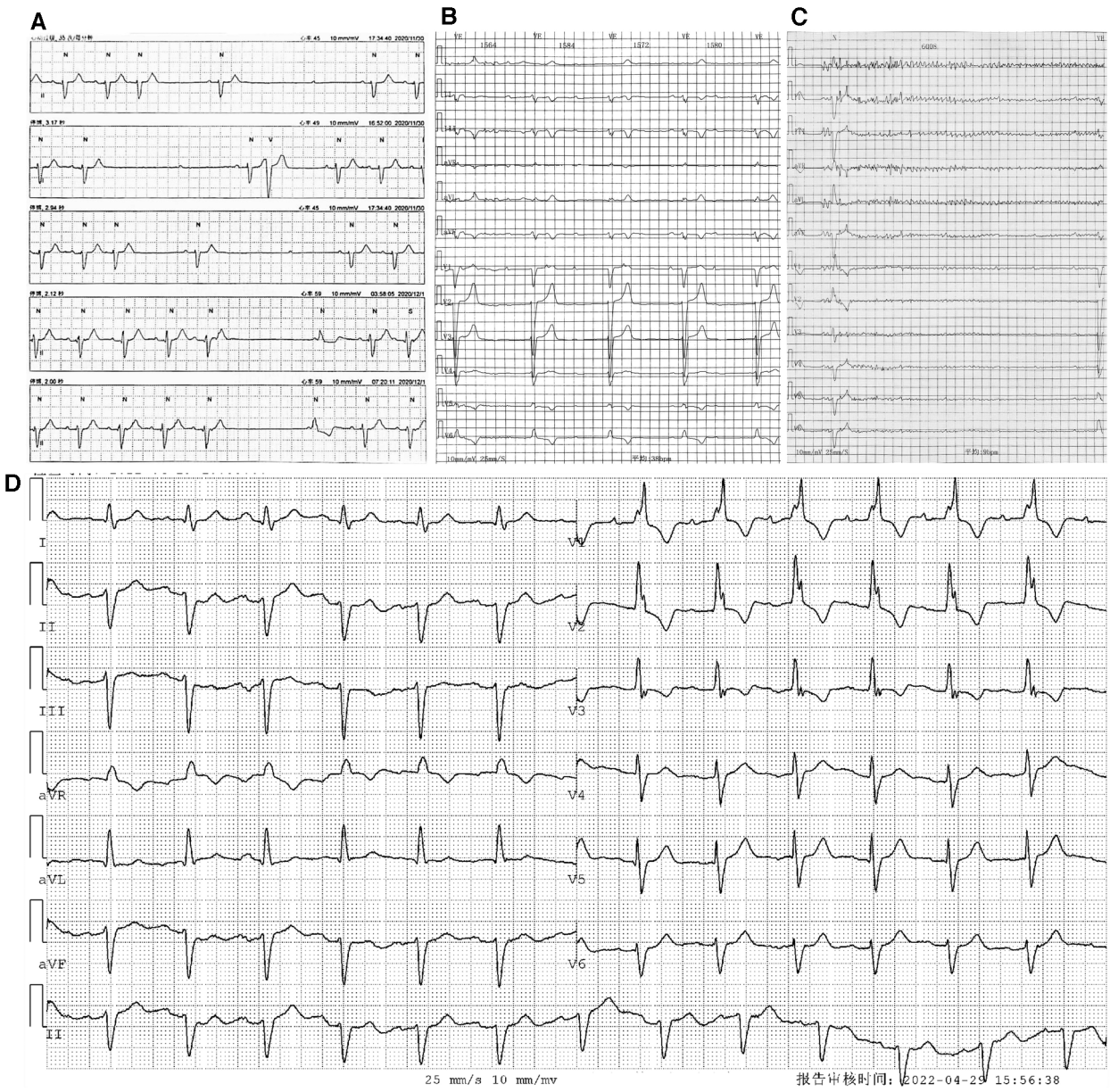

FIGURE 1
Holter monitoring of the patient. Holter monitoring in December 2020 (**A**) revealed an intermittent sinus pause and AVB. Holter monitoring after the first syncope episode in April 2022 (**B**,**C**) indicated an intermittent third-degree AVB with (**B**) and without (**C**) ventricular escapes. ECG without third-degree AVB (**D**) showed first-degree AVB, and the morphology of the QRS complex showed an RBBB pattern.

septum. The initial pacing site was the right ventricular septum. The QRS morphology in the pacing site showed a "w" pattern with a notch at the nadir of the QRS in lead V1 (Figure 2B). Then, the lead was screwed into the interventricular septum until a paced QRS (voltage output at 5 V @ 0.4 ms in the unipolar mode) of RBBB morphology with a terminal R-wave in lead V1 was obtained (Figure 2C). There was little difficulty in screwing the Model 3830 lead into the deep septum. The left bundle branch potential could be recorded when the lead was deeply screwed into the subendocardial area on the left side of the interventricular septum (Figure 2D). A threshold test was performed, and it showed that the transitions in the QRS morphology were quite subtle when pacing from high voltage (5 V @ 0.4 ms) to low voltage (0.5 V @ 0.4 ms); therefore, the test was non-conclusive. When pacing at high and low output voltages, consistent values of the stimulus to V6 R-wave peak time (V6RWPT) were recorded, as shown in Figures 2E,F. To confirm the left bundle branch capture, the LBBP ECG criteria were evaluated. The V6–V1 inter-peak interval was 41.67 ms (Figure 2F), and the stimulus to V6RWPT was 78.28 ms (Figure 2F). Because the left bundle branch potential to V6RWPT in intrinsic rhythm was 58.33 ms (Figure 2D), the difference between the potential to V6RWPT and the stimulus to V6RWPT was 19.95 ms. Because V6RWPT <80 ms fulfilled the

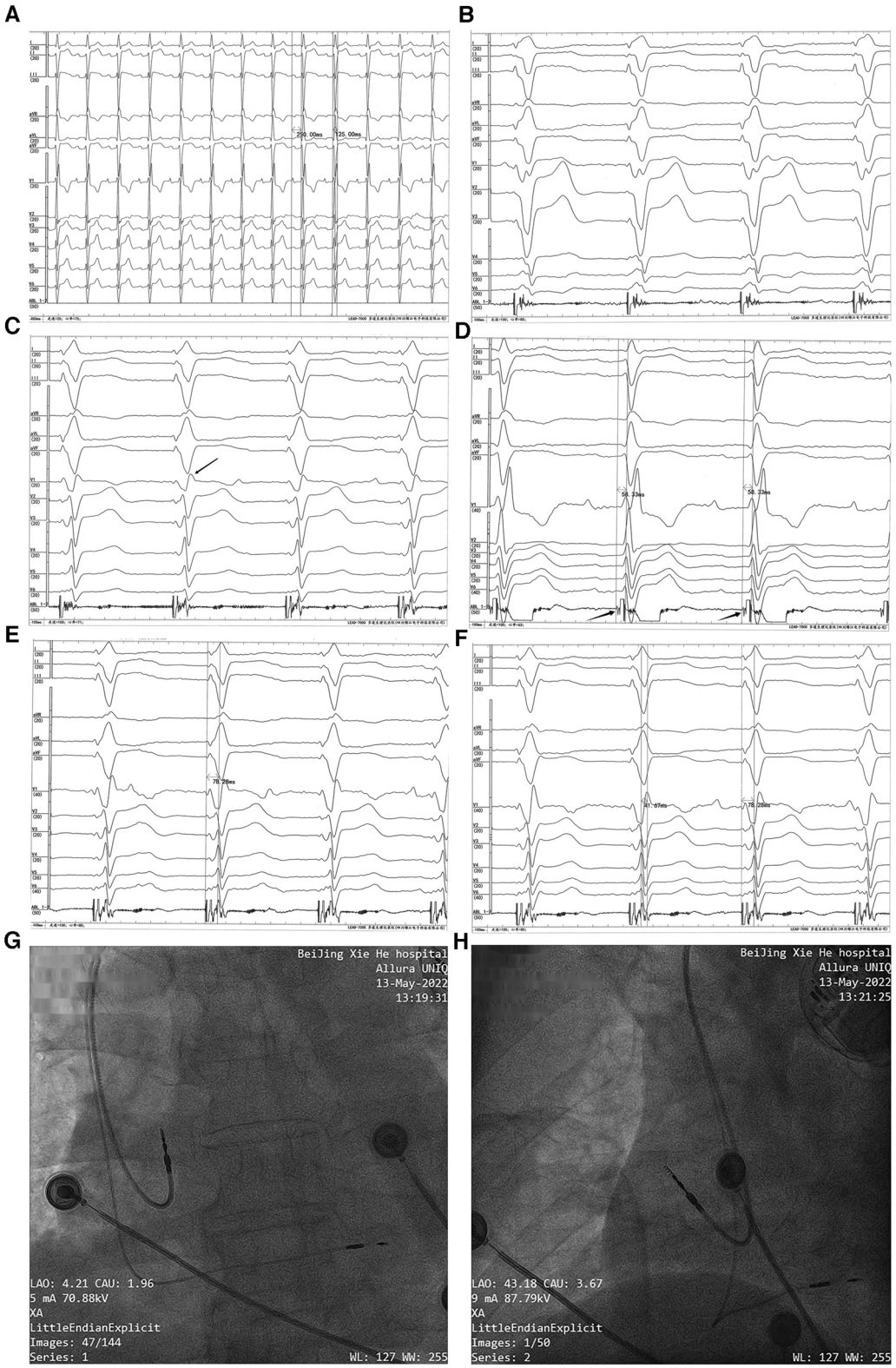

FIGURE 2
Permanent dual-chamber pacemaker implantation. Before the implantation procedure, the intrinsic ECG (**A**) showed first-degree AVB, RBBB, and LAFB (a sweep speed of 25 mm/s). Paced QRS morphology in the right ventricular septum (**B**) showed a "w" pattern with a notch at the nadir of the QRS in lead V1 (a sweep speed of 100 mm/s). With the lead screwed into the interventricular septum, the terminal R-wave of the paced QRS appeared in lead V1 (marked with a black arrow) (**C**) (a sweep speed of 100 mm/s). The left bundle branch potential (marked with a black arrow) was recorded from a Model 3830 lead tip (**D**) (unipolar, a sweep speed of 100 mm/s), and the left bundle branch potential to V6RWPT in the intrinsic rhythm was 58.33 ms. (**E**) Pacing at high voltage (5 V @ 0.4 ms) with the stimulus to V6RWPT of 78.28 ms (a sweep speed of 100 mm/s). (**F**) Pacing at low voltage (0.5 V @ 0.4 ms) with the stimulus to V6RWPT of 78.28 ms and a V6–V1 inter-peak interval of 41.67 ms (a sweep speed of 100 mm/s). (**G**,**H**) Positions of the pacing leads.

European Heart Rhythm Association (EHRA) criteria (14), the LBBP of our patient was confirmed. The threshold of left bundle branch capture measured in the unipolar mode was 0.5 V @ 0.4 ms, the R-wave amplitude measured in the bipolar mode was 21.0 mV, and the ventricular lead impedance was 774 Ω. The threshold of right atrium capture was 0.8 V @ 0.4 ms, the P-wave amplitude was 1.6 mV, and the atrial lead impedance was 922 Ω. The paced QRS duration was 106 ms. The pacing leads were connected to a generator (X3DR01 Astra S DR, Medtronic Inc.). The positions of the leads are shown in Figures 2G,H.

After pacemaker implantation, there was no occurrence of recurrent syncope. At the patient's 3-month follow-up visit, the pacing parameters were stable. The unipolar left bundle branch capture threshold was recorded at 0.75 V @ 0.4 ms, the unipolar pacing impedance was measured at 570 Ω, and the sensed bipolar R-wave amplitude was 20.0 mV. The right atrium capture threshold was recorded at 0.75 V @ 0.4 ms, the pacing impedance was measured at 323 Ω, and the sensed P-wave amplitude was 1.1 mV. At the 1-year follow-up visit, the patient's intrinsic rhythm was a sinus rhythm with first-degree AVB (Figure 3A); therefore, the left bundle branch capture threshold was measured by mandatory ventricular pacing, and the value was 0.75 V @ 0.4 ms. The sensed R-wave amplitude and pacing impedance were 20.0 mV and 532 Ω, respectively. The right atrium capture threshold was recorded at 1.0 V @ 0.4 ms, the pacing impedance was measured at 323 Ω, and the sensed P-wave amplitude was 0.8 mV. The stimulus to V6RWPT (78 ms) was stable at high (5.0 V @ 0.4 ms) and low (1.0 V @ 0.4 ms) output voltages when the left bundle branch was captured (Figures 3B,C). The atrial and ventricular pacing rates were 37.4% and 7.7%, respectively. In addition, no pacemaker-related complications, such as pocket infection, hematoma, lead dislodgement, and rupture, were reported. There was no reported occurrence of syncope, and the patient did not experience dyspnea on exertion.

The trends in the right atrial lead and LBBP lead threshold, sensing, and impedance are shown in Figure 4. The timeline of the present case is shown in Supplementary Table 1.

Discussion

Conduction system diseases are not uncommon in AL-CA patients. In a study of 157 AL-CA patients, first-degree AVB, RBBB, LBBB, and LAFB were present in 18%, 19%, 4%, and 29% of the patients, respectively (15). Recently, a large cohort study showed that 8.9% of the patients with cardiac amyloidosis received a pacemaker because of SND or AVB within 3 years after diagnosis (6). The pathogenesis of conduction system diseases in cardiac amyloidosis is multifactorial, including amyloid deposition causing a disruption of the transmission of electrical impulses along the conduction fibers and the cytotoxicity of amyloid precursor proteins (3).

In the general population with right ventricular pacing, a significant decline in LVEF was noted, and the incidence of pacing-induced cardiomyopathy was also significantly higher (16). Among patients with amyloid transthyretin cardiac amyloidosis (ATTR-CA) who have implantable devices, a higher conventional right ventricular pacing burden is associated with deleterious remodeling and congestive heart failure (9). Conduction system pacing techniques, such as His bundle pacing and LBBP, have been demonstrated to be superior to conventional right ventricular apex pacing because they achieve electrical synchrony of the left ventricle (7, 8). However, evidence of LBBP in infiltrative cardiomyopathy mainly caused by amyloidosis is scarce.

In the present case, LBBP was successfully used in an AL-CA patient with third-degree AVB. During the patient's 3-month and 1-year follow-up visits, no occurrence of pacemaker-related complication was reported, and the left bundle branch capture threshold, R-wave amplitude, and ventricular lead impedance remained stable. Although the extracellular deposition of amyloid fibrils in the myocardium and conduction system might potentially cause an increase in the ventricular pacing capture threshold, and the frequently encountered decreased QRS voltage might cause device undersensing, a previous retrospective observational study of 34 patients with AL- or ATTR-CA and a cardiac implantable electronic device showed that the mean right

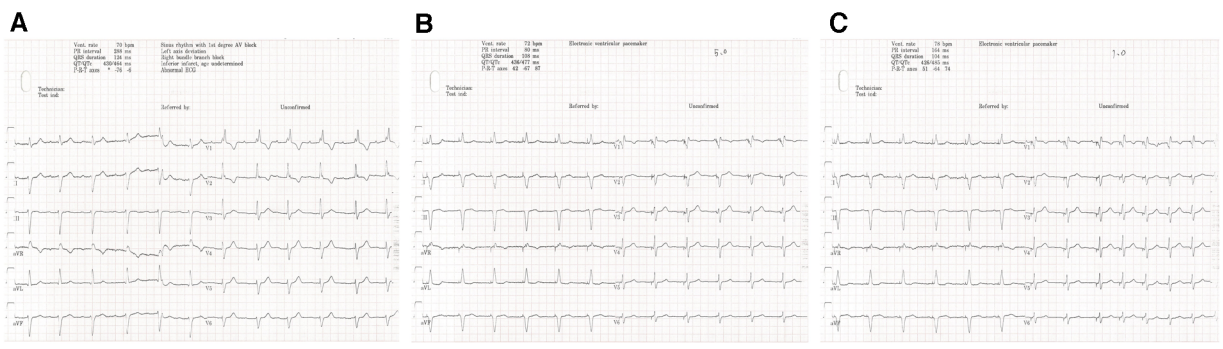

FIGURE 3
One-year follow-up visit. The intrinsic rhythm (A) was a sinus rhythm with first-degree AVB. The stimulus to V6RWPT (78 ms) was stable at high (5.0 V @ 0.4 ms) (B) and low (1.0 V @ 0.4 ms) (C) output voltages when the left bundle branch was captured.

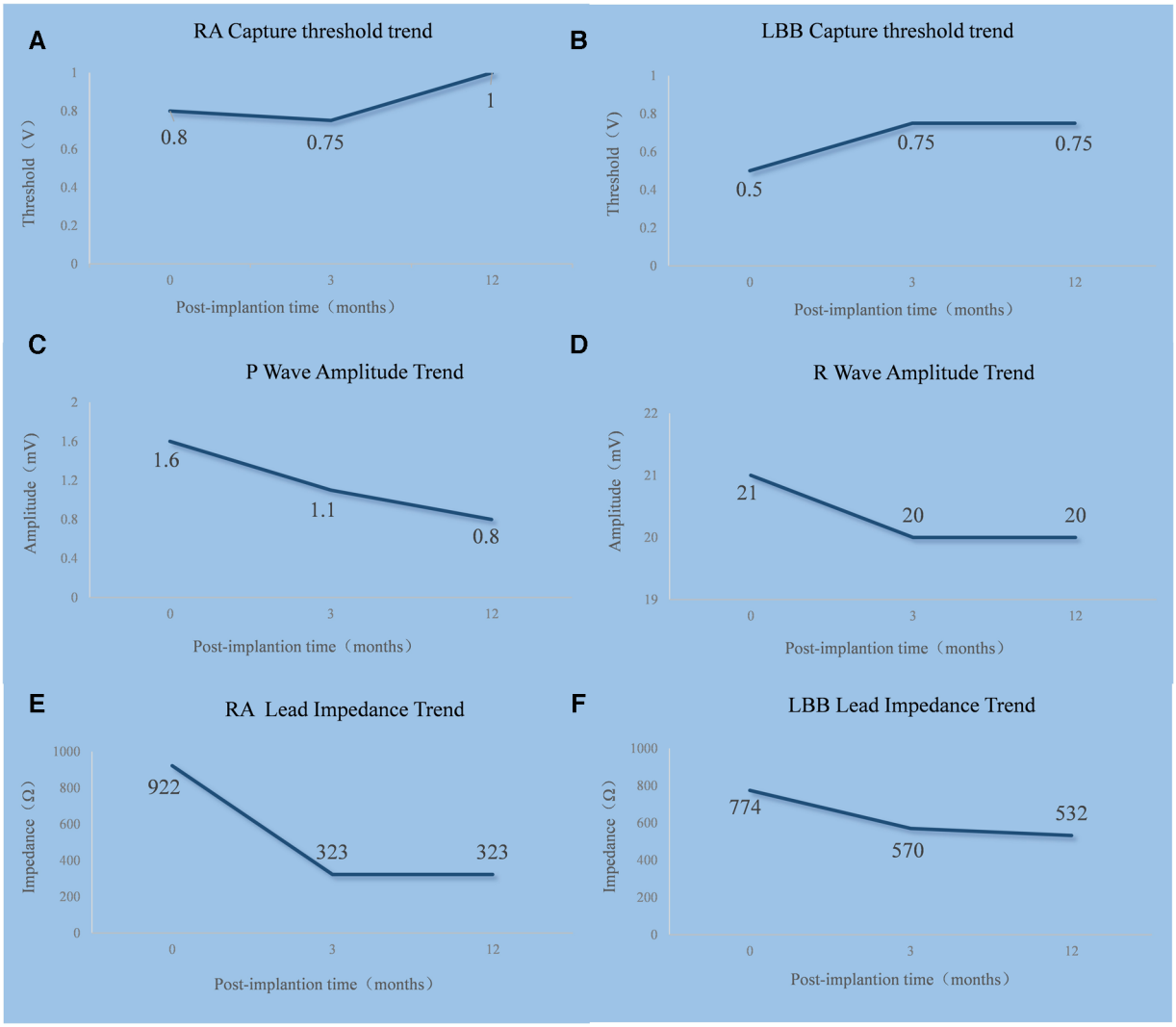

FIGURE 4
Trends in the RA lead (A,C,E) and LBBP lead (B,D,F) threshold, sensing, and impedance. RA, right atrium; LBB, left bundle branch.

ventricular capture threshold (0.8 ± 0.1 V at 3 years) and the mean right ventricular lead impedance (418 ± 28 Ω at 3 years) remained stable over a mean follow-up of 3.1 ± 4.0 years, but the mean right ventricular sensing was 10.6 ± 0.8 mV at 1 year, which decreased to 6.7 ± 1.2 mV at 3 years without resulting in device malfunction (17). Taha et al. reported a case of an ATTR-CA patient with LBBP who demonstrated a significant alleviation of heart failure symptoms and improvement in exercise capacity during 3- and 6-month follow-up visits with stable pacing thresholds (18). The lead parameters of our patient at follow-up were consistent with those of the previous studies (17, 18). Recently, Chinh et al. reported a retrospective cohort including 23 patients with ATTR-CA or AL-CA who underwent left bundle branch area pacing for bradycardia or cardiac resynchronization therapy. The sensed R-wave amplitude and pacing threshold were stable during a mean follow-up time of 7.7 months (19). Using stricter criteria of LBBP in our patient, we also found stable pacing parameters during follow-up visits, which was consistent with a study by Chinh et al. We speculated that the conduction capacity of the left bundle branch might be partially preserved in some AL-CA patients and that the left bundle branch could be captured with an acceptable threshold. LBBP appears to be a promising pacing modality in AL-CA patients requiring a pacemaker. However, further studies are needed to determine the long-term feasibility and safety of applying LBBP in AL-CA patients and to determine its effect on left ventricular function.

Conclusion

AL-CA with serious AVB might be a potential candidate for the application of LBBP. Further studies are needed to determine the long-term feasibility and safety of the application of LBBP in patients with AL-CA and to ascertain its effect on left ventricular function.

Limitations

There are several limitations in our study. First, an invasive electrophysiological study was not performed and we could not confirm the level of conduction block. Second, the baseline LVEF of the patient was normal and the ventricular pacing percentage was quite low; therefore, the present findings cannot be generalized to patients with left ventricular systolic dysfunction and high-burden ventricular pacing. Finally, syncope and a worsening of AVB occurred after light-chain amyloidosis recovery; therefore, other factors contributing to the development of AVB could not be completely excluded. However, only 25%–50% of all patients treated with chemotherapy achieve an organ response (20). The present case indicated that atrioventricular conduction worsening could develop even in patients with hematological remission after chemotherapy.

Data availability statement

The original contributions presented in the study are included in the article/**Supplementary Material**, and further inquiries can be directed to the corresponding authors.

Ethics statement

The studies involving humans were approved by the Ethics Committee of Peking Union Medical College Hospital, Chinese Academy of Medical Sciences; Peking Union Medical College, Beijing, China. The studies were conducted in accordance with the local legislation and institutional requirements. The participants provided their written informed consent to participate in this study. Written informed consent was obtained from the individual(s) for the publication of any potentially identifiable images or data included in this article.

Author contributions

JY: Data curation, Investigation, Writing – original draft. FK: Investigation, Software, Writing – original draft. PG: Data curation, Methodology, Writing – review & editing. TC: Conceptualization, Supervision, Writing – review & editing. YL: Conceptualization, Supervision, Writing – review & editing. ZC: Conceptualization, Data curation, Writing – review & editing. HD: Conceptualization, Data curation, Writing – review & editing. JLa: Conceptualization, Data curation, Writing – review & editing. LZ: Conceptualization, Data curation, Writing – review & editing. JF: Conceptualization, Data curation, Writing – review & editing. JW: Data curation, Writing – review & editing. XQ: Data curation, Writing – review & editing. KS: Data curation, Writing – review & editing. JLi: Data curation, Methodology, Writing – review & editing. QF: Conceptualization, Supervision, Writing – review & editing. DY: Conceptualization, Data curation, Funding acquisition, Investigation, Methodology, Project administration, Supervision, Writing – review & editing. KC: Conceptualization, Data curation, Methodology, Project administration, Resources, Supervision, Writing – review & editing.

Funding

The authors declare that financial support was received for the research, authorship, and/or publication of this article.

This study was supported by National High Level Hospital Clinical Research Funding (2022-PUMCH-A-183), China.

Acknowledgments

We would like to thank the nurses of the cardiac catheterization laboratory and the technicians responsible for pacemaker follow-up, who contributed to the diagnosis, therapy, and decision-making of the present case.

Conflict of interest

The authors declare that the research was conducted in the absence of any commercial or financial relationships that could be construed as a potential conflict of interest.

Publisher's note

Supplementary material

The Supplementary Material for this article can be found online at: https://www.frontiersin.org/articles/10.3389/fcvm.2023.1333484/full#supplementary-material

References

1. Ashutosh DW, Julian DG, Philip NH. Systemic amyloidosis. *Lancet*. (2016) 387:2641–54. doi: 10.1016/S0140-6736(15)01274-X

2. Pablo G-P, Claudio R, Yehuda A, Michael A, Cristina B, Antonio B, et al. Diagnosis and treatment of cardiac amyloidosis: a position statement of the ESC

working group on myocardial and pericardial diseases. *Eur Heart J*. (2021) 42:1554–68. doi: 10.1093/eurheartj/ehab072

3. Jack H, Wael J, Matthew M, Brett S, Mazen H, Patrick C, et al. Electrophysiological manifestations of cardiac amyloidosis. *JACC CardioOncol*. (2021) 3:506–15. doi: 10.1016/j.jaccao.2021.07.010

4. Rabah A, Derin T, Omar S, Frederick R. Conduction abnormalities and role of cardiac pacing in cardiac amyloidosis: a systematic review. *Pacing Clin Electrophysiol*. (2021) 44:2092–9. doi: 10.1111/pace.14375

5. Michael G, Jens CN, Mads BK, Yoav M, Angelo A, Israel MB, et al. 2021 ESC guidelines on cardiac pacing and cardiac resynchronization therapy. *Eur Heart J*. (2021) 42:3427–520. doi: 10.1093/eurheartj/ehab364

6. Aldostefano P, Maddalena R, Francesco C, Marco C, Beatrice M, Alberto C, et al. Incidence and risk factors for pacemaker implantation in light-chain and transthyretin cardiac amyloidosis. *Eur J Heart Fail*. (2022) 24:1227–36. doi: 10.1002/ejhf.2533

7. David JS, Merritt HR, Freddy D-CM, Siva KM, Naseer N, Pamela NP. Impact of physiologic pacing versus right ventricular pacing among patients with left ventricular ejection fraction greater than 35%: a systematic review for the 2018 ACC/AHA/HRS guideline on the evaluation and management of patients with bradycardia and cardiac conduction delay: a report of the American College of Cardiology/American Heart Association Task Force on Clinical Practice Guidelines and the Heart Rhythm Society. *Circulation*. (2019) 140:e483–503. doi: 10.1161/CIR.0000000000000629

8. Parikshit SS, Neil RP, Venkatesh R, Dipen VZ, Sujitraj D, Varun G, et al. Clinical outcomes of left bundle branch area pacing compared to right ventricular pacing: results from the Geisinger-Rush conduction system pacing registry. *Heart Rhythm*. (2022) 19:3–11. doi: 10.1016/j.hrthm.2021.08.033

9. Eoin D, Oussama MW, Walid IS, Bryan B, Mazen H, Michael M, et al. Cardiac devices in patients with transthyretin amyloidosis: impact on functional class, left ventricular function, mitral regurgitation, and mortality. *J Cardiovasc Electrophysiol*. (2019) 30:2427–32. doi: 10.1111/jce.14180

10. Hu YR, Li H, Gu M, Hua W, Niu HX, Zhang NX, et al. Comparison between His-bundle pacing and left bundle branch pacing in patients with atrioventricular block. *J Interv Card Electrophysiol*. (2021) 62:63–73. doi: 10.1007/s10840-020-00869-w

11. Alexandre RP, Atul V, Jeffrey K, Paula SS, Enes EG, Ajay P, et al. Left bundle branch area pacing in patients with atrioventricular conduction disease: a prospective multicenter study. *Heart Rhythm*. (2022) 19:1484–90. doi: 10.1016/j.hrthm.2022.04.033

12. Angela D, Morie AG, Robert AK, Martha QL, Mary FB, Terry MT, et al. Serum cardiac troponins and N-terminal pro-brain natriuretic peptide: a staging system for primary systemic amyloidosis. *J Clin Oncol*. (2004) 22:3751–7. doi: 10.1200/JCO.2004.03.029

13. Giovanni P, Angela D, Morie AG, Shaji K, Ashutosh W, Philip NH, et al. New criteria for response to treatment in immunoglobulin light chain amyloidosis based on free light chain measurement and cardiac biomarkers: impact on survival outcomes. *J Clin Oncol*. (2012) 30:4541–9. doi: 10.1200/JCO.2011.37.7614

14. Haran B, Marek J, Óscar C, Karol Č, Jan DP, Huang WJ, et al. EHRA clinical consensus statement on conduction system pacing implantation: endorsed by the Asia Pacific Heart Rhythm Society (APHRS), Canadian Heart Rhythm Society (CHRS), and Latin American Heart Rhythm Society (LAHRS). *Europace*. (2023) 25:1208–36. doi: 10.1093/europace/euad043

15. Claudio R, Giampaolo M, Candida CQ, Letizia R, Simone L, Ornella L, et al. Systemic cardiac amyloidoses: disease profiles and clinical courses of the 3 main types. *Circulation*. (2009) 120:1203–12. doi: 10.1161/CIRCULATIONAHA.108.843334

16. Pugazhendhi V, Angela N, Faiz AS, Mohamed A, Parikshit SS, Jess WO, et al. Permanent His-bundle pacing: long-term lead performance and clinical outcomes. *Heart Rhythm*. (2018) 15:696–702. doi: 10.1016/j.hrthm.2017.12.022

17. Michael RR, Rahul SL, Eric BM, Amanda CC, Ravi K, Sean DP, et al. Cardiac implantable electronic devices: a window into the evolution of conduction disease in cardiac amyloidosis. *JACC Clin Electrophysiol*. (2020) 6:1144–54. doi: 10.1016/j.jacep.2020.04.020

18. Taha A, Samra HL, Hassan L, Jae L, Mazen H, Roy C. Left bundle branch pacing in transthyretin cardiac amyloidosis and alternating bundle branch block. *JACC Case Rep*. (2020) 2:1004–8. doi: 10.1016/j.jaccas.2020.04.040

19. Chinh P-T, Darwin V-U, Melodie S-D, Yuleisy DRR, Cristina A-A, Eusebio AG-I, et al. Feasibility and safety of left bundle branch area pacing in cardiac amyloidosis. A single center experience. *Pacing Clin Electrophysiol*. (in press). doi: 10.1111/pace.14894 [Epub ahead of print].

20. Gregory PK, Angela D, Morie AG, Martha QL, Francis KB, Suzanne RH, et al. Kinetics of organ response and survival following normalization of the serum free light chain ratio in AL amyloidosis. *Am J Hematol*. (2015) 90:181–6. doi: 10.1002/ajh.23898

frontiers | Frontiers in Cardiovascular Medicine

TYPE Case Report
PUBLISHED 18 January 2024
DOI 10.3389/fcvm.2023.1309929

OPEN ACCESS

EDITED BY
Reto Asmis,
Wake Forest University, United States

REVIEWED BY
Sanjeev Bhattacharyya,
Barts Heart Centre, United Kingdom
Lukas Stolz,
Ludwig Maximilian University of Munich, Germany
Eustaquio Maria Onorato,
Istituto di Ricovero e Cura a Carattere Scientifico (IRCCS), Italy

*CORRESPONDENCE
Michael Cronin
michaelcronin@rcsi.ie

RECEIVED 08 October 2023
ACCEPTED 18 December 2023
PUBLISHED 18 January 2024

CITATION
Cronin M and McAdam B (2024) Case Report: Carcinoid heart disease with severe tricuspid regurgitation and concomitant patent foramen ovale causing severe hypoxia.
Front. Cardiovasc. Med. 10:1309929.
doi: 10.3389/fcvm.2023.1309929

Case Report: Carcinoid heart disease with severe tricuspid regurgitation and concomitant patent foramen ovale causing severe hypoxia

Michael Cronin* and Brendan McAdam

Department of Cardiology, Beaumont Hospital, Dublin, Republic of Ireland

This case report demonstrates a unique case of managing complex concomitant structural cardiac issues using transcatheter techniques in a frail patient. The primary regurgitant lesion in this case caused significant right to left shunting with severely debilitating hypoxaemia for the patient, requiring high volumes of ambulatory oxygen to compensate. We would like to highlight the role of multi-modality cardiac imaging demonstrated in this case, as well as the limited surgical data and poor outcomes in advanced disease with higher peri-operative complications. Finally, it should be noted that percutaneous correction of structural lesions may provide palliative relief but carries an uncertain risk of recurrence.

KEYWORDS

carcinoid heart disease, tricuspid regurgitation, patent foramen ovale, transcatheter, echocardiography

Introduction

Carcinoid heart disease (CHD) is a recognised rare cause of right-sided valvular heart disease (VHD) and remains a major cause of morbidity and mortality in the cardio-oncology population. This case demonstrates CHD complicated by tricuspid regurgitation (TR) causing right to left heart shunting via a stretched patent foramen ovale (PFO), with marked hypoxia and severe heart failure. The tricuspid valve (TV) has a complex anatomy that is essential to understanding the pathophysiology of TR in CHD (1), and multi-modal imaging is required in its evaluation, including transthoracic echocardiography (TTE), transoesophageal echocardiography (TOE), cardiac computed tomography (CT), and invasive catheterisation with fluoroscopy, as demonstrated in this clinical case. There remains a limited specific advice regarding the management of VHD in CHD, with poor surgical outcomes, low procedural numbers, and high anaesthetic risk in this frail population (2, 3). Our case demonstrates the narrow clinical window regarding intervention, when the TR is severe but the right ventricular (RV) function is intact. Secondary to the associated frailty and deconditioning within this population, transcatheter interventions are growing in availability, yet remain very much in their infancy with a lack of long-term data (4).

Case description

Patient information

A 61-year-old male presented with a rectal mass during a primary care visit in 2021 and was then referred to the local surgical outpatient department (OPD). His past medical history was significant for varicose veins with previous radiofrequency ablation and avulsion. He was a retired bus driver and an ex-smoker with occasional alcohol use. A CT scan of the abdomen conducted in November 2021 showed a bulky rectal mass with liver and retroperitoneal involvement. The results of a liver biopsy showed a "well-differentiated neuroendocrine tumour," and consequently, the local Medical Oncology service initiated treatment with lanreotide. During the subsequent 12 months of follow-up, he reported recurrent pedal oedema and dyspnoea, and was found to have a systolic murmur leading to a referral to the cardiology OPD for assessment. By this stage, everolimus was prescribed in addition to his lanreotide due to persistent symptoms of facial flushing and diarrhoea.

Diagnostic assessment

A full timeline of events can be seen in Figure 1. A TTE in April 2022 showed normal biventricular size and systolic function, with mild/moderate aortic incompetence (AI) and moderate/severe central TR. At this moment, the colour flow Doppler examination indicated that the intra-atrial septum (IAS) was found to be intact.

In early October of the same year, he needed to be admitted to the hospital due to an increasing need for oral diuretic. He had significant bilateral pedal oedema, bilateral basal lung crackles on auscultation, and an oxygen (O_2) requirement of 12 L via nasal cannulae to maintain adequate saturations. He had obvious facial flushing and prominent neck veins.

His N-terminal pro-B type natriuretic peptide (NT-pro-BNP) was 582 pg/ml, haemoglobin 13.1 g/dl, creatinine 104 µmol/L, and cardiac troponin T 19 ng/L (<14). The lung parenchyma was clear on chest x-ray. The arterial blood gas (ABG) on 60% FiO_2 showed mild respiratory alkalosis with type 1 respiratory failure (pH 7.5, paO_2 9.3kPa, pCO_2 4.9kPA, HCO_3 29.1 mEq/L, lactate 1.7 mmol/L). Electrocardiogram showed sinus tachycardia with right axis deviation. Viral panel was negative for seasonal variants. The CT pulmonary angiogram did not show any pulmonary embolus, vascular shunt, or interstitial lung disease to explain the hypoxia.

The updated TTE showed a preserved left ventricular function with interval RV dilatation exhibiting slightly reduced systolic function in the presence of severe TR, and a dilated right atrium (RA) (Supplementary Video S1). Upon evaluation by the clinical cardiology service, there was a suspicion of shunting across the IAS, and the TR trace by Doppler envelope was deemed

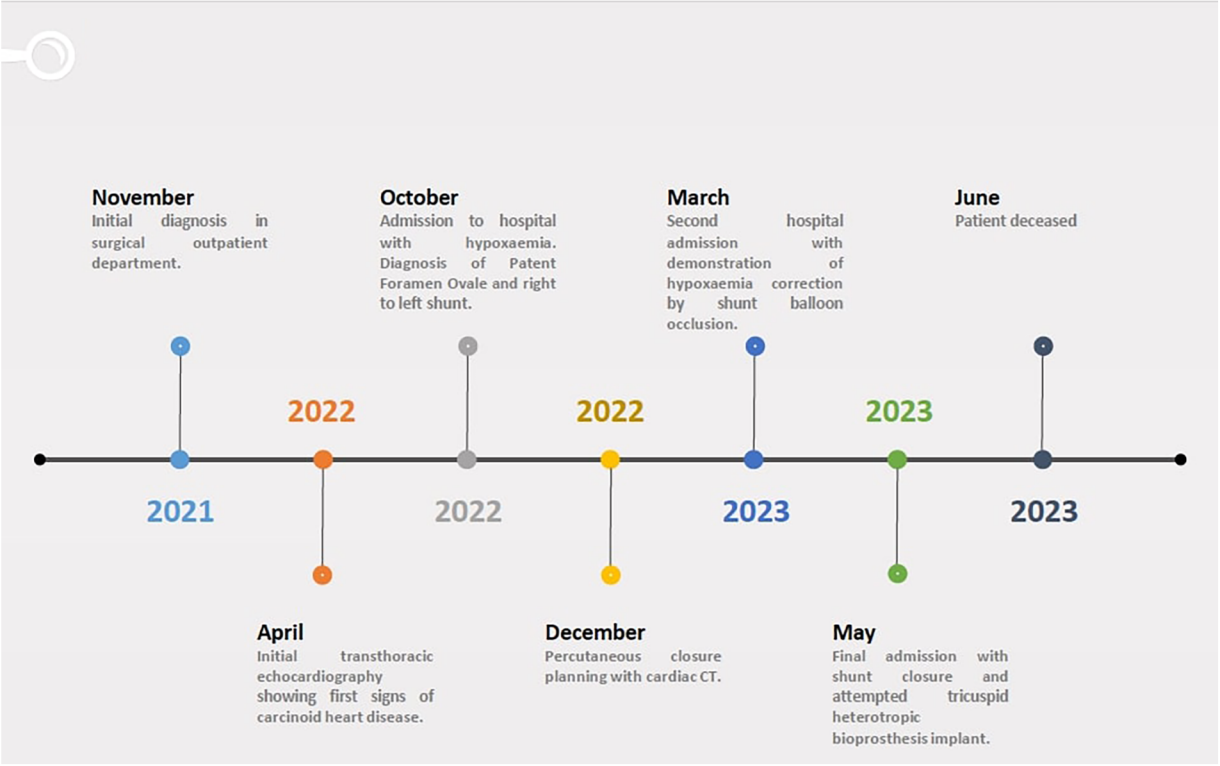

FIGURE 1
Timeline.

insufficiently accurate for quantifying pulmonary arterial pressure. The presence of a right-to-left shunt was confirmed using a bubble study with agitated saline (Supplementary Video S2). The presence of cardiac platypnea-orthodeoxia was confirmed using supine ABG (paO_2 7.4 kPa, SpO_2 90.3%) compared with standing ABG (paO_2 6.9 kPa, SpO_2 87.5%).

To further clarify the suspicion of an intra-cardiac shunt, a TOE was performed (Supplementary Video S1). This showed a mobile IAS with PFO by a strongly positive bubble study both with agitated saline and agitated gelofusin. The mitral valve (MV) exhibited mild/moderate regurgitation (vena contracta, 0.2 cm), and the trileaflet aortic valve (AV) was determined to exhibit moderate AI secondary to a coaptation defect and a small focal prolapse of the non-coronary cusp. Both of these valves demonstrated leaflet thickening suggestive of carcinoid, primarily believed to be secondary to the significant right to left shunt. Both right-sided valves showed severe regurgitation, with a dilated tricuspid annulus with leaflet thickening and malcoaptation.

With the information gathered thus far, it was elected to perform left (LHC) and right catheterisation (RHC). LHC showed largely patent coronary arteries, with a dominant right coronary artery, left ventricular end-diastolic pressure (EDP) of 8 mmHg, and no aortic stenosis on catheter pull back. RHC was performed via the right median cubital vein. It demonstrated normal pulmonary arterial pressures (22/1/7 mmHg), normal pulmonary capillary wedge pressure (mean 3 mmHg), but elevated right filling pressures (RA pressure peak 14/mean 9 mmHg) and V wave consistent with a known TR. RV EDP was elevated at 10 mmHg, with pulmonary vascular resistance of 1 Wood unit. The Qp:Qs ratio was calculated at 0.93, and the cardiac output (CO) was mildly reduced (CO 3.53l /min, cardiac index 2.21l /min by thermodilution). There was no significant saturation step-up amongst the venous blood gases collected (PA 49.9%, IVC 56.3%, mid RA 48.2%, high RA 51.9%, SVC 48.6%), with a resting radial arterial saturation of 87% at rest and dropping to 84% during exercise.

At this stage, the patient was discharged with a prescription for long-term O_2 therapy of 15 L O_2 via nasal prongs and enrolment in the outpatient palliative care services. He was maintained on bumetanide 1 mg BD and eplerenone 25 mg as a diuretic regimen at this stage. The case was presented at a surgical conference, and secondary to frailty, he was considered unsuitable for surgery, albeit the medical oncology team determining that he had a reasonable prognosis for his carcinoid syndrome. Consideration was given to a percutaneous PFO closure with a tricuspid valve intervention concomitantly given the risk of worsening heart failure (the heart team perceived that the right chambers were offloading pressure via the PFO, and occluding this shunt may abruptly halt this compensatory mechanism, leading to circulatory collapse). To this end, a cardiac CT was undertaken for percutaneous procedural planning. This demonstrated mildly enlarged right heart chambers with annular dilatation, but without annular or tricuspid leaflet calcification.

On review in the OPD 5 months later, his dyspnoea and pedal oedema had continued to worsen. He had been reviewed at the structural cardiology OPD and listed for a balloon occlusion of the PFO to assess RA pressures and O_2 saturations. It was felt that if the balloon occlusion improved the hypoxia, then an attempt at closure would be made if a heterotopic bioprosthesis was available.

Therapeutic intervention

Late in March 2023, he was readmitted with worsening pedal oedema and hypoxia, with pre-syncope and hypokalaemia from diuretic therapy. He was transferred for the purpose of performing balloon occlusion on his PFO. He underwent a procedure where a 10 Fr sheath was inserted into his right common femoral vein to occlude his PFO for 3 min. During this period, his radial arterial oxygen saturation improved from 90% pre-procedurally (on room air) to 100%, with no change in his RA pressures before (26/14 mmHg) vs. after (25/12 mmHg) the procedure. Since the procedure was scheduled for diagnostic purposes rather than therapeutic purposes, a permanent closure device, sized by cardiac CT, was not made available on the same day. ECG-gated CT on that day demonstrated a stretched PFO of 10.4 mm. It was thought at this stage that his PFO was now confirmed to be the primary cause of hypoxia, in the context of severe TR with a low cardiac output and right to left shunting and normal PA pressures. Following optimisation of his fluid status, he was once again allowed to go home in order to provide time for procedural preparation.

After 2 months, he was readmitted secondary to carcinoid crisis, requiring coronary care unit (CCU) care with octreotide infusion. He remained markedly hypoxaemic despite receiving 100% FiO_2 using high flow nasal cannulae. His medical condition was so severe that he needed the national inter-intensive care unit (ICU) transfer service to be transferred from his primary centre CCU to the structural intervention referral centre CCU for inpatient PFO closure and tricuspid valve heterotopic bioprosthesis insertion.

PFO closure was undertaken first, with bilateral femoral venous access, using intra-cardiac echocardiography for anatomo-morphological guidance. The PFO was crossed with a multipurpose catheter before the delivery of sheath for device deployment. Initial Amplatzer Talisman PFO 18 mm/18 mm Occluder (Model number 9-PFO-1818) was unable to oppose at the right atrial side, so a 30 mm/25 mm Amplatzer Talisman PFO Occluder (Model number 9-PFO-3025) was selected, with good opposition on both atrial sides (Supplementary Video S3). Occlusion was confirmed by venogram via pigtail in the hepatic veins near IVC/RA junction with no dye across the IAS (Supplementary Video S3). The O_2 saturations immediately normalised, with a reduction in supplemental O_2 requirements noted.

The procedure progressed to the deployment of the heterotopic bioprosthesis ("TricValve"). Attempts were made to advance the 27 Fr catheter for the deployment of the IVC valve against marked resistance. Pre-dilatation of the veins was attempted, without progression. The delivery sheath was removed and noted to be kinked and damaged at the tip. Due to operator concern, digital subtraction angiography was performed and confirmed

extravasation of contrast medium from the external iliac vein (still can be observed in Supplementary Video S3). This was occluded with an 8 mm balloon; however, even at higher atmospheric pressures, this failed to contain the extravasation. Therefore, a 10 mm Bentley covered stent was deployed at 6 atm with good balloon expansion, and cessation of extravasation on venogram. Venography of the left iliac system demonstrated similar issues regarding vascular size and was deemed not large enough to receive the delivery sheath. The procedure was stopped at this junction to allow the stent to undergo maturation and endothelialisation, with an intention to resume the procedure in 4 weeks to pass the IVC and SVC delivery systems via femoral access.

Follow-up and outcomes

Unfortunately, the patient became acutely delirious at the end of the case. A CT scan of the thorax/abdomen and pelvis showed a large haematoma in the right iliac fossa with multifocal infarction in the right kidney. A concomitant CT scan of the brain did not show acute pathology. In time, the patient was transferred back to his original hospital facility for ongoing CCU care. Ultimately, his condition proved fatal, with persistent delirium, intercurrent Clostridium difficile infection, and overwhelming carcinoid crisis leading to his premature demise. Upon discussion with the direct family members of the patient, autopsy was not undertaken.

Discussion

Carcinoid tumours are a type of neuroendocrine tumours that are typically located in the bronchus and GI tract. Carcinoid syndrome is a clinical phenomenon secondary to the release of vasoactive substances [serotonin, 5-hydroxytryptamine (5-HT), 5-hydroxytryptophan, histamine, bradykinin, tachykinins, and prostaglandins], leading to vasomotor changes (secretory diarrhoea, bronchospasm, and hypotension) (5). The diagnosis of a carcinoid tumour involves 24 h collection of urine for 5-HIAA level (end product of serotonin metabolism), chromogranin A levels, PET-CT for tumour location, and tissue biopsy as appropriate. The treatment focuses on reducing proliferation of the primary tumour, and symptomatic control, predominantly via somatostatin analogues, e.g., lanreotide, octreotide (6).

Carcinoid heart disease (CHD) as a sequelae occurs eventually in approximately 20%–50% of patients with carcinoid syndrome and remains a major cause of morbidity and mortality. It is a recognised rare cause of right-sided valvular heart disease, particularly primary TR and stenosis, with development of plaque-like, fibrous endocardial thickening on valves (mostly tricuspid and pulmonary due to metabolism of serotonin in the lung parenchyma). Clinical features include dyspnoea, fatigue, systolic murmur best heard along the sternal border, elevated jugular venous pressure (JVP) with a prominent V wave, ascites, and peripheral oedema (7). The involvement of the left-sided heart valves is uncommon due to the metabolism of 5-HT within the lungs, occurring in approximately one-third of patients. The reasons for left-sided valve disease include a PFO, bronchial carcinoid, or very high levels of 5-HT.

The tricuspid valve itself is the largest and most apically placed heart valve. There is a low-pressure difference between the right atria and ventricle with gradients across the valve expected to be <2 mmHg. It is thought of as four components: leaflets, papillary muscles, chordal attachments, and annulus, with typically three leaflets (anterior, posterior, and septal), but may be bicuspid or have more than three leaflets. Its complex anatomy is essential to understanding the pathophysiology of TR in carcinoid heart disease. Annular dilatation, right atrial and ventricular dilatation, and septal bowing are all recognised features within the clinical syndrome (1).

Symptomatic primary severe TR should have a surgical replacement as per the 2021 ESC/EACTS VHD guidelines (8). However, there is limited specific advice regarding CHD management in these guidelines. Overall, there is limited data, but the existing data indicate a poor outlook. The largest series published in 2019 (2) showed that over 30 years, 240 patients with CHD who underwent valvular heart surgery at Mayo Clinic had high peri-operative morbidity and mortality, particularly when RV dysfunction is present either pre- or post-operatively. The authors quoted a 2-year overall survival of 60%, and a 5-year survival of 34%, albeit with a reduction in early post-operative mortality in more recent times. Low operative numbers (TVR and PVR are relatively uncommon in adult cardiothoracic surgical practice) result in limited information regarding surgical technical aspects and valve replacement optimisation (3). Lastly, it is recognised that the implantation of bioprosthetic material in the context of active carcinoid is commonly associated with valve degeneration, particularly pulmonic implants (9).

PFO closure in isolation has been shown to benefit patients with carcinoid syndrome without valvular disease at 6 months regarding systemic arterial oxygenation, 6 m walk test, and New York Heart Association score (10). However, prospective data regarding the management of PFO and valvular heart disease are restricted to isolated case reports. This does not negate the value in the correction of carcinoid heart disease sequelae, as we have demonstrated an improvement in the symptoms and hypoxaemia of the patient in this case, as was also shown in other similar clinical scenarios (10). After correcting the hypoxaemia in this patient population, staged valvular repair/replacement can be considered at a subsequent junction.

We would suggest a multi-modal imaging approach to the evaluation of these patients, as demonstrated by the initial diagnosis and evaluation of the aetiology of valvular disease via transthoracic and transoesophageal echocardiography. Fluoroscopy, along with right heart catheterisation, is essential for shunt evaluation, and angiography is necessary for the exclusion of concomitant coronary artery disease. These procedures remain an integral part of the diagnostic pathway. ECG-gated cardiac CT is complementary for procedural planning for sizing of PFO closure device, and for the evaluation of tricuspid valve leaflet calcification if subsequent transcatheter correction is anticipated. Finally, we would suggest an expedited

approach as feasible for each medical facility in the diagnostic work-up and therapeutic intervention for this patient population, as demonstrated by the rapid deterioration of our patient throughout their clinical course.

Take home points

Carcinoid heart disease is a rare cause of right-sided valvular heart disease, particularly tricuspid regurgitation and stenosis. We demonstrate a case of carcinoid heart disease complicated by TR causing right to left heart shunting via a stretched PFO, with marked hypoxia and severe heart failure. We wish to highlight the role that multi-modality imaging played during this patient's journey. Unfortunately, there are limited surgical data regarding CHD, with poor outcomes in advanced disease and higher peri-operative complications. We encourage considering percutaneous palliative procedures as, albeit for a short period of time, the patient in this case improved subsequent to such interventions.

Data availability statement

The original contributions presented in the study are included in the article, further inquiries can be directed to the corresponding author/s.

Ethics statement

Ethical review and approval was not required for the study on human participants in accordance with the local legislation and institutional requirements. Written informed consent from the patients/participants next of kin was not required to participate in this study in accordance with the national legislation and the institutional requirements.

Author contributions

MC: Writing – original draft, Writing – review & editing. BM: Writing – review & editing.

Funding

The author(s) declare that no financial support was received for the research, authorship, and/or publication of this article.

Conflict of interest

The authors declare that the research was conducted in the absence of any commercial or financial relationships that could be construed as a potential conflict of interest.

Publisher's note

Supplementary material

The Supplementary Material for this article can be found online at: https://www.frontiersin.org/articles/10.3389/fcvm.2023.1309929/full#supplementary-material

References

1. Dahou A, Levin D, Reisman M, Hahn RT. Anatomy and physiology of the tricuspid valve. *JACC Cardiovasc Imaging*. (2019) 12(3):458–68. doi: 10.1016/j.jcmg.2018.07.032

2. Nguyen A, Schaff HV, Abel MD, Luis SA, Lahr BD, Halfdanarson TR, et al. Improving outcome of valve replacement for carcinoid heart disease. *J Thorac Cardiovasc Surg*. (2019) 158(1):99–107.e2. doi: 10.1016/j.jtcvs.2018.09.025

3. Albåge A, Montibello M. Surgical aspects of valve replacement in carcinoid heart disease. *J Card Surg*. (2021) 36(1):290–4. doi: 10.1111/jocs.15169

4. Alperi A, Almendárez M, Álvarez R, Moris C, Leon V, Silva I, et al. Transcatheter tricuspid valve interventions: current status and future perspectives. *Front Cardiovasc Med*. (2022) 9. doi: 10.3389/fcvm.2022.994502

5. Aluri V, Dillon JS. Biochemical testing in neuroendocrine tumors. *Endocrinol Metab Clin North Am*. (2017) 46(3):669–77. doi: 10.1016/j.ecl.2017.04.004

6. Wolin EM, Manon A, Chassaing C, Lewis A, Bertocchi L, Richard J, et al. Lanreotide depot: an antineoplastic treatment of carcinoid or neuroendocrine tumors. *J Gastrointest Cancer*. (2016) 47(4):366–74. doi: 10.1007/s12029-016-9866-9

7. Davar J, Connolly HM, Caplin ME, Pavel M, Zacks J, Bhattacharyya S, et al. Diagnosing and managing carcinoid heart disease in patients with neuroendocrine tumors: an expert statement. *J Am Coll Cardiol*. (2017) 69(10):1288–304. doi: 10.1016/j.jacc.2016.12.030

8. Vahanian A, Beyersdorf F, Praz F, Milojevic M, Baldus S, Bauersachs J, et al. 2021 ESC/EACTS guidelines for the management of valvular heart disease. *Eur Heart J*. (2022) 43(7):561–632. doi: 10.1093/eurheartj/ehab395

9. Honan KA, Hassan S, Deswal A, Herrmann J, Song J, Monlezun D, et al. Bioprosthetic valve monitoring in patients with carcinoid heart disease. *Front Cardiovasc Med*. (2023) 12(9):1072890. doi: 10.3389/fcvm.2022.1072890

10. Mansencal N, Mitry E, Pillière R, Lepère C, Gérardin B, Petit J, et al. Prevalence of patent foramen ovale and usefulness of percutaneous closure device in carcinoid heart disease. *Am J Cardiol*. (2008) 101(7):1035–8. doi: 10.1016/j.amjcard.2007.11.056

frontiers | Frontiers in Cardiovascular Medicine

TYPE Case Report
PUBLISHED 19 February 2024
DOI 10.3389/fcvm.2024.1328378

OPEN ACCESS

EDITED BY
Alessandro Inno,
Ospedale Sacro Cuore Don Calabria, Italy

REVIEWED BY
Luigi Tarantini,
IRCCS Local Health Authority of Reggio Emilia, Italy
Joshua Eric Levenson,
University of Pittsburgh Medical Center, United States

*CORRESPONDENCE
Paul J. Bröckelmann
paul.broeckelmann@uk-koeln.de

RECEIVED 05 December 2023
ACCEPTED 25 January 2024
PUBLISHED 19 February 2024

CITATION
Lewis RI, Seuthe K, Lennartz S, Weber J-P, Kreuzberg N, Klingel K and Bröckelmann PJ (2024) Case Report: Sudden very late-onset near fatal PD1 inhibitor-associated myocarditis with out-of-hospital cardiac arrest after >2.5 years of pembrolizumab treatment. Front. Cardiovasc. Med. 11:1328378. doi: 10.3389/fcvm.2024.1328378

Case Report: Sudden very late-onset near fatal PD1 inhibitor-associated myocarditis with out-of-hospital cardiac arrest after >2.5 years of pembrolizumab treatment

Richard I. Lewis[1], Katharina Seuthe[2], Simon Lennartz[3], Jan-Phillip Weber[4], Nicole Kreuzberg[5], Karin Klingel[6] and Paul J. Bröckelmann[1]*

[1]Department I of Internal Medicine, Center for Integrated Oncology Aachen Bonn Cologne Duesseldorf, Faculty of Medicine and University Hospital of Cologne, University of Cologne, Cologne, Germany, [2]Department III of Internal Medicine, Faculty of Medicine and University Hospital of Cologne, University of Cologne, Cologne, Germany, [3]Department of Radiology, Faculty of Medicine and University Hospital of Cologne, University of Cologne, Cologne, Germany, [4]Center for Hematology and Oncology, Oncology Cologne, Cologne, Germany, [5]Department of Dermatology, Faculty of Medicine and University Hospital of Cologne, University of Cologne, Cologne, Germany, [6]Cardiopathology, Institute for Pathology and Neuropathology, University Hospital Tübingen, Tübingen, Germany

Introduction: Immune checkpoint inhibitors have advanced the outcomes of many different types of cancer. A rare but extraordinarily severe complication of these agents resembles immune checkpoint inhibitor-related myocarditis, which typically occurs within the first few weeks after treatment initiation with a mortality of 25%–50%.

Case report: A 57-year-old woman had uneventfully received pembrolizumab for metastatic non-small cell lung cancer for over 2.5 years and was admitted after an out-of-hospital cardiac arrest due to ventricular fibrillation. After successful cardiopulmonary resuscitation, the initial diagnostic work-up showed elevated cardiac enzymes and a limited left-ventricular ejection fraction, while coronary angiography did not show relevant stenosis. Despite cardiac MRI being unsuggestive of myocarditis, myocardial biopsies were obtained and histologically confirmed anti-PD-1 antibody-associated myocarditis. After the initiation of prednisone at 1 mg/kg body weight, the patient gradually recovered and was discharged three weeks later with markedly improved cardiac function.

Conclusion: This case resembles the first description of a very late onset irMyocarditis, occurring over 2.5 years after the start of treatment. It demonstrates the importance of contemplating that severe immune-related toxicities with a sudden onset clinical presentation may occur even after long uneventful periods of anti-PD-1 immune checkpoint inhibitor treatment. Furthermore, it underlines the critical importance of myocardial biopsies in this setting, especially when cardiac MRI remains inconclusive. Moreover, it demonstrates the necessity and benefits of early immunosuppressive treatment if immune-related myocarditis is considered a differential diagnosis.

KEYWORDS

cancer immunotherapy, immune checkpoint inhibition, immune related adverse effects (irAEs), immune-related myocarditis, pembrolizumab

Introduction

Since the discovery of immune checkpoint inhibition (ICI) as a novel cancer treatment paradigm, an ever-growing group of substances rapidly became part of standard treatments across major cancer types. For many, ICI revolutionized outcomes and is thus increasingly used in curative intent (1). With a reported incidence between 0.04% and 1.14%, ICI-related myocarditis (irMyocarditis) is a relatively rare, yet potentially lethal immune-related adverse effect (irAE) (2). Importantly, irMyocarditis is considered an early irAE, with a median occurrence of 17 to 34 days after treatment initiation, and 76% of cases develop within the first six weeks of ICI (3–5). However, in the following, we present a rare case of histologically confirmed near fatal irMyocarditis, which occurred after over 2.5 years of pembrolizumab treatment. To our knowledge, this resembles the longest yet reported latency of irMyocarditis.

Case report

A 57-year-old woman experienced sudden cardiac arrest while attending a social event. After a no-flow time of approximately 1 min, a coincidentally present nurse initiated cardiopulmonary resuscitation (CPR). When paramedics arrived, approximately 10 min into CPR, the initial rhythm was ventricular fibrillation. The patient underwent a series of 3 defibrillations and received 200 mg of amiodarone before achieving a return of spontaneous circulation after a total of approximately 17 min.

The patient was then transferred to our center and initially presented with heart failure with a reduced left ventricular ejection fraction (Figure 1A; Supplementary Report S1), which was previously unknown. Laboratory results showed elevated cardiac enzymes (Supplementary Table S1), which further increased initially, likely due to the combination of CPR and myocarditis (Supplementary Table S2). The patient was initially neuro-protectively cooled for 24 h and was successfully weaned from ventilation after 36 h. Subsequently, the patient developed fever and intermittent tachycardic atrial fibrillation, which we treated with piperacillin/tazobactam for suspected aspiration pneumonia, electrolyte supplementation, and metoprolol. Electrocardiograms exhibited no signs of ischemia, even at supraventricular tachycardic frequencies of 180 /min (Figure 1B). Hence, we postponed coronary angiography and reviewed the patient's history.

Here we learned the patient had received chemotherapy and a total of 42 infusions of 200 mg pembrolizumab at 3-weekly intervals for over 2.5 years, following the diagnosis of metastatic non-small-cell lung cancer (NSCLC, UICC stage IV). We initiated intravenous prednisone (1 mg/kg body weight) as, despite being improbable, irMyocarditis was considered a differential diagnosis. Cardiac MRI was performed the consecutive day, and MRI-based tissue characterization using Lake Louise Criteria II (LLC II) showed neither myo-/pericardial late gadolinium enhancement nor pericardial thickening or effusion. Furthermore, T2-mapping was not prolonged with an exemplary midventricular septal T2 relaxation time of 60 ms (scanner-specific reference range: 58 ± 5 ms), while native T1 relaxation was prolonged with an exemplary mid-ventricular relaxation time of 974 ms.

In summary, MRI did not indicate peri-/myocarditis (Figure 1C; Supplementary Report S2). Hence, we performed coronary catheterization and etiologically ruled out ischemia (Supplementary Report S3). We then reviewed the case within our center's interdisciplinary CIO iTox Board, dedicated to the management of irAEs, and jointly opted for endomyocardial biopsies even though imaging was inconspicuous. Five samples from the left ventricle were collected and reviewed by an external reference pathologist (KK). The myocardium showed distinct focal but also diffuse interstitial fibrosis, indicative of inflammation, likely subclinically preceding the OHCA by months. In different areas, myocyte necrosis was observed in association with numerous CD3+ *T*-cells (100 /mm^2), a great number of CD68$^+$ macrophages with MHC II expression (200 /mm^2), and scattered CD20$^+$ B-lymphocytes, without eosinophilic granulocytes or multinucleated giant cells (Figure 1D). We further carried out nested PCR to rule out cardiotropic pathogens as the underlying cause. EBV-specific DNA sequences were detected at low copy numbers in both endomyocardial biopsies and peripheral leukocyte preparation, most certainly reflecting latent systemic virus persistence. Negative PCR results were obtained for a standardized panel of further cardio-pathogens (Supplementary Table S3). Furthermore, there were no clinical signs of myasthenia or myositis and the patient could not recall pathologies of the thymus, neither did the medical history or CT scans acquired reveal any such alterations.

Taken together, (immuno)histology was consistent with acute lymphocytic myocarditis, as eosinophilic myocarditis, giant cell myocarditis, or amyloidosis were histologically excluded, thus confirming irMyocarditis. Hence, we continued prednisone treatment, on which the patient's clinical condition continuously improved to the state prior to the event. The patient received an implantable cardioverter-defibrillator for secondary prevention, pembrolizumab was permanently discontinued, and with continued heart failure medication, the patient demonstrated normalized LVEF (Figure 1A). The NSCLC remains in remission 4 months after.

Discussion

Summarizing, while irMyocarditis resembles a comparably rare adverse event, it is associated with a high mortality of 25% to 50% (2). While previous case reports and systematic analyses on irMyocarditis exist (4, 6), the case presented herein is extraordinary in multiple aspects and thus provides compelling insights for the management of patients with (very) late-onset: Our patient experienced cardiac arrest after over 2.5 years of treatment without prior irAEs, although irMyocarditis typically manifests early after initiation (3). To our knowledge, this is the longest onset yet reported. With a rapidly growing number of patients treated with ICI, including in curative intent, this case

10.3389/fcvm.2024.1328378

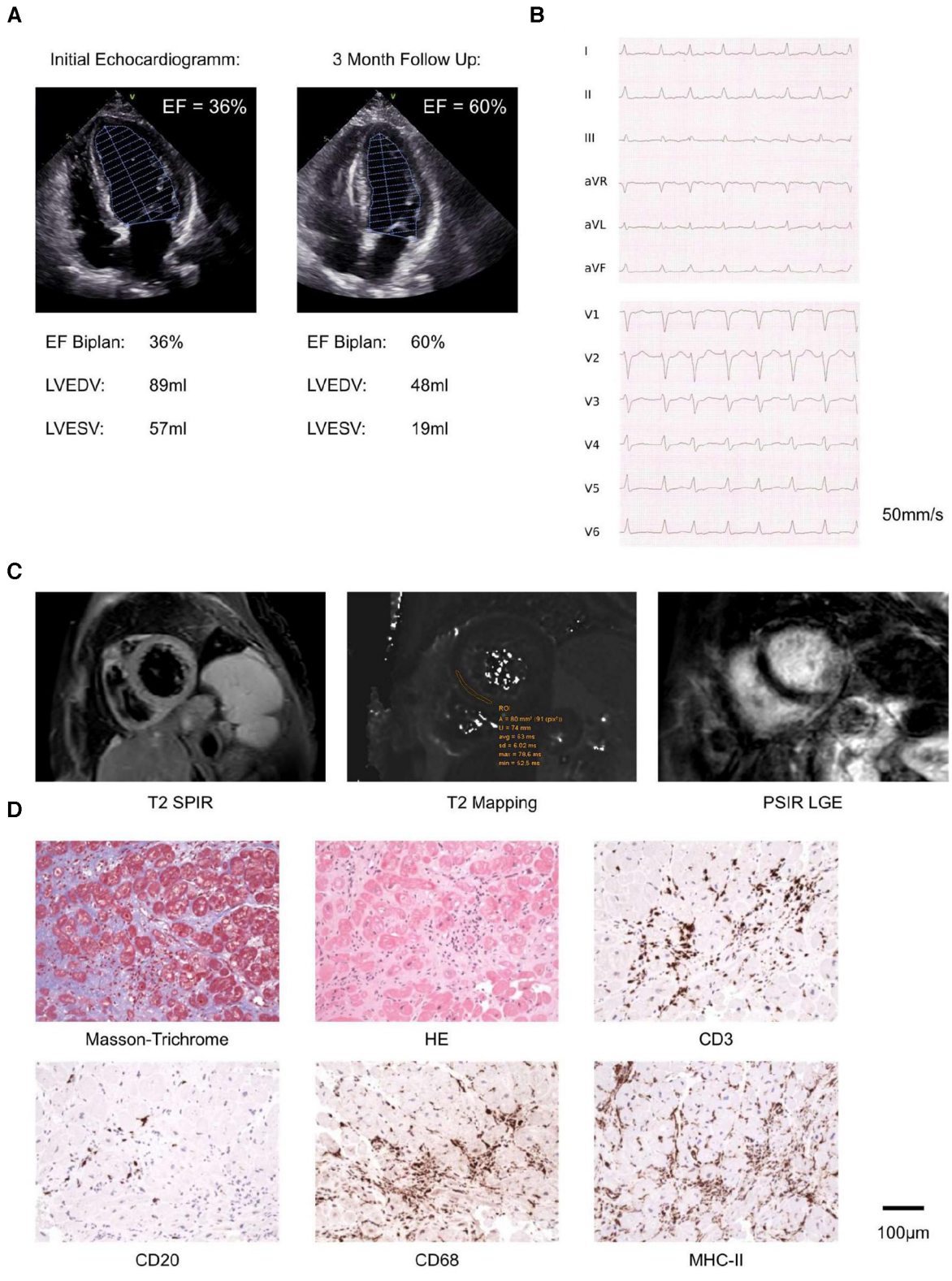

FIGURE 1
Diagnostics, including echocardiography, radiology and pathology: (**A**) representative images of initial echocardiography depicting reduced LVEF and 3 months follow up echocardiography depicting improved LVEF. (**B**) Electrocardiogram recorded during tachycardic (180/min) atrial fibrillation. (**C**) Representative images from cardiac MRI, recorded one day after initiation of prednisone. (**D**) Histopathology and Immunohistology of endomyocardial biopsies including Masson Trichrome, HE, CD3 (T lymphocytes), CD20 (B lymphocytes), CD68 (macrophages) and MHCII stains. Scale bar as indicated.

demonstrates the importance of vigilance for irAEs even after long treatment periods. Furthermore, it stresses that early initiation of immunosuppression appears critical for improved outcomes with negligible risks if the specific event may later be attributed to a different etiology and should hence be initiated even when irMyocarditis seems unlikely (7). Moreover, it highlights that irMyocarditis may be present even with inconspicuous MRI. Although cardiac MRI became a pivotal tool in diagnosing myocarditis over the last two decades, it is critical to contemplate that while demonstrating high specificity, sensitivity is reported to be 87% with LLC II (8). Additionally, previous studies showed that sensitivity of cardiac MRI is dependent on underlying cardiac pathology and lowest in cardiomyopathic causes of myocarditis (9). Thus, especially in the context of possible irMyocarditis with inconclusive MRI, myocardial biopsies remain the gold standard of diagnosis. Additionally, our case makes evident the importance of interdisciplinary teams for optimal management of such patients. By reviewing the case in our well-established CIO iTox Board, we swiftly coordinated diagnostics and early immunosuppression, which data suggests is critical for patients' outcomes (4, 5, 10). With the ever-growing number of ICI-based treatments and expansion beyond targeting PD-1 and CTLA-4, such interdisciplinary teams will become increasingly important in the future to manage these patients' therapies, especially when irAEs occur. Our case also once more demonstrates, that irAEs can occur after long uneventful treatment periods, which raises the question of optimal length of ICI-based treatments. To this end, initial data indicates the possibility to achieve long-lasting remissions with time-limited treatment periods, which might reduce the risk of irAEs (11). Although mechanisms underlying early-onset and CTLA-4-mediated irMyocarditis are more and more understood and led to the implementation of abatacept as an additional treatment option (12), the biology underlying anti-PD-1 and especially late-onset irMyocarditis is unknown. Hence, further translational studies are crucial to provide optimal care to patients.

Data availability statement

The original contributions presented in the study are included in the article/Supplementary Material, further inquiries can be directed to the corresponding author.

Ethics statement

Ethical approval was not required for the studies involving humans because the manuscript represents a case report. The patient's data was anonymized and the patient provided written informed consent to the manuscript, which they read and accepted in advance. The studies were conducted in accordance with the local legislation and institutional requirements. The participants provided their written informed consent to participate in this study. Written informed consent was obtained from the individual(s) for the publication of any potentially identifiable images or data included in this article.

Author contributions

RL: Conceptualization, Writing – original draft, Writing – review & editing, Data curation, Visualization. KS: Writing – review & editing, Data curation, Visualization. SL: Data curation, Visualization, Writing – review & editing. J-PW: Data curation, Visualization, Writing – review & editing. NK: Data curation, Writing – review & editing. KK: Data curation, Visualization, Writing – review & editing. PB: Conceptualization, Data curation, Investigation, Supervision, Visualization, Writing – original draft, Writing – review & editing.

Funding

The author(s) declare financial support was received for the research, authorship, and/or publication of this article.

PB is supported by a Mildred Scheel School of Oncology (MSSO) Postdoctoral Fellowship by the German Cancer Aid (No. 70113307).

Acknowledgments

The authors would like to express their sincere gratitude to the patient who generously allowed the utilization of their complete medical record for this case report. Their invaluable contribution has made this case report possible and greatly provides further insight to a to this date research and understanding of this medical case.

Conflict of interest

The authors declare that the research was conducted in the absence of any commercial or financial relationships that could be construed as a potential conflict of interest.

Publisher's note

Supplementary material

The Supplementary Material for this article can be found online at: https://www.frontiersin.org/articles/10.3389/fcvm.2024.1328378/full#supplementary-material

References

1. Tan S, Day D, Nicholls SJ, Segelov E. Immune checkpoint inhibitor therapy in oncology: current uses and future directions: JACC: Cardiooncology state-of-the-art review. *JACC CardioOncology*. (2022) 4(5):579–97. doi: 10.1016/j.jaccao.2022.09.004

2. Palaskas N, Lopez-Mattei J, Durand JB, Iliescu C, Deswal A. Immune checkpoint inhibitor myocarditis: pathophysiological characteristics, diagnosis, and treatment. *J Am Heart Assoc*. (2020) 9(2):e013757. doi: 10.1161/JAHA.119.013757

3. Varricchi G, Galdiero MR, Marone G, Criscuolo G, Triassi M, Bonaduce D, et al. Cardiotoxicity of immune checkpoint inhibitors. *ESMO Open*. (2017) 2(4):E000247. doi: 10.1136/esmoopen-2017-000247

4. Mahmood SS, Fradley MG, Cohen JV, Nohria A, Reynolds KL, Heinzerling LM, et al. Myocarditis in patients treated with immune checkpoint inhibitors. *J Am Coll Cardiol*. (2018) 71(16):1755–64. doi: 10.1016/j.jacc.2018.02.037

5. Osinga TE, Oosting SF, van der Meer P, de Boer RA, Kuenen BC, Rutgers A, et al. Immune Checkpoint Inhibitor–Associated Myocarditis. *Neth Heart J*. (2022) 30 (6):295–301. doi: 10.1007/s12471-021-01655-7

6. Wang DY, Salem JE, Cohen JV, Chandra S, Menzer C, Ye F, et al. Fatal toxic effects associated with immune checkpoint inhibitors: a systematic review and meta-analysis. *JAMA Oncol*. (2018) 4(12):1721–8. doi: 10.1001/jamaoncol.2018.3923

7. Maher VE, Fernandes LL, Weinstock C, Tang S, Agarwal S, Brave M, et al. Analysis of the association between adverse events and outcome in patients receiving a programmed death protein 1 or programmed death ligand 1 antibody. *J Clin Oncol*. (2019) 37(30):2730–7. doi: 10.1200/JCO.19.00318

8. Luetkens JA, Faron A, Isaak A, Dabir D, Kuetting D, Feisst A, et al. Comparison of original and 2018 Lake Louise criteria for diagnosis of acute myocarditis: results of a validation cohort. *Radiol Cardiothorac Imaging*. (2019) 1(3):e190010. doi: 10.1148/ryct.2019190010

9. Francone M, Chimenti C, Galea N, Scopelliti F, Verardo R, Galea R, et al. CMR sensitivity varies with clinical presentation and extent of cell necrosis in biopsy-proven acute myocarditis. *JACC Cardiovasc Imaging*. (2014) 7(3):254–63. doi: 10.1016/j.jcmg.2013.10.011

10. Escudier M, Cautela J, Malissen N, Ancedy Y, Orabona M, Pinto J, et al. Clinical features, management, and outcomes of immune checkpoint inhibitor–related cardiotoxicity. *Circulation*. (2017) 136(21):2085–7. doi: 10.1161/CIRCULATIONAHA.117.030571

11. Marron TU, Ryan AE, Reddy SM, Kaczanowska S, Younis RH, Thakkar D, et al. Considerations for treatment duration in responders to immune checkpoint inhibitors. *J Immunother Cancer*. (2021) 9(3):E001901. doi: 10.1136/jitc-2020-001901

12. Salem J-E, Bretagne M, Abbar B, Leonard-Louis S, Ederhy S, Redheuil A, et al. Abatacept/ruxolitinib and screening for concomitant respiratory muscle failure to mitigate fatality of immune-checkpoint inhibitor myocarditis. *Cancer Discovery*. (2023) 13(5):1100–15. doi: 10.1158/2159-8290.Cd-22-1180

frontiers | Frontiers in Oncology

TYPE Case Report
PUBLISHED 26 February 2024
DOI 10.3389/fonc.2024.1342748

OPEN ACCESS

EDITED BY
Reto Asmis,
Wake Forest University, United States

REVIEWED BY
Massimo Baudo,
Lankenau Institute for Medical Research, United States
Tareg Bey,
University of Texas MD Anderson Cancer Center, United States

*CORRESPONDENCE
Mingjie Pang
1836443709@qq.com

RECEIVED 22 November 2023
ACCEPTED 05 February 2024
PUBLISHED 26 February 2024

CITATION
Zhang Y and Pang M (2024) Unveiling the mystery: a rare case of localized malignant pericardial mesothelioma—case report. *Front. Oncol.* 14:1342748. doi: 10.3389/fonc.2024.1342748

Unveiling the mystery: a rare case of localized malignant pericardial mesothelioma—case report

Yan Zhang[1] and Mingjie Pang[2]*

[1]Department of Magnetic Resonance, The First People's Hospital of Yunnan Province, The Affiliated Hospital of Kunming University of Science and Technology, Kunming, Yunnan, China, [2]Department of Cardiology, The First People's Hospital of Yunnan Province, The Affiliated Hospital of Kunming University of Science and Technology, Kunming, Yunnan, China

Primary malignant pericardial mesothelioma (PMPM) is a rare pericardial malignant tumor. Most manifestations of PMPM are localized or diffuse masses surrounding the heart. The prognosis of diffuse PMPM is poor due to the difficulty of surgical resection. Although the edge of localized PMPM is clear and can be easily resected, the diagnosis of this disease is difficult. Timely diagnosis and proper treatment are key to a good prognosis. Here, we report a patient with localized PMPM and describe the method for the diagnosis of this disease.

KEYWORDS

24 h pericardial effusion drainage, wax tissue, late gadolinium enhancement cardiac magnetic resonance, localized malignant pericardial mesothelioma, PET-CT examination

1 Introduction

Primary malignant pericardial mesothelioma (PMPM) is a rare pericardial malignant tumor (1, 2). Most PMPM was found in autopsy, and the incidence rate was about 0.006%/0.0022% (3, 4). Malignant pericardial mesothelioma is clinically rare with a poor prognosis and an average survival time of 6–10 months (2). PMPM has not been reported locally. In this study, We present a rare case report of PMPM.

2 Case report

A 53-year-old female patient was admitted to our hospital for 6 months because of pericardial effusions. The patient had previous hypertension, with the highest blood pressure of 160/90 mmHg. She had no history of surgery or familial diseases. In the past, the patient had not experienced limb joint pain, morning stiffness, photosensitivity,

oral ulcers, hair loss, low-grade fever, and night sweats. She had no weight loss in the short term or recent infections. Physical examination during admission showed stable vital signs. The patient had no obvious symptoms, such as palpitations or chest tightness. On February 10, 2021, the patient underwent Color Doppler Echocardiography in a local hospital for physical examination, which revealed a pericardial effusion. The thickest part was about 4.8 cm, and the pericardium of the left ventricular free wall was thickened and irritable. A CT scan of the chest and abdomen, which was conducted in the local hospital, showed pericardial effusions and calcification in the right lung. Abdominal ultrasound showed no abnormality. Breast ultrasound revealed bilateral breast hyperplasia. Thyroid ultrasound detected TI-RADS3 type of cystic-solid nodules in the right lobe of the thyroid. Suspected pulmonary tuberculosis infection was assessed by local hospitals, and standardized pulmonary tuberculosis chemotherapy was administered. Echocardiography was performed on March 29 after a month of treatment, which showed that the amount of pericardial effusions significantly increased. The thickest part was about 4.8 cm, and the pericardium was localized, thickened, and irritable. The patient visited our hospital on June 21. In addition to the patient's information stated above, physical examination performed by a specialist showed an enlarged cardiac silhouette, a HR of 83, and a low heart sound. No pericardial friction sounds or abnormal heart sounds were detected.

The admission electrocardiogram showed a sinus rhythm with low voltage in the chest leads and right bundle branch block (Figure 1). Chest X-ray revealed an enlargement of the heart shadow, and chest CT indicated a large volume of pericardial effusions. The blood routine, ESR, and CRP of the patient were normal. No abnormalities were observed in liver and renal functions. The levels of troponin T and Pro-BNP, as well as tumor markers, were normal. Blood ANCA, ANA, RF, and other immune-related indexes were also normal. Blood EB and cytomegalovirus detection revealed no abnormalities. The detection of tuberculosis T cell, tuberculosis antibody, rpoB gene, and mutation of *Mycobacterium* nucleic acid also showed no abnormalities. Pericardial puncture was performed, and fluid was collected simultaneously to improve the relevant laboratory examination. The pericardial effusions were yellow and slightly muddy. The serous mucin qualitative test was positive (+), and the total number of cells was 68 × 10 ^ 6/L. No abnormalities were found in LDH, TP, ADA, GLU, CI, and CEA. Pathological

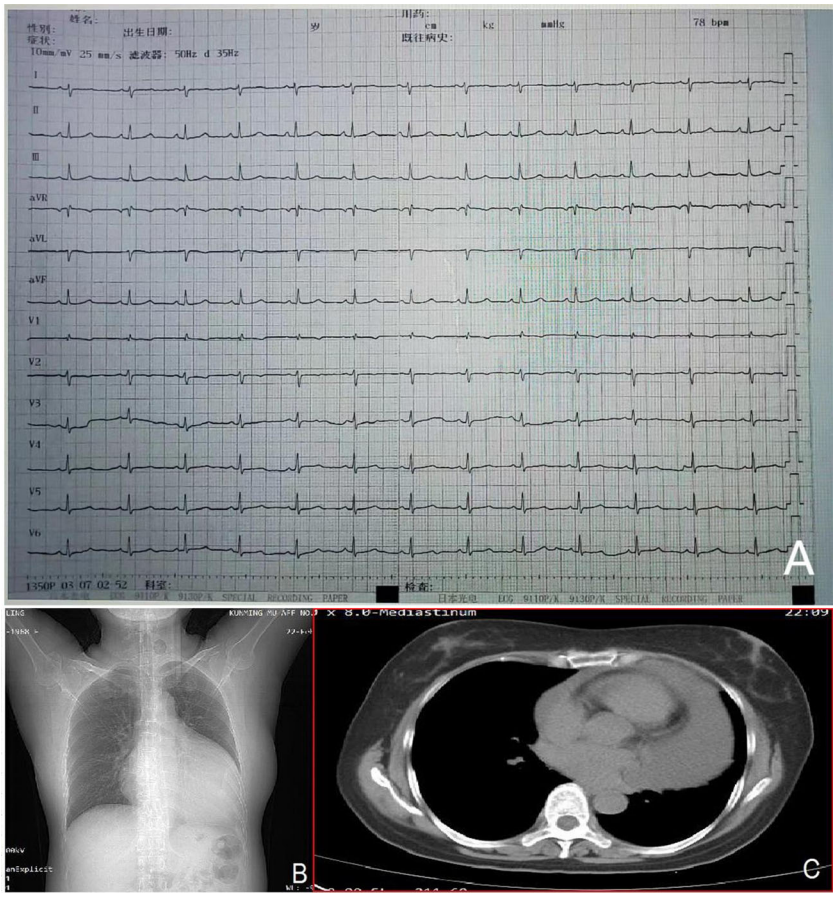

FIGURE 1
Admission electrocardiogram **(A)** showing a sinus rhythm with low voltage in the chest leads and right bundle branch block. Chest X-ray **(B)** indicating an enlarged heart shadow. Chest CT **(C)** suggesting a large volume of effusions in the pericardial cavity.

examination of pericardial effusions showed that some of the nuclei were large and deeply stained with a large number of red blood cells and a small number of atypical cells. Perfect PET-CT examination revealed no signs of malignant tumor but showed a slight pericardial thickening and adhesive and a small amount of pericardial effusions with encapsulated changes (Figure 2). Then, the late gadolinium enhancement cardiac magnetic resonance examination on the patient showed improvements, such as pericardial thickening, adhesive, lesions on the right ventricular margin, and pleural adhesion. The pericardial fat on the left ventricular free wall appeared blurred, and the fibrous pericardium on the left ventricular free wall exhibited thickening. Perfusion imaging indicated that the thickened hairy pericardium had moderate enhancement. The late gadolinium contrast agent enhancement (LGE) medium implied that the pericardial thickening exhibited delayed enhancement (Figure 3). During hospitalization, the second pericardiocentesis was performed, pericardial effusion was drained for 24 h, and the sediment was collected for wax-encapsulated pathological examination and immunohistochemistry. Immunohistochemical staining showed the following expression of tumor cells: CK7(+), CK20(−), Villin (−), TTF-1(−), WT-1(+), P16(+), CR(+), CDX-2(−), CA125(+), Pax-8(−), P53(+), CK19(+), CK8(+), CK5/6(+), Vim(+), ER(−), PR (−), and Ki-67(+). Collectively, these results suggested malignant mesothelioma (Figure 4). The patient was then transferred to the department of oncology, but the patient refused chemotherapy. For nearly a year and a half, the patient was followed up regularly. As of September 30, 2023, the patient had stable vital signs and had no metastasis in other body parts.

3 Discussion

Pericardial tumors are rare in clinical works, and most of them come from adjacent tissues and organs, such as malignant pleural tumors, malignant lung tumors, melanomas, or lymphomas. Primary pericardial malignant tumors are rare. The prevalence of PMPM in pericardial tumors is less than 0.002% (2). The cause of PMPM is also unknown. Notably, malignant pleural mesothelioma is usually associated with asbestos exposure (5), but patients mentioned in previous literature had no history of asbestos exposure and no obvious etiology (6). No particular age of onset was reported. Clinical symptoms in previous reports were not characteristic and regular, and the typical manifestation is the clinical presentation of pericardial effusions (6).

The prognosis of PMPM is poor, the survival time is short, and the reported survival time is about 2.5 years (7). A correct clinical diagnosis needs to be made as soon as possible. The lack of characteristic clinical manifestations of PMPM causes great challenges to the diagnosis of the disease. Thus, improving imaging and pathological examination is key to its diagnosis and differentiation, especially in cases of localized pericardial thickening. Imaging examination methods include cardiac color Doppler ultrasound, CT, PET-CT, and CMR. Color Doppler echocardiography and CT can detect pericardial effusions, pericardial thickening, or localized pericardial masses. Enhanced CT can also indicate the blood supply of tumors. PET-CT not only can detect pericardial effusions and masses but also can identify or exclude other tumors. In the current case, the pericardial focus of the patient is limited and flocculent, not a formed mass, which

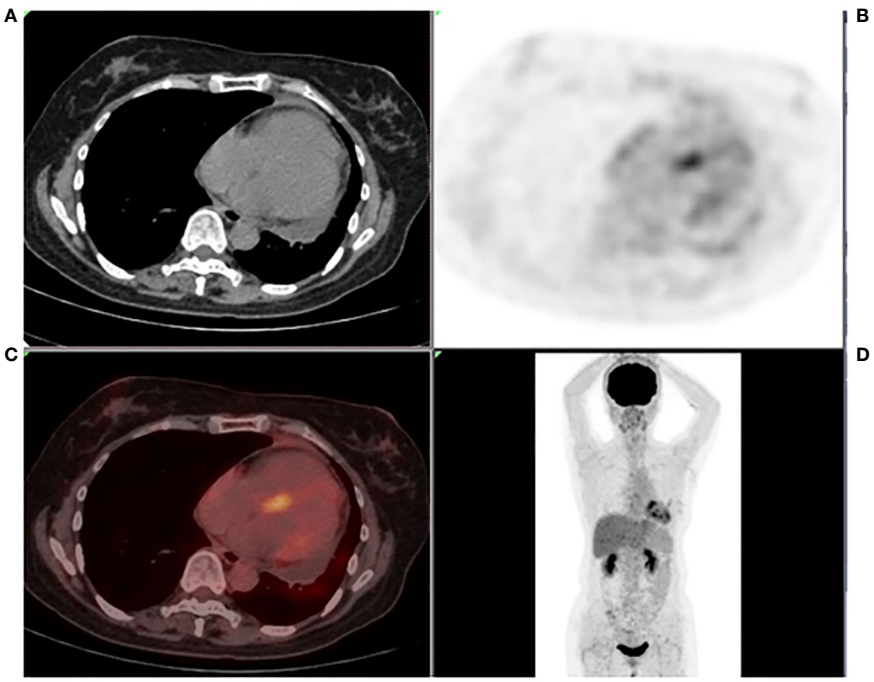

FIGURE 2
Systemic PET-CT **(A–D)** showing no clear signs of malignant tumor. The pericardium was slightly thickened and adhered, the metabolism increased slightly, and a small amount of effusions were observed in the pericardium with encapsulated changes.

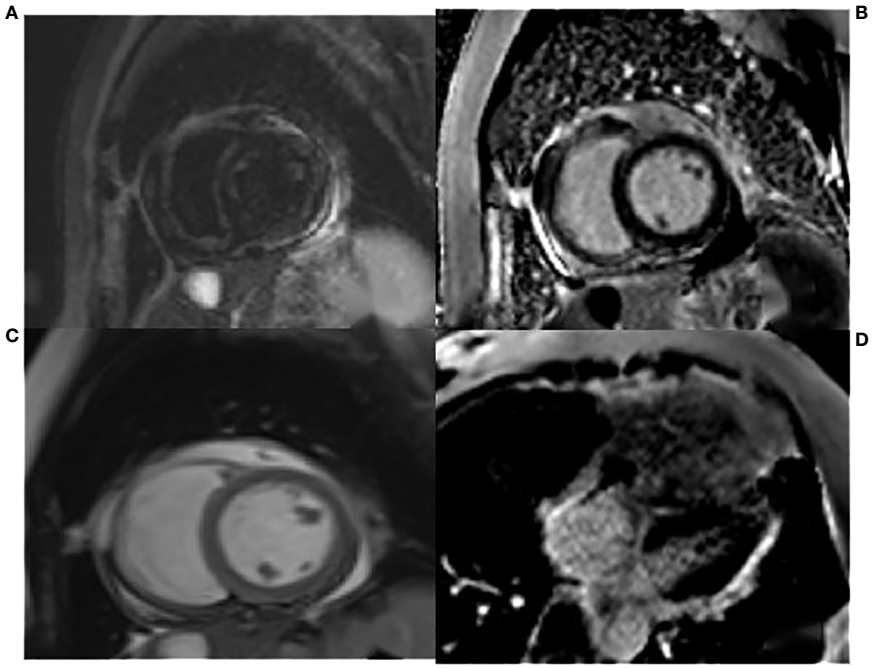

FIGURE 3
The T2WI fat suppression sequence in **(A)** showed pericardial thickening, adhesive, and lesions on the right ventricular margin adhering to the pleura. The cardiac movie sequence in **(C)** revealed that the fibrous pericardium of the right ventricular free wall adhered to the pleura, the serous pericardium was slightly thickened, and a small amount of pericardial effusions were observed. The LGE images of the two-chamber and four-chamber heart in **(B, D)** indicated thickening and enhancement of the fibrous pericardium.

causes difficulties in diagnosis. CMR has high soft tissue resolution and can be used for multi-parameter and multi-directional imaging. CMR can dynamically observe the relationship between cardiac movement and the pericardium. It can identify the delayed enhancement of the pericardium after thickening on LGE sequences, which is valuable in the localization and qualitative diagnosis of diseases.

In this case, the focus of the patient is limited, and the positive rate of pericardial effusion is low. A special way to collect pericardial effusions is necessary. The conventional method of retaining pericardial effusions involves collecting fluid immediately after puncture for laboratory examination and pathological examination. In this case, 24-hour pleural effusion was drained and filtered, and the sediment was collected and wrapped in wax blocks.

The sediment wrapped in wax blocks was investigated by pathological examination and immunohistochemistry. The use of wax tissue avoids a low positive rate of diagnosis and missed diagnosis caused by a small number of cells, overlapping accumulation of cells, uneven smear thickness, and multiple background impurities. Wax block tissue has various advantages, such as ease of acquisition, low cost, simple operation, and good specificity. At present, cell wax block diagnosis is the most effective and reliable technique to distinguish benign and malignant effusions. The combination of immunocytochemical staining can help in identifying the primary source, identify the pathological type of the tumor, and further conduct molecular pathological detection, which provides an objective basis for accurate treatment and prognosis of patients and is valuable for extensive clinical promotion (8, 9). In summary, localized pericardial thickening and massive pericardial effusions are easily missed and misdiagnosed in patients. At the same time, the positive rate of pleural effusion is low, which cannot be used as a diagnostic

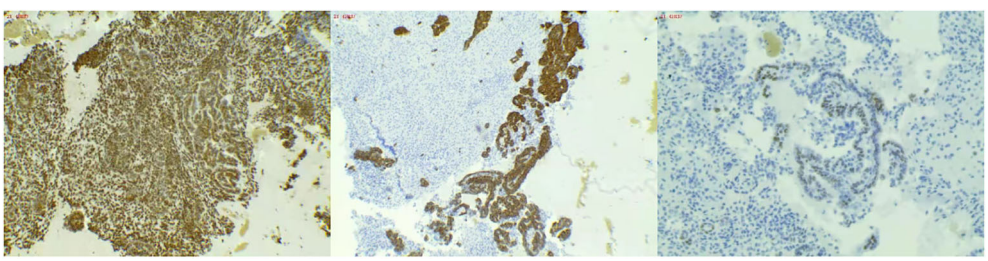

FIGURE 4
(Wax mass of pericardial effusion) HE morphology and immunohistochemical results consistent with malignant mesothelioma.

criterion of negative PMPM (10, 11). For such cases, various laboratory tests and imaging methods need to be improved, and special methods should be adopted for pleural effusion drainage and pathological examination. Best efforts should be made to avoid the progression of diseases and increase the survival rate of patients.

Data availability statement

The original contributions presented in the study are included in the article/supplementary material. Further inquiries can be directed to the corresponding author.

Ethics statement

The studies involving humans were approved by Ethics Committee of Yunnan First People's Hospital. The studies were conducted in accordance with the local legislation and institutional requirements. The participants provided their written informed consent to participate in this study. Written informed consent was obtained from the individual(s) for the publication of any potentially identifiable images or data included in this article.

Author contributions

YZ: Writing – original draft. MP: Writing – review & editing.

Funding

The author(s) declare financial support was received for the research, authorship, and/or publication of this article. This work was supported and funded by the National Natural Science Foundation of China (82160079) and Yunnan Provincial Department of Science and Technology - Kunming Medical University Joint Special Project on Applied Basic Research (202201AY070001-243). None of the funding sources participated in the preparation of the data and writing of the manuscript.

Conflict of interest

The authors declare that the research was conducted in the absence of any commercial or financial relationships that could be construed as a potential conflict of interest.

Publisher's note

References

1. Savarrakhsh A, Vakilpour A, Davani SZ, Daskareh M, Morsaghian M, Salari A, et al. Malignant primary pericardial mesothelioma presenting as effusive constrictive pericarditis: a case report study. *J Cardiothorac Surg* (2021) 16(1):298. doi: 10.1186/s13019-021-01684-8s

2. Pan L, Du J, Liu J, Liao H, Liu X, Guo X, et al. Tocilizumab treatment effectively improves coronary artery involvement in patients with Takayasu arteritis. *Clin Rheumatol* (2020) 39:2369–78. doi: 10.1007/s10067-020-05005-7

3. Chetrit M, Parent M, Klein AL. Multimodality imaging in pericardial diseases. *Panminerva Med* (2021) 63:301–13. doi: 10.23736/S0031-0808.21.04270-1

4. Martínez-Girón R, Liron P. Sudden cardiac death due to primary Malignant pericardial mesothelioma: brief report and literature review. *Respir Med Case Rep* (2019) 26:185–8. doi: 10.1016/j.rmcr.2019.01.011

5. Mensi C, Romano A, Berti A, Dore R, Riboldi L. A second case of pericardial mesothelioma mimicking systemic lupus erythematosus in the literature in over 30 years: a case report. *J Med Case Rep* (2017) 11(1):85–90. doi: 10.1186/s13256-017-1237-z

6. Song G, Bi W, Zhang X, Huang W, Zhou K, Ren W. Localized primary Malignant pericardial mesothelioma. *J Clin Ultrasound* (2019) 47(3):178–181. doi: 10.1002/jcu.22673

7. Bray F, Ferlay J, Soerjomataram I, Siegel RL, Torre LA, Jemal A. Global cancer statistics 2018: GLOBOCAN estimates of incidence and mortality worldwide for 36 cancers in 185 countries. *CA-A Cancer J Clin* (2018) 68(6):394–424. doi: 10.3322/caac.21492

8. McGehee E, Gerber DE, Reisch J, Dowell JE. Treatment and outcomes of primary pericardial mesothelioma: A contemporary review of 103 published cases. *Clin Lung Cancer* (2019) 20:e152–7. doi: 10.1016/j.cllc.2018.11.008

9. Yan Y, Lv W, Luo Y, Hu J, Yang J. Primary Malignant pericardial mesothelioma with a survival of 2.5 years: a case report. *Trans Cancer Res* (2022) 1:1455. doi: 10.21037/tcr

10. Seal S, Simon H. Primary pericardial mesothelioma: A rare but serious consideration. *Cureus* (2021) 13:e19966. doi: 10.7759/cureus.19966

11. Karagodin I, Nagle K, Scheidemantle B, Chung J, Paul J, Larsen P, Kalathiya R, et al. Metastatic pericardial mesothelioma: a rare case of constrictive pericarditis. *J Am Coll Cardiol* (2019) 73(9):2640–7. doi: 10.1016/S0735-1097(19)33246-2

frontiers | Frontiers in Cardiovascular Medicine

TYPE Case Report
PUBLISHED 28 February 2024
DOI 10.3389/fcvm.2024.1356134

OPEN ACCESS

EDITED BY
Monica Cattaneo,
MultiMedica (IRCCS), Italy

REVIEWED BY
Giulia Iannaccone,
Catholic University of the Sacred Heart, Italy
Wilhelm Mistiaen,
University of Antwerp, Belgium

*CORRESPONDENCE
Yongheng Zhang
mfqq_258383@sohu.com

†These authors have contributed equally to this work

RECEIVED 15 December 2023
ACCEPTED 05 February 2024
PUBLISHED 28 February 2024

CITATION
Liu J, Zheng Y, Zhang W, Xia J, Zhang Y and Tang L (2024) Case Report: A case of third-degree atrioventricular block associated with primary cardiac lymphoma.
Front. Cardiovasc. Med. 11:1356134.
doi: 10.3389/fcvm.2024.1356134

Case Report: A case of third-degree atrioventricular block associated with primary cardiac lymphoma

Jianping Liu[1†], Yong Zheng[1†], Weishan Zhang[2], Juan Xia[3], Yongheng Zhang[1*] and Long Tang[1]

[1]Department of Cardiovascular Surgery, Suining Central Hospital, Suining, Sichuan, China, [2]Department of Pathology, Suining Central Hospital, Suining, Sichuan, China, [3]Department of Hospital-Acquired Infection Control, Suining Central Hospital, Suining, Sichuan, China

Background: Primary cardiac lymphoma is an extremely rare malignant lymphoma, with clinical manifestations related to its location. We reported the diagnosis and treatment of primary cardiac lymphoma in a patient presented with atrioventricular block.
Case presentation: A 64 year-old man was admitted to our hospital because of symptoms of a tired heart and shortness of breath. The initial electrocardiogram revealed a third-degree atrioventricular block. Computed tomography scan showed an irregularly shaped right heart, irregular clusters, and relatively weakly enhanced areas in the right auricle, atrium, and ventricle. The local boundary between the lesion, pericardium, and left atrium was unclear, and the ventricular septum was irregular and thickened. Multiple irregular gray neoplasms with less smooth surfaces were observed, with a maximum diameter of approximately 7 cm. Pathological findings confirmed a non-germinal center B cell subtype of diffuse large B-cell lymphoma. After surgical resection of the tumor and implantation of a permanent pacemaker, the symptoms of the patient were significantly improved, allowing subsequent chemotherapy.
Conclusion: Surgical resection and placement of a permanent pacemaker were effective treatments for a patient with primary cardiac lymphoma presented with atrioventricular block.

KEYWORDS

cardiac lymphoma, atrioventricular block, diffuse large B-cell lymphoma, case report, diagnosis, treatment

1 Introduction

Primary cardiac tumors are particularly rare, with a prevalence ranging from 0.001% to 0.03%, with 1.3% of primary cardiac tumors and 0.5% of extranodal lymphomas being primary cardiac lymphomas (1). Primary cardiac lymphoma, which always involves the right atrium and ventricle, is three times more common in women than men, with 64 years being the median age for disease diagnosis (2). Primary cardiac lymphoma is defined as follows: (1) the heart or pericardium is affected by malignant lymphoma as demonstrated by autopsy (3); and (2) tumor tissue consisting of cardiac or pericardial lymphoma or lymphoma infiltration in the myocardium causing cardiac symptoms at initial diagnosis (4). Primary cardiac lymphomas are largely reported as isolated cases owing to their rarity and difficulty in their diagnosis. Thus, owing to late diagnosis, the

prognosis of primary cardiac lymphoma is poor, with the median survival after diagnosis being 7 months (5).

The main clinical manifestations of primary cardiac lymphoma are cardiac symptoms induced by lymphoma infiltration of the myocardium. Other signs may be observed, including mediastinal lymph node enlargement, pleural exudation, and pulmonary embolism (6). Primary cardiac lymphoma is easily misdiagnosed in patients presenting with atrioventricular block only (7). We reports a case of third-degree atrioventricular block secondary to primary cardiac lymphoma that provides theoretical and empirical evidence for the diagnosis and treatment of this disease.

2 Case description

A 64 year-old man was admitted to our hospital on September 2, 2022, owing to symptoms of a tachycardia and shortness of breath. Physical examination at admission revealed the following: body temperature: 36.5°C, heart rate: 51 times/min, pulse: 51 beats/min; blood pressure: 102/68 mmHg, poor spirit, edema of the trunk, yellow sclera, slight cyanosis of the lip, no filling of the jugular vein, coarse breath sounds in both lungs, no enlargement of the heart boundary, arrhythmia, soft abdomen, and severe pitting edema of the lower limbs. Moreover, laboratory tests revealed the following: cardiac troponin I (cTNI) < 0.02 ng/ml (normal range: <0.53 ng/ml), creatinine-kinase-MB: 5.49 ng/ml (normal range: <5.0 ng/ml), myohemoglobin: 216.82 ng/ml (normal range: <110 ng/ml), D-dimer: 1214.27 ng/ml (normal range: <200 ng/ml), and B-type natriuretic peptide: 2460.72 pg/ml (normal range: <100 pg/ml). Electrocardiography indicated sinus rhythm, third-degree atrioventricular block, full-lead low voltage, QT interval prolongation, and borderline escape rhythm. Echocardiography revealed a hypoechoic mass extending from the right atrium to the right ventricle and obstructing the forward flow of the tricuspid valve. The size of the mass was approximately 66 × 40 mm (Figure 1). Computed tomography revealed the following: (1) irregular shape of the right heart, with the enhanced right auricle, right atrium, and ventricle exhibiting irregular clusters and relatively weakly enhanced areas. The CT value after enhancement was approximately 70–90 HU, while the larger cross-section was approximately 6.2 × 6.9 cm. The local boundaries between the lesion, pericardium, and left atrium were unclear, while the ventricular septum was irregular and thickened; (2) the filling of the superior vena cava and left and right brachiocephalic veins was not uniform; (3) the pulmonary artery and its branches in the upper, middle, and lower lobes of the right lung were poorly developed, while the local lumen was suspected to be uneven, exhibiting a few patchy and slightly low-density shadows. A suspicious low density shadow was observed at the edge of the upper and lower pulmonary arteries of the left lung; (4) the two lungs were dispersed with flaky shadows of increased density, the volume of the lower lobe of the left lung was reduced, a dense shadow was present in some lung tissues, and the enhancement was visible; (5) the bronchial segment of the left inferior lobe of the lung was slightly narrowed, while part of the bronchus of the left inferior lobe was unclear; (6) pericardial effusion, bilateral pleural effusion, left interlobar fissure, and adjacent lung hypoinflation; (7) the thoracic section of the esophageal wall was slightly thickened, approximately 0.4 cm; (8) swelling of left axilla, chest wall, and back soft tissue; (9) abdominal fluid, the local adipose space in the abdominal area was seen as lamellar and slightly high-density shadows; (10) multiple small veins in inferior vena cava and right lobe of liver were developed in advance; and (11) the adipose space in the abdominal cavity was blurred, with multiple pieces being increasingly flocculent, while the fascia around both kidneys was thickened (Figure 2).

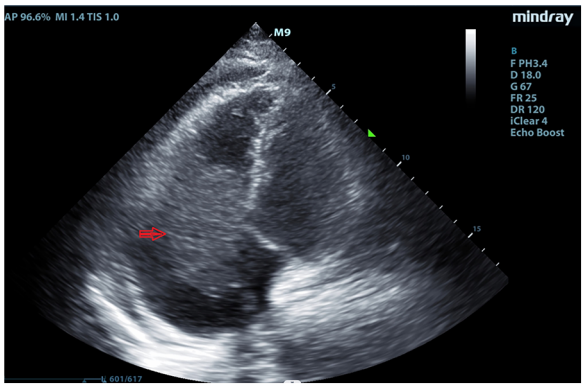

FIGURE 1
Echocardiography revealed a hypoechoic mass extending from the right atrium to the right ventricle in September 2, 2022.

September 3, 2022, hematological tests revealed the following: reduced lymphocyte ratio (8.1%, normal range: 20%–50%), platelet count (88×10^9, normal range: $100–300 \times 10^9$), prothrombin time activity (36%, normal range: 70%–130%), and level of plasma fibrinogen (1.7 g/L, normal range: 2–4 g/L), whereas elevated neutrophil ratio (76.3%, normal range: 40%–75%), level of high-sensitivity C-reactive protein (40.25 mg/L, normal range: 0–10 mg/L), prothrombin time (23.1 s, normal range: 9.6–12.8 s), international normalized ratio (2.05, normal range: 0.88–1.15), activated partial thromboplastin time (46 s, normal range: 24.8–33.8 s), and levels of D-dimer (8.52 μg/ml, normal range: <200 ng/ml), fibrinogen degradation product (25.5 μg/ml, normal range: 0–5 μg/ml), cTNI (74.8 pg/ml), myohemoglobin (476.54 ng/ml), N-terminal brain natriuretic peptide (700.7 pg/ml, normal range: <100 pg/ml), alanine transaminase (ALT) (1,202 U/L, normal range: 9–50 U/L), aspartate transaminase (AST) (806 U/L, normal range: 15–40 U/L), total bilirubin (72.1 μmol/L, normal range: <26 μmol/L), direct bilirubin (40.8 μmol/L, normal range: <4 μmol/L), indirect bilirubin (31.3 μmol/L, normal range: <22 μmol/L), urea (27.97 mmol/L, normal range: 3.6–9.5 mmol/L), creatinine (203 μmol/L, normal range: 57–111 μmol/L), and uric acid (1,265 *M*mol/L, normal range: 208–428 μmol/L). On September 4, 2022, the patient underwent preoperative preparation, and the right atrial and right ventricular masses were removed using

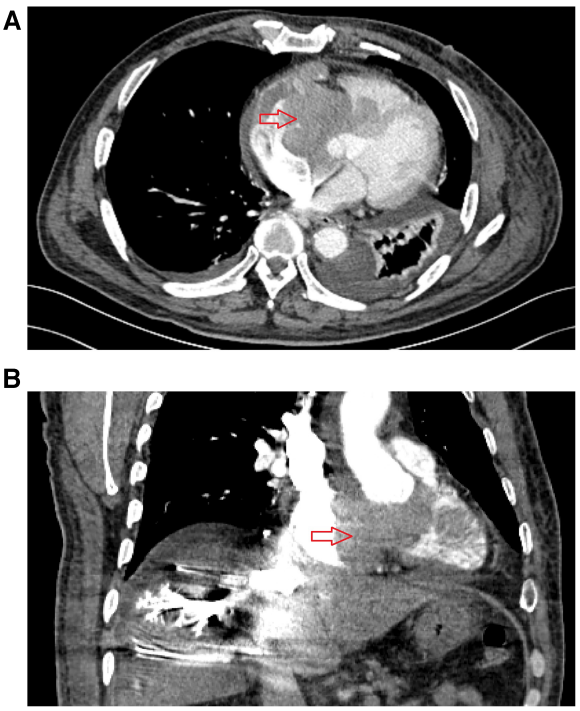

FIGURE 2
Preoperative enhanced computed tomography results for patient in September 2, 2022. (A) The cross-sectional image shows a mass in the right atrium, with irregular patchy enhancement in the right atrial appendage, right atrium, and right ventricular region, with a CT value of approximately 89 Hounsfield units. The interventricular septum is irregularly thickened. (B) Coronal view shows a mass in the right atrium, uneven opacification in some areas of the superior vena cava, delayed opacification of the inferior vena cava and veins in the right lobe of the liver.

tracheal intubation cardiopulmonary bypass. Pericardial mediastinal drainage was performed and a temporary cardiac pacemaker was implanted during surgery. Intraoperative findings included the following: (1) multiple irregular gray neoplasms in the right atrium, which was characterized by less smooth surfaces and a maximum diameter of approximately 7 cm. The base was located in the atrial septum, which had grown compact with the tricuspid valve without gaps. An increased number of mural thrombi were present around the tumor body of the right atrium, with some thrombi being embedded in the dressing muscle of the right atrium; (2) several new organisms with a diameter of approximately 3 cm were observed in the right ventricular chamber, which straddled the tricuspid valve opening, resulting in severe blockage of the tricuspid valve; (3) the tumor profile was yellow and fish-like; (4) some tumors were not densely adhered to the tricuspid septum, while the tricuspid ring was slightly enlarged, and the water injection test showed mild regurgitation. Postoperative pathological examination revealed a bunch of grayish white tissue with a total volume of $7.5 \times 6.5 \times 3$ cm. Focal hemorrhage and necrosis were observed in this section. Microscopically, the lymphocytic phenotype was diffuse and scattered among histiocytes, small lymphocytes, and nuclear fragments. Immunohistochemical examination revealed the following: medium large heterogeneous lymphocyte CD20 (+), CD19 (+), CD22 (+), CD10 (−), BCL-6 (+), MUM-1 (+), CD30 (−), BCL-2 (+, 90%), C-MYC (+, 50%), Ki-67(+, 90%), CD3 (−), CD5 (−), CyclinD1 (−), TDT (−), p53 (+, 70%), and PCK (−). Fluorescence *in situ* hybridization analysis showed no separation rearrangement of BCL-6, BCL-2, and MYC. Therefore, the patient was diagnosed as having the non-germinal center B cell (non-GCB) subtype of diffuse large B-cell lymphoma. BCL-2, C-MYC double expression. Bone marrow biopsy and flow cytometry revealed no lymphocytic infiltration. On September 5, 2022, the patient presented elevated levels of ALT (204 U/L), AST (297 U/L), total bilirubin (100 μmol/L), direct bilirubin (35 μmol/L), indirect bilirubin (65 μmol/L), urea (27.88 mmol/L), creatinine (280 μmol/L), uric acid (1,045 μmol/L), as well as increased prothrombin time (17.8 s), international normalized ratio (1.46), and activated partial thromboplastin time (50.9 s), whereas prothrombin time activity (55%), and the level of plasma fibrinogen (1.93 g/L) were significantly reduced. A permanent pacemaker was placed after the patient stabilized.

On October 19, 2022, echocardiography revealed an enlarged left atrium and a hypoechoic mass extending from the right atrium to the right ventricle with an irregular shape and a size of approximately 85×54 mm was (Figure 3A). The boundary between the mass and tricuspid septum was unclear, while the atrial septum was infiltrated by the mass, suggesting tumor recurrence and severe tricuspid stenosis. The patient was administered an rituximab, cyclophosphamide, doxorubicin, vincristine, and prednisone (R-CHOP) regimen. On November 1, 2022, echocardiography revealed the irregular shape of the right atrium, a solid mass measuring 25×21 mm, adhesion to the root of the tricuspid septum and lower atrial septum, enlargement of the left and right atria, widening of the aortic sinus, severe tricuspid regurgitation, and arrhythmia, with an ejection fraction of 71% (Figure 3B). Chest computed tomography showed exudation of the mediastinum and pericardium, slightly increased levels of blood and fluid, pneumonia, bilateral pleural effusion with atelectasis of the adjacent lung tissue, slightly narrowed left dorsal segment bronchus of the lower lobe of the lung due to compression, and aortic and coronary area calcification. Next-generation sequencing of the mass indicated a class I variation of *CD79B* (+), C.587A > C, which suggesting The adenine (A) at the 587th base position of the CD79B gene is replaced by cytosine (C). After three months post-surgery, the patient died due to severe lung infection following chemotherapy.

3 Discussion

Primary cardiac lymphoma, of which diffuse B-cell lymphoma is the main pathological type, is extremely rare. The disease often involves the right atrium, right ventricle, atrial septum, and inferior vena cava. We reported a patient with highly aggressive CD20 (+) B-cell lymphoma, which invaded the right atrium,

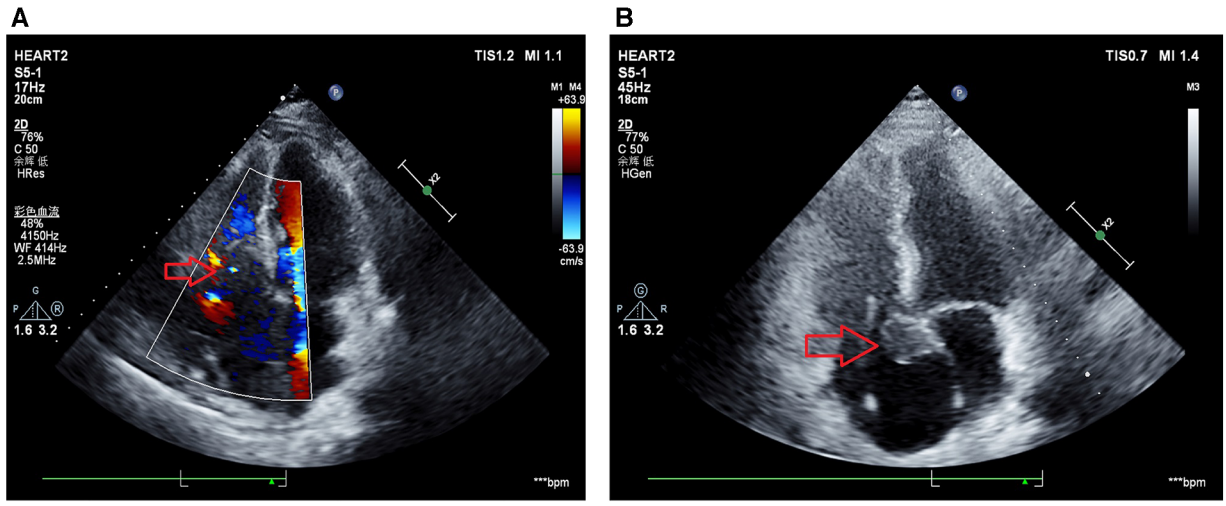

FIGURE 3
Echocardiography results after surgical resection. (A) Echocardiogram results at October 19, 2022 indicated a hypoechoic mass with irregular shape measuring approximately 85 mm × 54 mm is observed from the right atrium to the right ventricle. The boundary between the mass and the tricuspid valve is unclear, and the mass infiltrates the interatrial septum, suggesting tumor recurrence (with an increased size compared to pre-surgery) and severe tricuspid valve stenosis. (B) Echocardiogram results at November 1, 2022 indicated irregularly shaped solid mass in the right atrium, measuring 25 mm × 21 mm, adhering to the septal leaflet and inferior interatrial septum, with enlargement of the left and right atria, dilation of the aortic sinus, and severe tricuspid regurgitation.

right ventricle, and atrial septum and involved the tricuspid septum, resulting in severe tricuspid stenosis. The clinical manifestations of primary cardiac lymphoma lack specificity and are closely related to tumor size, location, and complications. Right heart tumors can cause venous congestion, and their enlargement aggravates the disease. Tumors can invade the atrioventricular valve and cause stenosis or incomplete closure of the valve. The main clinical symptoms include congestive heart failure (31%–78%), chest pain (19%–46%), and arrhythmia (8%–56%) (8, 9). Other less common symptoms include the superior vena cava syndrome (10–12), odynophagia (6), and embolic phenomena (13). In this paper, we noted that the patient presented with dyspnea, edema, multiple serous effusions, hepatic and renal dysfunction, coagulation dysfunction, sinus rhythm, third-degree atrioventricular block, full-lead low voltage, QT interval prolongation, and a borderline escape rhythm.

Numerous studies have reported cases of primary cardiac lymphoma accompanied by atrioventricular block (Table 1) (14–25). The age of patients included in these studies ranged from 36.0 to 80.0 years, with 58.3% of them being men. Of the 12 included patients, 2 had primary cardiac T-cell lymphoma and most had complete atrioventricular block. All patients underwent surgical resection, pacemaker implantation, and chemotherapy, resulting in the complete remission or reduced mass size of tumors and a better prognosis. The primary treatment for cardiac lymphoma was chemotherapy; however, some patients presented with extensive myocardial involvement, which could cause sudden cardiac arrest (26, 27). Thus, surgical resection was performed first in patients at high risk of sudden cardiac events due to cardiac involvement. An alternative method for treating atrioventricular block was surgical epicardial lead implantation, particularly in patients presenting with broad cardiac involvement. Complete atrioventricular block was always caused by infiltration of the conduction system by primary cardiac lymphoma, and pacemaker lead implantation was always performed owing to bradycardia-induced heart failure (27).

Accurate diagnosis at an early stage is particularly important for patients with primary cardiac lymphoma (28). Imaging examinations could be considered useful tools for detecting masses in the heart; however, imaging examinations do not provide a definitive diagnosis. However, echocardiography can provide information regarding the location, size, and activity of the tumor, tumor involvement in the atrioventricular valve, and cardiac function. Once echocardiography suggests a malignant tumor in the heart, computed tomography and cardiac magnetic resonance imaging can be performed to observe tumor infiltration and the relationship with surrounding tissues, providing information for surgical planning. Furthermore, positron emission tomography-computed tomography can comprehensively determine the presence of distant metastasis and the presence of other extracardiac tumors. These diagnostic tools can provide further information guiding personalized treatments. Of note, endomyocardial biopsy is considered a valuable tool for diagnosing intracardiac masses and arrhythmogenic cardiomyopathies (23). In our paper, the patient underwent echocardiography and computed tomography to detect the tumor location, while an endomyocardial biopsy was performed to assess the primary cardiac lymphoma.

TABLE 1 The summary results for primary cardiac lymphoma with atrioventricular block.

Study	Gender	Age (years)	Disease status	Clinical symptoms	Imaging diagnosis	Treatments	Prognosis
Frikha et al. (14)	Male	64.0	Non-Hodgkin large B-cell lymphoma	Cardiac tamponade and paroxysmal third-degree atrioventricular block	Echocardiography, computed tomography, coronary angiography	Surgical resection and R-CHOP	The size of the mass was reduced
Crisel et al. (15)	Male	55.0	Diffuse large B-cell lymphoma	Complete atrioventricular block	Echocardiography, cardiac magnetic resonance imaging	Pacemaker implantation and R-EPOCH	No identifiable tumor
Chen et al. (16)	Male	36.0	Primary diffuse cardiac large B-cell lymphoma	Atrioventricular block and paroxysmal ventricular tachycardia	Echocardiography, computed tomography	COP, CHOP, and R-CHOP	Adequate global systolic and diastolic functions, with significant reduction of myocardial thickness and resolution of pericardial effusion
Wang et al. (17)	Female	70.0	Primary cardiac T-cell lymphoma	Complete atrioventricular block and torsades de pointes	Echocardiography, computed tomography	CHOP	Complete remission
Sekar et al. (18)	Male	76.0	High-grade non-Hodgkin's lymphoma of B-cell type	Acute coronary syndrome and atrioventricular block	Echocardiography, computed tomography	R-GCVP	Tumor recurrence
Jang et al. (19)	Male	56.0	Diffuse large B-cell lymphoma	Atrioventricular block	Echocardiography, cardiac magnetic resonance imaging, positron emission tomography-computed tomography	Surgical resection, pacemaker implantation, R-CHOP	Complete remission
Usry et al. (20)	Female	80.0	C-MYC positive, EBV-negative, Burkitt lymphoma	Symptomatic complete heart block	Echocardiography, cardiac magnetic resonance imaging, coronary angiography	Pacemaker implantation and R-CHOP	The size of the mass was reduced
Al Mawed et al. (21)	Female	73.0	Diffuse large B-cell non-Hodgkin lymphoma of non-germ-cell type	Atrial flutter and atrioventricular block	Echocardiography, cardiac magnetic resonance imaging, positron emission tomography-computed tomography	Pacemaker implantation, R-mini-CHOP and R-CHOP	Complete remission
Hu et al. (22)	Male	70.0	Non-germinal centre diffuse large B-cell lymphoma	Complete atrioventricular block	Echocardiography, computed tomography, positron emission tomography-computed tomography	R-EPOCH	The size of the mass was reduced
Chen et al. (23)	Female	47.0	Primary cardiac T-cell lymphoma	Complete atrioventricular block	Echocardiography, cardiac magnetic resonance imaging, computed tomography, positron emission tomography-computed tomography	MTX-CHOP	Complete remission
Shigeno et al. (24)	Female	55.0	Diffuse large B-cell lymphoma	Complete atrioventricular block	Echocardiography, computed tomography	Surgical resection, epicardial lead implantation, R-CHOP	Complete remission
Mao et al. (25)	Male	64.0	Primary diffuse cardiac large B-cell lymphoma	Complete atrioventricular block	Echocardiography, computed tomography, positron emission tomography-computed tomography	Pacemaker implantation, R-COP and R-CDOP	The size of the mass was reduced

4 Conclusions

This paper described the clinical course of a patient with a non-GCB subtype of diffuse large B-cell lymphoma diagnosed via endomyocardial biopsy. Echocardiography and computed tomography were used as imaging diagnostic tools, and the patient underwent surgical resection of the right atrial and right ventricular masses through tracheal intubation cardiopulmonary bypass. Furthermore, a permanent pacemaker was placed after the patient stabilized, followed by administration of R-CHOP as the chemotherapy regimen. After chemotherapy, the size of the tumor was reduced, indicating remission.

Data availability statement

The original contributions presented in the study are included in the article/Supplementary Material, further inquiries can be directed to the corresponding author.

Ethics statement

Ethical approval was not required for the studies involving humans because standard care is performed in this case report. The studies were conducted in accordance with the local legislation and institutional requirements. The participants provided their written informed consent to participate in this study. Written informed consent was obtained from the individual(s) for the publication of any potentially identifiable images or data included in this article.

Author contributions

JL: Conceptualization, Data curation, Formal Analysis, Writing – original draft, Writing – review & editing. YZ: Conceptualization, Data curation, Formal Analysis, Writing – original draft, Writing – review & editing. WZ: Data curation, Formal Analysis, Writing – review & editing. JX: Data curation, Formal Analysis, Writing – review & editing. YZ: Conceptualization, Formal Analysis, Project administration, Writing – review & editing. LT: Data curation, Formal Analysis, Writing – review & editing.

Funding

The author(s) declare that no financial support was received for the research, authorship, and/or publication of this article.

Conflict of interest

The authors declare that the research was conducted in the absence of any commercial or financial relationships that could be construed as a potential conflict of interest.

Publisher's note

All claims expressed in this article are solely those of the authors and do not necessarily represent those of their affiliated organizations, or those of the publisher, the editors and the reviewers. Any product that may be evaluated in this article, or claim that may be made by its manufacturer, is not guaranteed or endorsed by the publisher.

References

1. He S, Cao Y, Qin W, Chen W, Yin L, Chai H, et al. Prevalence of primary cardiac tumor malignancies in retrospective studies over six decades: a systematic review and meta-analysis. *Oncotarget*. (2017) 8:43284–94. doi: 10.18632/oncotarget.17378

2. Sheppard M, Angelini A, Raad M, Savelieva I. Tumours of the heart. In: Camm AJF, Luscher T, Serruys PW, editors. *The ESC Textbook of Cardiovascular Medicine*. London: Blackwell (2006). p. 535–52.

3. Curtsinger CR, Wilson MJ, Yoneda K. Primary cardiac lymphoma. *Cancer*. (1989) 64:521–5. doi: 10.1002/1097-0142(19890715)64:2<521::AID-CNCR2820640227>3.0.CO;2-T

4. Zaharia L, Gill PS. Primary cardiac lymphoma. *Am J Clin Oncol*. (1991) 14:142–5. doi: 10.1097/00000421-199104000-00009

5. Miguel CE, Bestetti RB. Primary cardiac lymphoma. *Int J Cardiol*. (2011) 149:358–63. doi: 10.1016/j.ijcard.2010.02.016

6. Antoniades L, Eftychiou C, Petrou PM, Bagatzounis A, Minas M. Primary cardiac lymphoma: case report and brief review of the literature. *Echocardiography*. (2009) 26:214–9. doi: 10.1111/j.1540-8175.2008.00757.x

7. Montiel V, Maziers N, Dereme T. Primary cardiac lymphoma and complete atrio-ventricular block: case report and review of the literature. *Acta Cardiol*. (2007) 62:55–8. doi: 10.2143/AC.62.1.2019372

8. Gordon MJ, Danilova O, Spurgeon S, Danilov AV. Cardiac non-Hodgkin's lymphoma: clinical characteristics and trends in survival. *Eur J Haematol*. (2016) 97:445–52. doi: 10.1111/ejh.12751

9. Carras S, Berger F, Chalabreysse L, Callet-Bauchut E, Cordier J-F, Salles G, et al. Primary cardiac lymphoma: diagnosis, treatment and outcome in a modern series. *Hematol Oncol*. (2017) 35:510–9. doi: 10.1002/hon.2301

10. Habertheuer A, Ehrlich M, Wiedemann D, Mora B, Rath C, Kocher A. A rare case of primary cardiac B cell lymphoma. *J Cardiothorac Surg*. (2014) 9:14. doi: 10.1186/1749-8090-9-14

11. Johri A, Baetz T, Isotalo PA, Nolan RL, Sanfilippo AJ, Ropchan G. Primary cardiac diffuse large B cell lymphoma presenting with superior vena cava syndrome. *Can J Cardiol*. (2009) 25:e210–2. doi: 10.1016/S0828-282X(09)70110-2

12. van Rooijen CR, Scholtens AM, de Jong CN, Saraber CE, van de Donk NWCJ. Primary cardiac lymphoma with central nervous system relapse. *Clin Case Rep*. (2017) 5:1454–8. doi: 10.1002/ccr3.1094

13. Liu X, Liu P, Li J. EBV+ diffuse large B-cell lymphoma arising within atrial myxoma in Chinese immunocompetent patient. *Int J Clin Exp Pathol*. (2015) 8:2159–64.

14. Frikha Z, Abid L, Abid D, Mallek S, Frikha I, Abdennadher M, et al. Cardiac tamponade and paroxysmal third-degree atrioventricular block revealing a primary cardiac non-Hodgkin large B-cell lymphoma of the right ventricle: a case report. *J Med Case Rep*. (2011) 5:433. doi: 10.1186/1752-1947-5-433

15. Crisel RK, Knight BP, Kim SS. Reversible, complete atrioventricular block caused by primary cardiac lymphoma in a nonimmunocompromised patient. *J Cardiovasc Electrophysiol*. (2012) 23:1386–9. doi: 10.1111/j.1540-8167.2012.02343.x

16. Chen K-W, Chang J-H, Yeh S-P, Lu C-R. Primary cardiac B-cell lymphoma with atrioventricular block and paroxysmal ventricular tachycardia. *J Cardiothorac Surg*. (2012) 7:70. doi: 10.1186/1749-8090-7-70

17. Wang T-L, Lai C-H, Liou J-Y, Lo H-M, Shyu K-G. Complete AV block and torsades de pointes in a case of primary cardiac T-cell lymphoma. *Acta Cardiol Sin*. (2015) 31:245–8. doi: 10.6515/acs20141117a

18. Sekar B, Swami G, Ibrahim A, Hanna A, Payne MN, Seale JR, et al. 76-year-old Gentlemen with primary cardiac lymphoma presenting as acute coronary syndrome and atrioventricular block. *BJR Case Rep*. (2016) 2:20150466. doi: 10.1259/bjrcr.20150466

19. Jang G-W, Chung H, Kim W-S, Lee JM. Primary cardiac lymphoma manifesting as an atrioventricular block in a renal transplantation recipient. *JACC Case Rep*. (2020) 2:600–3. doi: 10.1016/j.jaccas.2020.01.028

20. Usry CR, Wilson AS, Bush KNV. Primary cardiac lymphoma manifesting as complete heart block. *Case Rep Cardiol*. (2020) 2020:3825312. doi: 10.1155/2020/3825312

21. Al Mawed M, Brockmeier J, Haertel D, Ellermeier M, Hartmann F, Gielen S. From inoperable to back to life: a case report of successfully treated obstructive right ventricular primary cardiac lymphoma. *Eur Heart J Case Rep*. (2022) 6:ytac051. doi: 10.1093/ehjcr/ytac051

22. Hu B, Zhao J, Liang X, Ren C, Li N, Liang C. A case of complete atrioventricular block associated with primary cardiac lymphoma reversed without cardiac pacemaker implantation. *J Int Med Res*. (2022) 50:3000605221089780. doi: 10.1177/03000605221089780

23. Chen P, Hao Y, Qiu X, Xiao X, Zhu W, Xu Y, et al. Case report: primary cardiac T-cell lymphoma with complete atrio-ventricular block diagnosed by endomyocardial biopsy. *Front Immunol*. (2022) 13:890059. doi: 10.3389/fimmu.2022.890059

24. Shigeno R, Okada T, Koyama T, Furukawa Y. Surgical resection and epicardial lead implantation for primary cardiac lymphoma with a complete atrioventricular block: a case report. *Eur Heart J Case Rep*. (2023) 7:ytad035. doi: 10.1093/ehjcr/ytad035

25. Mao J, Xu Y, Zhu M, Wang L, Hou Y. Case report: complete atrio-ventricular block successfully reversed in newly diagnosed primary cardiac B-cell lymphoma. *Front Med*. (2023) 10:1119286. doi: 10.3389/fmed.2023.1119286

26. Sultan I, Aranda-Michel E, Habertheuer A, Kilic A, Arnaoutakis G, Bianco V, et al. Long-term outcomes of primary cardiac lymphoma. *Circulation*. (2020) 142:2194–5. doi: 10.1161/CIRCULATIONAHA.120.047215

27. Ottaviani G, Matturri L, Rossi L, Jones D. Sudden death due to lymphomatous infiltration of the cardiac conduction system. *Cardiovasc Pathol*. (2003) 12:77–81. doi: 10.1016/S1054-8807(02)00168-0

28. Csizmar CM, Sachs Z, Cayci Z, Bu L, Linden MA. Primary cardiac lymphoma: three case reports and a review of the literature. *Open J Blood Dis*. (2021) 11:120–32. doi: 10.4236/ojbd.2021.114012

frontiers | Frontiers in Cardiovascular Medicine

TYPE Case Report
PUBLISHED 29 February 2024
DOI 10.3389/fcvm.2024.1337957

OPEN ACCESS

EDITED BY
Reto Asmis,
Wake Forest University, United States

REVIEWED BY
James Cotton,
Royal Wolverhampton Hospitals NHS Trust, United Kingdom
Matteo Nardin,
Asst degli Spedali Civili di Brescia, Italy

*CORRESPONDENCE
Cezar Iliescu
✉ ciliescu@mdanderson.org

RECEIVED 13 November 2023
ACCEPTED 29 January 2024
PUBLISHED 29 February 2024

CITATION
Ali A, Jewani P, Bourdillon M, Koutroumpakis E, Khalaf S, Charitakis K, Thompson K, Marmagkiolis K, Deswal A and Iliescu C (2024) Navigating P2Y12 inhibition in the labyrinth of cardio-oncology care: cangrelor bridging in patients with cancer.
Front. Cardiovasc. Med. 11:1337957.
doi: 10.3389/fcvm.2024.1337957

Navigating P2Y12 inhibition in the labyrinth of cardio-oncology care: cangrelor bridging in patients with cancer

Abdelrahman Ali[1], Poonam Jewani[1], Max Bourdillon[2], Efstratios Koutroumpakis[1], Shaden Khalaf[1], Konstantinos Charitakis[2], Kara Thompson[1], Konstantinos Marmagkiolis[1], Anita Deswal[1] and Cezar Iliescu[1]*

[1]Department of Cardiology, MD Anderson Cancer Center, Houston, TX, United States, [2]Division of Cardiology, Department of Medicine, McGovern Medical School, University of Texas, Houston, TX, United States

Cangrelor, a potent intravenous P2Y12 platelet inhibitor, has demonstrated effectiveness in reducing ischemic events without a corresponding increase in severe bleeding during percutaneous coronary intervention, as evidenced by the CHAMPION-PHOENIX trial. Its off-label role as a bridging antiplatelet agent for patients facing high thrombotic risks who must temporarily stop oral P2Y12 inhibitor therapy further underscores its clinical utility. This is the first case series to shed light on the application of cangrelor in cancer patients needing to pause dual antiplatelet therapy for a range of medical interventions, marking it as a pioneering effort in this domain. The inclusion of patients with a variety of cancer types and cardiovascular conditions in this series underlines the adaptability and critical role of cangrelor in managing the dual challenges of bleeding risk and the need for uninterrupted antiplatelet protection. By offering a bridge for high-risk cancer patients who have recently undergone percutaneous coronary intervention and need to halt oral P2Y12 inhibitors temporarily, cangrelor presents a practical solution. Early findings indicate it can be discontinued safely 2-4 h before medical procedures, allowing for the effective reintroduction of oral P2Y12 inhibitors without adverse effects. This evidence calls for expanded research to validate and extend these preliminary observations, emphasizing the importance of further investigation into cangrelor's applications in complex patient care scenarios.

KEYWORDS

coronary artery disease, cangrelor, thrombocytopenia, bridging, P2Y12 Inhibitors

Introduction

Cangrelor, an intravenous P2Y12 platelet inhibitor, has reduced the rate of ischemic events compared with oral P2Y12 inhibition, without causing significant increases in severe bleeding during percutaneous coronary intervention (PCI), as demonstrated by the CHAMPION-PHOENIX randomized controlled trial (RCT) (1). In addition, cangrelor has been used off-label as bridging antiplatelet therapy in patients with PCI at high thrombotic risk who require early (within 3–6 months) interruption of their oral P2Y12 inhibitor therapy (2). Advancements in cancer therapy have improved

patient survival rates, leading to an increased number of cardiac procedures, such as PCI, among patients treated for cancer. However, there is limited information on the utilization of cangrelor in patients with cancer, particularly in those with thrombocytopenia (3). In this study, we present a single-center case series of cangrelor bridging in patients with cancer and recent PCI that required temporary interruption of dual antiplatelet therapy (DAPT).

Case 1

A 69-year-old woman with a past medical history (PMH) of IgA kappa multiple myeloma (MM) with a history of autologous stem cell transplant on maintenance lenalidomide, end-stage renal disease on peritoneal dialysis, saphenous venous thrombosis, and coronary artery disease (CAD) with recent non-ST-segment elevation myocardial infarction (NSTEMI) had a PCI to the mid-left anterior descending artery (LAD) 3 months prior to presentation with melena and acute on chronic anemia (hemoglobin 5.6 g/dl). The patient was taking both clopidogrel and apixaban prior to admission and was noted to have an allergy to aspirin. On admission, both clopidogrel and apixaban were held due to concerns for gastrointestinal (GI) bleeding. The patient underwent a coronary angiogram with optical coherence tomography (OCT), which revealed suboptimal apposition of the previously implanted LAD stent (by approximately 20%). The interventional cardiology team recommended the initiation of cangrelor on day 3 of admission in anticipation of further GI evaluation. The patient underwent an upper GI endoscopy on hospital day 6 and no active bleeding was observed. Cangrelor infusion was discontinued after endoscopy, and clopidogrel was resumed with a 300 mg loading dose. The patient's apixaban was not resumed at discharge as the patient no longer had an indication for apixaban after consultation with the hematology service and also due to thrombocytopenia (39 K/μL).

Case 2

A 55-year-old woman with metastatic gallbladder adenocarcinoma, hypertension, type II diabetes, and CAD, who underwent a PCI of a bifurcating lesion of the distal right coronary artery (RCA) extending into posterolateral and posterior descending artery (PDA) branches with two drug-eluting stents (DES) 2 months prior to the current admission, presented with biliary obstruction. The patient was on DAPT with aspirin and clopidogrel prior to admission. The last dose of clopidogrel was administered on day 2 of hospitalization, and cangrelor was initiated on day 3 with the recommendation to hold 4 h prior to the planned procedure. The patient underwent an endoscopic retrograde cholangiopancreatography (ERCP) with stent placement on day 8. Cangrelor was discontinued postprocedure, and clopidogrel was restarted 2 days post procedure with a 300 mg loading dose, followed by standard 75 mg daily dosing.

Case 3

A 64-year-old man with relapsed diffuse large B-cell lymphoma s/p chimeric antigen receptor (CAR) *T*-cell therapy (10 days prior to presentation), atrial fibrillation, and ischemic cardiomyopathy (ICM) underwent a high-risk PCI (10 weeks prior to hospital admission) with three overlapping stents in the ostial to mid-LAD, and residual RCA chronic total occlusion, was hospitalized for fever and profound fatigue. The patient's home DAPT of aspirin and clopidogrel was initially continued during hospital stay. On hospital day 5, the patient received his last dose of clopidogrel, and cangrelor was initiated the following day in preparation for a planned endoscopic evaluation for cytomegalovirus colitis. Aspirin was discontinued 2 days after cangrelor initiation because of worsening thrombocytopenia (platelet count, 32 K/μl). Given the patient's clinical improvement, elevated cardiac risk, and altered mental status, colonoscopy was deferred, and clopidogrel was restarted without a loading dose (platelet count, 21 K/μl). He was discharged on clopidogrel monotherapy because of significant thrombocytopenia (platelet count <50 K/μl).

Case 4

A 74-year-old woman with metastatic ovarian cancer (including pulmonary metastases and peritoneal involvement), hypertension, and CAD s/p PCI to mid-LAD (3 weeks prior to presentation) presented with small bowel obstruction. She was on DAPT with aspirin and ticagrelor prior to admission. Resumption of the patient's DAPT was complicated by a strict nothing by mouth (NPO) status. Rectal aspirin was recommended, but the patient deferred in taking it. In lieu, heparin infusion was initiated on the first day of hospitalization, and she was eventually transitioned to cangrelor on day 4 of admission, as it was unclear when the patient would be able to resume oral antiplatelet therapy. A gastrostomy tube (G-tube) was placed by interventional radiology on day 8 of the patient's hospitalization, for which cangrelor was held 3 h prior to the procedure. DAPT was resumed the following day with a 180 mg loading dose of ticagrelor. The patient was eventually transitioned to home hospice care.

Case 5

An 82-year-old man with a history of IgG kappa MM, AL-amyloidosis, CAD s/p coronary artery bypass graft (CABG) with left internal mammary artery (LIMA) to the LAD and saphenous vein graft (SVG) to PDA, and a recent NSTEMI treated with DES implantation to the left main coronary artery (LMCA) into the left circumflex artery (LCX) 6 weeks prior, presented with a right intertrochanteric lytic lesion. This lesion was associated with a non-displaced pathological fracture, necessitating surgical stabilization. The patient was

on DAPT with aspirin and clopidogrel at home. While aspirin was continued on admission, clopidogrel was replaced with cangrelor. The procedure was performed on day 5 of hospitalization, and cangrelor was held for 2 h prior to procedure. Cangrelor infusion was resumed in the evening of the procedure, and the patient was transitioned back to clopidogrel with a loading dose of 300 mg two days later when the risk of bleeding was considered to be low by the primary team.

Case 6

A 68-year-old man with a history of a newly diagnosed metastatic mesenteric mass to the liver, hypertension, type II diabetes, ST-segment elevation myocardial infarction (STEMI) treated with PCI to the proximal LAD 5 months earlier, and moderate aortic valve stenosis, presented to the hospital for an elective interventional radiology (IR)-guided biopsy. The patient had been on DAPT with aspirin and clopidogrel. Upon admission, aspirin was continued, clopidogrel was discontinued, and cangrelor bridging was initiated. A liver biopsy was performed on day 6 of hospitalization, and cangrelor was held 3 h prior to the procedure. The following day, clopidogrel was resumed with a 300 mg loading dose. The biopsy revealed a metastatic well-differentiated neuroendocrine tumor.

Case 7

An 85-year-old man with a history of salivary duct carcinoma of the right lower eyelid, hypertension, and CAD with PCI to the distal RCA 6 months prior for NSTEMI was admitted for cangrelor bridging prior to excision of a malignant lesion of the eyelid. Both aspirin and clopidogrel were to be stopped in the perioperative period, given the high risk of bleeding due to extensive surgery and reconstruction within the orbit, and the risk of vision loss if bleeding occurred. On admission, periprocedural cangrelor bridging was initiated. After a 1-week washout, the patient underwent the procedure uneventfully. Aspirin and clopidogrel were resumed 2 days after the procedure (both without loading doses per request from the surgical team).

Discussion

Patients with cancer present an elevated risk for both bleeding and thrombotic events. Managing patients who have CAD and stents in the context of cancer therapy is a complex task due to the frequent need for a shortened duration of DAPT. This is the first single-center experience with bridging antiplatelet therapy using cangrelor in patients with cancer undergoing non-cardiac interventions. Landmark RCTs such as CHAMPION-PCI, CHAMPION-PLATFORM, and CHAMPION-PHOENIX excluded patients with active cancer (1, 4, 5). Moreover, patients with cancer were not included in the BRIDGE trial, which assessed bridging antiplatelet therapy with cangrelor in patients undergoing CABG (2). The BRIDGE trial specifically consisted of two stages, an initial dose-finding phase for cangrelor, followed by a randomized, double-blind, placebo-controlled trial of 210 patients with acute coronary syndrome (ACS) or with a coronary stent receiving P2Y12 inhibitor therapy and awaiting CABG surgery. The trial demonstrated that preoperative use of cangrelor was associated with a reduction in platelet reactivity without an increase in CABG surgery–related bleeding. The median duration of cangrelor infusion was 2.8 days and median time from discontinuation to surgical incision was 3.2 h.

Expert consensus from the Society for Cardiovascular Angiography and Interventions in late 2016 did not offer recommendations for bridging with cangrelor in patients with active cancer, who may have concomitant thrombocytopenia due to the limited collective experience accumulated in the short time from FDA approval of cangrelor was June 2015 (6). However, the document stated that thrombocytopenia does not have a protective role against ischemic events, and in some specific malignancies with blood dyscrasias, it poses an increased thrombotic risk (7).

All patients in this case series had active cancer, including multiple myeloma, neuroendocrine tumor, lymphoma, gallbladder cancer, and ovarian cancer. The mean duration of cangrelor bridging was approximately 4.5 days (Table 1), and all patients except one underwent a PCI for ACS within 6–24 weeks of admission. The dose of cangrelor used for all seven patients was 0.75 μg/kg/min, which is consistent with the BRIDGE trial (2). The age range of the patients was 55–85 years old. None of the patients experienced any bleeding or thrombotic events during bridging therapy or postprocedure. Cangrelor has a very short half-life of 3–6 min. In the BRIDGE trial, it was discontinued 1–6 h before surgery. In most of our patients, we halted cangrelor 2–4 h prior to surgery or procedure based on the primary team's advice for the procedure. To date, there is only one case report in the cardio-oncology literature describing cangrelor bridging to facilitate lung biopsy in a 67-year-old patient who underwent a PCI of the mid-LAD 16 months prior to biopsy on extended DAPT therapy (3). Details of the patient's initial clinical presentation for PCI were not reported nor the rationale stated for the extended DAPT therapy. In contrast, our case series included only those patients who underwent PCI within the preceding 6 months, Several with an acute coronary syndrome indication, and required DAPT interruption.

A significant proportion of patients receiving cancer therapy and the majority of patients with active hematological malignancies have thrombocytopenia. Cangrelor has been used in patients with thrombocytopenia but not specifically in patients with cancer (8, 9). Cancer and therapy can actively modify both bleeding and thrombotic risks. Two of our patients had profound thrombocytopenia (cases 1 and 3; Figure 1), but neither experienced bleeding events. In case 1, clopidogrel monotherapy

TABLE 1 Baseline characteristics of patients receiving cangrelor.

Baseline characteristics	Case 1	Case 2	Case 3	Case 4	Case 5	Case 6	Case 7
Age (years)	69	55	64	74	82	68	85
Sex	Female	Female	Male	Female	Male	Male	Male
Baseline platelet count (K/μL)	39	383	51	256	178	222	154
CAD presentation	N-STEMI	Unstable angina	ICM	N-STEMI	N-STEMI	TSEMI	N-STEMI
Duration between index PCI and presentation (weeks)	12	8	10	3	6	20	24
Procedure	Endoscopy	ERCP	Colonoscopy	G-tube placement	Orthopedic	IR-guided biopsy	Eyelid malignant lesion excision
Duration of therapy (days)	3	5	3	4	5	5	7
Concomitant aspirin	None	Yes	Discontinued	Discontinued	Yes	Yes	None
Bleeding within 30 days	None	None	None	None	None	None	None
Ischemic within 30 days	None	None	None	None	None	None	None
Stent type	NA	Orsiro DES	Synergy DES	Synergy DES	Synergy DES	Onyx DES	NA
Number of stents	NA	2	3	1	2	NA	NA

CAD, coronary artery disease; ICM, ischemic cardiomyopathy; ERCP, endoscopic retrograde cholangiopancreatography; G-tube, gastrostomy tube; IR, interventional radiology; N-STEMI, non-ST segment elevation myocardial infarction; STEMI, ST segment elevation myocardial infarction; NA, not available; DES, drug eluting stent.

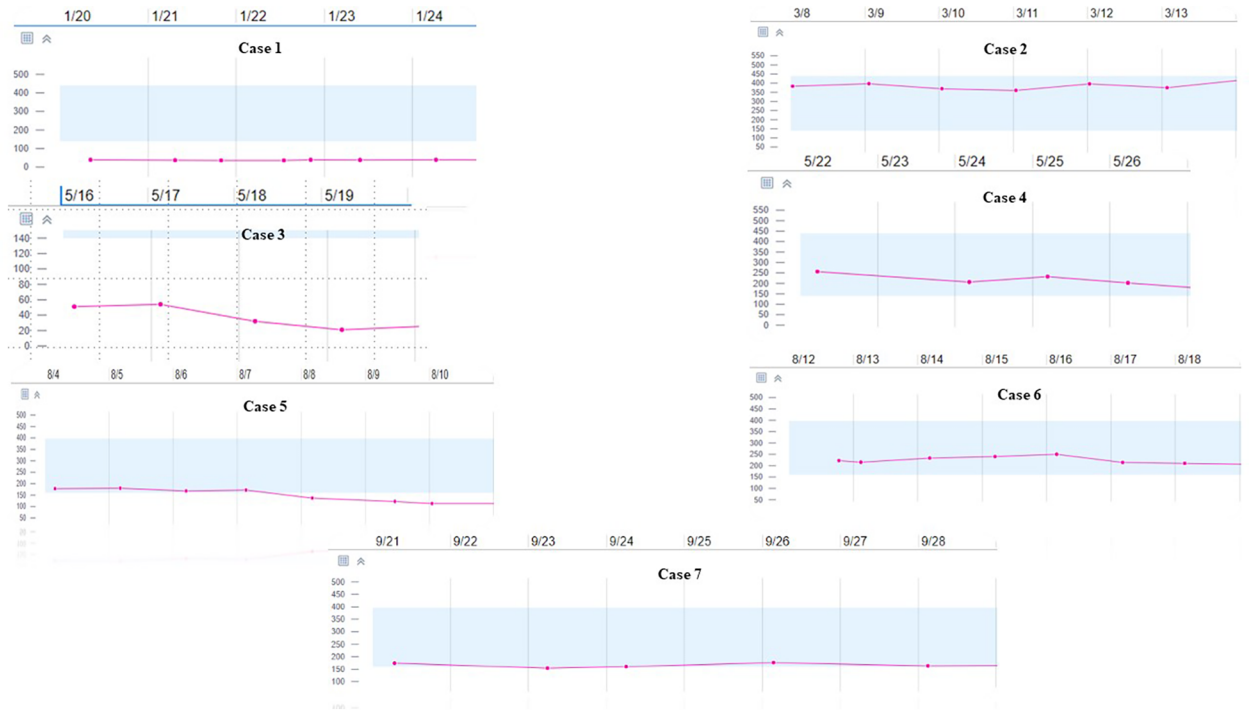

FIGURE 1
Trend of Platelet Count During Cangrelor Therapy.

was restarted after cangrelor bridging, and apixaban was not resumed as detailed, while case 3 was de-escalated to clopidogrel monotherapy at discharge due to persistent thrombocytopenia with a platelet count <50 K/μl. In a pooled analysis of the CHAMPION trials, acquired thrombocytopenia (platelet count <100 K/μl) occurred in 0.8% of the study cohort (10). In addition, periprocedural use of glycoprotein IIb/IIIa inhibitors was the strongest independent predictor of acquired thrombocytopenia. There was no statistical difference in the rate of acquired thrombocytopenia between patients who were randomized to receive either clopidogrel or cangrelor. A case report by Kabadi et al. highlighted the use of cangrelor bridging therapy in the setting of left ventricular assist device implantation in a patient with refractory cardiogenic shock post-STEMI. The patient developed acute thrombocytopenia with tirofiban use (9). However, the severity of thrombocytopenia (nadir $88 \times 10^3/mm^3$) was milder than that observed in our cardio-oncology population.

Conclusions

This report presents the use of an intravenous P2Y12 inhibitor for bridging high-risk cancer patients with recent PCI during temporary cessation of oral P2Y12 inhibitors. Preliminary data suggests that cangrelor can be used in patients with cancer and thrombocytopenia, and can be safely discontinued 2–4 h before the start of procedures. Most patients were reloaded with oral P2Y12 inhibitors without their experiencing any adverse outcomes. Tailored therapeutic strategies based on individual risks and procedures are critical. Larger prospective studies are required to address this knowledge gap, necessitating cardiology–oncology collaboration to enhance the care of this complex patient population.

Data availability statement

The original contributions presented in the study are included in the article/Supplementary Material, and further inquiries can be directed to the corresponding author.

Ethics statement

Written informed consent was not obtained from the individual(s) for the publication of any potentially identifiable images or data included in this article because no images are included in the case report. Some of the patients mentioned in this report have passed away. Written informed consent was obtained from the participant/patient(s) for the publication of this case report.

Author contributions

AA: Conceptualization, Data curation, Writing – original draft, Writing – review & editing. PJ: Writing – original draft, Writing – review & editing, Data curation. MB: Conceptualization, Writing – review & editing. EK: Writing – review & editing. SK: Writing – review & editing. KC: Writing – review & editing. KT: Writing – review & editing. KM: Writing – review & editing. AD: Supervision, Writing – review & editing. CI: Conceptualization, Supervision, Writing – review & editing.

Funding

The authors declare that no financial support was received for the research, authorship, and/or publication of this article.

Conflict of interest

The authors declare that the research was conducted in the absence of any commercial or financial relationships that could be construed as a potential conflict of interest.

Publisher's note

References

1. Bhatt DL, Stone GW, Mahaffey KW, Gibson CM, Steg PG, Hamm CW, et al. Effect of platelet inhibition with cangrelor during PCI on ischemic events. *N Engl J Med*. (2013) 368:1303–13. doi: 10.1056/NEJMoa1300815

2. Angiolillo DJ, Firstenberg MS, Price MJ, Tummala PE, Hutyra M, Welsby IJ, et al. Bridging antiplatelet therapy with cangrelor in patients undergoing cardiac surgery: a randomized controlled trial. *JAMA*. (2012) 307:265–74. doi: 10.1001/jama.2011.2002

3. Calnan MW, Crawford AN. A case report of cangrelor bridge therapy for a diagnostic bronchoscopy with biopsy. *J Pharm Pract*. (2020) 33:231–5. doi: 10.1177/0897190018795343

4. Bhatt DL, Lincoff AM, Gibson CM, Stone GW, McNulty S, Montalescot G, et al. Intravenous platelet blockade with cangrelor during PCI. *N Engl J Med*. (2009) 361:2330–41. doi: 10.1056/NEJMoa0908629

5. Harrington RA, Stone GW, McNulty S, White HD, Lincoff AM, Gibson CM, et al. Platelet inhibition with cangrelor in patients undergoing PCI. *N Engl J Med*. (2009) 361:2318–29. doi: 10.1056/NEJMoa0908628

6. Iliescu CA, Grines CL, Herrmann J, Yang EH, Cilingiroglu M, Charitakis K, et al. SCAI expert consensus statement: evaluation, management, and special considerations of cardio-oncology patients in the cardiac catheterization laboratory (endorsed by the Cardiological Society of India, and Sociedad Latino Americana de Cardiologia Intervencionista). *Catheter Cardiovasc Interv*. (2016) 87:E202–23. doi: 10.1002/ccd.26379

7. Bobbio-Pallavicini E, Gugliotta L, Centurioni R, Porta C, Vianelli N, Billio A, et al. Antiplatelet agents in thrombotic thrombocytopenic purpura (TTP). Results of a randomized multicenter trial by the Italian cooperative group for TTP. *Haematologica*. (1997) 82(4):429–35. PMID: 9299856

8. Cocozza S, Formigli D, Parente A, Pirozzi E, Franco V, Moscato F, et al. C83° use of cangrelor in a 63 years old men suffering from acute inferior ST–elevation myocardial infarction and severe idiopathic thrombocytopenic purpura: a case report. *Eur Heart J Suppl*. (2022) 24. doi: 10.1093/eurheartj/suac011.081

9. Kabadi RA, Danelich IM, Entwistle JW 3rd, Marhefka GD, Reeves G, Boyle AJ, et al. Use of cangrelor as a bridge to left ventricular assist device implantation in a patient with a recent drug-eluting stent who developed acute tirofiban-related thrombocytopenia. *Pharmacotherapy*. (2019) 39:521–5. doi: 10.1002/phar.2219

10. Groves EM, Bhatt DL, Steg PG, Deliargyris EN, Stone GW, Gibson CM, et al. Incidence, predictors, and outcomes of acquired thrombocytopenia after percutaneous coronary intervention: a pooled, patient-level analysis of the CHAMPION trials (cangrelor versus standard therapy to achieve optimal management of platelet inhibition). *Circ Cardiovasc Interv*. (2018) 11:e005635. doi: 10.1161/CIRCINTERVENTIONS.117.005635

frontiers | Frontiers in Cardiovascular Medicine

TYPE Case Report
PUBLISHED 22 March 2024
DOI 10.3389/fcvm.2024.1363235

OPEN ACCESS

EDITED BY
Reto Asmis,
Wake Forest University, United States

REVIEWED BY
Apurva Patel,
Gujarat Cancer & Research Institute, India
Jeremy Brownstein,
The Ohio State University, United States
Ana Paula Nunes Alves,
Federal University of Ceara, Brazil

*CORRESPONDENCE
Chunlan Tang
✉ chunlantangok@126.com
Liang Gong
✉ gongliang@tmmu.edu.cn

†These authors have contributed equally to this work and share first authorship

RECEIVED 30 December 2023
ACCEPTED 11 March 2024
PUBLISHED 22 March 2024

CITATION
Yang P, Xiong F, Zhu B, Gong L and Tang C (2024) Case Report: Two cases of advanced primary cardiac angiosarcoma treated with anlotinib and a retrospective analysis of the literature.
Front. Cardiovasc. Med. 11:1363235.
doi: 10.3389/fcvm.2024.1363235

Case Report: Two cases of advanced primary cardiac angiosarcoma treated with anlotinib and a retrospective analysis of the literature

Pan Yang, Fu Xiong, Bingjing Zhu, Liang Gong*† and Chunlan Tang*†

Department of Respiratory and Critical Care Medicine, First Affiliated Hospital of Army Medical University, Chongqing, China

Primary cardiac angiosarcoma is a rare malignant soft-tissue sarcoma derived from vascular endothelial cells or lymphatic endothelial cells, with a high malignancy, poor prognosis, and a lack of effective medical therapy. This article reports on two patients with primary cardiac angiosarcoma who received first-line treatment with multi-targeted anti-angiogenic agent, anlotinib monotherapy. The treatment rapidly controlled pleural and pericardial effusion, significantly reduced the tumor, improved symptoms, and showed satisfactory recent efficacy. This indicates that anlotinib offers a new first-line treatment option for advanced primary cardiac angiosarcoma.

KEYWORDS

cardiac angiosarcoma, pleural effusion, pericardial effusion, vascular targeting agents, anlotinib

Introduction

Primary cardiac angiosarcoma (PCA) is a rare malignant tumor originating from vascular endothelial cells or lymphatic endothelial cells, but it accounts for one-third to one-half of all cardiac sarcomas (1, 2). It usually occurs in the right atrium, but also in the right ventricle and pericardium. There is no gender difference in incidence rate. Most patients are between 40 and 59 years old at the time of diagnosis. They are highly invasive and can quickly invade adjacent structures. 47%–89% of patients have lung, liver or brain metastasis at the time of initial diagnosis (3, 4). Its prognosis is poor, with a median PFS of about 5 months and a median OS of about 12 months. Over 90% of patients experience metastasis or local recurrence within 2 years, and the 2-year survival rate is less than 30% (5). The clinical manifestations are not specific and largely depend on the location and extent of the tumor. Surgery is the primary treatment for PCA, followed by radiotherapy and/or chemotherapy, but the effects and effectiveness of radiotherapy and chemotherapy still require comprehensive study (6). Currently, traditional treatment methods have limited benefits for patients, and it is crucial to discover effective treatment approaches. Targeted therapy has emerged as a current research focus. Presently, research has confirmed that tumor-targeting drugs such as sorafenib, sunitinib and pazopanib have certain therapeutic effects on angiosarcoma (7–9). However, due to the limited number of cases, designing clinical trials is challenging, and large-scale randomized controlled clinical trials are still lacking,

resulting in the absence of a standard treatment plan. Anlotinib, a multi-target tyrosine kinase inhibitor, has inhibitory effects on targets such as VEGFR1, VEGFR2, VEGFR3, PDGFR, FGFR, etc., which is beneficial for controlling tumor invasion and metastasis. Additionally, anlotinib also acts on C-KIT targets and can inhibit the growth of tumor cells (10). The results of the ALTER0203 study demonstrated that compared to the control group, anlotinib significantly prolonged the median PFS in various subtypes of sarcoma (6.27 months vs. 1.47 months) and significantly improved the objective response rate (10.13% vs. 1.33%) and disease control rate (55.7% vs. 22.67%). Based on this, it has been approved by NMPA for monotherapy in patients with acinar soft tissue sarcoma, clear cell sarcoma, and other advanced soft tissue sarcoma who have previously received anthracycline-containing treatment. Our department admitted two cases of primary cardiac angiosarcoma. One case was primary in the pericardium, and the other was primary in the right atrium. After receiving monotherapy with anlotinib, satisfactory short-term efficacy was achieved. We will analyze these two cases based on the specific details.

Case 1 presentation

A 64-year-old Chinese male presented with chest pain, shortness of breath, edema in both lower limbs, and headaches at our hospital. He is a smoker with a smoking index of 20 pack years. Thoracic fluid B-ultrasound revealed bilateral pleural effusion (liquid dark areas with a distance of approximately 38 mm detected in the right chest, and liquid dark areas with a distance of approximately 107 mm detected in the left chest). Left chest closed drainage was performed, and the pleural fluid analysis showed bloody turbidity, a positive Li Fanta test, a total cell count of 191.824×10^9/L, a white blood cell count of 0.678×10^9/L, a monocyte percentage of 94%, and a multinucleated cell percentage of 6%. Chest fluid biochemistry revealed glucose levels of 6.04 mmol/L, total protein levels of 36.9 g/L, albumin levels of 27.6 g/L, globulin levels of 9.3 g/L, a white blood cell ratio of 2.97, lactate dehydrogenase levels of 386 IU/L, and adenylate dehydrogenase levels of 1.68 U/L. Chest enhanced CT scan showed a visible size of approximately 7.3 cm at the upper edge of the right atrium and a 5.7 cm irregular mass shadow with an unclear boundary adjacent to the right atrium and superior vena cava. The lesion exhibited significantly uneven enhancement on enhanced scans and closely adhered to the pericardium, causing significant uneven cystic enhancement and a small amount of pericardial effusion. Bilateral pleural effusion was observed, partially enveloped on the left, with thickening of the left pleura and irregular cystic enhancement of the anterior and lower pleura (Figures 1A,B). PET/CT scan indicated irregular thickening of the pericardium and left pleura, increased FDG metabolism, and a high possibility of malignancy. A large

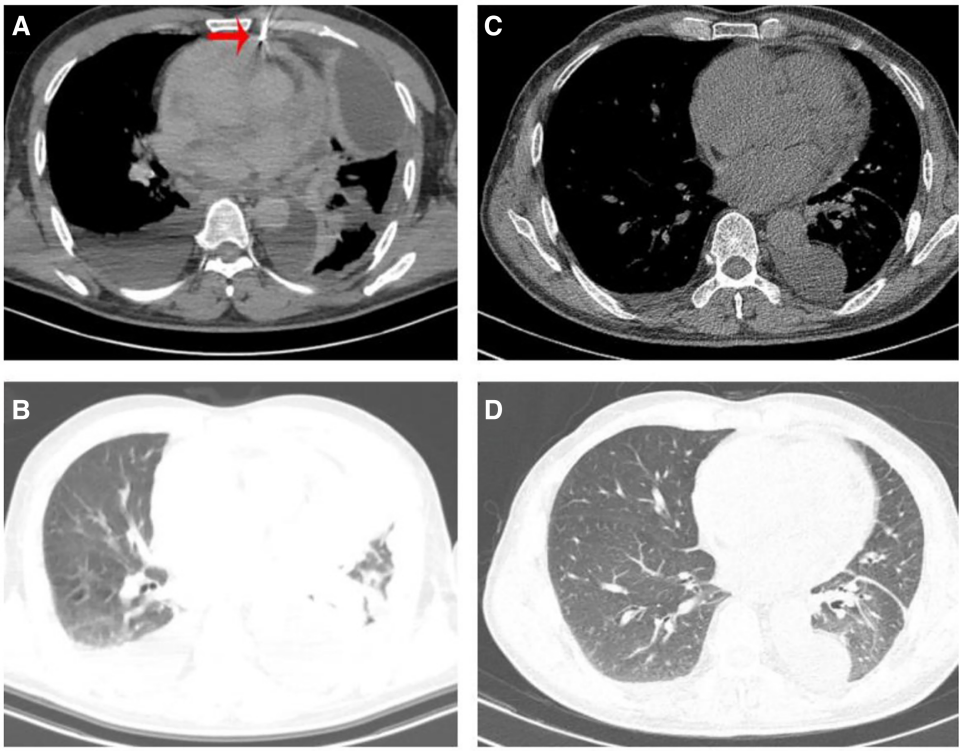

FIGURE 1
(A) Patient underwent CT guided pericardial biopsy. (A,B) Chest CT scan revealed bilateral pleural effusion, pericardial thickening, and pericardial effusion before treatment. (C,D) Chest CT showed a significance reduction in pleural and pericardial effusion after receiving one cycle of anlotinib treatment.

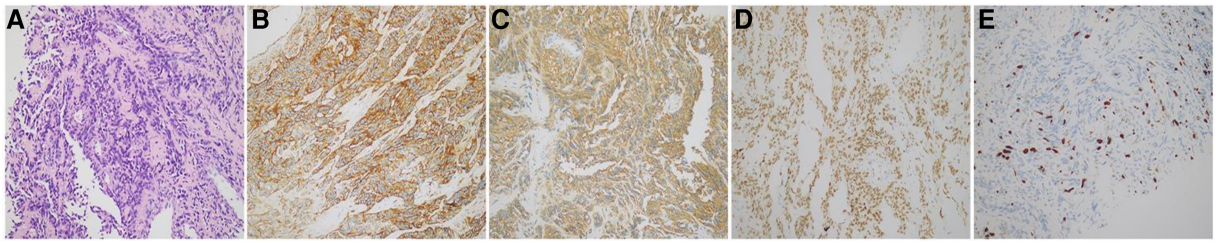

FIGURE 2
(A) Tumor cell staining of pericardial tissue (HE staining, ×20). (B–E) Staining of tumor markers in cellular tissues (immunohistochemical, ×20). (B) CD31 protein expression; (C) D2-40 protein expression; (D) ERG protein expression; (E) Ki-67 protein expression. Immunohistochemical results showed that D2-40 and ERG in tumor cells were diffusely positive; Ki-67 positive rate was about 30%; and CD31 in tumor cells were diffusely strongly positive.

amount of pleural effusion was present on the left side. Biopsy of the left pleura (in the 8th intercostal space of the left scapular line) suggested a high possibility of a vascular tumor, epithelioid endothelial cell tumor, or angiosarcoma in the left pleura. Immunohistochemical results showed CK (–), Vim (+), CEA (+), WT-1 (+), TTF-1 (–), P63 (–), Ki-67 (+, 30%), Napsina (–), CR (–), ERG (+), CD31 (+), CD45 (–), Desmin (–). To further clarify the diagnosis, a CT-guided pericardial biopsy was performed again, indicating that pericardial angiosarcoma had immunohistochemical features such as CK (–), TTF-1 (–), CR (–), D2-40 (+), P53 (–), Ki-67 (+, 10%), ERG (+), CD31 (+), HHV-8 (–), Desmin (–) (Figures 2A–E). Based on imaging and pathological diagnosis, it was determined to be a primary cardiac angiosarcoma with pleural metastasis (cTxN0M1, stage IV). The patient declined systemic chemotherapy. Approximately 700–1,000 ml of pleural effusion was drained daily. After 3 days of treatment with anlotinib, the patient's pleural effusion significantly decreased, and shortness of breath improved. Following one cycle of treatment (anlotinib, 12 mg oral/day, days 1–14, 21 days per cycle, 1cycle), the patient's symptoms significantly improved. Chest CT examination showed that the space-occupying lesion at the upper edge of the right atrium was smaller than before, and there was a significant decrease in pericardial and right pleural effusion (Figures 1C,D). The recent therapeutic effect was satisfactory. But due to economic reasons, the patient used anlotinib for only one treatment cycle and did not continue taking anlotinib orally. Subsequently, the patient's condition worsened, and the overall OS is five months.

Case 2 presentation

A 57-year-old Chinese male presented to our hospital with the main complaint of discovering bilateral pulmonary nodules six months ago and experiencing shortness of breath for the past three months. He has a pre-existing condition of hyperemia and is a heavy smoker with a smoking index of 40 pack years. On November 5, 2022, a physical examination revealed multiple scattered sub-solid ground glass shadows in both lungs, with a maximum length of approximately 25 mm. At that time, the patient did not experience any discomfort. After three months (February 2023), the patient developed shortness of breath after physical activity, which could be relieved by rest, but the patient did not pay attention to it. The shortness of breath gradually worsened with activity, and there was no improvement after receiving symptomatic treatment at an external hospital. Three months later (May 12, 2023), a chest enhanced CT scan showed larger scattered sub-solid ground glass shadows in both lungs compared to May 11, with a maximum length diameter of about 35 mm. Additionally, soft tissue density shadows were found in the right atrium, along with a small amount of pericardial effusion (Figures 3A–D). A PET/CT scan on May 16 revealed a large amount of fluid accumulation in the pericardial cavity, with a maximum diameter of about 1.8 cm. There was an increase in the arc-shaped soft tissue density around the root of the superior vena cava and the right atrium, accompanied by a significant increase in FDG uptake. The boundary with the adjacent pericardium and atrial wall was unclear, with SUVmax at 13.1. Multiple slightly lower density nodules of varying sizes were observed in the right lobe of the liver, with larger ones located in the parietal area of the liver, measuring approximately 2.2 cm in diameter with unclear boundaries. FDG uptake was slightly increased, with SUVmax at 4.4. Solid nodular shadows were scattered in both lungs, with visible halo signs. FDG uptake was slightly increased, with SUVmax at 2.1.

The patient was admitted to our hospital for treatment from May 5 to May 28. On May 29, a cardiac ultrasound revealed low echogenicity in the right atrium (visible range approximately 47 mm × 32 mm low echo), mild regurgitation of the mitral, tricuspid, and pulmonary valves, and moderate to large amounts of pericardial effusion (liquid dark areas with a spacing of 9 mm detected in the posterior left ventricular wall, liquid dark areas with a spacing of 18 mm detected in the anterior right ventricular wall, liquid dark areas with a spacing of 18 mm detected in the apex of the heart, liquid dark areas with a spacing of 19 mm detected in the lateral left ventricular wall, liquid dark areas with a spacing of 19 mm detected in the lateral right ventricular wall, and liquid dark areas with a spacing of 13 mm detected in the right atrium and lower right ventricle). A closed drainage of the pericardial cavity was performed, and routine analysis of the pericardial effusion showed bloody turbidity, positive Li Fanta test, total number of cells at

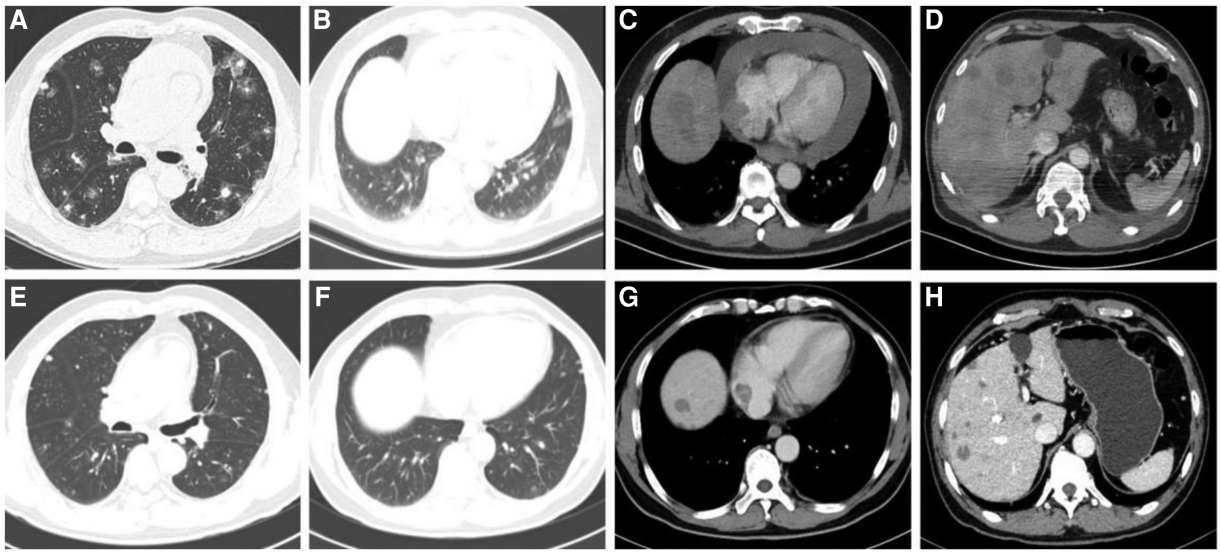

FIGURE 3
(A–D) Chest CT scan of the patient revealed dispersed sub-solid ground glass shadows in both lungs, soft tissue shadows in the right atrium, numerous nodular shadows in the liver, and a considerable pericardial effusion before treatment. (E,F) After 4 cycles of anlotinib treatment, the patient's numerous nodules in the lungs and liver showed significant reduction, the tumor lesion in the right atrium decreased, and pericardial effusion as managed.

$2{,}345.962 \times 10^9$/L, white blood cell count at 1.863×10^9/L, monocyte percentage at 68%, and multinucleated cell percentage at 32%. Chest fluid biochemistry: glucose level of 4.13 mmol/L, total protein level of 60.4 g/L, albumin level of 33.7 g/L, globulin level of 26.7 g/L, white blood cell ratio of 1.26, lactate dehydrogenase level of 262.80IU/L, adenylate dehydrogenase level of 14.6U/L. Liver enzyme display: ALT level of 1,487.2 IU/L, AST level of 1,452.9 IU/L, ALP level of 183 IU/L, daily drainage of approximately 500–700 ml of hemorrhagic pericardial effusion. Following admission, a lung biopsy revealed left lung alveolar epithelial and interstitial hyperplasia, mucinous degeneration, deposition of hemosiderin, and chronic tissue inflammation. Two exfoliative cytological examinations of the pericardial effusion showed the presence of a few inflammatory cells and mesothelial cells in the blood clot. To confirm the diagnosis, a liver puncture biopsy was performed (Figure 4A), which indicated angiosarcoma; CK (–), CD34 (stove+), P53 (2%+), Ki-67 (+, 10%), ERG (+), CD31 (+), S-100 (–), HMB45 (–), Desmin (–), SMA (stove+) (Figures 4B–E). Blood gene test results showed no clinically significant mutations, TMB: 6.8 mutations/Mb, and no detection of MSI-H. Based on imaging examination and pathological diagnosis, it was determined to be a primary cardiac angiosarcoma with bilateral lung and liver metastasis (cT1N0M1, stage IV). Starting from June 16, 2023, the patient received targeted treatment with anlotinib (anlotinib, 12 mg oral/day, days 1–14, 21 days per cycle, 11cycle). By June 18, 2023, the pericardial drainage fluid gradually decreased in volume and became lighter in color. After extracting 100 ml of pericardial effusion, no further extraction was necessary. Following the treatment, the patient experienced significant relief from shortness of breath, and their transaminase levels returned to normal. Subsequent CT scans revealed a significant reduction in tumor lesions in the right atrium, liver, and lungs, and the pericardial effusion was under control. No noticeable side effects

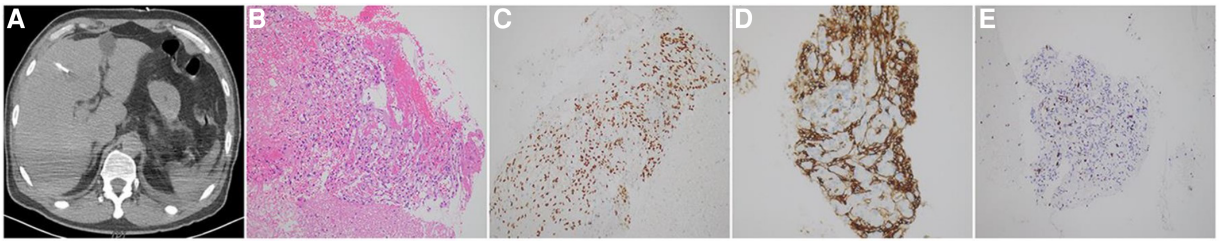

FIGURE 4
(A) CT guided liver biopsy. (B) Tumor cell staining of liver tissue (HE staining, ×20). (C–E) Tumor marker staining of liver cell tissue (immunohistochemical, ×20); (C) CD31 protein expression; (D) ERG protein expression; (E) Ki-67 protein expression. Immunohistochemical results showed that CD31 and ERG in tumor cells were diffusely positive; Ki-67 positive rate was about 10%.

from the medication were observed (Figures 3E–H). As of February 27, 2024, the patient has undergone 11 cycles of anlotinib treatment, resulting in partial remission with no notable drug side effects, PFS exceeding eight months.

Discussion

Among all cardiac tumors in adults, approximately 25% are malignant, with primary cardiac sarcoma representing around 95% of all malignant cardiac tumors. Notably, vascular sarcoma is the most frequently occurring type (11, 12). The key characteristic of PCA is its invasive growth and metastasis, frequently affecting the valve, pericardium, and even the coronary artery locally, or spreading throughout the body via the bloodstream (13). Early diagnosis of this condition is challenging, as its clinical symptoms are not typical. It often presents with manifestations such as chest tightness, shortness of breath, arrhythmia, or distant metastasis (14). The main clinical presentation of the two cases we reported is dyspnea, which is linked to tumor infiltration of the pericardium and pleura, resulting in pleural effusion and pericardial effusion. Early detection is challenging, thus imaging examinations hold significant diagnostic value for such patients. Imaging studies are crucial for diagnosing patients with cardiac sarcomas, with transthoracic echocardiography, chest CT, and MRI being commonly used methods. Whole body PET/CT is typically used to identify metastatic sites, while the gold standard for diagnosis is biopsy of the primary or metastatic site. Immunohistochemical markers like CD31, CD34, ERG, and Ki-67 are commonly used for angiosarcoma diagnosis. In our two patients, immunohistochemistry showed positive expression of CD31, ERG, and Ki-67, leading to a diagnosis of primary cardiac angiosarcoma based on imaging and pathology.

Surgical resection is not only the primary treatment for early or limited stage PCA, but also a predictive factor for patient survival (2).

Currently, for late-stage PCA patients who are ineligible for surgery, the treatment plan primarily involves the soft tissue sarcoma treatment plan. The most frequently prescribed medications are anthracyclines or paclitaxel drugs. First-line chemotherapy utilizing anthracyclines has shown remarkable tumor reduction in 25% of patients, with a median progression-free survival (PFS) of 4.9 months and a median overall survival (OS) of 9.9 months (15). In 2021, the Asian Sarcoma Consortium conducted a retrospective analysis of 276 patients with advanced angiosarcoma at 8 sarcoma academic centers. They compared the efficacy of first-line treatment regimens: paclitaxel (47.6% of patients) and liposome doxorubicin (19.6% of patients). The results revealed that paclitaxel monotherapy had a median PFS of 4.5 months, while liposome doxorubicin chemotherapy had a median PFS of 2.8 months. The median OS was 11.9 months for paclitaxel and 10.6 months for liposome doxorubicin. However, the difference between the two treatments was not statistically significant (16). Another phase III randomized controlled trial (EORTC 62012) examined the effectiveness of combination chemotherapy. The study revealed that while the doxorubicin combined with ifosfamide group had a significantly higher overall effective rate compared to the doxorubicin group (26% vs. 14%, $P < 0.0006$), there was no statistically significant difference in overall survival (OS). This lack of significance may be attributed to the heightened toxicity associated with the combination therapy group (17). There was no significant difference in median progression-free survival (PFS) between the doxorubicin and gemcitabine combined with docetaxel groups (23.3 weeks vs. 23.7 weeks). Although this study did not find any advantages of combining gemcitabine with docetaxel as a first-line treatment option (18), it does offer new treatment possibilities for patients with cardiac dysfunction or PCA. Due to the cumulative cardiac toxicity of doxorubicin and cyclophosphamide, the current treatment options for cardiac angiosarcoma mainly involve combining doxorubicin and cyclophosphamide with paclitaxel, docetaxel, or gemcitabine (19–23). However, the median OS for late-stage PCA patients does not surpass 8 months. Nevertheless, because PCA is rare and mostly documented as a case study, there is currently no established treatment method for late-stage cardiac angiosarcoma. It is crucial to investigate new treatment methods and strategies.

Tumor cell growth, invasion, and metastasis are reliant on the tumor microenvironment (TME), which includes tumor blood vessels. These vessels are frequently distorted and dysfunctional, with varying vascular permeability, excessive proliferation, and loss of wall hierarchy. This abnormal vascular system promotes tumor growth, metastasis, and treatment resistance, while selectively blocking the infiltration of certain immune cell types, such as cytotoxic T cells (24, 25). Vascular endothelial growth factor (VEGF) is a crucial factor in tumor angiogenesis (26, 27). For most solid tumors, such as sarcomas, targeted drugs that inhibit tumor angiogenesis primarily focus on VEGF and VEGFR. These drugs work by blocking the formation of new blood vessels, thus impeding the blood supply to the tumor. Additionally, they normalize the tumor blood vessels, which helps in suppressing tumor growth, development, and metastasis. Moreover, they enhance the response to other treatments (28). Typically, it is frequently combined with chemotherapy, immunotherapy, and radiation therapy for cancer treatment.

Angiosarcoma, a malignant tumor originating from vascular or lymphatic endothelial cells, may have unique advantages in anti-tumor angiogenesis. Ren et al. reported a case of a 99-year-old Chinese man diagnosed with angiosarcoma on his head and face. Due to his advanced age and extensive lesions, chemotherapy options were limited and surgery was challenging. As a result, he received monotherapy with anlotinib for 10 months (12 mg/day, D1-14, 21 days per cycle). The lesions on his head and face significantly decreased, and he tolerated the adverse drug reactions well (29). Both of our cardiac angiosarcoma patients received anlotinib treatment for approximately 3 days, leading to a notable decrease in the rapid expansion of pleural and pericardial effusion, as well as swift relief from symptoms like breathing difficulties. This outcome is attributed to anlotinib's ability to impede blood supply, normalize tumor blood vessels, and reduce vascular

permeability. Subsequent assessments revealed partial remission of the target lesion in a short timeframe, which is linked to anlotinib's inhibition of the C-kit gene, thereby impeding tumor cell growth. Neither patient experienced significant toxic side effects, and their quality of life notably improved. In 2019, Case 1 was treated with anlotinib at a monthly expense of 10,227 RMB. Currently, anlotinib is available in hospitals at a monthly cost of 5,760 RMB, a notable reduction from the 2019 price. Anlotinib also offers a free medication policy. After self-paying for 9 courses of anlotinib, patients can receive free medication until disease progression. Therefore, anlotinib could be considered a novel first-line treatment choice, either as a standalone therapy or in combination, for patients with advanced cardiac angiosarcoma presenting with significant pleural or pericardial effusion.

For patients with unresectable angiosarcoma, chemotherapy and radiotherapy are the primary treatment methods, although their efficacy is limited. However, they still provide clinical benefits to patients. Previously, we investigated the use of anlotinib chemotherapy combined with immunotherapy in other types of sarcomas. In a phase II single-arm prospective study, we explored the use of epirubicin in combination with anlotinib as a first-line treatment for advanced unresectable soft tissue sarcoma. The study showed impressive efficacy, with a median progression-free survival (PFS) of 11.5 months, an objective response rate (ORR) of 13.33%, and a disease control rate (DCR) of 80.0%. The safety profile was also good (30). At the 2023 ASCO conference, mid-term data was presented on the safety and efficacy of combining Penpulimab, anlotinib, and epirubicin as a first-line treatment for soft tissue sarcoma. The results showed a median PFS of 10.55 months, an ORR of 12.50% (4/24), and a DCR of 68.75% (14/24), indicating favorable safety. Therefore, the combination of anlotinib and other treatment methods such as chemotherapy, immunization, and palliative radiotherapy is worth further exploration in the treatment of advanced angiosarcoma, in order to maximize patient survival.

Data availability statement

The original contributions presented in the study are included in the article/Supplementary Material, further inquiries can be directed to the corresponding authors.

Ethics statement

The requirement of ethical approval was waived by Ethics Committee of the Southwest Hospital, Army Medical University (Third Military Medical University for the studies on humans because This article is a retrospective analysis of individual cases, therefore exempting ethics. The studies were conducted in accordance with the local legislation and institutional requirements. Written informed consent for participation was not required from the participants or the participants' legal guardians/next of kin in accordance with the national legislation and institutional requirements. The human samples used in this study were acquired from a by- product of routine care or industry. Written informed consent was obtained from the individual(s) for the publication of any potentially identifiable images or data included in this article.

Author contributions

PY: Conceptualization, Data curation, Investigation, Writing – original draft, Methodology. FX: Data curation, Writing – original draft. BZ: Formal Analysis, Writing – original draft. LG: Writing – review & editing, Methodology. CT: Methodology, Project administration, Writing – review & editing.

Funding

The author(s) declare financial support was received for the research, authorship, and/or publication of this article.

This work was funded by the Army Medical University Foundation of China (XZ-2019-505-015).

Conflict of interest

The authors declare that the research was conducted in the absence of any commercial or financial relationships that could be construed as a potential conflict of interest.

Publisher's note

References

1. Randhawa JS, Budd GT, Randhawa M, Ahluwalia M, Jia X, Daw H, et al. Primary cardiac sarcoma: 25-year Cleveland clinic experience. *Am J Clin Oncol.* (2016) 39 (6):593–9. doi: 10.1097/COC.0000000000000106

2. Yin K, Luo R, Wei Y, Wang F, Zhang Y, Karlson KJ, et al. Survival outcomes in patients with primary cardiac sarcoma in the United States. *J Thorac Cardiovasc Surg.* (2021) 162(1):107–115.2. doi: 10.1016/j.jtcvs.2019.12.109

3. Hammami MB, Al-Wawi MZ, Fazel H, Oudih M. Incidence, prognostic significance, and survival outcomes of primary cardiac sarcoma: an updated population-based retrospective study. *Anatol J Cardiol*. (2021) 25(2):104–10.

4. Bangolo A, Fwelo P, Iyer KM, Klinger S, Tavares L, Dey S, et al. Primary cardiac sarcoma: clinical characteristics and prognostic factors over the past 2 decades. *Diseases*. (2023) 11(2):74. doi: 10.3390/diseases11020074

5. Stergioula A, Kokkali S, Pantelis E. Multimodality treatment of primary cardiac angiosarcoma: a systematic literature review. *Cancer Treat Rev*. (2023) 120:102617. doi: 10.1016/j.ctrv.2023.102617

6. Davis JS, Allan BJ, Perez EA, Neville HL, Sola JE. Primary pediatric cardiac malignancies: the SEER experience. *Pediatr Surg Int*. (2013) 29(5):425–9. doi: 10.1007/s00383-013-3261-4

7. Bugarin-Estrada E, Villanueva-Castro E, Medina-Franco H. Soft tissue angiosarcoma of the breast in a patient with Klippel-Trenaunay-Weber syndrome. *Cir Cir*. (2018) 86(6):566–9. doi: 10.24875/CIRU.18000306

8. Ogata D, Yanagisawa H, Suzuki K, Oashi K, Yamazaki N, Tsuchida T. Pazopanib treatment slows progression and stabilizes disease in patients with taxane-resistant cutaneous angiosarcoma. *Med Oncol*. (2016) 33(10):116. doi: 10.1007/s12032-016-0831-z

9. Ray-Coquard I, Italiano A, Bompas E, Le Cesne A, Robin YM, Chevreau C, et al. Sorafenib for patients with advanced angiosarcoma: a phase II trial from the French sarcoma group (GSF/GETO). *Oncologist*. (2012) 17(2):260–6. doi: 10.1634/theoncologist.2011-0237

10. Khalil DN, Smith EL, Brentjens RJ, Wolchok JD. The future of cancer treatment: immunomodulation, CARs and combination immunotherapy. *Nat Rev Clin Oncol*. (2016) 13(5):273–90. doi: 10.1038/nrclinonc.2016.25

11. Centofanti P, Di Rosa E, Deorsola L, Dato GM, Patane F, La Torre M, et al. Primary cardiac tumors: early and late results of surgical treatment in 91 patients. *Ann Thorac Surg*. (1999) 68(4):1236–41. doi: 10.1016/S0003-4975(99)00700-6

12. Butany J, Leong SW, Carmichael K, Komeda M. A 30-year analysis of cardiac neoplasms at autopsy. *Can J Cardiol*. (2005) 21(8):675–80. doi: 10.1016/s0828-282x(06)70247-1

13. Patel SD, Peterson A, Bartczak A, Lee S, Chojnowski S, Gajewski P, et al. Primary cardiac angiosarcoma—a review. *Med Sci Monit*. (2014) 20:103–9. doi: 10.12659/MSM.889875

14. Meng Q, Lai H, Lima J, Tong W, Qian Y, Lai S. Echocardiographic and pathologic characteristics of primary cardiac tumors: a study of 149 cases. *Int J Cardiol*. (2002) 84(1):69–75. doi: 10.1016/S0167-5273(02)00136-5

15. Constantinidou A, Sauve N, Stacchiotti S, Blay JY, Vincenzi B, Grignani G, et al. Evaluation of the use and efficacy of (neo)adjuvant chemotherapy in angiosarcoma: a multicentre study. *ESMO Open*. (2020) 5(4):e000787. doi: 10.1136/esmoopen-2020-000787

16. Chen TW, Pang A, Puhaindran ME, Maw MM, Loong HH, Sriuranpong V, et al. The treatment landscape of advanced angiosarcoma in Asia-A multi-national collaboration from the Asian sarcoma consortium. *Cancer Sci*. (2021) 112(3):1095–104. doi: 10.1111/cas.14793

17. Young RJ, Natukunda A, Litiere S, Woll PJ, Wardelmann E, van der Graaf WT. First-line anthracycline-based chemotherapy for angiosarcoma and other soft tissue sarcoma subtypes: pooled analysis of eleven European organisation for research and treatment of cancer soft tissue and bone sarcoma group trials. *Eur J Cancer*. (2014) 50(18):3178–86. doi: 10.1016/j.ejca.2014.10.004

18. Seddon B, Strauss SJ, Whelan J, Leahy M, Woll PJ, Cowie F, et al. Gemcitabine and docetaxel versus doxorubicin as first-line treatment in previously untreated advanced unresectable or metastatic soft-tissue sarcomas (GeDDiS): a randomised controlled phase 3 trial. *Lancet Oncol*. (2017) 18(10):1397–410. doi: 10.1016/S1470-2045(17)30622-8

19. Look Hong NJ, Pandalai PK, Hornick JL, Shekar PS, Harmon DC, Chen YL, et al. Cardiac angiosarcoma management and outcomes: 20-year single-institution experience. *Ann Surg Oncol*. (2012) 19(8):2707–15. doi: 10.1245/s10434-012-2334-2

20. Hirai T, Miwa K, Furusho H, Yasuda T. Coronary intervention for severe stenosis in the ostial right coronary artery with cardiac angiosarcoma: a case report. *Eur Heart J Case Rep*. (2022) 6(1):ytab505. doi: 10.1093/ehjcr/ytab505

21. Yeh JK, Tsai YS, Chen YP, Roan JN, Chang HY. Right atrium angiosarcoma with feeding vessels from right coronary artery: a case report. *Eur Heart J Case Rep*. (2022) 6(1):ytac025. doi: 10.1093/ehjcr/ytac025

22. Stacchiotti S, Palassini E, Sanfilippo R, Vincenzi B, Arena MG, Bochicchio AM, et al. Gemcitabine in advanced angiosarcoma: a retrospective case series analysis from the Italian rare cancer network. *Ann Oncol*. (2012) 23(2):501–8. doi: 10.1093/annonc/mdr066

23. Jiang L, Xu X, Davies H, Shi K. The effect of ifosfamide, epirubicin, and recombinant human endostatin therapy on a cardiac angiosarcoma: a case report. *Medicine (Baltimore)*. (2019) 98(17):e15290. doi: 10.1097/MD.0000000000015290

24. Bejarano L, Jordao MJC, Joyce JA. Therapeutic targeting of the tumor microenvironment. *Cancer Discov*. (2021) 11(4):933–59. doi: 10.1158/2159-8290.CD-20-1808

25. Viallard C, Larrivee B. Tumor angiogenesis and vascular normalization: alternative therapeutic targets. *Angiogenesis*. (2017) 20(4):409–26. doi: 10.1007/s10456-017-9562-9

26. Bergers G, Benjamin LE. Tumorigenesis and the angiogenic switch. *Nat Rev Cancer*. (2003) 3(6):401–10. doi: 10.1038/nrc1093

27. Jiang X, Wang J, Deng X, Xiong F, Zhang S, Gong Z, et al. The role of microenvironment in tumor angiogenesis. *J Exp Clin Cancer Res*. (2020) 39(1):204. doi: 10.1186/s13046-020-01709-5

28. Apte RS, Chen DS, Ferrara N. VEGF In signaling and disease: beyond discovery and development. *Cell*. (2019) 176(6):1248–64. doi: 10.1016/j.cell.2019.01.021

29. Ren B, Wang W, Tan J, Yuan B, Chen G, Mo X, et al. Efficacy of anlotinib for the treatment of angiosarcoma of the face and neck: a case report. *Front Oncol*. (2021) 11:596732. doi: 10.3389/fonc.2021.596732

30. Wang ZM, Zhuang RY, Guo X, Zhang CL, You Y, Chen LS, et al. Anlotinib plus epirubicin followed by anlotinib maintenance as first-line treatment for advanced soft-tissue sarcoma: an open-label, single-arm, phase II trial. *Clin Cancer Res*. (2022) 28(24):5290–6. doi: 10.1158/1078-0432.CCR-22-1903

frontiers | Frontiers in Oncology

TYPE Case Report
PUBLISHED 05 April 2024
DOI 10.3389/fonc.2024.1362347

OPEN ACCESS

EDITED BY
Reto Asmis,
Wake Forest University, United States

REVIEWED BY
Numrah Fadra,
Mayo Clinic, United States
Bjorn Cools,
University Hospital Leuven, Belgium

*CORRESPONDENCE
Akihiro Nishiyama
an0510@staff.kanazawa-u.ac.jp
Shinji Takeuchi
takeuchi@staff.kanazawa-u.ac.jp

RECEIVED 28 December 2023
ACCEPTED 25 March 2024
PUBLISHED 05 April 2024

CITATION
Nishiyama A, Sato S, Sakaguchi H, Kotani H, Yamashita K, Ohtsubo K, Mizuguchi K, Ikeda H, Iino K, Takemura H and Takeuchi S (2024) Case report: Navigating treatment pathways for cardiac intimal sarcoma with *PDGFRβ* N666K mutation. *Front. Oncol.* 14:1362347. doi: 10.3389/fonc.2024.1362347

Case report: Navigating treatment pathways for cardiac intimal sarcoma with *PDGFRβ* N666K mutation

Akihiro Nishiyama[1*], Shigeki Sato[1], Hiroyuki Sakaguchi[1], Hiroshi Kotani[1], Kaname Yamashita[1], Koushiro Ohtsubo[1], Keishi Mizuguchi[2], Hiroko Ikeda[2], Kenji Iino[3], Hirofumi Takemura[3] and Shinji Takeuchi[1*]

[1]Department of Medical Oncology, Kanazawa University Hospital, Kanazawa, Japan, [2]Department of Diagnostic Pathology, Kanazawa University Hospital, Kanazawa, Japan, [3]Department of Cardiovascular Surgery, Kanazawa University, Kanazawa, Japan

In the realm of rare cardiac tumors, intimal sarcoma presents a formidable challenge, often requiring innovative treatment approaches. This case report presents a unique instance of primary intimal sarcoma in the left atrium, underscoring the critical role of genomic profiling in guiding treatment. Initial genomic testing unveiled a somatic, active mutation in *PDGFRβ* (*PDGFRβ* N666K), accompanied by *MDM2* and *CDK4* amplifications. This discovery directed the treatment course toward pazopanib, a PDGFRβ inhibitor, following irradiation. The patient's response was remarkable, with the therapeutic efficacy of pazopanib lasting for 16.3 months. However, the patient experienced a recurrence in the left atrium, where subsequent genomic analysis revealed the absence of the *PDGFRβ* N666K mutation and a significant reduction in PDGFRβ expression. This case report illustrates the complexities and evolving nature of cardiac intimal sarcoma treatment, emphasizing the potential of PDGFRβ signaling as a strategic target and highlighting the importance of adapting treatment pathways in response to genetic shifts.

KEYWORDS

intimal sarcoma, *PDGFRβ* N666K mutation, precision oncology, MDM2 amplification, CDK4 amplification

1 Introduction

Primary cardiac tumors are rare, with an incidence of 0.001%–0.003% worldwide (1), and intimal sarcoma is the most frequent subtype of cardiac sarcoma (2). Intimal sarcoma occurs in the innermost layer of large vessels, such as the pulmonary arteries. The clinical outcome is poor, with a median survival of only 12–13 months after radical surgery (3); thus, the development of effective treatment for intimal sarcoma is an unmet need. Gene profiling analyses of intimal sarcoma revealed that *MDM2* amplification and/or overexpression is frequently detected and is now considered one of the criteria for diagnosing intimal sarcoma (2). Moreover, a previous case report suggested that PDGFRβ may be involved in the tumorigenesis of intimal sarcoma (4). However, organized data on genetic findings of cardiac intimal sarcoma are limited.

2 Case description

A 45-year-old male patient, experiencing constitutional symptoms including palpitations and cough for four months, was admitted to Kanazawa University Hospital. Transthoracic echocardiography revealed a 5-cm-sized mass in the left atrium, possibly adhering to the mitral valve leaflets (Figure 1A). This mass

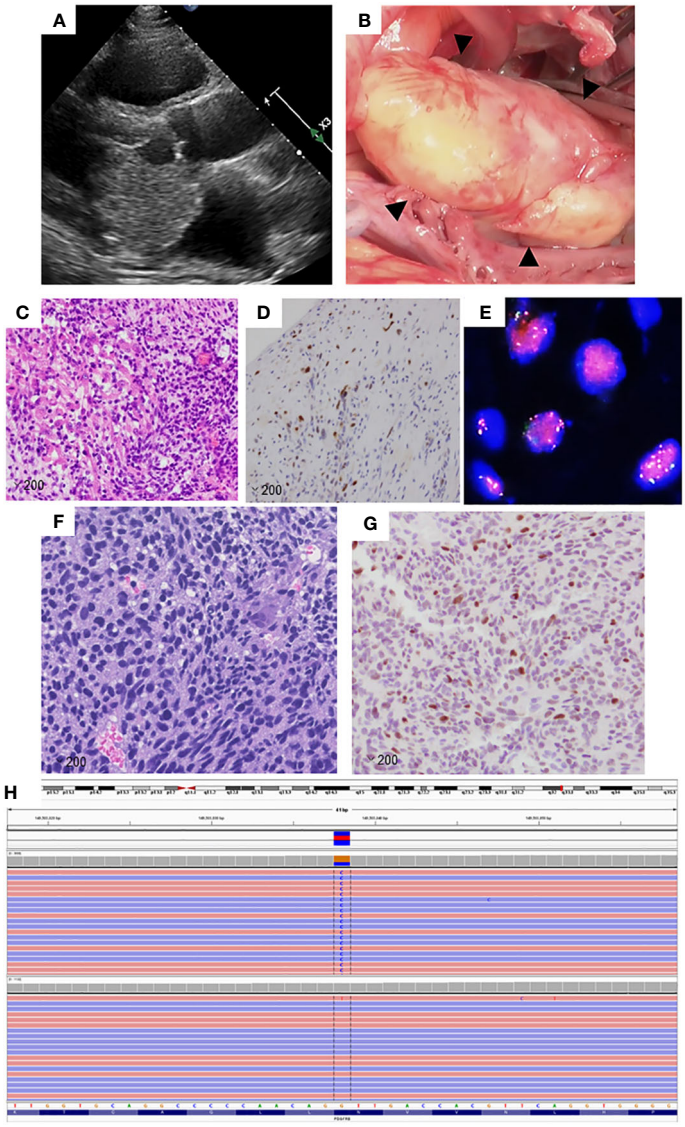

FIGURE 1
(A) Transthoracic echocardiography image of the primary lesion in the left atrium. **(B)** Perioperative image of the primary lesion in the left atrium. **(C)** The primary lesion shows the proliferation of spindle cells with a high nuclear-cytoplasmic ratio, magnification: ×200. **(D)** Tumor cells in the primary lesion showed positive immunoreactivity for MDM2 (magnification: ×200). **(E)** Fluorescence *in situ* hybridization analysis revealed the amplification of MDM2. Signals for MDM2 are presented in red, while those of CEP 12 are shown in green. **(F)** The left tailor muscle metastatic lesion consists of spindle cells and resembles the primary lesion (magnification: ×200). **(G)** The tumor cells in the metastatic lesion showed positive immunoreactivity for MDM2, magnification: ×200. **(H)** Illustration of *PDGFRβ* ^{N666K} using a next-generation sequencing platform as visualized in the Integrative Genomics Viewer.

resulted in pulmonary hypertension and low cardiac output. Emergent surgical excision of the mass was performed (Figure 1B), and pathological examination confirmed the diagnosis of intimal sarcoma in the left atrium, characterized by *MDM2* amplification and overexpression (Figures 1C–E).

Subsequently, the patient developed brain metastasis and underwent two sessions of Gamma Knife therapy. Despite these treatments, multiple bone metastases emerged, necessitating chemotherapy with doxorubicin, followed by eribulin. Although these regimens effectively controlled the bone metastases, a new lesion appeared in the left tailor muscle. A biopsy of this muscle mass was performed for comprehensive genomic testing. Histological analysis confirmed the left tailor muscle tumor as a metastatic intimal sarcoma, also displaying MDM2 overexpression (Figures 1F, G). The patient underwent palliative radiation therapy (60 Gy) targeting the left tailor muscle metastasis and continued with eribulin therapy. However, the thoracolumbar and sternal metastases progressed, manifesting as new lesions.

Genomic testing of the left tail muscle metastasis revealed the presence of *PDGFRβ* N666K mutation, along with the amplification of *MDM2* and *CDK4*, both located on the long arm of chromosome 12 (Figure 1H). The *PDGFRβ* N666K had an allele frequency of 35.9%, and the copy numbers for *MDM2* and *CDK4* were 8.48 and 9.09, respectively. Due to pain resulting from the thoracolumbar and sternal metastases, the patient underwent external irradiation (30 Gy). Pazopanib, a sarcoma-approved drug active against PDGFRs, was initiated as a third-line treatment. Prior to the induction of pazopanib, the patient had several irradiated lesions, including metastases in the brain, left tailor muscle, sternum, and thoracolumbar spine, and a non-irradiated left adrenal metastasis. Pazopanib demonstrated a favorable and prolonged effect without requiring dose reduction, with the only side effect being a change in hair color. Unfortunately, 16.3 months after pazopanib initiation, a local recurrence in the left atrium was observed. For non-brain metastatic lesions, the relapse-free survival period was 619 days (Figure 2).

Salvage surgery was performed to remove the recurrent lesion, but local recurrence was detected after one and a half months. Owing to the inability to undergo another surgery, the patient received palliative radiation therapy for the treatment of a recurrent lesion in the left atrium (Supplementary Figure 1A). Further genomic testing on the left atrium recurrence sample (Table 1) resulted in the establishment of a patient-derived cell line from this sample, after obtaining the ethical review approval and patient consent (Supplementary Figure 1B). The recurrent lesion lacked the *PDGFRβ* N666K mutation and showed minimal PDGFRβ expression, in contrast to the clear PDGFRβ positivity observed in the primary and left tail muscle metastasis lesions (Supplementary Figures 2A-C).

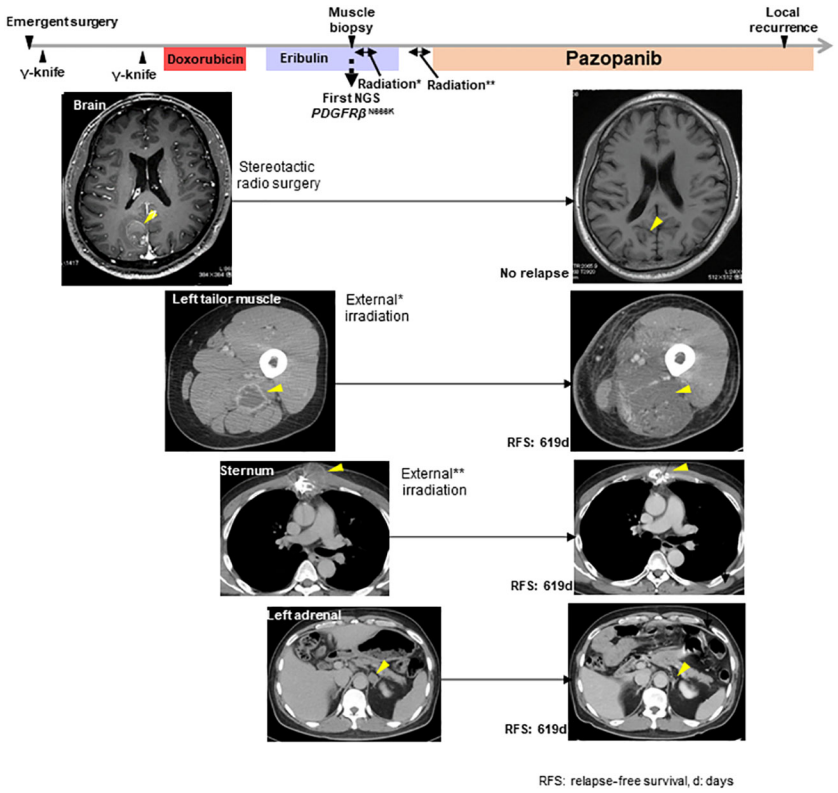

FIGURE 2
The clinical course from the initial operation to the local recurrence in the left atrium and the response of metastatic lesions to radiation or pazopanib. *indicated the external irradiation delivered to the left tailor muscle lesion. **indicated the external irradiation delivered to the sternum lesion. The yellow arrowheads show the target lesions.

TABLE 1 Difference between first genomic test results and second genomic test results by next-generation sequencing.

Detected Gene alterations	VAF or Copy number	
	1st NGS	2nd NGS
***PDGFRβ* N666K**	35.9%	Not detected
***MDM2* amplification**	CN 8.48	CN 33.5
***CDK4* amplification**	CN 9.09	CN 7.07
***CDKN2A* loss**	Not detected	Detected
***TP53* A198V**	47.5%	50.1%

NGS, next-generation sequencing; VAF, variant allele frequency; CN, copy number.

Subsequently, new metastatic lesions developed in the right atrium and the greater curvature of the stomach. The patient received palliative radiotherapy to prevent sudden death and gastrointestinal hemorrhage. Ultimately, disease progression occurred 44.6 months after the initial surgery.

3 Discussion

This case of cardiac intimal sarcoma with the *PDGFRβ* N666K mutation provides significant insights into the molecular landscape of this rare tumor type. Neuville et al.'s study on 42 cardiac intimal sarcomas reported MDM2 overexpression and *MDM2*/*CDK4* amplification (2). Additionally, *PDGFRβ* mutations, found in 15.3% of patients with intimal sarcomas, have been linked to oncogenesis in mesenchymal tumors (4–6). Notably, *PDGFRβ* D850V, M772V, R709H, and E472D mutations in intimal sarcoma have been previously documented (4, 5, 7). However, the *PDGFRβ* N666K mutation detected in our patient is the first instance in intimal sarcoma, underscoring its novelty and importance.

The oncogenic role of the PDGFRβ signaling pathway is further supported by the response of *PDGFRβ* N666K-transfected Ba/F3 cells to inhibitors like imatinib, nilotinib, or ponatinib, and its ability to induce cancer *in vivo* (6). The presence of *PDGFRβ* N666K in the primary lesion and the left tail muscle metastasis, as evidenced by the clear PDGFRβ positivity on the cell membrane (Supplementary Figures 2A, B), suggests that these lesions were driven by this mutation. However, the recurrence's resistance to pazopanib and the lack of *PDGFRβ* N666K mutation therein indicate a complex and evolving tumor biology.

Table 2 compares the efficacy of pazopanib in the present patient with those used in previous case reports (8–11). Results showed a significantly longer progression-free survival and better response, suggesting that *PDGFRβ* mutations may be a viable therapeutic target. However, the *CDK4* amplification and loss of CDKN2A observed in the recurrent lesion, coupled with increased sensitivity to abemaciclib, a CDK4/6 inhibitor, over pazopanib (Supplementary Figure 1C), highlight the necessity for tailored treatment approaches (12, 13). Although MDM2 acts as a negative regulator of TP53 by promoting its degradation and inhibiting tumor suppressor activity, the presence of TP53 mutations complicates the therapeutic landscape. Even if MDM2 inhibitors successfully block the MDM2-TP53 interaction, they are incapable of restoring TP53 function due to these underlying *TP53* alterations. Regrettably, the presence of a TP53 pathogenic variant precluded participation in studies involving MDM2 inhibitors such as milademetan (14), further emphasizing the need for a focus on alternative pathways influencing the cell cycle, specifically through *CDK4* amplification and *CDKN2A* loss, as pivotal resistance mechanisms.

Our study has some limitations. Pazopanib is a multi-kinase inhibitor, which could obscure the specific impact of the drug on the *PDGFRβ* N666K mutation (10). Furthermore, as four lesions, excluding the left adrenal metastasis, had undergone irradiation before pazopanib administration, the distinct effect of the drug on these lesions remains uncertain.

4 Conclusion

This case highlights the potential of precision medicine for cardiac intimal sarcoma, showcasing the benefits of genomic testing in identifying specific alterations such as *PDGFRβ* N666K, *MDM2* amplification, and *CDK4* amplification. The prolonged efficacy observed with pazopanib following irradiation in a *PDGFRβ* N666K-positive patient emphasizes the potential of targeted therapies in improving the prognosis of patients with cardiac intimal sarcoma. This case report underscores the evolving nature of cancer treatment and the necessity for individualized therapeutic strategies.

TABLE 2 Efficacy of pazopanib as treatment for intimal sarcoma in the present and previous case reports.

Authors	Age (years)/sex	Gene alteration	Line of pazopanib	Response rate	Progression-free survival
Funatsu et al. (8)	71/F	Not reported	2nd	PR	2.0 months
Kollar et al. (9)	67.2* M/F 1/1	Not reported	2nd	PR	Not reported
Sai et al. (10)	33/F	Not reported	1st	SD	5.8 months
Frezza et al. (11)	51* M/F 7/5	Not reported	1st/2nd/further 1/3/8	PR/SD/PD 1/4/7	3.7* months
Present case	46/M	*PDGFRβ* ^{N666K}	3rd	CR	16.3 months

*Median number.
CR, complete response; PR, partial response; SD, stable disease; PD, progressive disease.

Data availability statement

The original contributions presented in the study are included in the article/Supplementary Material, further inquiries can be directed to the corresponding author/s.

Ethics statement

Written informed consent was obtained from the individual(s) for the publication of any potentially identifiable images or data included in this article.

Author contributions

AN: Writing – original draft, Writing – review & editing. SS: Writing – review & editing. HS: Writing – review & editing. HK: Writing – review & editing. KY: Writing – review & editing. KO: Writing – review & editing. KM: Writing – review & editing. HI: Writing – review & editing. KI: Writing – review & editing. HT: Writing – review & editing. ST: Writing – review & editing.

Funding

The author(s) declare financial support was received for the research, authorship, and/or publication of this article. This work was supported by the Japan Society for the Promotion of Science (JSPS) KAKENHI Grant Number 20K08516 to ST.

Acknowledgments

We thank the patient and his family for providing informed consent for the processing of his data for this publication. Additionally, we thank SRL Co., Ltd. for providing the sequence data for *PDGFRβ* N666K.

Conflict of interest

The authors declare that the research was conducted in the absence of any commercial or financial relationships that could be construed as a potential conflict of interest.

Publisher's note

Supplementary material

The Supplementary Material for this article can be found online at: https://www.frontiersin.org/articles/10.3389/fonc.2024.1362347/full#supplementary-material

SUPPLEMENTARY FIGURE 1
The radiographic findings of the local recurrence in the left atrium and the experiment using the recurrence tissue. **(A)** The yellow arrowheads indicated the recurrence lesions. These lesions responded to palliative radiotherapy. **(B)** The appearance of the cell line established from the recurrence tissue. **(C)** The sensitivity of the patient-derived cell line to pazopanib or abemaciclib was determined through cell viability assays.

SUPPLEMENTARY FIGURE 2
Immunohistochemistry staining of *PDGFRβ* (Cell Signaling Technology; PDGF Receptor β (C82A3) Rabbit mAb #4564). **(A)** The primary lesion exhibited an adequate expression of *PDGFRβ*. **(B)** The left tailor muscle metastasis lesion demonstrated a high expression of *PDGFRβ*. **(C)** The local recurrence lesion in the left atrium had a low expression of *PDGFRβ*.

References

1. Neragi-Miandoab S, Kim J, Vlahakes GJ. Malignant tumours of the heart: a review of tumour type, diagnosis and therapy. *Clin Oncol*. (2007) 19:748–56. doi: 10.1016/j.clon.2007.06.009

2. Neuville A, Collin F, Bruneval P, Parrens M, Thivolet F, Gomez-Brouchet A, et al. Intimal sarcoma is the most frequent primary cardiac sarcoma: clinicopathologic and molecular retrospective analysis of 100 primary cardiac sarcomas. *Am J Surg Pathol*. (2014) 38:461–9. doi: 10.1097/PAS.0000000000000184

3. Dewaele B, Floris G, Finalet-Ferreiro J, Fletcher CD, Coindre JM, Guillou L, et al. Coactivated platelet-derived growth factor receptor α and epidermal growth factor receptor are potential therapeutic targets in intimal sarcoma. *Cancer Res*. (2010) 70:7304–14. doi: 10.1158/0008-5472.CAN-10-1543

4. Roszik J, Khan A, Conley AP, Livingston JA, Groisberg R, Ravi V, et al. Unique aberrations in intimal sarcoma identified by next-generation sequencing as potential therapy targets. *Cancers (Basel)*. (2019) 11:1283. doi: 10.3390/cancers11091283

5. Ito Y, Maeda D, Yoshida M, Yoshida A, Kudo-Asabe Y, Nanjyo H, et al. Cardiac intimal sarcoma with *PDGFRβ* mutation and co-amplification of *PDGFRα* and *MDM2*: an autopsy case analyzed by whole-exome sequencing. *Virchows Arch*. (2017) 471:423–8. doi: 10.1007/s00428-017-2135-x

6. Arts FA, Chand D, Pecquet C, Velghe AI, Constantinescu S, Hallberg B, et al. PDGFRB mutants found in patients with familial infantile myofibromatosis or overgrowth syndrome are oncogenic and sensitive to imatinib. *Oncogene*. (2016) 35:3239–48. doi: 10.1038/onc.2015.383

7. Fu X, Niu W, Li J, Kiliti AJ, Al-Ahmadie HA, Iyer G, et al. Activating mutation of PDGFRB gene in a rare cardiac undifferentiated intimal sarcoma of the left atrium: a case report. *Oncotarget*. (2017) 8:81709–16. doi: 10.18632/oncotarget.20700

8. Funatsu Y, Hirayama M, Shiraishi J, Asakura T, Wakaki M, Yamada E, et al. Intimal sarcoma of the pulmonary artery treated with pazopanib. *Intern Med*. (2016) 55:2197–202. doi: 10.2169/internalmedicine.55.6199

9. Kollár A, Jones RL, Stacchiotti S, Gelderblom H, Guida M, Grignani G, et al. Pazopanib in advanced vascular sarcomas: an EORTC Soft Tissue and Bone Sarcoma Group (STBSG) retrospective analysis. *Acta Oncol*. (2017) 56:88–92. doi: 10.1080/0284186X.2016.1234068

10. Sai S, Imamura Y, Kiyota N, Jimbo N, Toyoda M, Funakoshi Y, et al. Relationship between PDGFR expression and the response to pazopanib in intimal sarcoma of the pulmonary artery: a case report. *Mol Clin Oncol*. (2021) 14:6. doi: 10.3892/mco.2020.2168

11. Frezza AM, Assi T, Lo Vullo SL, Ben-Ami E, Dufresne A, Yonemori K, et al. Systemic treatments in MDM2 positive intimal sarcoma: a multicentre experience with anthracycline, gemcitabine, and pazopanib within the World Sarcoma Network. *Cancer*. (2020) 126:98–104. doi: 10.1002/cncr.32508

12. Dickson MA, Schwartz GK, Keohan ML, D'Angelo SP, Gounder MM, Chi P, et al. Phase 2 trial of the CDK4 inhibitor palbociclib (PD0332991) at 125 mg dose in well-differentiated or dedifferentiated liposarcoma. *JAMA Oncol.* (2016) 2:937–40. doi: 10.1001/jamaoncol.2016.0264

13. Fennell DA, King A, Mohammed S, Greystoke A, Anthony S, Poile C, et al. Abemaciclib in patients with p16ink4A-deficient mesothelioma (MiST2): a single-arm, open-label, phase 2 trial. *Lancet Oncol.* (2022) 23:374–81. doi: 10.1016/S1470-2045(22)00062-6

14. Koyama T, Shimizu T, Kojima Y, Sudo K, Okuma HS, Shimoi T, et al. Clinical activity and exploratory resistance mechanism of milademetan, an MDM2 inhibitor, in intimal sarcoma with MDM2 amplification: an open-label phase Ib/II study. *Cancer Discov.* (2023) 13:1814–25. doi: 10.1158/2159-8290.CD-23-0419

frontiers | Frontiers in Cardiovascular Medicine

TYPE Case Report
PUBLISHED 17 May 2024
DOI 10.3389/fcvm.2024.1378655

OPEN ACCESS

EDITED BY
Reto Asmis,
Wake Forest University, United States

REVIEWED BY
Massimo Baudo,
Lankenau Institute for Medical Research, United States
Silvia Vanni,
IRST, Italy

*CORRESPONDENCE
Zhaohui Wang
joseking7628592@outlook.com

RECEIVED 30 January 2024
ACCEPTED 06 May 2024
PUBLISHED 17 May 2024

CITATION
Hu L, Wang Z, Chen Y and Zhang X (2024) Case Report: Assessment of primary myxofibrosarcoma in the left atrium using multimodal ultrasonography.
Front. Cardiovasc. Med. 11:1378655.
doi: 10.3389/fcvm.2024.1378655

Case Report: Assessment of primary myxofibrosarcoma in the left atrium using multimodal ultrasonography

Liyan Hu[1], Zhaohui Wang[2]*, Yu Chen[1] and Xiaowei Zhang[3]

[1]Department of Ultrasonography, People's Hospital of Dong yang, Dong yang, Zhejiang, China, [2]Department of Cardiac Surgery, People's Hospital of Dong yang, Dong yang, Zhejiang, China, [3]Department of Pathology, People's Hospital of Dong yang, Dong yang, Zhejiang, China

Primary myxofibrosarcoma of the heart, a rare cardiac malignancy, was diagnosed in a middle-aged female patient exhibiting progressive dyspnea following transthoracic echocardiography and pathological analysis. Postoperatively, the patient underwent chemotherapy and Lenvatinib mesylate therapy, with regular check-ups confirming her survival. After 10 months the patient is still alive and well.

KEYWORDS

myxofibrosarcomas, cardiac tumor, multimodal ultrasonography, contrast-enhanced ultrasound (CEUS) imaging, cardiac surgery

Introduction

Primary cardiac tumors are extremely rare, with a reported prevalence of 0.002% to 0.03% in postmortem studies. Myxomas account for approximately 25% of all primary cardiac tumors, while the remainder are benign (1). The majority (95%) of these primary malignant tumors are vascular sarcomas (2). Fibrosarcoma, also known as myxofibrosarcoma, is a rare tumor that can manifest in any chamber of the heart but is most commonly found in the left atrium. The tumor tissue is characterized by the presence of a mucinous stroma (3). Primary cardiac myxofibrosarcoma is very aggressive. Although only a few cases have been reported, studies have shed light on clinical presentation, pathological features, and treatment strategies (4–7). Moreover, the diagnostic value of ultrasonography, particularly cardiac contrast echocardiography, has not been widely discussed.

Case presentation

A 59-year-old woman presented with a two-month history of chest tightness and shortness of breath that worsened significantly in the last 12 h prior to admission. Previous episodes of chest discomfort and dyspnea occurred during physical activity and were alleviated by rest. Upon admission, she was experiencing orthopnea and acute emesis. The patient had a past history of hypertension and diabetes for 2 years. Her breathing sounded slightly rough. Her heart rate was at 104 beats per min, and she had a rhythmic systolic rumble (grade 2/6) in the mitral region but no lower limb swelling.

Laboratory results indicated a serum troponin level of 0.043 ng/ml, normal serum creatinine, and an elevated B-type natriuretic peptide (BNP) level of 3,170 pg/ml.

A transthoracic echocardiogram revealed two masses in the left atrial cavity. The larger mass measured 7.2 × 3.2 cm and was located proximally to the mitral valve. The smaller lesion measured 2.5 × 2.4 cm and was directly linked to the mitral valve. The masses were characterized by irregular shapes, clear boundaries, and uneven echogenicity. During diastole, the small mass prolapsed into the left ventricular inflow tract, generating a 35 mmHg pressure differential. The transthoracic echocardiogram also found mitral orifice obstruction with mild regurgitation; moderate pulmonary hypertension; mild tricuspid regurgitation; small amount of pericardial effusion, Pressure difference halved time 149 ms, and no significant abnormalities were observed in the residual valves. Some specific data is shown in Table 1. Based on ultrasound findings, a preliminary diagnosis of a left atrial mass was made, with suspicion of malignancy.

Contrast-enhanced echocardiography was recommended, revealing rapid perfusion of the contrast material into the right and left atria and ventricles. After a few cardiac cycles, the mass was substantially enhanced, almost matching the surrounding myocardium, confirming the likelihood of a malignant tumor (Figure 1, Supplementary Video 1).

On February 8, 2023, the patient underwent surgery for the left atrial lesions. The surgical approach was median sternotomy. cardiopulmonary bypass was used in the surgery through Aortic Cannulation and bicaval cannulation. More than 2 lesions, with different sizes, were found in the left atrial. The cardiac tumors exhibited fragility and spanned from the roof of the left atrium to the edge of the mitral valve. The left atrial tumors were excised en block, accompanied by the removal of a portion of the endocardium. Finally, a 3 cm × 4 cm size Cow pericardial patch was used to rebuild the atrial septum. Subsequent to the surgical procedure, postoperative pathology analysis identified a cardiac malignant tumor consistent with myxofibrosarcoma. This diagnosis was substantiated through immunohistochemistry and microscopic morphology examination (Figures 2, 3). Immunohistochemical staining results were as follows: CK(AE1/AE3)(−), EMA(−), Vimentin(+), CD31(−), CD34(−), D2-40(−), Desmin(−), SMA(small amount+), MyoD1(−), S-100(−), Ki-67 (+ approximately 30%); F8(−), Actin(−), MSA(−), caldesmon(+),

TABLE 1 Transthoracic echocardiogram data.

Name	Value	Name	Valve
Ejection fraction	74%	Left atrium	41 mm
Fraction shortening	41%	Right atrium	40 mm
Left ventricular end-diastolic volume	32 mm	Pulmonary artery systolic pressure	74 mmHg
Mitral valve orifice area	1.48 cm^2	Mean mitral valve pressure gradient	35 mmHg
Maximum diastolic mitral orifice flow rate	4.02 m/s	Maximum velocity of tricuspid regurgitation	4.23 m/s

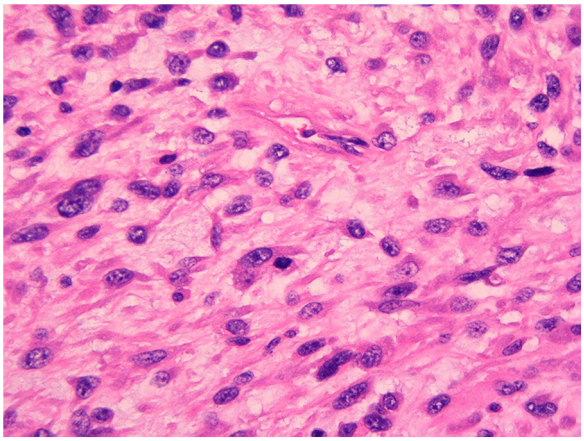

FIGURE 2
Primary myxofibrosarcoma of the left atrium.

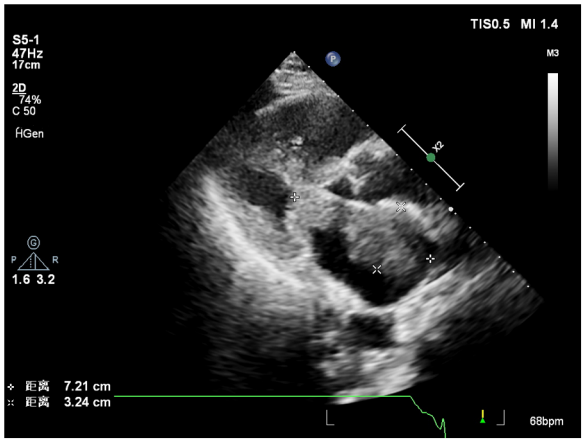

FIGURE 1
The larger mass close to the mitral valve.

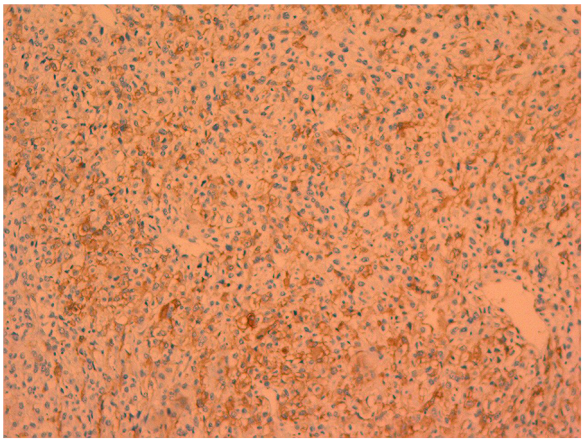

FIGURE 3
Smooth muscle actin positive.

B-catenin(−), HMB45(−), SOX-10(−), CD117(−), DOG-1(−), TFE3(+).calretinin(−), WT-1(+), Bcl-2(−), CD99(+).

The patient recovered well after surgery without any surgical complications. The symptoms of chest tightness and shortness of breath disappeared when the patient was discharged. PET-CT examination was performed after the operation, revealing that the patient had multiple metastatic lesions in the liver and left femur. Subsequently, the patient underwent 6 cycles of chemotherapy, comprising albumin-bound Paclitaxel 200 mg, Liposomal Doxorubicin 40 mg, and Anlotinib 10 mg.

At 8 months post-surgery, a 41 × 24 mm mass in the left atrium was detected using transthoracic echocardiography. The lesion had an irregular shape, uneven echogenicity, and an ill-defined boundary with the atrial septum. The maximum velocity of blood flow through the mitral valve was measured to be 1.39 meters per s. The maximum and mean pressure gradients across the valve were found to be 8 and 4 mmHg, respectively. During the contrast-enhanced ultrasound examination, perfusion of the contrast agent was observed in the mass. However, the enhancement degree was lower than that of the adjacent myocardium, leading to the diagnosis of tumor recurrence. (Figure 4, Supplementary Video 2). Considering tumor recurrence, Lenvatinib Mesylate was added as an anti-tumor therapy. The patient was followed up monthly in our hospital. Having gone through the series of treatments (Table 2), she complained of nothing but feeling a little weakness with firm support from family members and meticulous care from medical staff, she kept an Optimistic attitude.

TABLE 2 A timeline with relevant data.

Time	Event
2023-02-05	Admitted to the Cardiology Department
2023-02-06	An echocardiogram revealed two masses in the left atrial cavity
2023-02-07	Coronary angiography results in negative
2023-02-07	Transferred to the Cardiac Surgery Department
2023-02-08	Cardiac tumor resection surgery. Frozen sections indicated that mesenchymal tumor flap cells were abundant, necrotic, and tended to be borderline or low-grade malignant.
2023-02-17	Primary Myxofibrosarcoma was substantiated through immunohistochemistry and microscopic morphology examination; Discharged.
2023-03-21	PET-CT revealed that the patient had multiple metastatic lesions in the liver and left femur.
From 2023 to 04 to 2023-10	6 cycles of chemotherapy: Paclitaxel 200 mg, Liposomal Doxorubicin 40 mg, and Anlotinib 10 mg.
2023-10	Routine outpatient follow-up. An echocardiogram revealed a recurrent mass in the left atrial cavity. Lenvatinib Mesylate was added as an anti-tumor therapy.
From 2023 to 11 to 2024-03	Routine outpatient follow-up.

Discussion

Left atrial myxofibrosarcoma is usually characterized by low or moderate echogenic masses attached to the left atrial valve or wall (3). These lesions often exhibit unclear boundaries from surrounding normal tissue, irregular shapes, and uneven echogenicity. Additionally, they are frequently large, sessile, and possess a broad base. They may also invade the pulmonary veins and exhibit other features. In the present case, one of the masses oscillated around the mitral valve orifice during the cardiac cycle, obstructing the valve orifice during diastole. This resulted in symptoms of mitral stenosis, such as chest tightness and dyspnea. Distinguishing left atrial myxofibrosarcoma from left atrial myxoma is crucial. The American Society of Echocardiography guidelines recommend the differentiation of intracardiac masses using ultrasound enhancement agents (8). Benign cardiac tumors, predominantly myxomas, typically exhibit sparse neovascularization, with the myxoid matrix composed of acidic mucopolysaccharides (9, 10). In contrast, malignant tumors, such as myxofibrosarcomas, grow rapidly and feature abundant new blood vessels, densely distributed with a dilated lumen, resulting in significant enhancement during angiography (11). Of note, conventional ultrasonography revealed that the mass had an irregular shape, uneven echogenicity, no peduncle, and a wide base, which required differentiation from a thrombus. Of note, thrombi do not exhibit enhanced imaging due to a lack of blood vessel supply, a feature distinguishing them from malignant tumors (8, 12). Postoperatively, a follow-up transthoracic echocardiography was conducted 8 months later, unveiling the recurrence of the tumor in the left atrium. Further characterization through contrast-enhanced ultrasound indicated sparse enhancement of the left atrial mass, with the degree of enhancement lower than that observed in the surrounding myocardium.

This observation contrasts with the preoperative contrast-enhanced ultrasonography, which demonstrated significant enhancement in the mass akin to the adjacent myocardium. The altered enhancement pattern may be attributed to the effects of chemotherapy and Lenvatinib Mesylate. Lenvatinib Mesylate is a tyrosine kinase (RTK) receptor inhibitor that

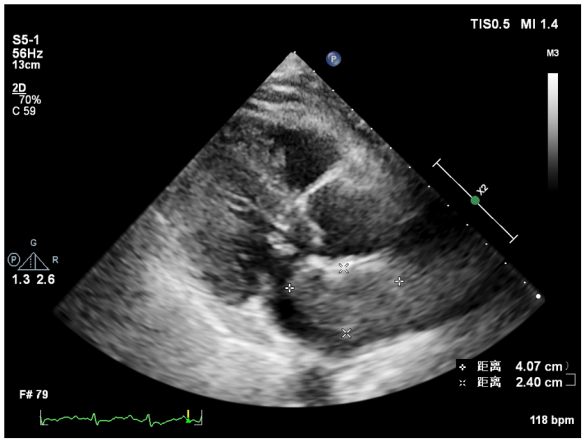

FIGURE 4
Recurrent tumor in the left atrium.

inhibits the kinase activity of the vascular endothelial growth factor (VEGF) receptors VEGFR1(FLT1), VEGFR2(KDR) and VEGFR3(FLT4). Moreover, it also inhibits RTKs involved in other proangiogenic and tumorigenic pathways, including fibroblast growth factor (FGF), receptors FGFR1, 2, 3, and 4, and platelet-derived growth factor (PDGF) receptors PDGFRa, KIT, and RET.

According to case reports and guidelines, the most widely adopted treatment strategies are surgery combined with chemotherapy and targeted anti-tumor drugs (3, 7, 8, 10). However the outcomes are not satisfactory, the median survival for patients that had complete surgical resection was 17 months compared to 6 months with incomplete resection. Reviewing the entire treatment process, the left heart tumor grew into the left atrium and obstructed flow, thereby presenting with heart failure and high BNP. For this reason, surgery was indicated urgently for the relief of symptoms. But the shortage of this case is the time of PET-CT examination. We could know more about the situation of the patient if the PET-CT was completed before surgery. Since PCT-CT is very expensive, self-funded, and not reimbursed by medical insurance, not everyone can afford it.

Multimodal ultrasound technologies, including two-dimensional echocardiography, color Doppler, and Contrast-enhanced echocardiography, were used to diagnose myxofibrosarcoma and detect hemodynamic changes in this case.

When considering the therapeutic options for primary cardiac myxofibrosarcoma (MFS), it is evident that beyond early diagnosis, identifying the most effective treatment strategy is crucial. Emerging genomic approaches offer promising tools for stratifying patients based on their chemosensitivity, allowing for a more personalized and targeted treatment plan. The study showed that Comparative genomic analysis between myxofibrosarcoma and undifferentiated pleomorphic sarcoma patient samples has pinpointed distinct genetic expressions, with certain genes being up-regulated in UPS and others in MFS (13). Genomic profiling of 7,494 sarcomas, representing a diverse range of histologies, can potentially alter or refine diagnostic outcomes for over 10% of cases. This approach uncovers targetable genetic aberrations in approximately 31.7% of patients, with specific kinase rearrangements noted in 2.6% and a significant tumor mutational burden in 3.9%, thereby enhancing therapeutic decision-making in sarcoma treatment (14). Although this study did not incorporate genomic analysis, we acknowledge the importance of such methodologies and recommend their consideration in future research to enhance our understanding of tumor biology and chemotherapeutic sensitivity.

This study has several limitations that warrant acknowledgment. Firstly, due to financial constraints, a preoperative PET-CT scan was not performed on the patient, which limited our comprehensive assessment of tumor metastasis. Secondly, while we utilized multimodal ultrasonography for detailed tumor evaluation, the study did not include genomic analysis that could have provided further insights into the tumor's characteristics and response to chemotherapy. Additionally, the small sample size may limit the generalizability of our findings to the broader population of MFS patients. Future studies should aim to include a larger cohort and consider integrating genomic analyses to refine treatment strategies.

Summary

Early detection and treatment of cardiac myxofibrosarcoma are paramount, given its rapid progression and rarity. The integration of echocardiography with contrast-enhanced ultrasound enhances the diagnostic accuracy of cardiac myxofibrosarcoma, facilitating precise diagnosis and aiding in treatment planning. Given the potential for incomplete tumor resection, vigilant follow-up is imperative, and we advocate for echocardiographic monitoring every 3 months. As of the latest update, the patient is still alive and is undergoing regular check-ups.

Data availability statement

The raw data supporting the conclusions of this article will be made available by the authors, without undue reservation.

Ethics statement

The studies involving humans were approved by Medical Ethics Committee of Dongyang People's Hospital. The studies were conducted in accordance with the local legislation and institutional requirements. The participants provided their written informed consent to participate in this study. Written informed consent was obtained from the individual(s) for the publication of any potentially identifiable images or data included in this article.

Author contributions

LH: Writing – review & editing, Writing – original draft, Visualization, Validation, Supervision, Resources, Project administration, Methodology, Investigation, Data curation, Conceptualization. ZW: Writing – review & editing, Writing – original draft, Visualization, Validation, Supervision, Software, Resources, Project administration, Methodology, Investigation, Funding acquisition, Formal Analysis, Data curation, Conceptualization. YC: Writing – review & editing, Writing – original draft, Validation, Software, Project administration, Data curation. XZ: Writing – original draft, Software, Resources, Data curation.

Funding

The author(s) declare that no financial support was received for the research, authorship, and/or publication of this article.

Conflict of interest

The authors declare that the research was conducted in the absence of any commercial or financial relationships that could be construed as a potential conflict of interest.

Publisher's note

All claims expressed in this article are solely those of the authors and do not necessarily represent those of their affiliated organizations, or those of the publisher, the editors and the reviewers. Any product that may be evaluated in this article, or claim that may be made by its manufacturer, is not guaranteed or endorsed by the publisher.

Supplementary material

The Supplementary Material for this article can be found online at: https://www.frontiersin.org/articles/10.3389/fcvm.2024.1378655/full#supplementary-material

SUPPLEMENTARY VIDEO 1
Contrast-enhanced ultrasonography of the mass. Scan the QR code to watch the video.

SUPPLEMENTARY VIDEO 2
Contrast-enhanced ultrasonography of the recurrent tumor. Scan the QR code to watch the video.

References

1. Butany J, Nair V, Naseemuddin A, Nair GM, Catton C, Yau T. Cardiac tumours: diagnosis and management. *Lancet Oncol*. (2005) 6(4):219–28. doi: 10.1016/S1470-2045(05)70093-0

2. Bruce CJ. Cardiac tumours: diagnosis and management. *Heart*. (2011) 97 (2):151–60. doi: 10.1136/hrt.2009.186320

3. Lazaros GA, Matsakas EP, Madas JS, Toli DI, Nikas DJ, Kershaw MA, et al. Primary myxofibrosarcoma of the left atrium: case report and review of the literature. *Angiology*. (2008) 59(5):632–5. doi: 10.1177/0003319707306079

4. Reddy KVC, Kumar P, Sanzgiri P, George AM. Primary cardiac myxofibrosarcoma with osteoid differentiation mimicking a left atrial myxoma: a rare entity. *J Cardiol Cases*. (2020) 22(5):253–6. doi: 10.1016/j.jccase.2020.07.013

5. Ujihira K, Yamada A, Nishioka N, Iba Y, Maruyama R, Nakanishi K, et al. A case report of primary cardiac myxofibrosarcoma presenting with severe congestive heart failure. *J Cardiothorac Surg*. (2016) 11(1):95. doi: 10.1186/s13019-016-0490-3

6. Verhemel S, Protty M, Rodrigus I, Paelinck B, Claeys M. De-differentiated myxofibrosarcoma metastasis in the right atrium: an invasive but diagnostic approach. *JACC Case Rep*. (2019) 1(2):151–5. doi: 10.1016/j.jaccas.2019.06.021

7. Wang ZH, Lv XH, Pu JH, Yang MF, Chen LJ. Treatment of primary cardiac angiosarcoma in a 35 weeks pregnant woman. *J Card Surg*. (2021) 36(9):3452–5. doi: 10.1111/jocs.15751

8. Palaskas N, Thompson K, Gladish G, Agha AM, Hassan S, Iliescu C, et al. Evaluation and management of cardiac tumors. *Curr Treat Options Cardiovasc Med*. (2018) 20(4):29. doi: 10.1007/s11936-018-0625-z

9. Amano J, Kono T, Wada Y, Zhang T, Koide N, Fujimori M, et al. Cardiac myxoma: its origin and tumor characteristics. *Ann Thorac Cardiovasc Surg*. (2003) 9(4):215–21.

10. Wang H, Li Q, Xue M, Zhao P, Cui J. Cardiac myxoma: a rare case series of 3 patients and a literature review. *J Ultrasound Med*. (2017) 36(11):2361–6. doi: 10.1002/jum.14264

11. Fidler IJ. Critical factors in the biology of human cancer metastasis. *Am Surg*. (1995) 61(12):1065–6.

12. Porter TR, Mulvagh SL, Abdelmoneim SS, Becher H, Belcik JT, Bierig M, et al. Clinical applications of ultrasonic enhancing agents in echocardiography: 2018 American society of echocardiography guidelines update. *J Am Soc Echocardiogr*. (2018) 31(3):241–74. doi: 10.1016/j.echo.2017.11.013

13. Vanni S, Fausti V, Fonzi E, Liverani C, Miserocchi G, Spadazzi C, et al. Unveiling the genomic basis of chemosensitivity in sarcomas of the extremities: an integrated approach for an unmet clinical need. *Int J Mol Sci*. (2023) 24(8):6926. doi: 10.3390/ijms24086926

14. Gounder MM, Agaram NP, Trabucco SE, Robinson V, Ferraro RA, Millis SZ, et al. Clinical genomic profiling in the management of patients with soft tissue and bone sarcoma. *Nat Commun*. (2022) 13(1):3406. doi: 10.1038/s41467-022-30496-0

frontiers | Frontiers in Oncology

TYPE Case Report
PUBLISHED 21 May 2024
DOI 10.3389/fonc.2024.1340115

OPEN ACCESS

EDITED BY
Christian Cadeddu Dessalvi,
University of Cagliari, Italy

REVIEWED BY
Andres Daniele,
Instituto de Oncología Ángel H. Roffo, Argentina
Massimiliano Camilli,
Agostino Gemelli University Polyclinic (IRCCS), Italy

*CORRESPONDENCE
Qiaowen Li
Stevenxzf@sina.com
Jinduan Lin
2020620649@gzhmu.edu.cn

RECEIVED 29 February 2024
ACCEPTED 02 May 2024
PUBLISHED 21 May 2024

CITATION
Shu H, Xiao D, Han S, Du Y, Lin J and Li Q (2024) A case of left atrial intimal sarcoma with rhabdomyosarcoma differentiation: a case report and literature review. *Front. Oncol.* 14:1340115. doi: 10.3389/fonc.2024.1340115

A case of left atrial intimal sarcoma with rhabdomyosarcoma differentiation: a case report and literature review

Hongyun Shu[1], Duan Xiao[2], Sisi Han[1], Yongkang Du[1], Jinduan Lin[3]* and Qiaowen Li[4]*

[1]Department of Cardiovascular Medicine, The Affiliated Qingyuan Hospital of Guangzhou Medical University, Qingyuan, China, [2]Department of Rehabilitation, The First Affiliated Hospital of Jinan University, Guangzhou, China, [3]Department of Laboratory Medicine, The Affiliated Qingyuan Hospital of Guangzhou Medical University, Qingyuan, China, [4]Institute of Gerontology, Guangzhou Geriatric Hospital, Guangzhou Medical University, Guangzhou, China

Primary cardiac malignancies are rare, with cardiac sarcomas being the main type. Among these, intimal sarcomas are the most common. However, they tend to occur in the great vessels and are rare in the heart, with only a few isolated cases reported. We report a challenging case of a patient with left atrial intimal sarcoma with rhabdomyosarcoma differentiation. The patient was admitted after a physical examination detected left heart occupancy, and initial imaging suspected a left atrial thrombus. The patient then underwent extracorporeal circulation-assisted open cardiac surgery with resection of an atrial mass. The postoperative pathological findings were suggestive of an arterial intimal sarcoma, which included areas of rhabdomyosarcoma differentiation within the tumor tissue. Unfortunately, the patient's tumor recurred 4 months later, and she died due to treatment failure. This case highlights the rarity and risk of misdiagnosis of cardiac intimal sarcoma. Additionally, we aim to improve the understanding of intimal sarcoma through a review of immunohistochemistry and gene amplification techniques.

KEYWORDS

primary cardiac tumors, intimal sarcoma, rhabdomyosarcoma, diagnosis, treatment

Introduction

Primary cardiac tumors are rare, with an incidence of 0.001–0.03% based on autopsy results, of which approximately 25% are malignant (1). Primary cardiac malignancies lack specific clinical manifestations. Intracardiac masses can obstruct blood flow and invade cardiac valves, causing symptoms of congestive heart failure, including syncope, dyspnoea,

angina pectoris, and peripheral oedema (2). Various arrhythmias may be associated with the formation of scar-like material around the sarcoma tissue, and some tumors may invade the pericardium (3).

Intimal sarcoma (IS) is an extremely rare malignant mesenchymal tumor and is also known as a spindle cell tumor, which occurs mostly in large vessels such as the pulmonary arteries and less commonly in the heart (4). Neuville et al. retrospectively analyzed 100 primary cardiac tumors and classified them according to murine double minute 2 (MDM2) amplification and found that ISs were the most common among primary cardiac malignancies (42%); they are characterized by rapid invasion into the lumen, possessing high mitotic activity (5); and because of the heterogeneous nature of IS, which, based on morphology and immunohistochemistry, is speculated to originate from subendothelial multifunctional stem cells that can differentiate into vascular, rhabdomyosarcoma or osteosarcoma histotypes, has led to the need for genetic testing, in addition to morphological and immunohistochemical tests, if necessary, in determining the final diagnosis (6, 7). Due to the rarity of these diseases, there is a lack of standard treatment and surgical resection is still the preferred option. These tumors have a high degree of malignancy, susceptibility to recurrence and metastasis, and a very poor prognosis. Here, we will describe a case of IS of the left atrium in a patient with postoperative histologic findings suggestive of IS with areas of rhabdomyosarcoma differentiation.

Case presentation

A 78-year-old woman presented to the outpatient clinic for "COVID-19" infection. Transthoracic echocardiography (TTE) revealed a left atrial hypoechoic mass measuring 85 mm × 55 mm × 35 mm. This mass was located in the left atrium and had a wide base connecting it to the left atrial wall. During diastole, part of the hypoechoic mass was visible, allowing blood flow to be expelled into the left ventricle through the mitral valve orifice. Additionally, mild mitral regurgitation was observed. Notably, TTE showed that the left ventricular ejection fraction (LVEF) was preserved at 68% (Figure 1), and the patient did not present any symptoms regarding the cardiovascular system. An enhanced computed tomography (CT) scan of the chest, abdomen, and coronary arteries on admission showed a filling defect in the left atrium, which was likewise considered to be atrial tethering (Figure 2). Cardiac CT and coronary angiography showed coronary atherosclerosis, including moderate stenosis of the left anterior descending branch in the middle part of the lumen and slight stenosis of the distal part of the right coronary artery. In addition, several suspicious lymph nodes were found in the mediastinum and adjacent to the great vessels. Laboratory tests revealed an N-terminal pro-B-type natriuretic peptide (NT-pro-BNP) level of 1030 pg/mL (normal range <450 pg/mL for those under 50 years old and <900 pg/mL for those over 50 years old) and a fibrinogen level of 4.88 g/L (normal range 2–4 g/L). The remainder of the admission tests did not indicate any abnormalities.

The patient underwent resection of the atrial tumor due to the large size of the mass and impaired valve function. During the surgery, we observed greyish-yellow and greyish-white tissue almost filling the left atrium. The mass had a solid, greyish-yellow, translucent section with focal necrosis (Figure 3). We performed a complete resection of the mass along its tip and used radiofrequency ablation to excise a small mass located between the pulmonary artery opening and the left atrium. No residual tumor mass was visible to the naked eye. We clipped a pericardial patch to fill the defect in the posterior wall of the left atrium. Additionally, a drainage tube was placed in the right thoracic cavity to facilitate the drainage of the pleural effusion. The endotracheal tube was removed two days after the operation, and the patient had a successful recovery. Postsurgery, bedside DR screening revealed scattered exudates in both lungs and pleural effusion without any notable features. The patient did not exhibit symptoms of heart failure, such as shortness of breath. On the 7th day after the operation, the patient was discharged from the hospital and started receiving palliative care. Further adjuvant radiotherapy and chemotherapy measures were not pursued.

In the postoperative routine pathological evaluation, the tumor was microscopically observed to consist of a dense cellular zone and a sparse cellular zone. The tumor cells had an oval shape and were clearly anisotropic, with long, oval nuclei, pale cytoplasm staining, weakly defined cell borders, and apoptosis fragmentation that was easily noticeable. Certain cells had rich, reddish-stained cytoplasm,

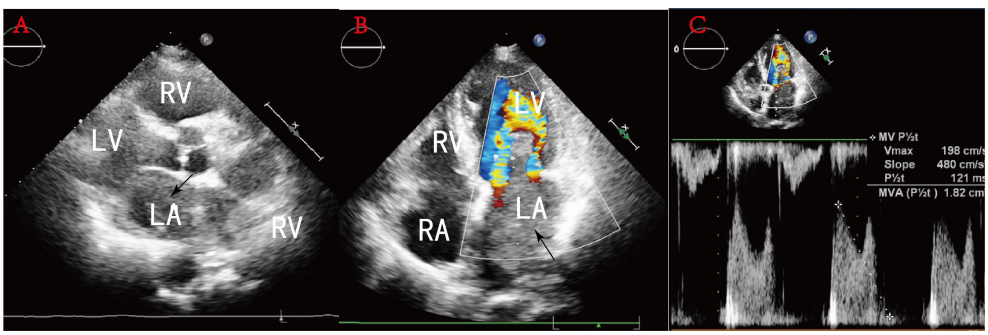

FIGURE 1
(A) Sternal fat left ventricular long-axis view: a hypoechoic mass is seen in the left atrium, and some of this hypoechoic mass is seen entering the left ventricle during diastole through the mitral orifice. **(B)** No obvious blood flow is seen in the mass. **(C)** Pulsed Doppler flow spectra at the mitral valve orifice: mild mitral regurgitation.

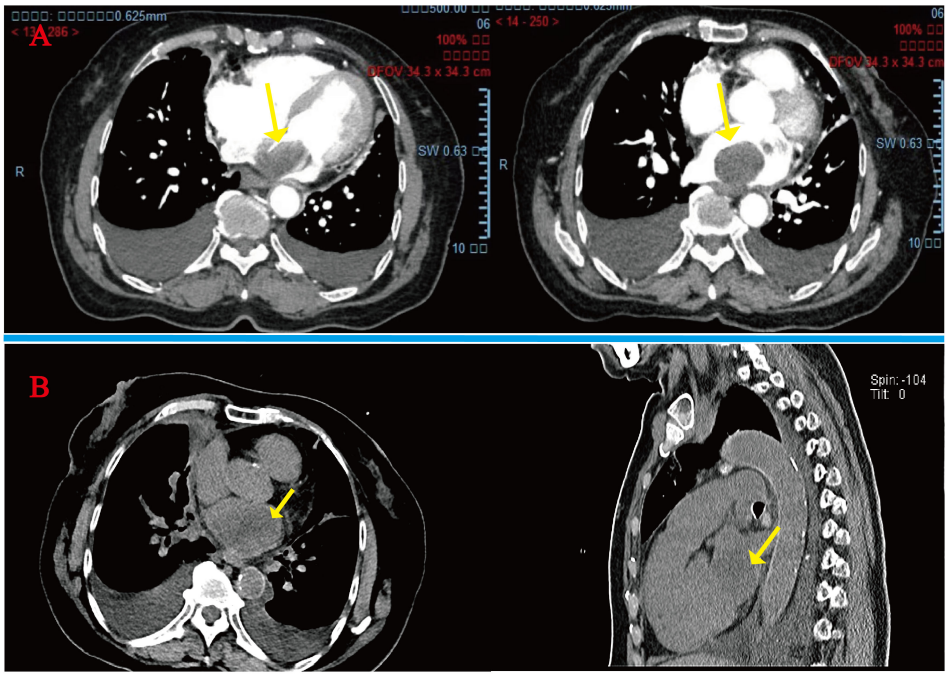

FIGURE 2
(A) Initial admission preoperative enhanced CT scan of the chest and abdomen: arrows indicate a homogeneous low-density mass almost entirely occupying the left atrium, extending into the left auricle and pulmonary artery opening. **(B)** Readmission CT tomography scan of the chest at 4 months postoperatively: tumor recurrence is seen at the arrows.

and their nuclei were skewed to one side. In the sparse cellular zone, the visual appearance of the stroma resembled mucus. The immunohistochemistry results revealed that vimentin, CD99, CD34, CD31, and CD56 were all positive. Desmin, SMA, MyoD1, and myogenin all showed focal positive expression, although 10% of the samples had Ki67. MDM2, S-100, β-catenin, STAT6, EMA, H3K27M, H3K27Me3, P16, GFAP and CD57 all yielded negative results (Figure 3). The tumor was confirmed to be IS and rhabdomyosarcoma based on the immunohistochemical results and the final pathologic evaluation.

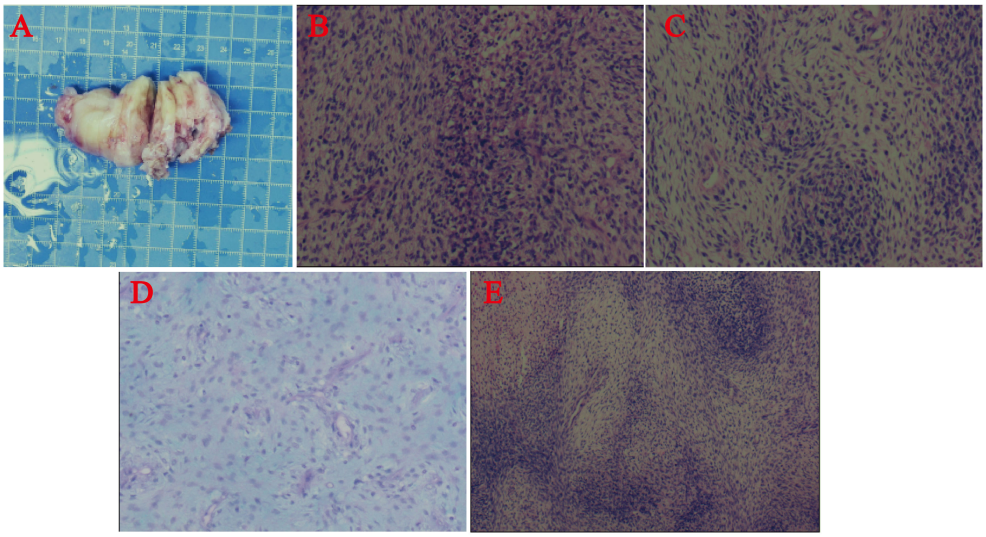

FIGURE 3
(A) Surgical resection of the cardiac mass. Postpathological histology and immunohistochemistry. **(B-E)** Under the microscope, the tumor was composed of dense and sparse cells, the tumor cells were spindle-shaped, with poorly defined cell boundaries, pale cytoplasm, long oval nuclei, obvious anisotropy, easy-to-see nuclear schizophrenia, and mucus-like stroma in the sparse cell area. Some of the cells are rich in cytoplasm and reddish stained, and the nuclei were biased to one side.

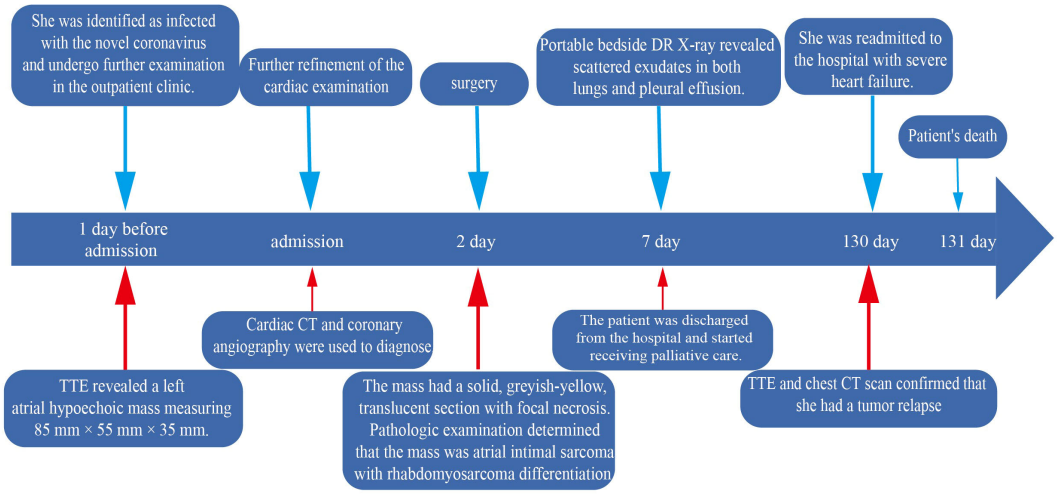

FIGURE 4
Complete timeline, including diagnosis (surgery) and treatment.

However, after the fourth month of surgery, she was readmitted to the hospital with severe heart failure symptoms, and a bedside TTE revealed a solid left atrial space causing mitral orifice obstruction, tricuspid regurgitation (moderate-to-severe), severe pulmonary hypertension, and a chest CT scan revealed a hypodense shadow in the left atrium and a large amount of pleural effusion. (Figure 2), We considered tumor recurrence and started urgent anti-heart failure therapy. The patient's oxygen saturation level was extremely low, and we performed ventilator-assisted ventilation. However, on the second day after admission, the patient's shortness of breath worsened, her consciousness appeared fuzzy, and she passed away after resuscitation (Figure 4).

Discussion

Cardiac IS are rare, primarily originating in the left heart, with a lack of specificity in clinical presentation. They are often incidentally detected due to comorbidities of other diseases, typically over 40 years old. Patients with IS may be asymptomatic or have clinical manifestations of mechanical obstruction or atrioventricular block secondary to the location of the mass, and Rahmouni et al. reported a patient with IS presenting with cardiogenic shock (8). As we have reported in this article, the patient did not present with any cardiac-related symptoms at the time of her initial visit and was only accidentally found to have a cardiac occupancy on physical examination, and the TTE and CT scan revealed that an atrial thrombus was a possibility. However, the patient denied a history of atrial fibrillation, and coagulation tests did not suggest abnormally elevated levels of D-dimer, so we ruled out an atrial thrombus. The most likely diagnosis was "cardiac myxomas", and surgery was performed for "left atrial cardiac myxomas". After completing the histopathological examination, we established the diagnosis of IS and found areas of rhabdomyosarcoma differentiation microscopically, which was supported by the focal positivity of immunohistochemistry for MyoD1 and myogenin, which is rare in cardiac IS. The classification of similar tumors in the heart remains difficult due to the lack of diagnostic consensus among soft tissue pathologists, and the diagnosis of undifferentiated pleomorphic sarcoma versus IS is currently debatable due to the extreme similarities in their biological behaviors. However, based on the cases that have been reported and the related reports, the diagnosis of IS is preferred when the following two basic criteria are met: ① occurrence within the lumen of a large blood vessel in the pulmonary or systemic circulation or within the lumen of the heart; and ② a primary high-grade sarcoma, with or without an anisotropic component (9). Moreover, histopathological and immunohistochemical examinations are important. Immunohistochemistry of IS shows positive MDM2 expression, but MDM2 is eventually overexpressed and amplified by fluorescence *in situ* hybridization (FISH), quantitative PCR (qPCR) or array comparative genomic hybridization (CGH) to distinguish IS and other cardiac sarcoma tissue subtypes (10). Currently, the classification of cardiac sarcomas is based on histological features. Nevertheless, understanding its molecular characteristics is important for understanding the unique biology of IS and may assist in the use of molecularly targeted agents (1).Chen et al.'s preliminary investigation of 70 primary cardiac sarcomas after molecular analysis revealed potentially actionable aberrations, including MDM2 and PDGFRA amplification. Fu et al.'s analysis of 410 cancer-associated gene copy numbers from a patient with IS identified PDGFRA, MDM2, KIT genomic amplification, and CDKN2A and CDKN2B deletions in that case, confirming the emerging concept of considering PDGFR signaling as a diagnostic biomarker specific for IS (11). Tamborini sequenced the mutational hotspots of the corresponding genes and showed that these genes had no gain-of-function alterations, further supporting the notion that autocrine/paracrine loops may be responsible for receptor activation, insights that justify the use of PDGFR small-molecule inhibitors (such as imatinib, sunitinib, and nilotinib) either alone or in combination with other therapies (6).

We went through many twists and turns in determining the diagnosis. In fact, the IS is uncommon and the initial pathologic and

radiologic features may be confused with those of other malignant or even benign cardiac tumors (12). Multimodal noninvasive imaging techniques play a complementary role in the preoperative diagnosis of cardiac tumors, including noninvasive and rapid TTE for the evaluation of the localization of the mass as well as the structures it invades. Typical myxomas mostly adhere to the interatrial septum with a smooth and shiny surface, and they are usually pedicled and attached to the ovale fossa (13). However, in our case, the mass observed on echocardiography was identified as being attached to the free wall of the left atrium. Furthermore, the attachment of the mass was broad, which indicates a sign of malignancy. CT can assess tissue features, vascularity, adjacent infiltrates and extracardiac metastases, and cardiac magnetic resonance imaging (MRI) is the standard diagnostic tool (14). 18F-FDG positron emission computed tomography (PET/CT) infers the presence of a malignant process based on the FDG uptake of the mass, and IS has a high FDG uptake (15, 16).

For IS, complete surgical resection is preferred (17). However, this is often impossible due to the surrounding vital structures, making tumor recurrence unavoidable, and in this case, it was rare to have such a rapid recurrence at only 4 months. In addition to this, the prognosis for IS remains very poor, with most primary cardiac malignancies having a survival of only 9 to 27 months (1). Anthracycline-based chemotherapy regimens are a potentially effective medical option for IS. Frezza's retrospective analysis of two chemotherapy regimens in 72 patients with IS showed that the real-world overall response rate (rwORR) was 38% in the anthracycline-based treatment group (18). For patients with localized disease, the median recurrence-free survival (RFS) was 14.6 months, and for patients with advanced disease, the median progression-free survival (PFS) was 7.7 months. For gemcitabine and pazopanib, the rwORR was 8%, and the median PFS was 3.2 and 3.7 months, respectively. Because of the significant risk of radiation-induced heart disease following high-dose radiotherapy in heart radiotherapy, high-dose radiotherapy is rarely used in cardiac malignancies, forcing clinicians to adopt a reduced-dose or segmented approach to radiation therapy, Fatima et al. observed superior survival in patients who received 40–50 Gy of postoperative radiation therapy compared with surgery alone (19).

We finally clarified the diagnosis of a malignant tumor: IS, which determined the possible future treatment, although this was based on the final postpathological histology and immunohistochemistry. In our case, we have summarized several key insights: First, IS symptoms are insidious, as in our patient, who did not present with cardiac discomfort prior to surgery. Secondly, non-invasive imaging tests other than PET/CT seem to have difficulty in recognizing the features of IS. Finally, diagnosis and surgery as early as possible will provide patients with more therapeutic options, including radiotherapy and chemotherapy.

Conclusion

Given the complexity of IS and their poor prognosis, the mass should be accurately evaluated preoperatively. Patients with atrial fibrillation are at risk of atrial thrombosis, whereas left ventricular thrombosis is associated with impaired left ventricular contraction (20). To achieve negative intraoperative margins as much as possible, when tumor resection is limited, patients with defined tumor subtypes may benefit from gene-targeted therapy with PDGFRA or MDM2, especially for those with less differentiated IS.

Data availability statement

The original contributions presented in the study are included in the article/supplementary material. Further inquiries can be directed to the corresponding authors.

Ethics statement

The studies involving humans were approved by The Ethics Review Board of the Sixth Affiliated Hospital of Guangzhou Medical University. The studies were conducted in accordance with the local legislation and institutional requirements. The participants provided their written informed consent to participate in this study. Ethical approval was not required for the study involving animals in accordance with the local legislation and institutional requirements because no animal experiments were performed. Written informed consent was obtained from the individual(s) for the publication of any potentially identifiable images or data included in this article.

Author contributions

HS: Writing – original draft, Investigation, Software. QL: Writing – review & editing. JL: Writing – original draft, Writing – review & editing. DX: Writing – review & editing. SH: Writing – review & editing. YD: Writing – original draft.

Funding

The author(s) declare that no financial support was received for the research, authorship, and/or publication of this article.

Acknowledgments

We would like to thank the study participants for their dedication, motivation and perseverance, as well as their delving into this rare case, which made these findings possible. I would like to thank the cooperation of the surgical team and the pathology department for providing the pathological data.

Conflict of interest

The authors declare that the research was conducted in the absence of any commercial or financial relationships that could be construed as a potential conflict of interest.

Publisher's note

References

1. Chen TW, Loong HH, Srikanthan A, Zer A, Barua R, Butany J, et al. Primary cardiac sarcomas: A multi-national retrospective review. *Cancer Med*. (2019) 8:104–10. doi: 10.1002/cam4.1897

2. Vander Salm TJ. Unusual primary tumors of the heart. *Semin Thorac Cardiovasc Surg*. (2000) 12:89–100. doi: 10.1053/ct.2000.5080

3. Kumar S, Barbhaiya C, Nagashima K, Choi EK, Epstein LM, John RM, et al. Ventricular tachycardia in cardiac sarcoidosis: characterization of ventricular substrate and outcomes of catheter ablation. *Circ Arrhythm Electrophysiol*. (2015) 8:87–93. doi: 10.1161/circep.114.002145

4. Durieux R, Tchana-Sato V, Lavigne JP, Radermecker MA, Moonen M, Scagnol I, et al. Recurrent cardiac intimal sarcoma misdiagnosed as a myxoma or Malignant transformation of a cardiac myxoma? *J Card Surg*. (2021) 36:357–62. doi: 10.1111/jocs.15200

5. Neuville A, Collin F, Bruneval P, Parrens M, Thivolet F, Gomez-Brouchet A, et al. Intimal sarcoma is the most frequent primary cardiac sarcoma: clinicopathologic and molecular retrospective analysis of 100 primary cardiac sarcomas. *Am J Surg Pathol*. (2014) 38:461–9. doi: 10.1097/pas.0000000000000184

6. Tamborini E, Casieri P, Miselli F, Orsenigo M, Negri T, Piacenza C. Analysis of potential receptor tyrosine kinase targets in intimal and mural sarcomas. *J Pathol*. (2007) 212:227–35. doi: 10.1002/path.2177

7. Chen D, Zhu G, Wang D, Zhang Z, Fang W, Qu Z. Clinicopathological and immunohistochemical features of pulmonary artery sarcoma: A report of three cases and review of the literature. *Oncol Lett*. (2016) 11:2820–6. doi: 10.3892/ol.2016.4308

8. Rahmouni K, Al Abri Q, Janelle M, Nguyen VH, Sabapathy C, Bernier PL, et al. Intimal cardiac sarcoma in an adolescent presenting with sudden cardiogenic shock. *Pediatr Blood Cancer*. (2021) 68:e29083. doi: 10.1002/pbc.29083

9. Cho H, Song IH, Jo U, Jeong JS, Koo HJ, Yang DH, et al. Primary cardiac sarcomas: A clinicopathologic study in a single institution with 25 years of experience with an emphasis on MDM2 expression and adjuvant therapy for prognosis. *Cancer Med*. (2023) 12:16815–28. doi: 10.1002/cam4.6303

10. Vinod P, Jabri A, Hegde V, Lahorra J, Cutler D. Functional mitral stenosis: imposture of primary cardiac intimal sarcoma. *Cardiol Res*. (2018) 9:307–13. doi: 10.14740/cr748w

11. Fu X, Niu W, Li J, Kiliti AJ, Al-Ahmadie HA, Iyer G, et al. Activating mutation of PDGFRB gene in a rare cardiac undifferentiated intimal sarcoma of the left atrium: a case report. *Oncotarget*. (2017) 8:81709–16. doi: 10.18632/oncotarget.20700

12. Marques Mendes E, Ferreira A, Felgueiras P, Silva A, Ribeiro C, Guerra D, et al. Primary intimal sarcoma of the left atrium presenting with constitutional symptoms. *Oxf Med Case Rep*. (2017) 2017:omx031. doi: 10.1093/omcr/omx031

13. Griborio-Guzman AG, Aseyev OI, Shah H, Sadreddini M. Cardiac myxomas: clinical presentation, diagnosis and management. *Heart*. (2022) 108:827–33. doi: 10.1136/heartjnl-2021–319479

14. Ye N, Lan L, Hu H, Liu J, Xu H. Case report: The diagnostic challenge of primary cardiac intimal sarcoma. *Front Cardiovasc Med*. (2023) 10:1089636. doi: 10.3389/fcvm.2023.1089636

15. Janssen N, Verheyen J, Albert A. Right atrial intimal sarcoma on 18F-FDG PET/CT. *Clin Nucl Med*. (2020) 45:e307–8. doi: 10.1097/rlu.0000000000003051

16. Klein MA, Scalcione LR, Youn T, Shah RA, Katz DS, Sung WW, et al. Intensely hypermetabolic lipomatous hypertrophy of the interatrial septum on 18-FDG PET with MRI and CT correlation. *Clin Nucl Med*. (2010) 35:972–3. doi: 10.1097/RLU.0b013e3181f9dfeb

17. Pomp J, van Asselen B, Tersteeg RHA, Vink A, Hassink RJ, van der Kaaij NP, et al. Sarcoma of the heart treated with stereotactic MR-guided online adaptive radiation therapy. *Case Rep Oncol*. (2021) 14:453–8. doi: 10.1159/000513623

18. Frezza AM, Assi T, Lo Vullo S, Ben-Ami E, Dufresne A, Yonemori K, et al. Systemic treatments in MDM2 positive intimal sarcoma: A multicentre experience with anthracycline, gemcitabine, and pazopanib within the World Sarcoma Network. *Cancer*. (2020) 126:98–104. doi: 10.1002/cncr.32508

19. Fatima J, Duncan AA, Maleszewski JJ, Kalra M, Oderich GS, Gloviczki P, et al. Primary angiosarcoma of the aorta, great vessels, and the heart. *J Vasc Surg*. (2013) 57:756–64. doi: 10.1016/j.jvs.2012.09.023

20. Poterucha TJ, Kochav J, O'Connor DS, Rosner GF. Cardiac tumors: clinical presentation, diagnosis, and management. *Curr Treat Opt Oncol*. (2019) 20:66. doi: 10.1007/s11864–019-0662–1

frontiers | Frontiers in Cardiovascular Medicine

TYPE Case Report
PUBLISHED 07 June 2024
DOI 10.3389/fcvm.2024.1367893

OPEN ACCESS

EDITED BY
Reto Asmis,
Wake Forest University, United States

REVIEWED BY
Liang Guo,
Bristol Myers Squibb, United States
Zhejun Cai,
Zhejiang University, China

*CORRESPONDENCE
Jin Qin
✉ Qinjin_lch@163.com

†These authors have contributed equally to this work

RECEIVED 09 January 2024
ACCEPTED 21 May 2024
PUBLISHED 07 June 2024

CITATION
Dai M, Chen Y and Qin J (2024) Atrioventricular re-entrant tachycardia and atrioventricular node re-entrant tachycardia in a patient with cancer under chemotherapy: a case report and literature review.
Front. Cardiovasc. Med. 11:1367893.
doi: 10.3389/fcvm.2024.1367893

Atrioventricular re-entrant tachycardia and atrioventricular node re-entrant tachycardia in a patient with cancer under chemotherapy: a case report and literature review

Meiyan Dai[1†], Yue Chen[2†] and Jin Qin[1*]

[1]Division of Cardiology, Department of Internal Medicine, Tongji Hospital, Tongji Medical College, Huazhong University of Science and Technology, Wuhan, China, [2]Department and Institute of Infectious Disease, Tongji Hospital, Tongji Medical College, Huazhong University of Science and Technology, Wuhan, China

Cardio-oncology is a new field of interest in cardiology focusing on the detection and treatment of cardiovascular diseases, such as arrhythmias, myocarditis, and heart failure, as side-effects of chemotherapy and radiotherapy. The association between chemotherapeutic agents and arrhythmias has previously been established. Atrial tachyarrhythmias, particularly atrial fibrillation, are most common, but ventricular arrhythmias, including those related to treatment-induced QT prolongation, and bradyarrhythmias can also occur. However, the association between chemotherapeutic agents and atrioventricular re-entrant tachycardia (AVRT)/atrioventricular node re-entrant tachycardia (AVNRT) remains poorly understood. Here, we report a patient with new-onset AVRT/AVNRT and lung cancer who underwent chemotherapy. We considered that chemotherapy or cancer itself may have been a trigger for the initiation of paroxysmal AVRT/AVNRT, and that radiofrequency catheter ablation was effective in treating this type of tachycardia. Here, possible mechanisms and potential genes (mostly ion channels) involved in AVRT/AVNRT are summarized and the mechanisms underlying the possible regulatory patterns of cancer cells and chemotherapy on ion channels are reviewed. Finally, we considered that ion channel abnormalities may link cancer or chemotherapy to the onset of AVRT/AVNRT. The aim of the present study was to highlight the association between chemotherapeutic agents and AVRT/AVNRT and to provide new insights for future research. Understanding the intermediate mechanisms between chemotherapeutic agents and AVRT/AVNRT may be beneficial in preventing chemotherapy-evoked AVRT/AVNRT (and/or other arrhythmias) in future.

KEYWORDS

chemotherapy, arrhythmia, cancer, ion channel, case report

1 Introduction

Cancer is a major disease threatening human health, accounting for nearly one in six deaths (1). Some cancers that have historically been associated with high fatality and mortality rates now have high cure rates, converting malignancy into a chronic disease (2). However, an increasing number of patients with cancer are at risk of the adverse effects of cancer therapy. Cancer therapy-related cardiac dysfunction is a serious side-effect of

chemotherapy, occurring in approximately 10% of patients (3). Cancer therapy has been linked to myocyte damage, such as heart failure, thrombogenesis, pericardial pathology, hypertension, ischemia, vasospasm, and myocarditis (4–6). However, few reports have addressed cancer treatment-induced arrhythmia until recently.

Chemotherapeutic agents, such as anthracyclines, alkylating agents, antimetabolites, histone deacetylase (HDAC) inhibitors, immunomodulatory drugs, platinum compounds, proteasome inhibitors, multitargeted tyrosine kinase inhibitors, vascular endothelial growth factor (VEGF) signaling pathway inhibitors, and immune check point inhibitors, are suggested to be associated with a broad range of arrhythmias, including sinus bradycardia and tachycardia, premature atrial complexes, supraventricular tachycardia (SVT), premature ventricular complexes (PVCs), and ventricular tachycardia (VT) (2, 7–11). Accelerated apoptosis, inflammation, mitochondrial dysfunction, oxidative stress, and impairment of intracellular calcium (Ca^{2+}) handling have been implicated in cancer therapy-induced arrhythmia (12–14). However, the detailed mechanisms through which chemotherapeutic agents cause arrhythmia remain unclear.

In terms of various arrhythmias, previous studies have reported the association between chemotherapeutic agents and SVT. SVT can be categorized as follows: atrioventricular re-entrant tachycardia (AVRT), atrioventricular node re-entrant tachycardia (AVNRT), atrial tachycardia, sinus tachycardia, sinus nodal re-entrant tachycardia, inappropriate sinus tachycardia, multifocal atrial tachycardia, junctional ectopic tachycardia, and non-paroxysmal junctional tachycardia. AVNRT and AVRT are types of paroxysmal supraventricular tachycardia (PSVT) that result from the presence of congenital re-entry circuits long before the development of cancer (15, 16). Currently, the association between cancer therapy and re-entrant tachycardia, such as AVNRT and/or AVRT, is poorly established.

Here, we report a case of new-onset AVRT/AVNRT in a patient with lung cancer who underwent chemotherapy. This case suggests that chemotherapy for cancer, or even the cancer itself, might be a possible trigger for the onset of AVRT/AVNRT. Moreover, as the direct mechanisms underlying cancer therapy-induced arrhythmia (especially AVNRT/AVRT) remain unclear, we summarize relevant evidence from available mechanistic studies. This study may provide insights into the development of new strategies and drugs to prevent and treat cancer therapy agent-induced arrhythmias.

2 Case report

2.1 Chemotherapy as a trigger for AVRT/AVNRT

A 65-year-old man with a history of lung cancer and chemotherapy, admitted to hospital on 4 October 2023 with a 2-week history of right-sided chest pain, was diagnosed with lung adenocarcinoma (LUAD) (cT2N2MIaIVa). The patient denied a history of hypertension, diabetes, mental illness, or cardiovascular/cerebrovascular disease and did not receive any daily pharmacological treatment. The patient did not refer to any arrhythmia relevant to his medical history. On 12 October 2023, he was treated with pemetrexed and nedaplatin (NDP; intravenous injection) and endostatin (intrapleural infusion). On 30 October, he received a bevacizumab intravenous injection. During the course of the disease, the patient's serum electrolyte level was dynamically monitored, and the electrolyte balance was basically maintained; in particular, the serum potassium level was maintained at approximately 4.0–4.5 mmol/L. On 5 November, he complained of hourly palpitations and tachycardic episodes. A 12-lead electrocardiogram (ECG) showed a narrow QRS complex tachycardia (Figure 1A), which was refractory to intravenous therapy with propafenone and adenosine triphosphate. A subsequent transesophageal electrogram indicated a possible slow-fast AVNRT and orthodromic AVRT (Figures 1B–D). After obtaining patient and family consent, electrophysiology study and radiofrequency catheter ablation were performed using the Carto 3^{TM} system. A decapolar catheter was advanced into the coronary sinus (CS) and a quadripolar catheter was positioned in the right ventricular apex. The patient was in normal sinus rhythm at baseline with proximal to distal coronary sinus activation. During the electrophysiology study, fixed retrograde atrial conduction was observed under ventricular pacing, with the earliest atrial activation at CS7/8. Coronary sinus pacing showed the jump-up phenomenon, and a narrow QRS tachycardia was stably induced. A combined analysis of electrophysiology study with transesophageal electrogram, a left posterior septal accessory pathway, and AVNRT were considered. The ablation catheter gained access to the left ventricle via a retrograde aortic approach, and the earliest atrial activation and local VA fusion was detected at CS7/8 under ventricular pacing (Figure 2A). After ablation with a 35 W discharge, the earliest atrial activation changed to CS1/2 with ventricular pacing (Figure 2B). Therefore, the patient appeared to have another concealed left lateral accessory pathway (Figure 2C). After ablation with a 35 W discharge, the local VA fusion was separated under ventricular pacing. Ventricular decremental pacing and ventricular extrastimuli did not demonstrate ventriculoatrial conduction anymore, while atrial extrastimulus testing demonstrated dual AV node physiology. During the coronary sinus stimulation with S1S2, the jumping phenomenon was observed, even though it could not induce tachycardia. After intravenous infusion of isoproterenol, coronary sinus stimulation revealed the jumping phenomenon and induced narrow QRS wave tachycardia stably. During tachycardia, the retrograde A wave in the coronary sinus electrode remained in a straight line, leading to the diagnosis of slow-fast atrioventricular nodal re-entrant tachycardia. A slow pathway ablation was performed (Figure 2D), eliminating the dual AV node physiology even with programed atrial stimulation with and without isoproterenol. The patient reported no palpitations during a follow-up phone call 4 months after the procedure.

2.2 Genes/pathways associated with AVRT/AVNRT

AVNRT occurs when a re-entry circuit is formed within or in close proximity to an AV node (17). Dual AV nodal conduction is a

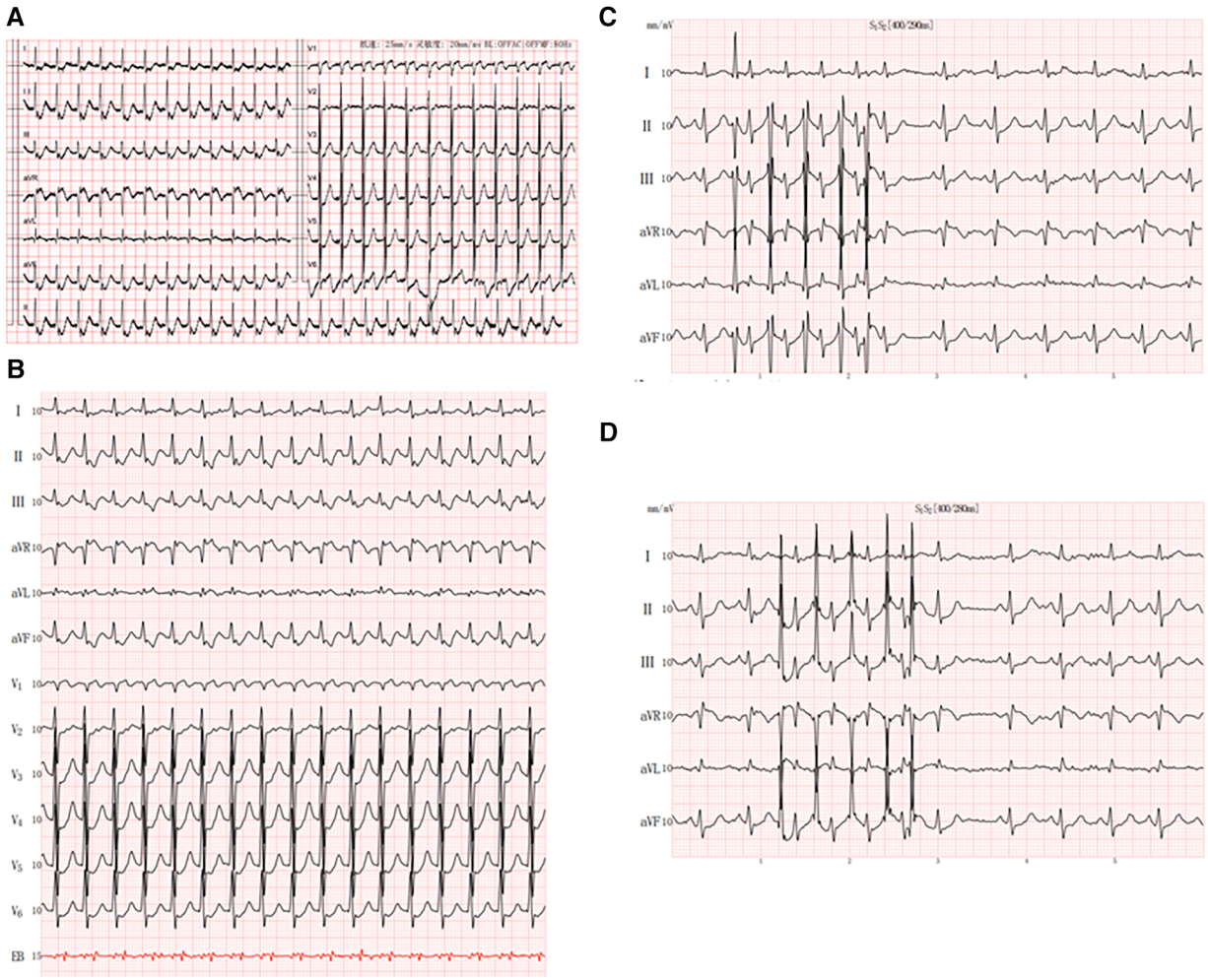

FIGURE 1
Patient characteristics: (A) 12-lead electrocardiogram showed a small-complex supraventricular tachycardia; (B) esophageal electrocardiogram showed RP′ < P′R and RP′ interval of 120 ms in V1; (C,D) jumping phenomenon caused by S_2R stimulation.

congenital abnormality that develops during prenatal cardiogenesis (18). AVRT is a macro-re-entrant tachycardia with an anatomically congenital circuit consisting of two distinct pathways (19). While these are congenital abnormalities, some studies have reported that the onset of AVNRT/AVRT can be triggered through several factors.

AVNRT is twice as common in women as in men and is the most common arrhythmia encountered during pregnancy, with approximately 44% of patients with known AVNRT experiencing symptoms during pregnancy (20, 21). Women with AVNRT are known to be significantly younger at symptom onset than men (22); therefore, sex hormones may also trigger tachycardia.

It has been suggested that AVNRT is an ion channel disease. Familial clustering indicates the involvement of genetic factors in AVNRT pathophysiology. Andreasen et al. reported that 26.4% of patients with AVNRT had ≥1 variant in genes affecting sodium handling, namely, *SCN3A*, *SCN5A*, *SCN10A*, *SCN8A*, *SCN4A*, *SCN1A*, *SCN2B*, and *SCN9A*, and 19.0% of patients with AVNRT had variants in genes affecting calcium handling (*RYR2*, *RYR3*, *CACNB2*, *ATP2A2*, *CACNA1C*, *CACNA1D*, *CACNA1I*, and *CACNA1G*) in the heart. Moreover, variants in *HCN1–4* and *KCNE3* have also been associated with AVNRT (23).

One study performed whole-exome sequencing (WES) in 82 patients with AVNRT and in 100 controls. They reported that the genes *SCN1A*, *PRKAG2*, *RYR2*, *CFTR*, *NOS1*, *PIK3CB*, *GAD2*, and *HIP1R* and the related pathways mediated by these genes, such as neuronal system/neurotransmitter release cycles or ion channels/cardiac conduction, might be involved in AVNRT (24, 25).

In terms of another type of PSVT, AVRT had a similar incidence in both young and older adults. The male/female ratio was similar across all age ranges (26). Familial Wolff–Parkinson–White syndrome (WPW), which is a common cause of AVRT, is well recognized as a cardiovascular disease, partly due to mutations in genes such as *PRKAG2* (27, 28). Pathogenic variants of MYH7 and rare *de novo* variants of genes associated with arrhythmia and cardiomyopathy (*ANK2*, *NEBL*, *PITX2*, and *PRDM16*) have been suggested as the genetic basis of WPW (29).

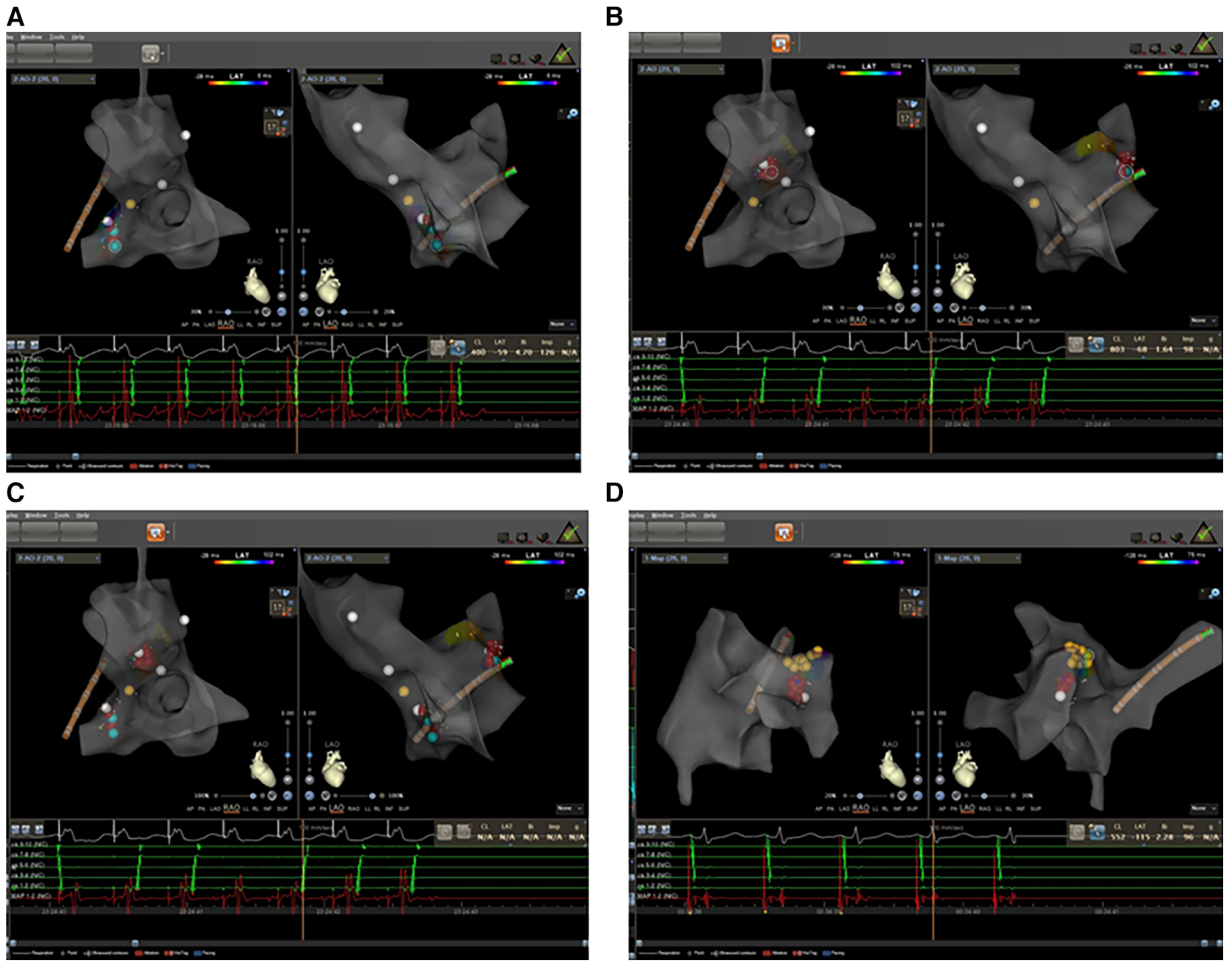

FIGURE 2
Electrophysiology study was performed with zero-fluoroscopy-approach-guided Carto 3TM system. (A) The earliest atrial activation was at CS7/8 with fixed retrograde atrial conduction under ventricular pacing. (B) The earliest atrial activation changed to CS1/2 with fixed retrograde atrial conduction under ventricular pacing. (C) The ablation targets of left lateral and septal accessory pathways. (D) The ablation targets of slow pathway modification. Red dots: ablation target; yellow dots: His bundle.

Therefore, compared with AVRT, AVNRT appears to be more intricately linked to ion channels if not caused by ion channel dysfunction, and the onset of symptoms is largely influenced by ion channels (Figure 3).

2.3 Regulation of ion channels in cancers

Previous studies have reported the dysregulation of ion channels in cancer cells. One study reported that the voltage-gated K^+ channel of Kv10.1 (EAG1) was aberrantly expressed in human pancreatic ductal adenocarcinoma (30). Moreover, EAG1 channels have been detected in approximately 70% of tumor biopsies originating from various cancers (31). Another K^+ channel, KCNQ1 (potassium voltage-gated channel subfamily Q Member 1), is also associated with the development of colorectal cancer (CRC) (32). In breast and prostate cancers, decreased expression of the K^+ channel KCNA3 has been found to be associated with an increased tumor grade. The K^+ channel HERG1 (KCNH2) is upregulated in CRCs. The K^+ channels EAG2 (KCNH5) and KCNT2 are highly expressed in the medulloblastoma of pediatric brain tumors. KCNA5, KCNQ1, and KCNN4 are also abnormally expressed in certain cancers (33).

Na^+ channels include the voltage-gated sodium channel (VGSC) and ligand-gated sodium channel (LGSC) subfamilies. VGSC contains nine subtypes of Nav1.1–Nav1.9, including both α and β subunits. The expression of Nav1.5, Nav1.6, and Nav1.7 is upregulated in many cancer types, such as prostate, breast, lung, and cervical cancer, and leukemia (34).

Dysregulation of Ca2+ channels has also been shown to be involved in the development of various types of cancer (35, 36). For example, in breast cancer, prostate cancer, and leukemia, the voltage-gated Ca2+ channels are upregulated (37). Notably, ion channel-related proteins in cancer cells are secreted by small extracellular vesicles (sEVs). Proteomic profiling of small extracellular vesicles secreted by human pancreatic cancer cells has shown the presence of KCNN4, KCNK5, and KCNMA1 in extracellular vesicles (38). KCNN4 has also been reported to be

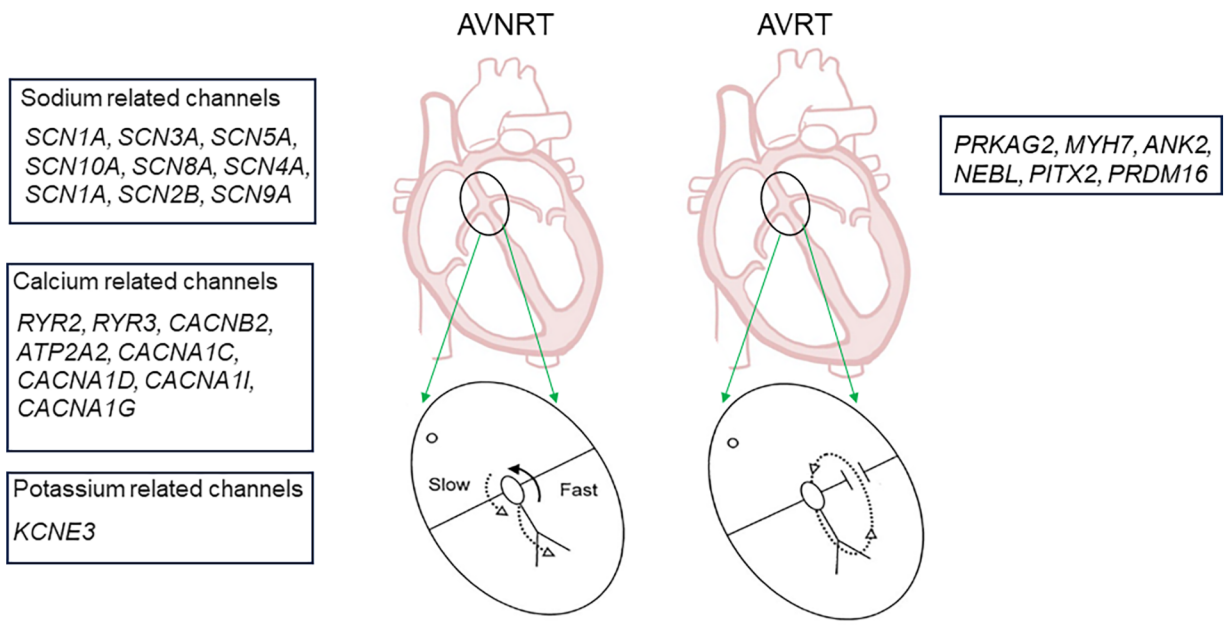

FIGURE 3
Genes that are potentially associated with AVNRT and AVRT.

detectable in cancer extracellular vesicles in breast, colon, and melanoma cancers. KCNAB3 is expressed in the extracellular vesicles of ovarian cancer cells. KCNQ1 and KCNH8 are present in the EVs of colon cancer. KCNAB2 is measurable in extracellular vesicles in breast, colon, and kidney cancers, and in leukemia and melanoma. KCNH4 has been detected in the extracellular vesicles of breast and lung cancer cells. The Ca2+ channel CACNA2D2 has been detected in breast, colon, melanoma, and ovarian extracellular vesicles. CACNA2D1 is highly expressed in breast, brain, lung, melanoma, and prostate cancer extracellular vesicles. CACNA1E has been detected in the extracellular vesicles of the breast, brain, colon, kidney, and ovaries (39, 40). sEVs can efficiently translocate to the cardiomyocytes (41, 42). Mechanistically, cancer cell-derived sEVs carrying aberrant ion channels that translocate into the heart may mediate ion homeostasis between cancer cells and cardiomyocytes.

Ion homeostasis affects cancer apoptosis and cell migration, and regulates the release of neurotransmitters, hormones, and growth factors in both normal cells (such as myocytes) and neoplastic cells (43, 44). Cancer cell secretions appear to indirectly induce ion channel dysfunction in myocytes. After treatment with cancer cell secretions, the maximum depolarization velocity and action potential amplitude in human-induced pluripotent stem cell (iPSC)-derived cardiomyocytes were reduced. Moreover, the action potential duration was prolonged, the peak Na^+ and transient outward currents decreased, and late Na^+ and slowly activating delayed rectifier K^+ currents increased. Mechanistically, DNA methylation of ion channel genes via activation of TGF-β/PI3K signaling might contribute to ion channel dysfunction (45).

Moreover, cancer cells metabolize glucose via glycolysis, and hypoxia can further aggravate dependence on glycolytic fueling, resulting in the overproduction of lactic acid (46, 47). Elevated circulating lactate levels have been documented in patients with various types of cancers (breast, prostate, colorectal, lung, and ovarian) (48–51). Lactate potently regulates ion channels in the muscle cells. For example, Ca^{2+}-activated K^+ channels (KCa channels) are activated by lactate in smooth muscle cells. Keung and Li reported that lactate activates KATP channels in guinea pig myocytes, and Han et al. reported that lactate induces the opening of KATP channels in rabbit ventricular myocytes (52, 53). Lactate has also been shown to modify the fast sodium current through hyperpolarization in guinea pig myocytes (54), which may contribute to the development of arrhythmia.

Investigators have found that tumor cells secrete neurotrophic growth factors, axon guidance molecules, VEGF, and chemical messengers (55–57). Many cancer cells synthesize and release catecholamines. Norepinephrine levels are higher in pancreatic cancer tissue than in normal tissue (58). Plasma norepinephrine and epinephrine concentrations are significantly upregulated in patients with oral and oropharyngeal squamous cell carcinoma (SCC) compared with those in patients with no cancer (59). Plasma-free metanephrine and normetanephrine levels are elevated in patients with gastric carcinoma and lung cancer (60, 61). Catecholamines play major roles in the induction of cardiac ion channel dysfunction and rhythm disorders (62).

The possible mechanisms linking cancer cells and the dysregulation of myocyte-localized ion channels are summarized in Figure 4.

2.4 Regulation of ion channels under chemotherapy

Ion channels are key regulators of cancer cell pathophysiology (63). Anticancer therapeutics appear to play non-negligible roles in the regulation of ion homeostasis in tumor cells.

Zhang et al. reported that paclitaxel, considered the most significant advance in chemotherapy in the past two decades, accelerates Ca^{2+} oscillations through increasing the IP3R opening frequency (64). Kang et al. showed that trifluoperazine, a well-known antipsychotic drug with anticancer effects, suppresses glioblastoma invasion through binding to the Ca^{2+}-binding protein calmodulin subtype 2 (CaM2) (65).

The chemotherapeutic drug cisplatin activates the K^+ channel KCa3.1, with the activation effect most likely due to the increase in intracellular Ca^{2+} concentration (66). Reduction in the activity of KCa3.1 has also been demonstrated with oxaliplatin treatment (67).

In non-tumor tissues/cells, chemotherapy can induce ion channel dysfunction. The development of acute oxaliplatin-induced peripheral neuropathy has been suggested to be due to changes in voltage-gated sodium channels, voltage-gated calcium channels, and in the TREK-1 two-pore-domain background K^+ channel (68–70). Chemotherapy directly alters the ion channel activities of cardiomyocytes. Chemotherapy drugs and HDAC inhibitors have been associated with QTc prolongation and arrhythmias, and blockade of the KCNH2 by HDAC inhibitors may be a mechanistic explanation (71). Ibrutinib upregulates calmodulin kinase 2 expression and increases the phosphorylation of ryanodine receptor 2 (RyR) in the cardiomyocyte endoplasmic reticulum, impairing intracellular calcium handling and triggering ectopic electrical activity (72). PD-1 deficiency results in premature mortality due to high-titer IgG autoantibodies against cardiac troponin I, augmenting the voltage-dependent L-type calcium current in normal cardiomyocytes (73). Anti-HER2 therapy also causes calcium homeostasis dysfunction within cardiomyocytes, leading to Reactive Oxygen Species (ROS) activation within the myocardium, similar to that caused by anthracyclines or other antineoplastic agents (74). Calcium oscillations in cardiac cells that alter automaticity have been proposed to be the mechanism underlying Bruton kinase inhibitor-induced cardiac toxicity (75).

The possible mechanisms linking chemotherapy with dysfunction of myocyte-localized ion channels are summarized in Figure 5.

2.5 Chemotherapy associated arrhythmias in LUAD

It has been suggested that chemotherapeutic agents are associated with a variety of arrhythmias. Combination chemotherapy of pemetrexed and carboplatin is a standard

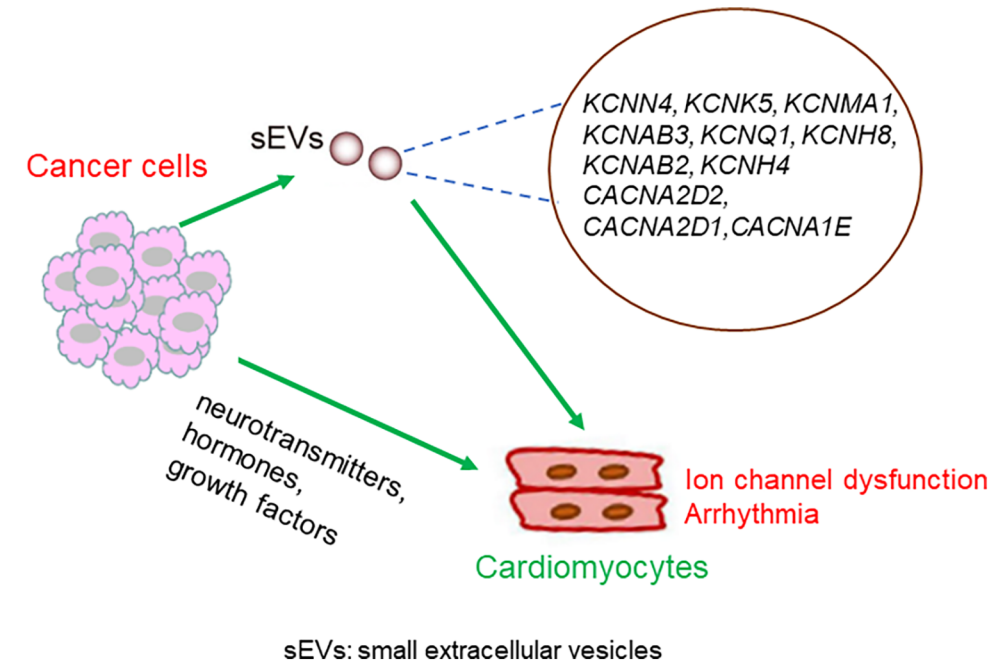

FIGURE 4
Possible mechanisms underlying the crosstalk between cancer cells and cardiomyocytes. Molecules secreted from cancer cells translocate into the heart, either through sEVs or other forms of particles, and regulate the expression or activity of cardiomyocytes localized ion channels. Alternatively, neurotransmitters, hormones, and growth factors secreted from cancer cells might mediate the crosstalk between cancer cells and cardiomyocytes.

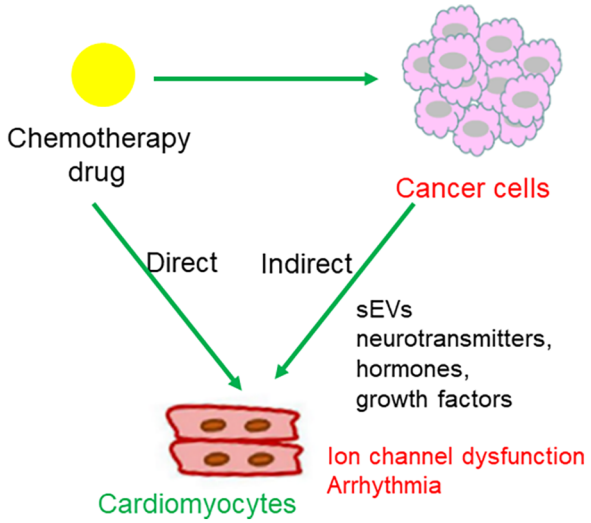

FIGURE 5
Regulatory pattern of chemotherapy drugs on cardiomyocytes. (1) Chemotherapeutic agents act upon cancer cells, leading to cancer cell death and subsequent release of chemical messages to indirectly influence cardiomyocytes localized ion channels; (2) direct action of chemotherapeutic agents on ion channels in cardiomyocytes.

treatment approach for non-small cell lung cancer (NSCLC). A case report showed pemetrexed and carboplatin appear to have triggered sinus arrhythmia in a patient undergoing multiple courses of chemotherapy (76). However, the mechanisms underlying the case of sinus arrhythmia are unclear. NDP is a second-generation platinum derivative, which has similar antitumor activity to cisplatin with less nephrotoxicity and gastrointestinal toxicity. NDP-induced cardiotoxicity is rare, although it has been presented that three patients who were treated with NDP developed chemotherapy-induced serious arrhythmias. The three cases developed sinus tachycardia and atrial premature beats, complete left bundle branch block, and bigeminy ventricular premature contraction, in the second, sixth, and second cycles, respectively (77). The arrhythmias in these patients were resolved after drug treatment, withdrawal of chemotherapy, or adjustment of chemotherapy regimens.

Treatment with bevacizumab increases the risk of arterial adverse events, particularly cardiac and cerebral ischemia, venous adverse events, bleeding, and arterial hypertension (78). However, bevacizumab-associated arrhythmia is also rare. One case reported a patient with lung adenocarcinoma who was treated with bevacizumab monotherapy, and a poor R-wave increase with slight ST segment elevation in V1-V3 leads and ventricular arrhythmia were detected. The patient's chest tightness and rapid heartbeat disappeared after the amiodarone treatment. The ECG monitoring results returned to normal (79).

It has been hypothesized that chemotherapeutic drug-associated cardiotoxicity occurs due to electrolyte imbalance or disturbance of the sinoatrial node. Herein, it is important to note that our patient developed ANRT and AVNRT during the first course of chemotherapy, without any electrolyte imbalance. However, it is important to consider that multiple factors, including chemotherapeutic drug combination, the selective cardiotoxicity of this chemotherapeutic regimen, aging, and heart disease-related risk factors, are all likely to have contributed to our patient's situation.

KCNQ1 is implicated in long QT syndrome (LQTS) and cardiac arrhythmia; the clinical significance and biological role of KCNQ1 in LUAD is also described. The potential mechanism of KCNQ1 underlying LUAD progression may lie in the perturbation of genes relevant to the cell cycle and DNA replication. However, KCNQ1-inhibitor gefitinib, which is the first-generation targeted therapy for non-small cell lung cancer, was implicated in the induction of heart QT prolongation in a guinea pig model, thereby raising a concern of arrhythmia when gefitinib is used for NSCLC treatment (80).

3 Conclusions and perspectives

An estimated 32%–40% of the population has dual atrioventricular nodal physiology; however, only a minority develop AVNRT (81). The incidence of AVNRT is 35 per 10,000 person-years or 2.29 per 1,000 persons, and it is the most common form of non-sinus tachydysrhythmia in young adults (82). Regarding AVRT, one study reported a tachyarrhythmia rate of 1.0% per year in individuals with a WPW pattern (83). Therefore, the onset of AVNRT or AVRT in patients with dual atrioventricular nodal pathways or accessory atrioventricular pathways is rare, and when they occur, they are usually attributed to stress in relation to pregnancy, exertion, caffeine, alcohol, beta-agonists (salbutamol), or sympathomimetics (amphetamines) (84, 85). Chemotherapeutic agents directly promote various arrhythmias, such as atrial fibrillation (AF) and ventricular ectopic beats. However, chemotherapy-induced AVRT/AVNRT has rarely been reported. Here, we present a typical case of chemotherapy-related AVRT/AVNRT. Moreover, we propose the following potential mechanisms underlying chemotherapeutic agent-induced AVRT/AVNRT: (1) molecules secreted from cancer cells translocate into the heart, either through sEVs or other forms of particles, regulating the expression or activity of cardiomyocyte-localized ion channels; (2) chemotherapeutic agents act on cancer cells, leading to cancer cell death and the subsequent release of chemical messages to indirectly influence cardiomyocyte-localized ion channels; and (3) direct action of chemotherapeutic agents on ion channels in cardiomyocytes.

Animal models are of vital importance for investigating the cause-effect relationship and detailed mechanisms between chemotherapy and arrhythmias, such as AVRT/AVNRT. Mice are the primary animal models for studying arrhythmias, particularly genetic arrhythmia syndromes. *RYR2* mutations have been found to be implicated in several arrhythmia disorders, including catecholaminergic polymorphic ventricular tachycardia (CPVT), PVC ventricular fibrillation, and AF (86). KCNQ1 or CACNA1C (Cav1.2) overexpression has been associated with LQTS, sympathetic stimulation-induced early after depolarizations

(EADs), and VT; mice with HCN4 (HCN4) ablation exhibited bradycardia, exit block, SVT, VT, and complete block (86). However, mouse models of AVRT/AVNRT have not been well established, partly because of technical difficulties in performing esophageal electrophysiological examinations or intracardiac electrophysiological studies on mice. Therefore, in the absence of an effective animal model, it is difficult to determine the exact pathophysiological basis of AVNRT. Further studies are required to establish animal models and develop electrophysiological examination technologies for small animals (such as mice). For *in vitro* studies, patient-specific iPSC-derived cardiomyocytes and human iPSC-derived 3D organotypic cardiac microtissues might be attractive experimental platforms to investigate the regulation of secretions from cancer cells and chemotherapeutic agents on ion channel activities on a large scale (87, 88). Moreover, high-throughput sequencing and mass spectrometry methods would allow for the systemic investigation of the regulation of ion channels by different types of chemotherapeutic agents. Further studies are required to identify the chemotherapeutic agents that are strongly associated with ion channel dysfunction. In clinical practice, agents that do not cause ion channel dysfunction are preferred.

Mechanistically, the direct regulation of cardiomyocytes by chemotherapeutic agents and the indirect regulation of cancer cells (with or without chemotherapy) on cardiomyocytes, such as sEV-mediated cancer-myocyte crosstalk, should be thoroughly investigated. Cell co-culture and Transwell experiments are helpful for studying complicated cancer-myocyte crosstalk.

In terms of treatment, arrhythmias are considered one of the clinical manifestations of heart failure and cardiomyopathy. Permanent treatment, such as ablation therapy, should be considered for arrhythmias with high success or cure rates, such as atrial flutter, AVNRT, AVRT, and atrial tachycardia (89). In this case, SVT was refractory to intravenous therapy with propafenone and reappeared repeatedly until ablation therapy successfully prevented the onset of AVNRT/AVRT after chemotherapy. Therefore, radiofrequency ablation may be an option for patients with arrhythmias after chemotherapy and poor response to antiarrhythmic drugs.

Data availability statement

The original contributions presented in the study are included in the article/Supplementary Material, further inquiries can be directed to the corresponding author.

Ethics statement

Written informed consent was obtained from the individual(s) for the publication of any potentially identifiable images or data included in this article.

Author contributions

MD: Writing – original draft. YC: Writing – original draft. JQ: Writing – review & editing.

Funding

The authors declare financial support was received for the research, authorship, and/or publication of this article.

This work was supported by grants from the National Natural Science Foundation of China (81800334). The funders had no role in study design, data collection and analysis, manuscript preparation, or decision to publish.

Acknowledgments

We thank our colleague Huaping Li for stimulating discussions. We would like to thank Editage (www.editage.com) for English language editing.

Conflict of interest

The authors declare that the research was conducted in the absence of any commercial or financial relationships that could be construed as a potential conflict of interest.

Publisher's note

References

1. Siegel RL, Miller KD, Jemal A. Cancer statistics, 2020. *CA Cancer J Clin*. (2020) 70 (1):7–30. doi: 10.3322/caac.21590

2. Buza V, Rajagopalan B, Curtis AB. Cancer treatment-induced arrhythmias: focus on chemotherapy and targeted therapies. *Circ Arrhythm Electrophysiol*. (2017) 10(8):e005443. doi: 10.1161/CIRCEP.117.005443

3. Perez IE, Taveras Alam S, Hernandez GA. Cancer therapy-related cardiac dysfunction: an overview for the clinician. *Clin Med Insights Cardiol*. (2019) 13:1179546819866445. doi: 10.1177/1179546819866445

4. Rowinsky EK, McGuire WP, Guarnieri T, Fisherman JS, Christian MC, Donehower RC. Cardiac disturbances during the administration of taxol. *J Clin Oncol*. (1991) 9(9):1704–12. doi: 10.1200/JCO.1991.9.9.1704

5. Bloom MW, Hamo CE, Cardinale D, Ky B, Nohria A, Baer L, et al. Cancer therapy-related cardiac dysfunction and heart failure: part 1: definitions, pathophysiology, risk factors, and imaging. *Circ Heart Fail*. (2016) 9(1):e002661. doi: 10.1161/CIRCHEARTFAILURE.115.002661

6. Sorrentino MF, Kim J, Foderaro AE, Truesdell AG. 5-fluorouracil Induced cardiotoxicity: review of the literature. *Cardiol J*. (2012) 19(5):453–8. doi: 10.5603/CJ.2012.0084

7. Kilickap S, Barista I, Akgul E, Aytemir K, Aksoy S, Tekuzman G. Early and late arrhythmogenic effects of doxorubicin. *South Med J*. (2007) 100(3):262–5. doi: 10.1097/01.smj.0000257382.89910.fe

8. Olsen EA, Kim YH, Kuzel TM, Pacheco TR, Foss FM, Parker S, et al. Phase IIb multicenter trial of vorinostat in patients with persistent, progressive, or treatment refractory cutaneous T-cell lymphoma. *J Clin Oncol*. (2007) 25(21):3109–15. doi: 10.1200/JCO.2006.10.2434

9. Fahdi IE, Gaddam V, Saucedo JF, Kishan CV, Vyas K, Deneke MG, et al. Bradycardia during therapy for multiple myeloma with thalidomide. *Am J Cardiol*. (2004) 93(8):1052–5. doi: 10.1016/j.amjcard.2003.12.061

10. Khozin S, Blumenthal GM, Zhang L, Tang S, Brower M, Fox E, et al. FDA approval: ceritinib for the treatment of metastatic anaplastic lymphoma kinase-positive non-small cell lung cancer. *Clin Cancer Res*. (2015) 21(11):2436–9. doi: 10.1158/1078-0432.CCR-14-3157

11. Steinberg JS, Cohen AJ, Wasserman AG, Cohen P, Ross AM. Acute arrhythmogenicity of doxorubicin administration. *Cancer*. (1987) 60(6):1213–8. doi: 10.1002/1097-0142(19870915)60:6<1213::AID-CNCR2820600609>3.0.CO;2-V

12. Yang X, Li X, Yuan M, Tian C, Yang Y, Wang X, et al. Arrhythmias and device therapies in patients with cancer therapy-induced cardiomyopathy. *Heart Rhythm*. (2021) 18(7):1223–9. doi: 10.1016/j.hrthm.2021.02.017

13. Yang X, Li X, Yuan M, Tian C, Yang Y, Wang X, et al. Anticancer therapy-induced atrial fibrillation: electrophysiology and related mechanisms. *Front Pharmacol*. (2018) 9:1058. doi: 10.3389/fphar.2018.01058

14. Duan J, Tao J, Zhai M, Li C, Zhou N, Lv J, et al. Anticancer drugs-related QTc prolongation, torsade de pointes and sudden death: current evidence and future research perspectives. *Oncotarget*. (2018) 9(39):25738–49. doi: 10.18632/oncotarget.25008

15. Marzlin KM. Atrioventricular nodal reentrant tachycardia. *AACN Adv Crit Care*. (2017) 28(1):84–8. doi: 10.4037/aacnacc2017887

16. Sugumar H, Tung M, Leather R, Lane C, Sterns LD, Novak PG. Atrioventricular nodal non re-entrant tachycardia (AVNNT). *Heart Lung Circ*. (2017) 26(5):524–5. doi: 10.1016/j.hlc.2016.07.014

17. Akhtar M, Jazayeri MR, Sra J, Blanck Z, Deshpande S, Dhala A. Atrioventricular nodal reentry. Clinical, electrophysiological, and therapeutic considerations. *Circulation*. (1993) 88(1):282–95. doi: 10.1161/01.CIR.88.1.282

18. Hayes JJ, Sharma PP, Smith PN, Vidaillet HJ. Familial atrioventricular nodal reentry tachycardia. *Pacing Clin Electrophysiol*. (2004) 27(1):73–6. doi: 10.1111/j.1540-8159.2004.00388.x

19. Marzlin KM, Webner C. Atrioventricular reentrant tachycardia. *AACN Adv Crit Care*. (2017) 28(2):223–8. doi: 10.4037/aacnacc2017151

20. Silversides CK, Harris L, Haberer K, Sermer M, Colman JM, Siu SC. Recurrence rates of arrhythmias during pregnancy in women with previous tachyarrhythmia and impact on fetal and neonatal outcomes. *Am J Cardiol*. (2006) 97(8):1206–12. doi: 10.1016/j.amjcard.2005.11.041

21. Porter MJ, Morton JB, Denman R, Lin AC, Tierney S, Santucci PA, et al. Influence of age and gender on the mechanism of supraventricular tachycardia. *Heart Rhythm*. (2004) 1(4):393–6. doi: 10.1016/j.hrthm.2004.05.007

22. Deneke T, Müller P, Lawo T, Lemke B, Horlitz M, Calcum B, et al. Gender differences in onset of symptoms in AV nodal re-entrant and accessory pathway-mediated re-entrant tachycardia. *Herzschrittmacherther Elektrophysiol*. (2009) 20(1):33–8. doi: 10.1007/s00399-009-0036-7

23. Andreasen L, Ahlberg G, Tang C, Andreasen C, Hartmann JP, Tfelt-Hansen J, et al. Next-generation sequencing of AV nodal reentrant tachycardia patients identifies broad spectrum of variants in ion channel genes. *Eur J Hum Genet*. (2018) 26(5):660–8. doi: 10.1038/s41431-017-0092-0

24. Luo R, Zheng C, Yang H, Chen X, Jiang P, Wu X, et al. Identification of potential candidate genes and pathways in atrioventricular nodal reentry tachycardia by whole-exome sequencing. *Clin Transl Med*. (2020) 10(1):238–57. doi: 10.1002/ctm2.25

25. Huang J, Luo R, Zheng C, Cao X, Zhu Y, He T, et al. Integrative analyses identify potential key genes and calcium-signaling pathway in familial atrioventricular nodal reentrant tachycardia using whole-exome sequencing. *Front Cardiovasc Med*. (2022) 9:910826. doi: 10.3389/fcvm.2022.910826

26. Brembilla-Perrot B, Houriez P, Beurrier D, Claudon O, Burger G, Vançon AC, et al. Influence of age on the electrophysiological mechanism of paroxysmal supraventricular tachycardias. *Int J Cardiol*. (2001) 78(3):293–8. doi: 10.1016/S0167-5273(01)00392-8

27. Gollob MH, Green MS, Tang AS, Gollob T, Karibe A, Ali Hassan AS, et al. Identification of a gene responsible for familial Wolff-Parkinson-White syndrome. *N Engl J Med*. (2001) 344(24):1823–31. doi: 10.1056/NEJM200106143442403

28. Gollob MH, Seger JJ, Gollob TN, Tapscott T, Gonzales O, Bachinski L, et al. Novel PRKAG2 mutation responsible for the genetic syndrome of ventricular preexcitation and conduction system disease with childhood onset and absence of cardiac hypertrophy. *Circulation*. (2001) 104(25):3030–3. doi: 10.1161/hc5001.102111

29. Coban-Akdemir ZH, Charng WL, Azamian M, Paine IS, Punetha J, Grochowski CM, et al. Wolff-Parkinson-White syndrome: de novo variants and evidence for mutational burden in genes associated with atrial fibrillation. *Am J Med Genet A*. (2020) 182(6):1387–99. doi: 10.1002/ajmg.a.61571

30. Lastraioli E, Perrone G, Sette A, Fiore A, Crociani O, Manoli S, et al. hERG1 channels drive tumour malignancy and may serve as prognostic factor in pancreatic ductal adenocarcinoma. *Br J Cancer*. (2015) 112(6):1076–87. doi: 10.1038/bjc.2015.28

31. Lastraioli E, Perrone G, Sette A, Fiore A, Crociani O, Manoli S, et al. Potassium channels in cell cycle and cell proliferation. *Philos Trans R Soc Lond B Biol Sci*. (2014) 369(1638):20130094. doi: 10.1098/rstb.2013.0094

32. Rapetti-Mauss R, Bustos V, Thomas W, McBryan J, Harvey H, Lajczak N, et al. Bidirectional KCNQ1:β-catenin interaction drives colorectal cancer cell differentiation. *Proc Natl Acad Sci U S A*. (2017) 114(16):4159–64. doi: 10.1073/pnas.1702913114

33. Fan JJ, Huang X. Ion channels in cancer: orchestrators of electrical signaling and cellular crosstalk. *Rev Physiol Biochem Pharmacol*. (2022) 183:103–33. doi: 10.1007/112_2020_48

34. Fraser SP, Ozerlat-Gunduz I, Brackenbury WJ, Fitzgerald EM, Campbell TM, Coombes RC, et al. Regulation of voltage-gated sodium channel expression in cancer: hormones, growth factors and auto-regulation. *Philos Trans R Soc Lond B Biol Sci*. (2014) 369(1638):20130105. doi: 10.1098/rstb.2013.0105

35. Buchanan PJ, McCloskey KD. Ca(V) channels and cancer: canonical functions indicate benefits of repurposed drugs as cancer therapeutics. *Eur Biophys J*. (2016) 45(7):621–33. doi: 10.1007/s00249-016-1144-z

36. Wang CY, Lai MD, Phan NN, Sun Z, Lin YC. Meta-analysis of public microarray datasets reveals voltage-gated calcium gene signatures in clinical cancer patients. *PLoS One*. (2015) 10(7):e0125766. doi: 10.1371/journal.pone.0125766

37. Hu S, Li L, Huang W, Liu J, Lan G, Yu S, et al. CAV3.1 knockdown suppresses cell proliferation, migration and invasion of prostate cancer cells by inhibiting AKT. *Cancer Manag Res*. (2018) 10:4603–14. doi: 10.2147/CMAR.S172948

38. Servage KA, Stefanius K, Gray HF, Orth K. Proteomic profiling of small extracellular vesicles secreted by human pancreatic cancer cells implicated in cellular transformation. *Sci Rep*. (2020) 10(1):7713. doi: 10.1038/s41598-020-64718-6

39. Hurwitz SN, Rider MA, Bundy JL, Liu X, Singh RK. Proteomic profiling of NCI-60 extracellular vesicles uncovers common protein cargo and cancer type-specific biomarkers. *Oncotarget*. (2016) 7(52):86999–7015. doi: 10.18632/oncotarget.13569

40. Kalra H, Simpson RJ, Ji H, Aikawa E, Altevogt P, Askenase P, et al. Vesiclepedia: a compendium for extracellular vesicles with continuous community annotation. *PLoS Biol*. (2012) 10(12):e1001450. doi: 10.1371/journal.pbio.1001450

41. Zhao H, Chen X, Hu G, Li C, Guo L, Zhang L, et al. Small extracellular vesicles from brown adipose tissue mediate exercise cardioprotection. *Circ Res*. (2022) 130(10):1490–506. doi: 10.1161/CIRCRESAHA.121.320458

42. Gan L, Xie D, Liu J, Bond Lau W, Christopher TA, Lopez B, et al. Small extracellular microvesicles mediated pathological communications between dysfunctional adipocytes and cardiomyocytes as a novel mechanism exacerbating ischemia/reperfusion injury in diabetic mice. *Circulation*. (2020) 141(12):968–83. doi: 10.1161/CIRCULATIONAHA.119.042640

43. Stewart TA, Yapa KT, Monteith GR. Altered calcium signaling in cancer cells. *Biochim Biophys Acta*. (2015) 1848(10 Pt B):2502–11. doi: 10.1016/j.bbamem.2014.08.016

44. Rizzuto R, De Stefani D, Raffaello A, Mammucari C. Mitochondria as sensors and regulators of calcium signalling. *Nat Rev Mol Cell Biol*. (2012) 13(9):566–78. doi: 10.1038/nrm3412

45. Zhong R, Zhang F, Yang Z, Li Y, Xu Q, Lan H, et al. Regulation of ion channel function in human-induced pluripotent stem cell-derived cardiomyocytes by cancer cell secretion through DNA methylation. *Front Cardiovasc Med*. (2022) 9:839104. doi: 10.3389/fcvm.2022.839104

46. Tosatto A, Sommaggio R, Kummerow C, Bentham RB, Blacker TS, Berecz T, et al. The mitochondrial calcium uniporter regulates breast cancer progression via HIF-1α. *EMBO Mol Med*. (2016) 8(5):569–85. doi: 10.15252/emmm.201606255

47. Vander Heiden MG, Cantley LC, Thompson CB. Understanding the warburg effect: the metabolic requirements of cell proliferation. *Science*. (2009) 324(5930):1029–33. doi: 10.1126/science.1160809

48. Kerslake R, Panfilov S, Mustafa N, Hall M, Kyrou I, Randeva HS, et al. Elevated circulating lactate levels and widespread expression of its cognate receptor, hydroxycarboxylic acid receptor 1 (HCAR1), in ovarian cancer. *J Clin Med*. (2022) 12(1):217. doi: 10.3390/jcm12010217

49. Cheung SM, Husain E, Masannat Y, Miller ID, Wahle K, Heys SD, et al. Lactate concentration in breast cancer using advanced magnetic resonance spectroscopy. *Br J Cancer*. (2020) 123(2):261–7. doi: 10.1038/s41416-020-0886-7

50. Graboń W, Otto-Ślusarczyk D, Chrzanowska A, Mielczarek-Puta M, Joniec-Maciejak I, Słabik K, et al. Lactate formation in primary and metastatic colon

cancer cells at hypoxia and normoxia. *Cell Biochem Funct*. (2016) 34(7):483–90. doi: 10.1002/cbf.3211

51. Suh EH, Geraldes C, Chirayil S, Faubert B, Ayala R, DeBerardinis RJ, et al. Detection of glucose-derived D- and L-lactate in cancer cells by the use of a chiral NMR shift reagent. *Cancer Metab*. (2021) 9(1):38. doi: 10.1186/s40170-021-00267-4

52. Keung EC, Li Q. Lactate activates ATP-sensitive potassium channels in Guinea pig ventricular myocytes. *J Clin Invest*. (1991) 88(5):1772–7. doi: 10.1172/JCI115497

53. Han J, So I, Kim EY, Earm YE. ATP-sensitive potassium channels are modulated by intracellular lactate in rabbit ventricular myocytes. *Pflugers Arch*. (1993) 425(5-6):546–8. doi: 10.1007/BF00374883

54. Tanaka H, Habuchi Y, Lu LL, Furukawa T, Morikawa J, Yoshimura M. Modulation of sodium current by lactate in guinea pig ventricular myocytes. *Cardiovasc Res*. (1994) 28(10):1507–12. doi: 10.1093/cvr/28.10.1507

55. O'Donnell M, Chance RK, Bashaw GJ. Axon growth and guidance: receptor regulation and signal transduction. *Annu Rev Neurosci*. (2009) 32:383–412. doi: 10.1146/annurev.neuro.051508.135614

56. Palm D, Entschladen F. Neoneurogenesis and the neuro-neoplastic synapse. *Prog Exp Tumor Res*. (2007) 39:91–8. doi: 10.1159/000100049

57. Zhang Y, Huang H, Coleman M, Ziemys A, Gopal P, Kazmi SM, et al. VEGFR2 activity on myeloid cells mediates immune suppression in the tumor microenvironment. *JCI Insight*. (2021) 6(23):e150735. doi: 10.1172/jci.insight.150735

58. Ceyhan GO, Bergmann F, Kadihasanoglu M, Altintas B, Demir IE, Hinz U, et al. Pancreatic neuropathy and neuropathic pain—a comprehensive pathomorphological study of 546 cases. *Gastroenterology*. (2009) 136(1):177–86.e1. doi: 10.1053/j.gastro.2008.09.029

59. Bastos DB, Sarafim-Silva BAM, Sundefeld M, Ribeiro AA, Brandão JDP, Biasoli É R, et al. Circulating catecholamines are associated with biobehavioral factors and anxiety symptoms in head and neck cancer patients. *PLoS One*. (2018) 13(8):e0202515. doi: 10.1371/journal.pone.0202515

60. Mehedințeanu AM, Sfredel V, Stovicek PO, Schenker M, Târtea GC, Istrătoaie O, et al. Assessment of epinephrine and norepinephrine in gastric carcinoma. *Int J Mol Sci*. (2021) 22(4):2042. doi: 10.1007/s11481-019-09891-w

61. Nilsson MB, Le X, Heymach JV. β-adrenergic signaling in lung cancer: a potential role for beta-blockers. *J Neuroimmune Pharmacol*. (2020) 15(1):27–36. doi: 10.1007/s11481-019-09891-w

62. Manolis AA, Manolis TA, Apostolopoulos EJ, Apostolaki NE, Melita H, Manolis AS. The role of the autonomic nervous system in cardiac arrhythmias: the neuro-cardiac axis, more foe than friend? *Trends Cardiovasc Med*. (2021) 31(5):290–302. doi: 10.1016/j.tcm.2020.04.011

63. Capatina AL, Lagos D, Brackenbury WJ. Targeting ion channels for cancer treatment: current progress and future challenges. *Rev Physiol Biochem Pharmacol*. (2022) 183:1–43. doi: 10.1007/112_2020_46

64. Zhang K, Heidrich FM, DeGray B, Boehmerle W, Ehrlich BE. Paclitaxel accelerates spontaneous calcium oscillations in cardiomyocytes by interacting with NCS-1 and the InsP3R. *J Mol Cell Cardiol*. (2010) 49(5):829–35. doi: 10.1016/j.yjmcc.2010.08.018

65. Kang S, Hong J, Lee JM, Moon HE, Jeon B, Choi J, et al. Trifluoperazine, a well-known antipsychotic, inhibits glioblastoma invasion by binding to calmodulin and disinhibiting calcium release channel IP3R. *Mol Cancer Ther*. (2017) 16(1):217–27. doi: 10.1158/1535-7163.MCT-16-0169-T

66. Lee EL, Hasegawa Y, Shimizu T, Okada Y. IK1 channel activity contributes to cisplatin sensitivity of human epidermoid cancer cells. *Am J Physiol Cell Physiol*. (2008) 294(6):C1398–406. doi: 10.1152/ajpcell.00428.2007

67. Huang MH, Huang YM, Wu SN. The inhibition by oxaliplatin, a platinum-based anti-neoplastic agent, of the activity of intermediate-conductance Ca^{2+}-activated K^+ channels in human glioma cells. *Cell Physiol Biochem*. (2015) 37(4):1390–406. doi: 10.1159/000430404

68. Lehky TJ, Leonard GD, Wilson RH, Grem JL, Floeter MK. Oxaliplatin-induced neurotoxicity: acute hyperexcitability and chronic neuropathy. *Muscle Nerve*. (2004) 29(3):387–92. doi: 10.1002/mus.10559

69. Alberti P, Canta A, Chiorazzi A, Fumagalli G, Meregalli C, Monza L, et al. Topiramate prevents oxaliplatin-related axonal hyperexcitability and oxaliplatin induced peripheral neurotoxicity. *Neuropharmacology*. (2020) 164:107905. doi: 10.1016/j.neuropharm.2019.107905

70. Sałat K. Chemotherapy-induced peripheral neuropathy—part 2: focus on the prevention of oxaliplatin-induced neurotoxicity. *Pharmacol Rep*. (2020) 72(3):508–27. doi: 10.1007/s43440-020-00106-1

71. Herrmann J. Adverse cardiac effects of cancer therapies: cardiotoxicity and arrhythmia. *Nat Rev Cardiol*. (2020) 17(8):474–502. doi: 10.1038/s41569-020-0348-1

72. Jiang L, Li L, Ruan Y, Zuo S, Wu X, Zhao Q, et al. Ibrutinib promotes atrial fibrillation by inducing structural remodeling and calcium dysregulation in the atrium. *Heart Rhythm*. (2019) 16(9):1374–82. doi: 10.1016/j.hrthm.2019.04.008

73. Nishimura H, Okazaki T, Tanaka Y, Nakatani K, Hara M. Autoimmune dilated cardiomyopathy in PD-1 receptor-deficient mice. *Science*. (2001) 291(5502):319–22. doi: 10.1126/science.291.5502.319

74. Maurea N, Coppola C, Piscopo G, Galletta F, Riccio G, Esposito E, et al. Pathophysiology of cardiotoxicity from target therapy and angiogenesis inhibitors. *J Cardiovasc Med (Hagerstown)*. (2016) 17(Suppl 1):S19–26. doi: 10.2459/JCM.0000000000000377

75. Romisher A, Carver J, Schuster SJ, Svoboda J, Vandegrift A, Rago A, et al. Bruton's tyrosine kinase inhibition is associated with manageable cardiac toxicity. *Blood*. (2015) 126(23):4529. doi: 10.1182/blood.V126.23.4529.4529

76. Quan X, Zhang H, Xu W, Cui M, Guo Q. Sinus arrhythmia caused by pemetrexed with carboplatin combination: a case report. *Heliyon*. (2022) 8(10):e11006. doi: 10.1016/j.heliyon.2022.e11006

77. Song YJ, Fan T, Quan CY, Cao SH, Zhang Y, Shao XH. Nedaplatin-induced arrhythmia: retrospective analysis of three cases. *J Coll Physicians Surg Pak*. (2017) 27(10):657–9.

78. Totzeck M, Mincu RI, Rassaf T. Cardiovascular adverse events in patients with cancer treated with bevacizumab: a meta-analysis of more than 20 000 patients. *J Am Heart Assoc*. (2017) 6(8):e006278. doi: 10.1161/JAHA.117.006278

79. Li J, Zhang F, Lu Y. Bevacizumab-induced arrhythmia in a patient with lung adenocarcinoma: a case report. *Medicine (Baltimore)*. (2023) 102(35):e34799. doi: 10.1097/MD.0000000000034799

80. Chang KT, Wu HJ, Liu CW, Li CY, Lin HY. A novel role of arrhythmia-related gene KCNQ1 revealed by multi-omic analysis: theragnostic value and potential mechanisms in lung adenocarcinoma. *Int J Mol Sci*. (2022) 23(4):2279. doi: 10.3390/ijms23042279

81. D'Este D, Bertaglia E, Zanocco A, Reimers B, Pascotto P. Electrophysiological properties of the atrioventricular node and ageing: evidence of a lower incidence of dual nodal pathways in the elderly. *Europace*. (2001) 3(3):216–20. doi: 10.1053/eupc.2001.0175

82. Markowitz SM, Lerman BB. A contemporary view of atrioventricular nodal physiology. *J Interv Card Electrophysiol*. (2018) 52(3):271–9. doi: 10.1007/s10840-018-0392-5

83. Fitzsimmons PJ, McWhirter PD, Peterson DW, Kruyer WB. The natural history of Wolff-Parkinson-White syndrome in 228 military aviators: a long-term follow-up of 22 years. *Am Heart J*. (2001) 142(3):530–6. doi: 10.1067/mhj.2001.117779

84. Jazayeri MR, Massumi A, Mihalick MJ, Hall RJ. Sinus node reentry: case report and review of electrocardiographic and electrophysiologic features. *Tex Heart Inst J*. (1985) 12(3):249–52.

85. Fox DJ, Tischenko A, Krahn AD, Skanes AC, Gula LJ, Yee RK, et al. Supraventricular tachycardia: diagnosis and management. *Mayo Clin Proc*. (2008) 83(12):1400–11. doi: 10.4065/83.12.1400

86. Blackwell DJ, Schmeckpeper J, Knollmann BC. Animal models to study cardiac arrhythmias. *Circ Res*. (2022) 130(12):1926–64. doi: 10.1161/CIRCRESAHA.122.320258

87. Karakikes I, Ameen M, Termglinchan V, Wu JC. Human induced pluripotent stem cell-derived cardiomyocytes: insights into molecular, cellular, and functional phenotypes. *Circ Res*. (2015) 117(1):80–8. doi: 10.1161/CIRCRESAHA.117.305365

88. Ergir E, Oliver-De La Cruz J, Fernandes S, Cassani M, Niro F, Pereira-Sousa D, et al. Generation and maturation of human iPSC-derived 3D organotypic cardiac microtissues in long-term culture. *Sci Rep*. (2022) 12(1):17409. doi: 10.1038/s41598-022-22225-w

89. Huizar JF, Ellenbogen KA, Tan AY, Kaszala K. Arrhythmia-induced cardiomyopathy: JACC state-of-the-art review. *J Am Coll Cardiol*. (2019) 73(18):2328–44. doi: 10.1016/j.jacc.2019.02.045

frontiers | Frontiers in Cardiovascular Medicine

TYPE Case Report
PUBLISHED 13 June 2024
DOI 10.3389/fcvm.2024.1398311

OPEN ACCESS

EDITED BY
Reto Asmis,
Wake Forest University, United States

REVIEWED BY
Maruti Haranal,
U N Mehta Institute of Cardiology and Research, India
Tareg Bey,
University of Texas MD Anderson Cancer Center, United States

*CORRESPONDENCE
Jinjing Wang
jinjingwangls@163.com

RECEIVED 09 March 2024
ACCEPTED 17 May 2024
PUBLISHED 13 June 2024

CITATION
Luo S, Li Y, Li J, Zeng J and Wang J (2024) Case Report: Primary malignant mesothelioma of the left atrium easily misdiagnosed as myxoma.
Front. Cardiovasc. Med. 11:1398311.
doi: 10.3389/fcvm.2024.1398311

Case Report: Primary malignant mesothelioma of the left atrium easily misdiagnosed as myxoma

Shuai Luo, Yao Li, Jin Li, Jiafei Zeng and Jinjing Wang*

Department of Pathology, Affiliated Hospital of Zunyi Medical University, Zunyi, Guizhou, China

Background: Malignant mesothelioma (MM) is a rare and aggressive tumor that is found in the pleura and peritoneum. A few cases of MM in the pericardium and tunica vaginalis testis have been reported. Moreover, primary occurrence in the atrium is extremely rare. The visual appearance of this tumor is similar to that of a common atrial myxoma, which makes it challenging for clinicians and radiologists to diagnose and treat this disease.
Case demonstration: An 18-year-old woman presented with symptoms of chest pain, shortness of breath, cough, and expectoration for 7 days. Echocardiography was performed on the patient, which revealed an atrial mass. Myxoma was one of the differential diagnoses. The tumor was an elliptical mass with tips, and the cut surface was jelly-like, similar to myxoma. After surgery, a pathologic examination of the biopsied tumor confirmed epithelial-type MM. During postoperative follow-up, no recurrence of the tumor was observed.
Conclusions: MM originating in the atrium is considered to be extremely rare. Consequently, clinicians can easily misdiagnose atrial MM as a myxoma. Moreover, to confirm the diagnosis, histopathologic biopsy, histomorphological characterization, immunohistochemistry, and molecular genetic testing are required. Therefore, clinical diagnosis and treatment of MM are challenging.

KEYWORDS

left atrium, malignant mesothelioma, diagnosis, differential diagnosis, myxoma

Background

Malignant mesothelioma (MM) is characterized as a tumor with an epithelial–mesenchymal transition. The pleura is reported as the most common site of occurrence, accounting for 90% of patient cases. Other sites of occurrence include the peritoneum and pericardium. In a few cases, the tunica vaginalis testis has been reported as the site of occurrence. The atrium is considered an extremely rare primary site for MM. The histomorphology of MM has been observed to be varied, and familiarity with the histologic pattern of MM is required for making any diagnosis or differential diagnosis. In this study, a case report of a patient with MM diagnosed at our hospital is presented. In addition, the relevant literature is reviewed to analyze the pathomorphological characteristics and clinical features, with the aim of improving clinicians' understanding of MM.

Abbreviation
MM, malignant mesothelioma.

Case demonstration

An 18-year-old woman presented with symptoms of chest pain and shortness of breath after activity. She had a cough and expectoration for 7 days because of an infection in the upper respiratory tract. Upon admission, a physical examination was conducted, which showed a symmetrical thorax without malformation and symmetrical respiratory movement in both lungs. On auscultation, coarse respiratory sounds were heard, and wet rales were detected at the bottom of both lungs. Her blood pressure was 113/50 mmHg. The heart rate was 115 beats/min. Echocardiography revealed echo groups in the left atrium, obstruction and mild regurgitation of the mitral valve, moderate regurgitation of the tricuspid valve, and mild regurgitation of the valve (Figure 1). Left atrial myxoma was considered a differential diagnosis. There was no uplift or depression in the precardiac area, and the heart boundary was enlarged to the left lower region. The rhythm was steady, and diastolic murmurs were audible in the apical area. The patient had no history of trauma or surgery, and no other significant findings were noted. The patient underwent tumor resection under direct intracardiac visualization with the use of general anesthesia and extracorporeal circulation. During surgery, the mass was found in the left atrium. It was endogenous, with poor mobility. The tip of the mass was attached to the atrial septum. The rest of the right atrium and ventricle did not have a clear mass.

A gross pathological examination indicated a grayish-white, jelly-like mass with a size of 5 cm × 5 cm × 4 cm, and the tip was approximately 5 mm. No envelope was seen. Microscopic examination identified numerous fissures in the tumor tissue. Glandular ducts and microcystic structures were seen (Figure 2). The tumor stroma and mucosa were fibrous; the cells were epithelioid and either vacuolated or cuboidal. The cytoplasm was acidophilic and abundant; the nucleus was large and deeply stained. The karyoplasmic index was high, and the nucleolus was clearly visible (Figure 3). Immunohistochemistry showed calretinin (Figure 4), and CK5/6, CK, D2-40, WT-1, and vimentin were positively expressed. TTF-1, napsin A, CEA, CK7, CD31, CD34, and other markers were negative. The percentage of the Ki-67 positive index was approximately 40.

Based on the histological and immunohistochemical results, the pathologic diagnosis was confirmed as left atrial epithelioid MM.

The patient did not receive postoperative radiotherapy, and no recurrence was seen on repeat echocardiography after 3 months.

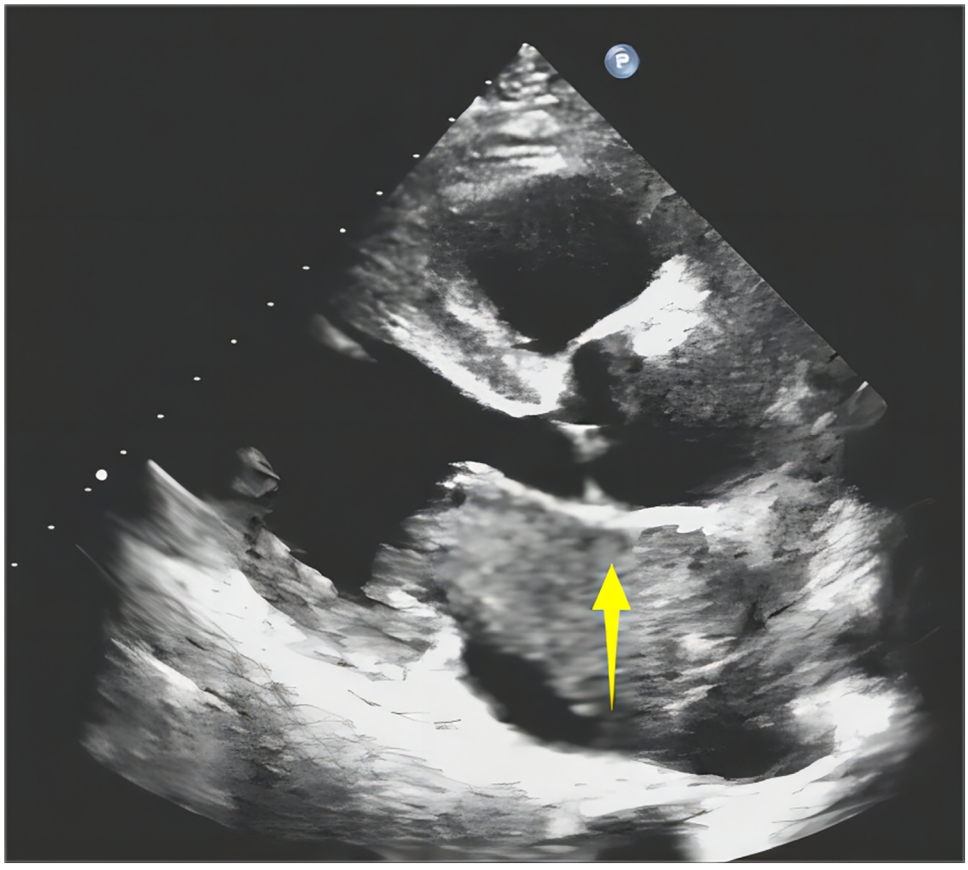

FIGURE 1
Ultrasonography shows a left atrial isoechoic mass (↑).

10.3389/fcvm.2024.1398311

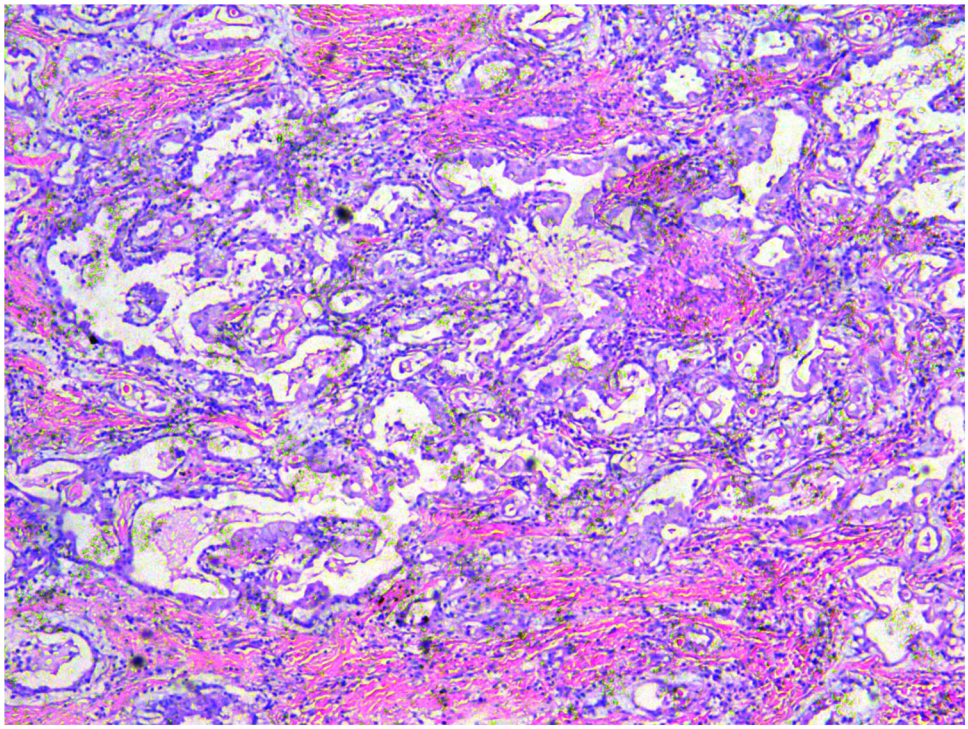

FIGURE 2
A microcystic or gridded arrangement, similar to adenomatoid tumors, H&E ×100.

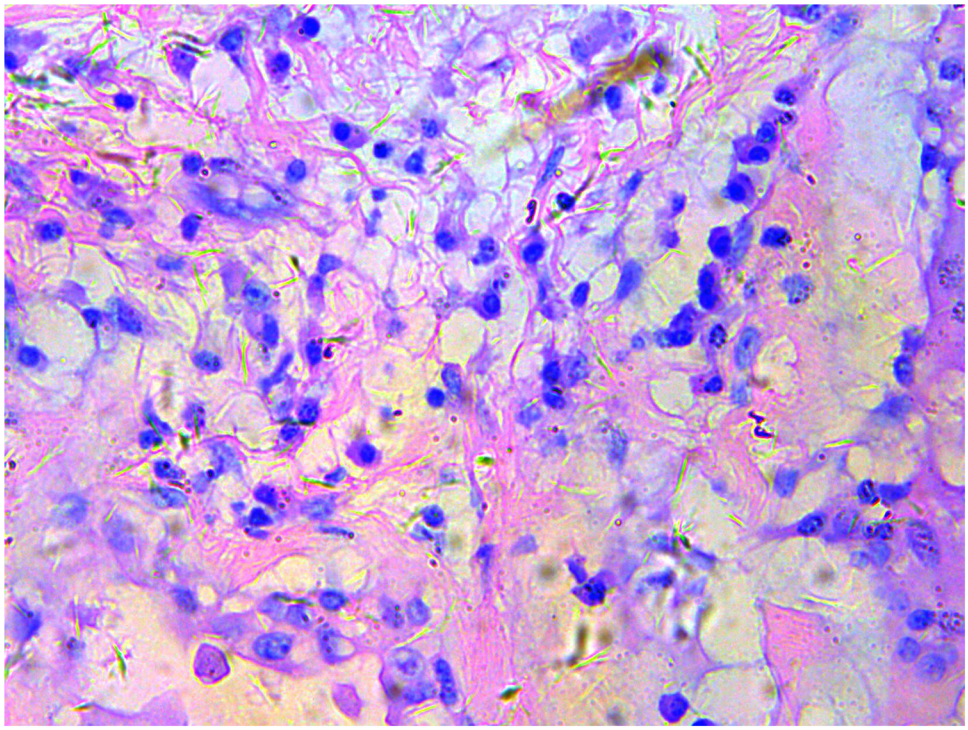

FIGURE 3
Epithelioid cells are vacuolar or cubic, with acidophilic and abundant cytoplasm and large deeply stained nuclei; H&E ×200.

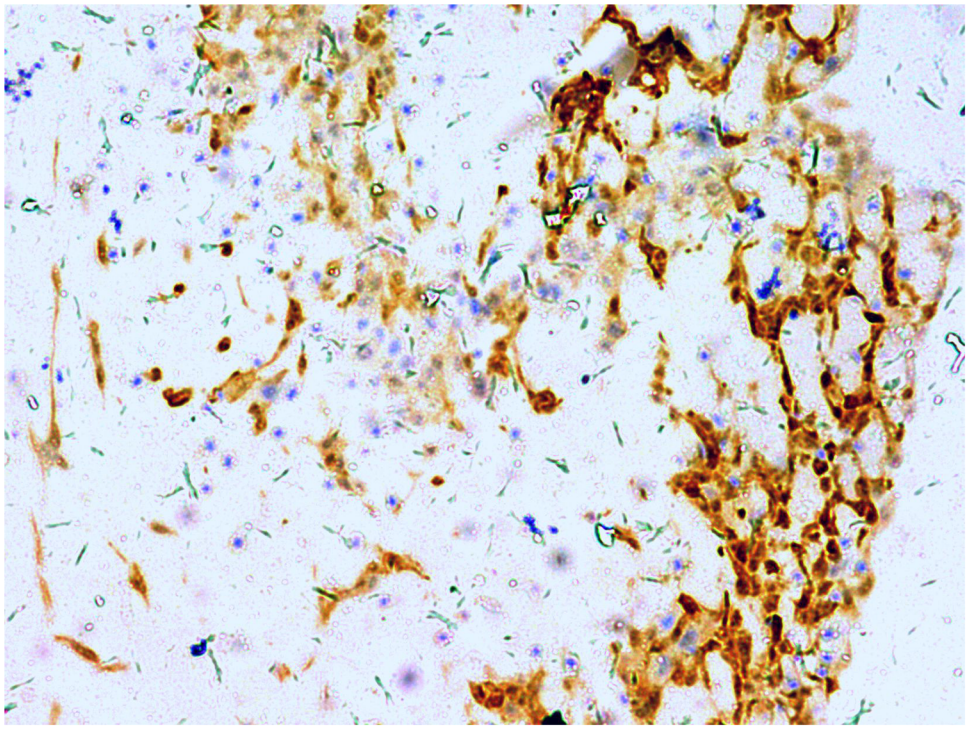

FIGURE 4
Calretinin is positive for diffuse cell membrane; EnVision, ×200.

Discussion

MM is a rare and aggressive tumor occurring in the pleura and peritoneum. In a few patient cases, the pericardium, tunica vaginalis testis, and female reproductive organ system have been reported as the sites of occurrence (1). MM is mainly diagnosed in patients over the age of 60 and is found to have a higher prevalence in men. The majority of cases of mesothelioma are attributed to occupational asbestos exposure (2). However, other causes of mesothelioma are associated with exposure to erionite, simian vacuolating virus 40 (SV40) infection, radiation, chronic inflammation, and genetic susceptibility (3). Nevertheless, recent studies have reported that younger female patients less exposed to asbestos have a higher frequency of prior radiotherapy and a higher family history of breast cancer than older patients (4). The patient reported in this study was an 18-year-old woman with no history of asbestos exposure or tumors. The tumor was confined within the left atrium without pleural involvement. This is an extremely rare occurrence of tumors and has been reported in only a few cases (5).

The origin of MM is not fully understood, but in our patient, the tumor was found to have originated from mesothelial cells. Studies have demonstrated that the tumor may originate from subcellular mesothelial cells, which can differentiate in various directions (6). Clinical manifestations depend on the location of the tumor. Furthermore, when the heart is the primary site, specific manifestations are not typically observed. Patients are admitted to the hospital with chest pain and shortness of breath after physical activity. Upon ultrasonographic examination, a strong echo with a luminescent cluster is observed, within which echogenic areas of varying size can be detected. The boundaries of these findings are not well defined. These ultrasonographic findings bear a resemblance to those of cardiac tumors, myxomas, and other conditions (7). Therefore, MM can be commonly misdiagnosed based on clinical manifestations and imaging results. Accurate diagnosis should be based on a combination of histopathology, immunohistochemistry, and molecular examinations.

MM is classified as a heterogeneous tumor based on its histomorphology. According to its histologic morphology, it is categorized into three subtypes: epithelioid, sarcomatoid, and biphasic (8). Among these subtypes, epithelioid mesothelioma is considered to be more prevalent than sarcomatoid and biphasic forms.

The most common morphologic variants of epithelioid mesothelioma are tubular, papillary, solid, and trabecular. Psammoma bodies may appear in any of these variants. Other uncommon variants include micropapillary, adenomatoid (microcystic), clear cell, migratory, metaplastic, small cell, and lymphohistiocytic (8, 9). Generally, epithelioid tumors contain polygonal, vacuolated, ovoid, or cuboidal cells that mimic reactive mesothelial cells and respond to various types of injury. However, a poorly differentiated epithelioid tumor with pathological mitotic signs was seen in our patient (10).

Sarcomatoid mesothelioma is the least common but most aggressive of the three histologic types of mesothelioma (11). The sarcomatoid types are usually characterized by a fascicular or irregularly arranged proliferation of spindle cells with varying

degrees of nuclear atypia and mitotic figures. Sarcomatoid tissues rarely have heterologous differentiation, such as osteoid, bone, or cartilage (8, 12). The fibrous reactive mesenchyme in epithelioid mesothelioma may be sparse or prominent with varying degrees of cellularity, which makes it challenging to distinguish it from a true sarcomatoid component. In these cases, immunohistochemistry may be helpful in showing the presence of BRCA1-associated protein 1 (BAP-1) and demonstrating a lack of expression in the sarcomatoid mesothelioma region (13).

Biphasic MM is characterized by the presence of mixed tumors consisting of epithelioid and sarcomatoid types, with each type constituting at least 10% of the tumors (8). In our patient, we reported an epithelioid malignant MM with vacuolated or cuboidal tumor cells arranged in microcystic or lattice-like patterns, resembling an adenomatoid tumor.

Immunohistochemical markers play a crucial role in histologic and differential diagnoses. However, it has been observed that no antibody can achieve 100% sensitivity and 100% specificity. Consequently, the Guidelines for the Diagnosis and Treatment of Malignant Pleural Mesothelioma recommend combining immunohistochemical markers with at least two positive and two negative markers to diagnose MM (1). Antibodies that can detect mesothelioma expression markers, including calretinin, WT1, D2-40, and CK5/6, were chosen. Immunohistochemical indices including CEA, TTF-1, Napsin A, MOC31, Ber-EP4, and BAP1 were not expressed (8, 10). P53 has also been reported to be often abnormally expressed in MM, which can be distinguished from reactive mesothelial hyperplasia. SOX6, as a new immunohistochemical marker of MM, has similar sensitivity to CR and D240 in differentiating epithelial MPM from lung adenocarcinoma, but it has better specificity. In addition, studies have shown that the expression of SOX6 was more sensitive than that of WT-1 (8, 10).

It has been demonstrated through studies (6) that partial loss of 1p21M-22, 3p14–25, 4q, 6q, 9p21, 13q13–14, 14q, and haploid chromosome 22, along with repetitive loss of 17p12-pter, are associated with molecular genetic changes in MM. Fluorescence *in situ* hybridization has revealed that deletion of the p16 gene is observed in approximately 35% of MM cases.

(1) During diagnosis, various primary and secondary tumors must be differentiated from MM. In the case presented here, the tumor growth site was rare, and the histological morphology was non-specific. Consequently, the possibility of misdiagnosis is high, and certain diseases listed here need to be ruled out.

(2) Reactive mesothelial hyperplasia: Although reactive mesothelial hyperplasia may show atypia, it is not significant. There are no tubules and no papillae formation, which would suggest MM. Furthermore, the most reliable morphological criterion for MM proliferation is a true infiltration of the mesenchyme (14). Currently, BAP-1 immunohistochemistry and p16 fluorescent *in situ* hybridization are the most effective analytical methods to identify benign and malignant mesothelial lesions (13, 15, 16). Studies have demonstrated that the lack of BAP-1 and p16 expression in MMs contributes to benign and malignant mesothelial cell proliferation.

(3) Myxoma in the atrium is the most common type of primary atrial tumor, and hence, it is common to misdiagnose MM as myxoma. Further, myxoma can also express CK and calretinin, which needs to be combined with the histopathology of myxoma (the whole tumor shows a large number of mucoid matrix and scattered tumor cells in the form of strips, networks, or single arrangements). Some of them can be arranged around the blood vessels, which will lead to the formation of a perivascular ring and will be often accompanied by scattered lymphocyte and plasma cell infiltration, bleeding, and hemosiderin deposition. The tumor may present with secondary changes, including fibrosis, cystic change, necrosis, thrombosis, calcification, ossification and Gamna-Gandy body. Myxoma immunohistochemistry demonstrates positivity for S100, CD34 and CD31, while it is negative for markers such as WT1, D2-40 and CK5/6. In terms of molecular genetics, approximately two-thirds of atrial myxomas exhibit mutations in the PRKAR1A gene (7).

(4) Atrial fibrosarcoma: This is an extremely rare and pure malignant spindle cell mesothelioma. The histologic morphology is similar to that of fibrosarcoma. However, the longitudinal and transverse cell bundles are not as obvious as in fibrosarcoma. The migratory components between epithelial mesothelial cells and spindle cells can be seen in the tumor tissues after a careful examination. The expression of CK and calretinin can be differentiated from that of fibrosarcoma.

(5) Synovial sarcoma is characterized by a histological pattern similar to that of MM, and biphasic differentiation can be achieved. The epithelioid component can be a synovial-like cuboidal epithelium or adenoidal columnar epithelium. The sarcomatoid component cells can be fibroblast-like and perivascular-like. In addition, biphasic expression is often observed in immunohistochemistry, with calretinin being focally positive. However, an important point differentiating synovial sarcoma from MM is negative WT1, with a t(X; 18) or SS18-SSX gene fusion (17). Synovial sarcomas are most commonly found in the extremities and rarely metastasize to the atrium.

(6) Metastatic adenocarcinoma can be challenging to differentiate from malignant epithelioid MM when the latter presents with only glandular and adenoid structures without malignant spindle cells. However, adenocarcinoma is generally positive for CEA, TTF-1, and napsin A and negative for calretinin and vimentin, whereas in MM, the scenario is reversed (18). If estrogen receptor, progesterone receptor, and gross cystic disease fluid protein 15 (GCDFP-15) expressions are positive, metastatic breast cancer is considered (19). In the case of the patient in this study, no tumor was seen at any other site, and the patient had no history of tumor.

Treatment and prognosis

The prognosis for MM is poor. The average survival time of a patient usually does not exceed 12 months (20). There is currently no standard and effective treatment available, and complete

surgical resection is usually the mainstay of therapy. However, it is sometimes challenging to achieve complete surgical resection. Our patient was followed up for 3 months, following which she had no tumor recurrence or metastasis. Pemetrexed/cisplatin combination chemotherapy has been widely used in treating MM. However, the efficacy rate after chemotherapy ranges between 30% and 40%, and the long-term survival rate remains poor (21). With the advent of next-generation sequencing technology, such as BAP-1 (13), neurofibromatosis type 2 (22), and cyclin-dependent kinase inhibitor 2A (p16/CDKN2A) (23), other gene therapies are currently under investigation. Therefore, differential diagnosis and treatment are based on genetic data that require further research.

Data availability statement

The original contributions presented in the study are included in the article/Supplementary Material, further inquiries can be directed to the corresponding author.

Ethics statement

This case report was approved by the Ethics Committee of the Affiliated Hospital of Zunyi Medical University. Written informed consent was obtained from the patient and the patient's family for publication of this clinical case report.

Author contributions

SL: Writing – review & editing, Writing – original draft. YL: Writing – original draft. JL: Writing – review & editing, Data curation. JZ: Writing – review & editing, Data curation. JW: Writing – review & editing.

Funding

The authors declare that no financial support was received for the research, authorship, and/or publication of this article.

Acknowledgments

The authors would like to thank all the reviewers who participated in the review. They also thank Bullet Edits Limited for the language editing and proofreading of the manuscript.

Conflict of interest

The authors declare that the research was conducted in the absence of any commercial or financial relationships that could be construed as a potential conflict of interest.

Publisher's note

References

1. Husain AN, Colby T, Ordonez N, Krausz T, Attanoos R, Beasley MB, et al. Guidelines for pathologic diagnosis of malignant mesothelioma: 2012 update of the consensus statement from the International Mesothelioma Interest Group. *Arch Pathol Lab Med*. (2013) 137(5):647. doi: 10.5858/arpa.2012-0214-OA

2. Peto J, Decarli A, La Vecchia C, Levi F, Negri E. The European mesothelioma epidemic. *Br J Cancer*. (1999) 79(3–4):666. doi: 10.1038/sj.bjc.6690105

3. Carbone M, Pass HI, Miele L, Bocchetta M. New developments about the association of SV40 with human mesothelioma. *Oncogene*. (2003) 22(33):5173. doi: 10.1038/sj.onc.1206552

4. Vivero M, Bueno R, Chirieac LR. Clinicopathologic and genetic characteristics of young patients with pleural diffuse malignant mesothelioma. *Mod Pathol*. (2018) 31 (1):122. doi: 10.1038/modpathol.2017.108

5. Mingfu Y, Zaigen Z, Yali W, Jinliang T, Fei X. Clinicopathological analysis of 45 cases of primary cardiac tumors. *J Diagn Pathol*. (2001) 6(06):10–2. doi: 10.3969/j.issn.1007-8096.2001.06.002.

6. Xiaojing Z, Li L, Congyang W, Yan W. Malignant mesothelioma clinicalpathological analyses of 6 cases. *J Diagn Pathol*. (2022) 29(06):542. doi: 10.3969/j.issn.1007-8096.2022.06.014

7. Yingchun Y, Xinyou W, Yanhong Y, Ming G. Primary malignant mesothelioma of right atrium: a clinicopathologic observation. *J Diagn Pathol*. (2006) 1(01):70–1. doi: 10.3969/j.issn.1007-8096.2006.01.019

8. Travis WD, Brambilla E, Burke AP, Marx A, Nicholson AG. Introduction to the 2015 world health organization classification of tumors of the lung, pleura, thymus, and heart. *J Thorac Oncol*. (2015) 10(9):1240. doi: 10.1097/JTO.0000000000000663

9. Allen TC, Cagle PT, Churg AM, Colby TV, Gibbs AR, Hammar SP, et al. Localized malignant mesothelioma. *Am J Surg Pathol*. (2005) 29(7):866. doi: 10.1097/01.pas.0000165529.78945.dc

10. Husain AN, Colby TV, Ordóñez NG, Allen TC, Attanoos RL, Beasley MB, et al. Guidelines for pathologic diagnosis of malignant mesothelioma 2017 update of the consensus statement from the International Mesothelioma Interest Group. *Arch Pathol Lab Med*. (2018) 142(1):89. doi: 10.5858/arpa.2017-0124-RA

11. Klebe S, Brownlee NA, Mahar A, Burchette JL, Sporn TA, Vollmer RT, et al. Sarcomatoid mesothelioma: a clinical-pathologic correlation of 326 cases. *Mod Pathol*. (2010) 23(3):470. doi: 10.1038/modpathol.2009.180

12. Klebe S, Mahar A, Henderson DW, Roggli VL. Malignant mesothelioma with heterologous elements: clinicopathological correlation of 27 cases and literature review. *Mod Pathol*. (2008) 21(9):1084. doi: 10.1038/modpathol.2008.125

13. Cigognetti M, Lonardi S, Fisogni S, Balzarini P, Pellegrini V, Tironi A, et al. BAP1 (BRCA1-associated protein 1) is a highly specific marker for differentiating mesothelioma from reactive mesothelial proliferations. *Mod Pathol*. (2015) 28 (8):1043. doi: 10.1038/modpathol.2015.65

14. Qiying L, Bo P, Jian W. Pathologic diagnosis of malignant mesothelioma. *J Clin Exp Pathol*. (2014) 30(10):1156. doi: 10.13315/j.cnki.cjcep.2014.10.019

15. Churg A, Sheffield BS, Galateau-Salle F. New markers for separating benign from malignant mesothelial proliferations: are we there yet? *Arch Pathol Lab Med*. (2016) 140(4):318. doi: 10.5858/arpa.2015-0240-SA

16. Chung CT, Santos Gda C, Hwang DM, Ludkovski O, Pintilie M, Squire JA, et al. FISH assay development for detecting p16/CDKN2A deletion in malignant pleural mesothelioma. *J Clin Pathol.* (2010) 63(7):630. doi: 10.1136/jcp.2010.076794

17. Miettinen M, Limon J, Niezabitowski A, Lasota J. Calretinin and other mesothelioma markers in synovial sarcoma: analysis of antigenic similarities and differences with malignant mesothelioma. *Am J Surg Pathol.* (2001) 25(5):610. doi: 10.1097/00000478-200105000-00007

18. Bishop JA, Sharma R, Illei PB. Napsin A and thyroid transcription factor-1 expression in carcinomas of the lung, breast, pancreas, colon, kidney, thyroid, and malignant mesothelioma. *Hum Pathol.* (2010) 41(1):20. doi: 10.1016/j.humpath.2009.06.014

19. Ordóñez NG, Sahin A. Diagnostic utility of immunohistochemistry in distinguishing between epithelioid pleural mesotheliomas and breast carcinomas: a comparative study. *Hum Pathol.* (2014) 45(7):1529. doi: 10.1016/j.humpath.2014.03.006

20. Sobhani N, Corona SP, Bonazza D, Ianza A, Pivetta T, Roviello G, et al. Advances in systemic therapy for malignant mesothelioma: future perspectives. *Future Oncol.* (2017) 13(23):2083. doi: 10.2217/fon-2017-0224

21. Kaiyan C, Chunying K, Dan S, Weimin M. Analysis of the pathogenesis, diagnosis and treatment of malignant mesothelioma in China. *Chin J Thorac Cardiovasc Surg.* (2017) 33(07):443. doi: 10.3760/cma.j.issn.1001-4497.2017.07.018

22. Petrilli AM, Fernández-Valle C. Role of merlin/NF2 inactivation in tumor biology. *Oncogene.* (2016) 35(5):537. doi: 10.1038/onc.2015.125

23. Guo G, Chmielecki J, Goparaju C, Heguy A, Dolgalev I, Carbone M, et al. Whole-exome sequencing reveals frequent genetic alterations in BAP1, NF2, CDKN2A, and CUL1 in malignant pleural mesothelioma. *Cancer Res.* (2015) 75(2):264. doi: 10.1158/0008-5472.CAN-14-1008

frontiers | Frontiers in Oncology

TYPE Case Report
PUBLISHED 17 June 2024
DOI 10.3389/fonc.2024.1356592

OPEN ACCESS

EDITED BY
Luigi De Maria,
University of Bari Aldo Moro, Italy

REVIEWED BY
Massimo Baudo,
Lankenau Institute for Medical Research, United States
Mohamed Rahouma,
NewYork-Presbyterian, United States

*CORRESPONDENCE
Yujiu Wang
yujiuwang0543@126.com

†These authors have contributed equally to the work

RECEIVED 29 February 2024
ACCEPTED 05 June 2024
PUBLISHED 17 June 2024

CITATION
Wang A, Liu B, Dong S and Wang Y (2024) Case report: A case of primary cardiac malignant mesothelioma. *Front. Oncol.* 14:1356592. doi: 10.3389/fonc.2024.1356592

Case report: A case of primary cardiac malignant mesothelioma

Ao Wang†, Baohui Liu†, Shengjun Dong and Yujiu Wang*

Department of Cardiovascular Surgery, Binzhou Medical University Hospital, Binzhou, Shandong, China

Primary cardiac malignant tumors are extremely rare, making up about 10% of all primary cardiac tumors. Most of these tumors are primary sarcomas, with primary mesothelioma being even less common. This report details a 53-year-old male patient diagnosed with primary cardiac malignant mesothelioma. The patient had symptoms of chest pain and difficulty breathing. A CT scan showed an enlarged heart, fluid around the heart, and irregular thickening of the pericardium. Diagnosis was confirmed through a surgical biopsy, which showed the presence of malignant mesothelioma. After the procedure, the patient received appropriate cardiac support. Although stable at discharge, the patient unfortunately died three months later due to severe wheezing. There may be a potential link between exposure to radioactive iodine treatment and this outcome. This case highlights the diagnostic and treatment challenges of primary cardiac malignant tumors and reminds physicians to consider this rare disease when evaluating patients with similar symptoms.

KEYWORDS

primary cardiac malignant tumors, mesothelioma, surgical treatment, radiation therapy, case report

1 Introduction

The incidence of primary cardiac tumors is extremely low, with most being benign and only 10% classified as malignant (1, 2). Among the malignant cases, angiosarcoma and poorly differentiated sarcomas are the most common types, making primary cardiac malignant mesothelioma even rarer. (3–5) (Table 1). The discovery of patients often occurs incidentally during imaging examinations conducted for unrelated reasons, resulting in a missed opportunity for timely treatment (10). We present a case report of a 53-year-old male patient diagnosed with primary cardiac malignant mesothelioma, whose symptoms were alleviated following surgical intervention. This report provides comprehensive insights into the diagnosis, treatment, and prognosis of this particular case, aiming to enhance understanding of the disease.

TABLE 1 Four cases of cardiac mesothelioma were previously reported.

Title	Reporting time	Gender	Risk Factors	Main symptoms	Location	Treatment	Prognosis
Cardiac mesothelioma (6)	1991						
Cardiac mesothelioma (7)	1996						
Primary cardiac mesothelioma presenting with fulminant recurrent pericarditis: a case report (8)	2023	male	BNT162b2 COVID-19 vaccine	Recurrent pericardial effusion, chest pain , dyspnea	the entire heart and the great vessels	NSAIDs, colchicine, prednisone, Pericardiocentesis, Resection of the pericardium	The patient passed away three weeks post-surgery
Case report and analysis of the literature on sarcomatous mesothelioma of the left atrium (9)	2023	female		Dyspnea, palpitations, syncopal, signs of global heart failure	Within the left atrium	Cardiac mass resection, mitral valve replacement	The patient succumbed to tumor recurrence in the left atrium 9 months post-surgery

However, the original records for the 1991 and 1996 cases could not be obtained. The remaining patients succumbed to heart mesothelioma within one year after undergoing surgery.

2 Case report

The patient, a 53-year-old man, presented with chest tightness and wheezing of unknown cause for one year, which had worsened over the past two days. Physical examination revealed weak breath sounds in the left lung and distant heart sounds. Chest CT showed an enlarged heart, irregular thickening of the pericardium with predominant dirty layer, pericardial effusion, bilateral pleural effusion, and enlarged lymph nodes around the great vessels of the upper mediastinum. Venipuncture examination for tumor markers was negative except for slightly elevated ferritin (403.10 ng/ml). The patient had a history of hyperthyroidism and hyperthyroid heart disease treated with methimazole, propranolol, and two courses of iodine-131 (I-131) radiotherapy. In 2021, he underwent pericardiocentesis twice at another medical facility due to worsening chest tightness and wheezing caused by significant pericardial effusion. Preoperative bedside echocardiography revealed reduced motion in the middle and lower segments of the ventricular septum, left ventricular lateral wall, left ventricular anterior wall, inferior apical segment of the left ventricular wall, and middle segment of the left ventricular posterior wall. However, the remaining segments exhibited acceptable levels of ventricular wall motion amplitude and systolic thickening rate. The ejection fraction was measured at 42%, with a ventricular septum thickness of 8 mm, a left ventricular end-diastolic diameter of 45 mm, and a left ventricular posterior wall thickness of 8 mm. Additionally, a fluid dark area was detected within the pericardial cavity. The end-diastolic width measurements were as follows: 27 mm posterior to the left ventricle, 35 mm lateral to the left ventricle, 14 mm anterior to the right ventricle, 16 mm lateral to the right atrium, and 39 mm for both the right atrium and inferior apex regions. Doppler ultrasound indicated mild regurgitation in both the aortic and bicuspid valves along with minimal tricuspid valve regurgitation.

After the patient's thyroid function improved, he underwent surgical treatment at our hospital, specifically a thoracotomy and cardiac tumor biopsy procedure (Figure 1). The diagnosis was reconfirmed through a repeated preoperative transesophageal echocardiogram (TEE) (Figure 2). During the chest incision, increased tension was observed in the pericardial cavity. A pericardial window was created near the aortic root, revealing an overflow of pale-yellow liquid. We extracted samples of this pericardial effusion to relieve cardiac compression and closely monitored changes in heart rate and blood pressure. In total, approximately 1200 ml of pale-yellow pericardial effusion was aspirated. The pericardium showed thickening and signs of inflammation, with fibrin deposition and adhesion. Upon

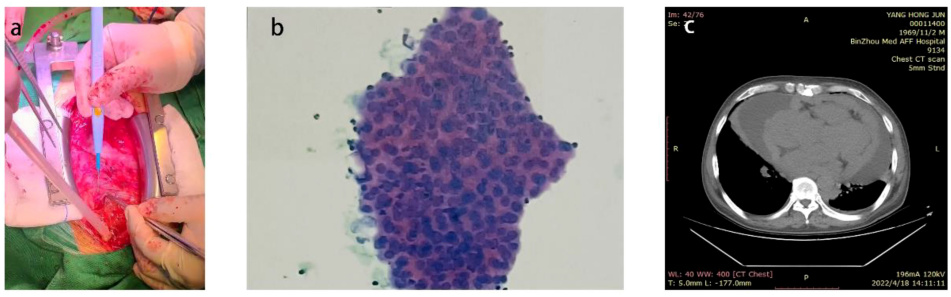

FIGURE 1
(A) The patient presented with a significant volume of pericardial effusion within the pericardial cavity. **(B)** Pathological results of pericardial effusion **(C)** Preoperative chest CT prompted a large number of pericardial effusion.

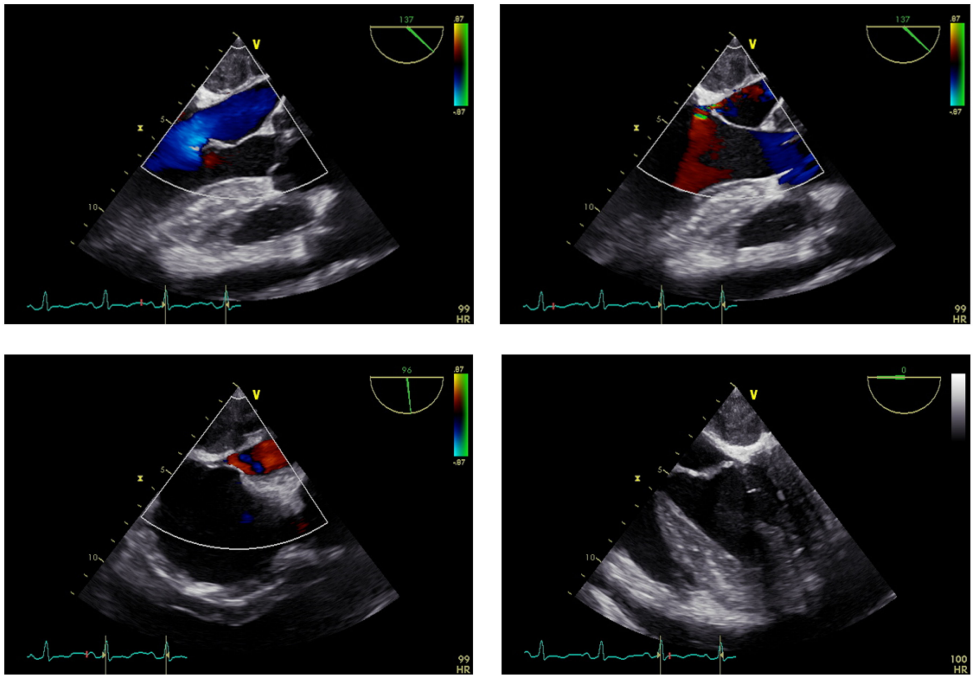

FIGURE 2
Preoperative TEE examination results.

separation and exploration, it was discovered that the entire heart, as well as its inlet and outlet, were enveloped by a densely connected cardiac mass adhering to the epicardium. The mass exhibited significant rigidity, resulting in impaired cardiac function (Figure 3). After thorough analysis, surgical removal of the tumor was deemed unfeasible. Therefore, only a portion of the cardiac mass and pericardium were excised for pathological examination. To prevent recurrence of tamponade caused by massive pericardial effusion, partial resection of the left pericardium and mediastinal pleura was performed to establish communication between the pericardial sac and thoracic cavity. Hemostasis was strictly maintained during surgery, with the placement of one drainage tube each in the pericardial sac, mediastinum, and left thoracic cavity before layered closure of the chest wall incision. Intraoperative blood loss totaled 100 ml without necessitating transfusion. The patient's blood pressure measured 117/73 mmHg, heart rate was 125 beats per minute, and SpO_2 level was 98%.

Following the surgical procedure, the patient received a comprehensive treatment regimen that included cardiotonic agents, diuretics, vasodilators, heart rate modulation, and supplemental thyroxine. Three days post-operation, bedside echocardiography revealed bilateral chamber enlargement with normal chamber diameter. The interventricular septum and left ventricular free wall thickness were within normal limits, while ventricular wall motion amplitude and thickening of shrinkage rate were observed. The ejection fraction was measured at 56%. Additionally, the interventricular septum thickness was found to be 9 mm, the left ventricular end-diastolic diameter before and after the operation was 46 mm, and the left ventricular posterior wall thickness was 9 mm. Pericardial cavity and liquid dark space measurements showed a width of 9 mm for the left ventricle after diastole, 18 mm for the left

FIGURE 3
(A) Photographs of the heart during surgery **(B)** The pericardium pathological results **(C)** Pathological results of cardiac mass.

ventricle side, 9 mm for the right side, 16 mm below the roof on the right side before diastole, and an apex measurement of 12 mm. Doppler ultrasound indicated mild aortic regurgitation, mild mitral regurgitation, and moderate tricuspid regurgitation. Furthermore, estimated pulmonary artery systolic pressure was recorded at 42 mmHg per month. Despite being eligible for both heart transplantation and tumor-related treatment, the patient preferred to be discharged to recuperate at home. Consequently, on the fifth day after surgery, the patient was discharged. The patient spent 46 hours in the intensive care unit and underwent mechanical ventilation for 43 hours. Their hospital stay lasted a total of 21 days. Upon discharge, the patient exhibited satisfactory recovery from the operation, with a well-healed chest incision showing no signs of redness, swelling, or exudation. The patient's condition remained stable without fever, cough, or sputum, and they were able to engage in mild activities without discomfort. The physical examination at discharge revealed strong heart sounds and a consistent rhythm. The patient was instructed to take digoxin tablets, furosemide tablets, spironolactone tablets, sustained-release potassium chloride tablets, bisoprolol fumarate tablets, and levothyroxine sodium tablets upon discharge. During follow-up, the patient experienced persistent wheezing symptoms two weeks after being discharged but relied solely on oral medication and home rest without specialized intervention. Unfortunately, the patient succumbed to his condition three months post-discharge.

Analysis of tumor markers in the pericardial effusion revealed significant elevations in CA19–9 (49.85 U/ml), CA125 (75.28 U/ml), non-small cell carcinoma (451.30 ng/ml), squamous cell carcinoma-associated antigen (17.71 ng/ml), and carbohydrate antigen 50 (35.10 IU/ml). Additionally, there were notable increases in CA15–3 (75.28 U/ml) but no elevation in CA72–4 (0.88 U/ml), neuron-specific enolase (8.57 ng/ml), or CA-242 (1.08 IU/ml). The pathology of the pericardial effusion revealed the presence of tumor cells in both the smear and sediment. Pathological examination of the cardiac mass demonstrated diffuse proliferation of epithelioid cells, exhibiting non-specificity, nucleoli, mitotic figures, adenoid structure, and solid nest arrangement of cells. Immunohistochemical staining showed positive expression for CK+, CR+, Vimentin+, focal positivity for CK7+, MC+, and D2–40+; negative expression for CK20-, and weakly positive WT-1+. The Ki-67 proliferation index was approximately 20%, suggesting a tendency towards epithelioid malignant mesothelioma. Histopathological examination of the pericardium revealed hyperplasia of epithelioid cells without atypia, nucleoli, or mitotic figures. Adenoid structure and solid nests were observed within the cell arrangement. Immunohistochemical staining showed positive expression for CK19+ and scattered weak positivity for MC; negative expression for galectin-3-. Additionally, there was positive expression for CK7+ but negative expression for CK20- and Villin-. These findings further support a diagnosis consistent with epithelioid malignant mesothelioma.

3 Discussion

Mesothelioma is a rare cancer originating from mesothelial cells, primarily affecting the pleura, peritoneum, and pericardium. The main subtypes of mesothelioma include epithelioid mesothelioma, sarcomatoid mesothelioma, and biphasic mesothelioma (11). Each subtype exhibits distinct pathological features, clinical manifestations, and prognoses. Epithelioid mesothelioma is the most common subtype, characterized by tumor cells with epithelioid features. It grows slowly and generally has a favorable prognosis. Sarcomatoid mesothelioma, on the other hand, displays sarcomatoid characteristics with rapid growth and aggressive invasion, leading to a poor prognosis. The primary treatments include chemotherapy or radiotherapy, while immunotherapy is less effective compared to epithelioid mesothelioma. Biphasic mesothelioma comprises both cell types mentioned above and has an intermediate prognosis between the two subtypes. The treatment approach primarily involves comprehensive management with surgery, chemotherapy, and radiotherapy; however, further exploration is needed for immunotherapy (11–13).

Primary cardiac malignant tumors are exceedingly rare, and primary cardiac malignant mesothelioma is even more uncommon. Consequently, a lack of understanding of this condition may result in misdiagnosis and delayed treatment. Additionally, pericardial effusion frequently accompanies cardiac malignancies. Tumors in the atria or atrioventricular valve region may present with symptoms that resemble mitral or tricuspid valve stenosis (3). Tumor infiltration into the myocardium can cause symptoms characteristic of restrictive cardiomyopathy, primarily manifesting as heart failure (14). These findings are consistent with the current case. In May 2020, our hospital's endocrinology clinic observed that patients presenting with chest tightness and chest pain may have been experiencing symptoms of heart disease. Cardiac color Doppler ultrasound revealed left ventricular hypertrophy, reduced left ventricular wall motion, decreased left ventricular diastolic function, mild tricuspid regurgitation, pericardial effusion, and an ejection fraction of 56%. At this time, the patient had received one dose of iodine-131. From 2021 to 2022, the patient's symptoms of chest tightness and asthma worsened along with orthopnea. Subsequent cardiac color Doppler ultrasounds also showed a significant amount of pericardial effusion. Despite multiple visits to various hospitals during this period (with diagnoses including hyperthyroidism, arrhythmia, pericardial effusion, and pericarditis), no cardiac tumor was identified. It is evident that primary cardiac malignant mesothelioma can be easily misdiagnosed and lead to delayed treatment due to its rarity and lack of specific clinical symptoms.

The role of CT in diagnosing various primary malignant tumors is crucial, serving as an important adjunct. It enables visualization of tumor invasion and provides information on the extent of tumor attachment (15). However, in this case, the patient's chest CT scan revealed only cardiac enlargement, pericardial effusion, and irregular thickening of the visceral pericardium, without definitive evidence of neoplastic disease. The detection of tumor markers in venous serum lacks specificity for common identification; however, there is a clear association between pericardial effusion and tumor marker detection. Therefore, it can be inferred that relying solely on imaging and serum tumor marker detection may not completely exclude the possibility of primary cardiac malignant mesothelioma,

especially if the patient presents with recurrent pericardial effusion, cardiac enlargement, and pericardial thickening.

The patient exhibits significant risk factors for cardiac malignancy. It remains unclear whether there is a history of I-131 radiation therapy. While it is evident that radiation therapy can cause side effects, such as cardiac structural alterations and various cardiovascular disorders, there are few reports and studies on radiation-induced heart disease, including I-131 therapy-related cardiac tumors (16). No other potential exposures have been identified, and no occupational exposures associated with the patient's career as a truck driver have been found.

Current treatment modalities for cardiac malignant tumors include surgical intervention, radiotherapy, and chemotherapy. The postoperative survival rate is closely associated with the completeness of surgical resection (17). In this case, the tumor extensively involved the entire heart, including its entrances and exits, and adhered closely to the epicardium. Due to the difficulty of surgical resection, only palliative treatment was administered, resulting in a grim prognosis for the patient.

Data availability statement

The raw data supporting the conclusions of this article will be made available by the authors, without undue reservation.

Ethics statement

Written informed consent was obtained from the individual(s) for the publication of any potentially identifiable images or data included in this article.

Author contributions

AW: Writing – original draft, Writing – review & editing. BL: Investigation, Writing – review & editing. SD: Investigation, Writing – review & editing. YW: Investigation, Writing – review & editing.

Funding

The author(s) declare financial support was received for the research, authorship, and/or publication of this article. We deeply appreciate the generous support provided by Natural Science Foundation of Shandong Province(No.ZR2020QH017) and Provincial Key Specialty Discipline Construction Funds of Shandong Province(No.SLCZDZK-16).

Conflict of interest

The authors declare that the research was conducted in the absence of any commercial or financial relationships that could be construed as a potential conflict of interest.

Publisher's note

All claims expressed in this article are solely those of the authors and do not necessarily represent those of their affiliated organizations, or those of the publisher, the editors and the reviewers. Any product that may be evaluated in this article, or claim that may be made by its manufacturer, is not guaranteed or endorsed by the publisher.

References

1. Rahouma M, Baudo M, Shmushkevich S, Chadow D, Mohamed A, Girardi L, et al. Sex differences in primary Malignant cardiac tumors: A multi-institutional cohort study from National Cancer Database. *J Card Surg*. (2022) 37(5):1275–86. doi: 10.1111/jocs.16359

2. Rahouma M, Arisha MJ, Elmously A, Ahmed El-Sayed MM, Spadaccio C, Mehta K, et al. Cardiac tumors prevalence and mortality: A systematic review and meta-analysis. *Int J Surg*. (2020) 76:178–89. doi: 10.1016/j.ijsu.2020.02.039

3. Hoffmeier A, Sindermann JR, Scheld HH, Martens S. Cardiac tumors–diagnosis and surgical treatment. *Dtsch Arztebl Int*. (2014) 111:205–11. doi: 10.3238/arztebl.2014.0205

4. Kodali D, Seetharaman K. Primary cardiac angiosarcoma. *Sarcoma*. (2006) 2006:39130. doi: 10.1155/srcm/2006/39130

5. Cardoso M, Canale L, Ramos R, Salvador Jr ES, Lachtermacher S. Cardiac angiosarcoma. *Case Rep Cardiol*. (2011) 2011:340681. doi: 10.1155/2011/340681

6. Krishnarathnam K, Subramanian S. Cardiac mesothelioma. *J Assoc Phys India*. (1991) 39:499–500.

7. Natsume T. Cardiac mesothelioma. *Ryoikibetsu Shokogun Shirizu*. (1996) 1996 (14):263–4.

8. Schwartzenberg S, Shapira Y, Rubachevski V, Sharony R. Primary cardiac mesothelioma presenting with fulminant recurrent pericarditis: a case report. *Eur Heart J Case Rep*. (2023) 7(3):ytad100. doi: 10.1093/ehjcr/ytad100

9. Rouabeh W, Cherif T, Mgarrech I, Ajmi N, Kortas C, Jerbi S, et al. Case report and analysis of the literature on sarcomatous mesothelioma of the left atrium. *Int J Surg Case Rep*. (2023) 109:108537. doi: 10.1016/j.ijscr.2023.108537

10. Poterucha TJ, Kochav J, O'Connor DS, Rosner GF. Cardiac tumors: clinical presentation, diagnosis, and management. *Curr Treat Opt Oncol*. (2019) 20:66. doi: 10.1007/s11864-019-0662-1

11. Patterson D, Ball K. 62 Single-centre DGH experience of using immunotherapy for Malignant mesothelioma. *Lung Cancer*. (2024) 190:107623. doi: 10.1016/j.lungcan.2024.107623

12. Cantini L, Laniado I, Murthy V, Sterman D, Aerts JGJV. Immunotherapy for mesothelioma: Moving beyond single immune check point inhibition. *Lung Cancer*. (2022) 165:91–101. doi: 10.1016/j.lungcan.2022.01.016

13. Mansfield AS, Wang XF, Wigle DA, Watt C, Masters GA, Kelley K, et al. Neoadjuvant immunotherapy in sarcomatoid mesothelioma (Alliance A082101). *J Clin Oncol*. (2023) 41:TPS8602–TPS8602. doi: 10.1200/JCO.2023.41.16_suppl.TPS8602

14. Heath D. Pathology of cardiac tumors. *Am J Cardiol*. (1968) 21:315–27. doi: 10.1016/0002-9149(68)90136-7

15. Araoz PA, Eklund HE, Welch TJ, Breen JF. CT and MR imaging of primary cardiac Malignancies. *Radiographics*. (1999) 19:1421–34. doi: 10.1148/radiographics.19.6.g99no031421

16. Curigliano G, Cardinale D, Suter T, Plataniotis G, de Azambuja E, Sandri MT, et al. Cardiovascular toxicity induced by chemotherapy, targeted agents and radiotherapy: ESMO Clinical Practice Guidelines. *Ann Oncol*. (2012) 23 Suppl 7: vii155–66. doi: 10.1093/annonc/mds293

17. Taguchi S. Comprehensive review of the epidemiology and treatments for Malignant adult cardiac tumors. *Gen Thorac Cardiovasc Surg*. (2018) 66:257–62. doi: 10.1007/s11748-018-0912-3

frontiers | Frontiers in Oncology

TYPE Case Report
PUBLISHED 17 June 2024
DOI 10.3389/fonc.2024.1331472

OPEN ACCESS

EDITED BY
Reto Asmis,
Wake Forest University, United States

REVIEWED BY
Tareg Bey,
University of Texas MD Anderson Cancer Center, United States
Fu Peng,
Sichuan University, China

*CORRESPONDENCE
Shi Li
lishi890427@163.com
Fang Zhao
cedilanid@163.com

†These authors have contributed equally to this work and share first authorship

RECEIVED 01 November 2023
ACCEPTED 01 May 2024
PUBLISHED 17 June 2024

CITATION
Zhang L, Zheng Y, Chen G, Zhao F and Li S (2024) Case report: Phosphoinositide 3-kinase inhibitor with fulvestrant in a patient with ER+/HER2- metastatic breast carcinoma induced fatal arrhythmias: a preventable event?
Front. Oncol. 14:1331472.
doi: 10.3389/fonc.2024.1331472

Case report: Phosphoinositide 3-kinase inhibitor with fulvestrant in a patient with ER+/HER2- metastatic breast carcinoma induced fatal arrhythmias: a preventable event?

Li Zhang[1†], Yanlei Zheng[1†], Gao Chen[1], Fang Zhao[2*] and Shi Li[1*]

[1]Department of Intensive Care Medicine, Hubei Cancer Hospital, Tongji Medical College, Huazhong University of Science and Technology, Wuhan, China, [2]Department of Cardiology, ZhongNan Hospital of Wuhan University, Wuhan, China

Phosphoinositide 3-kinase (PI3K) inhibitors have shown synergistic anticancer effects with endocrine therapy against ER+/PIK3CA-mutated breast cancer. PI3K inhibitors for cancer therapy are becoming more common. There is an increasing need to understand their cardiac adverse events. In this report, we describe the features of near-fatal mixed arrhythmias in a patient who was undergoing a phase Ib clinical study of PI3Kα inhibitor with fulvestrant. Subsequently, the patient survived by cardiopulmonary resuscitation and therefore did not die. This case highlights that PI3K inhibitors can induce QT/QTc prolongation and predispose patients to TdP. The combination of QT/QTc prolongation in combination with prolonged cardiac repolarization, such as an AV block during treatment with PI3Kα inhibitor, may aggravate the occurrence of TdP. It is likely to be a safer strategy to adjust the standard of discontinuing drugs and continuing drugs (QTc interval was <500 and <60 ms at baseline) or choose other types of alternative treatment options. This report provided some ideas for clinicians to identify early and prevent the occurrence of fatal arrhythmias during anticancer treatment.

KEYWORDS

phosphoinositide 3-kinase inhibitor, QT/QTc, atrioventricular block, torsade de pointes, electrocardiogram

Introduction

With different kinds of new anticancer drugs emerging, many heart-related adverse drug reactions (ADRs) have appeared (1). One crucial and potentially harmful marker is prolonged cardiac repolarization, which is reflected by a prolonged QT interval in the ECG (1, 2). Prolongation of the QT can develop into severe ventricular arrhythmia of the torsade de

pointes (TdP), which can induce sudden death (3). The phosphoinositide 3-kinase (PI3K) pathway plays a key role in cell growth, survival, apoptosis, metabolism, and myocardial contractility (4, 5). The combination therapy of PI3K inhibitors has presented a better clinical activity particularly in patients who have PIK3CA-mutated tumors (6). PI3K signaling could control cardiac repolarization and increase action potential duration by regulating multiple ion channels (7, 8). However, mixed arrhythmias which are caused by PI3K inhibitors have not been reported previously. This report provides clinical empirical evidence, which we hope will help healthcare practitioners to identify and prevent potential severe arrhythmia during treatment with PI3K inhibitors.

Case presentation

A 73-year-old woman had a radical mastectomy for right breast cancer 6 years earlier and had no other history. This was followed by oral letrozole (2.5 mg/day) for approximately 5 years, oral exemestane (2.5 mg/day) for 8 weeks, oral chidamide (30 mg/3 day) for 4 weeks, and discontinuation of the drug 3 months before admission. The carcinoma recurred after a series of anticancer therapies failed. The patient's repeated immunohistochemistry test results were as follows: ER (40%, +), PR (-), HER2 (0), KI67 (LI: 40%), and PI3KCA mutation. The initial laboratory tests were in the normal range (Table 1; Figure 1). A 12-lead ECG showed premature ventricular contraction (PVC), frequent bigeminy, and QT/QTc (398/410 ms) (Figure 2A). The patient met the project criteria of a phase Ib study of PI3K inhibitor with fulvestrant in PI3KCA-mutated metastatic breast cancer (project number: HS-10352–102), signed the informed consent, enrolled in the clinical study, and started to take the drug orally (4 mg/day). She took it for 28 days. The patient had no chronic disease, as only the trial drug was taken orally during the study. The ECG revealed frequent PVC, frequent bigeminy, and QT/QTc (440/446 ms) a week after the start of the study (Figure 2A). The laboratory results were in the normal ranges, but the ECG revealed QT/QTc of 410/457 ms, frequent PVC, frequent bigeminy, and second-degree AV block 2 weeks after the study (Figures 1A, 2A). The initial AV block was assessed as CTCAE V5.0 grade 1–2, and the study continued. We still found frequent PVC, frequent bigeminy, second-degree AV block, and QT/QTc (424/471 ms) 3 weeks after the study started (Figure 2A). At 4 weeks, the ECG showed QT/QTc of 524/534 ms and an almost complete AV block (Figure 2A). The second-degree AV block turned to an almost complete AV block, which was assessed as CTCAE V5.0 grade 3. The patient immediately withdrew from the clinical study and had a permanent pacemaker implanted.

We implanted a single-chamber permanent pacemaker (VVI). The ECG revealed QT/QTc of 456/456 ms, normal pacemaker sensing, and an almost complete AV block (Figure 2B). The laboratory results were also in the normal range. CTCAE V5.0 grade 3 turned to grades 1–2, so we adjusted the dose of the PI3K inhibitor (2 mg/day) and kept her on it for 28 days (Figure 1). We still observed a gradual prolongation of the QT/QTc (470/470 ms) after a week, QT/QTc (486/478 ms) after 2 weeks, and a consistently complete AV block (Figure 2B). The patient suddenly lost consciousness with no pulse after 12 days of dose adjustment. Continuous cardiopulmonary resuscitation (CPR) was performed, and the patient was transferred to the ICU. The patient's circulation eventually recovered with short episodes of ventricular tachycardia (VT), and TdP frequently occurred (Figure 2B). The chest X-ray result revealed that the location of the cardiac pacemaker was normal (Figure 2B). We achieved hemodynamic stability with a continuous infusion of magnesium sulfate (4 mg/min) and isoprenaline (1–3 μg/min), and the patient maintained a normal potassium level.

The patient was transferred to the ICU of another hospital for further antiarrhythmic therapy on the next day. The echocardiography showed a weakened systolic function and LVEF of approximately 40% (Figure 1). The laboratory tests results are shown in Figure 1. The ECG showed prolongation of the QT/QTc, frequent PVC, and almost complete AV block for 4 days (Figure 2C). The patient still had occasional short episodes of TdP on the 5th day, but the myocardial enzymes were gradually declining, and the chest X-ray result revealed that the location of the cardiac pacemaker was normal (Figure 2C). Finally, the patient recovered consciousness, was weaned from mechanical ventilation, and was discharged from the ICU after 2 weeks.

Discussion and conclusion

Numerous clinical reports have shown that PI3K inhibitors combined with endocrine therapy in HR+/HER2- advanced breast carcinoma could prolong progression-free survival (PFS) and enhance the overall response rate (ORR), clinical benefit rate (CBR), and median overall survival (OS) compared with control treatments (9, 10). According to FDA drug instructions, monitoring blood glucose and glycosylated hemoglobin before and after treatment with PI3K inhibitors is important (11). One study reported an incidence of hyperglycemia of 65%, an incidence of diarrhea of 58%, and a non-infectious pneumonia onset of 1.8% during alpelisib treatment. However, its adverse cardiovascular drug reactions are not reported in the clinic.

The patient had no chest pain or other cardiac symptoms, but the occurrence of fatal arrhythmias seems to be traceable. She could be observed to have experienced a second-degree AV block approximately 2 weeks after the start of the study, and the second-degree AV block worsened to almost a complete AV block throughout the study. Whether PI3K inhibitors induce AV block is unknown and has rarely been reported. The effect of PI3K inhibitors on AV block is permanent or temporary and requires extensive clinical data. We also observed a gradual prolongation of the QT/QTc during the study. ECG revealed a QT/QTc (524/534 ms) of approximately 120 ms above baseline and complete AV block after 4 weeks. We observed the QT/QTc (456/456 ms) to be below 60 ms from baseline and complete AV block after the pacemaker was implanted. Her cardiac risk seemed to have been removed, only to develop cardiac arrest when she had an adjusted drug dose. We recorded three ECG changes of QT/QTc gradual prolongation, which eventually led to cardiac arrest. There is no threshold of QTc prolongation at which TdP is certain to occur. The QTc greater than 500 ms has been associated with a twofold to threefold higher risk for TdP, and each 10-ms increase contributes to approximately 5% to 7% exponential increase in risk (12). Therefore, it

TABLE 1 Patient data and laboratory findings on admission.

Years	73	
Gender	Female	
Chief compliant	Right breast cancer surgery 6 years ago, and right breast recurrence 9 months	
Past medical history	Occasional premature atrial contraction and premature ventricular contraction	
Drug therapy	Intravenous AC-T chemotherapy for 8 weeks after surgery Oral letrozole(2.5mg/day) for approximately 5 years Intravenous nab-P drugs(100mg/3weeks) for 6 weeks Followed oral Exemestane(2.5mg/bid) for 56days followed oral chidamide(30mg/3days) for 28days	
Blood pressure	135/71mmHg	
	Normal range	value
Leukocyte count	3.5-9.5×10^9/L	5.1
Neutrophil count	1.8-6.3×10^9/L	2.15
Lymphocyte count	1.1-3.2×10^9/L	2.22
Platelet count	125-350×10^9/L	200
Erythrocyte count	3.5-5.5×10^{12}/L	3.23
Prothrombin time	9.4-12.5s	13.5
Activated partial Thromboplastin time	25.1-36.5s	32.3
D-dimer	0-0.5mg/L	2.82
Creatin kinase	18-198U/L	88
Creatine kinase-MB	0-5ng/mL	2.55
Hypersensitive troponin I	0-0.04ng/ml	0.019
Brain natriuretic peptide	0-100pg/ml	21.66
Alanine aminotransferase	0-40U/L	13.3
Aspartate aminotransferase	0-40U/L	17.1
Total bilirubin	0-20umol/L	8.91
Blood urea nitrogen	2.8-7.6mmol/L	4.7
Blood glucose	3.9-6.1mmol/L	5.39
Creatinine	41-111umol/L	50
Calcium	1.97-2.85mmol/L	2.18
Potassium	3.5-5.4mmol/L	4.29
Sodium	135-148mmol/L	141.5
Magnesium	0.75-1.25mmol/l	1.01
Lung CT scan	Right chest wall tumor and abnormal density shadow of right ribs	

appears that it is difficult to predict when to stop the PI3K therapy. We found (1, 2) no evidence showing that fulvestrant can lead to QT prolongation, so we can speculate that PI3K inhibitors lead to the prolongation of the QT/QTc. Whether it is correlated with the dose of the drug is unknown. The drug effects on cardiac conduction function require further clinical data and pharmacokinetic studies.

We might find some clues to prevent the occurrence of fatal arrhythmia in this case. Firstly, we should fully assess the medical history, including older age (>65 years), sex, a congenital long QT syndrome (LQTS), a high baseline QTc, hypothyroidism, and induced QTc prolonged by other drugs (1, 2). Secondly, the risk classification of anticancer drugs and supportive drugs should also be fully estimated, and evaluation of the risk of QTc prolongation is necessary for moderate–high risk drugs (13, 14). Thirdly, monitoring the ECG and electrolyte levels is also crucial and the easiest way to get it. The latter report (1) also emphasized the standard of discontinuing the drugs when the QTc interval was ≥500 or ≥60 ms above baseline until the QTc interval was <500 or <60 ms above baseline. Electrolyte imbalances directly increase the risk of developing TdP, just as several drugs that cause QTc prolongation corrected the target value

10.3389/fonc.2024.1331472

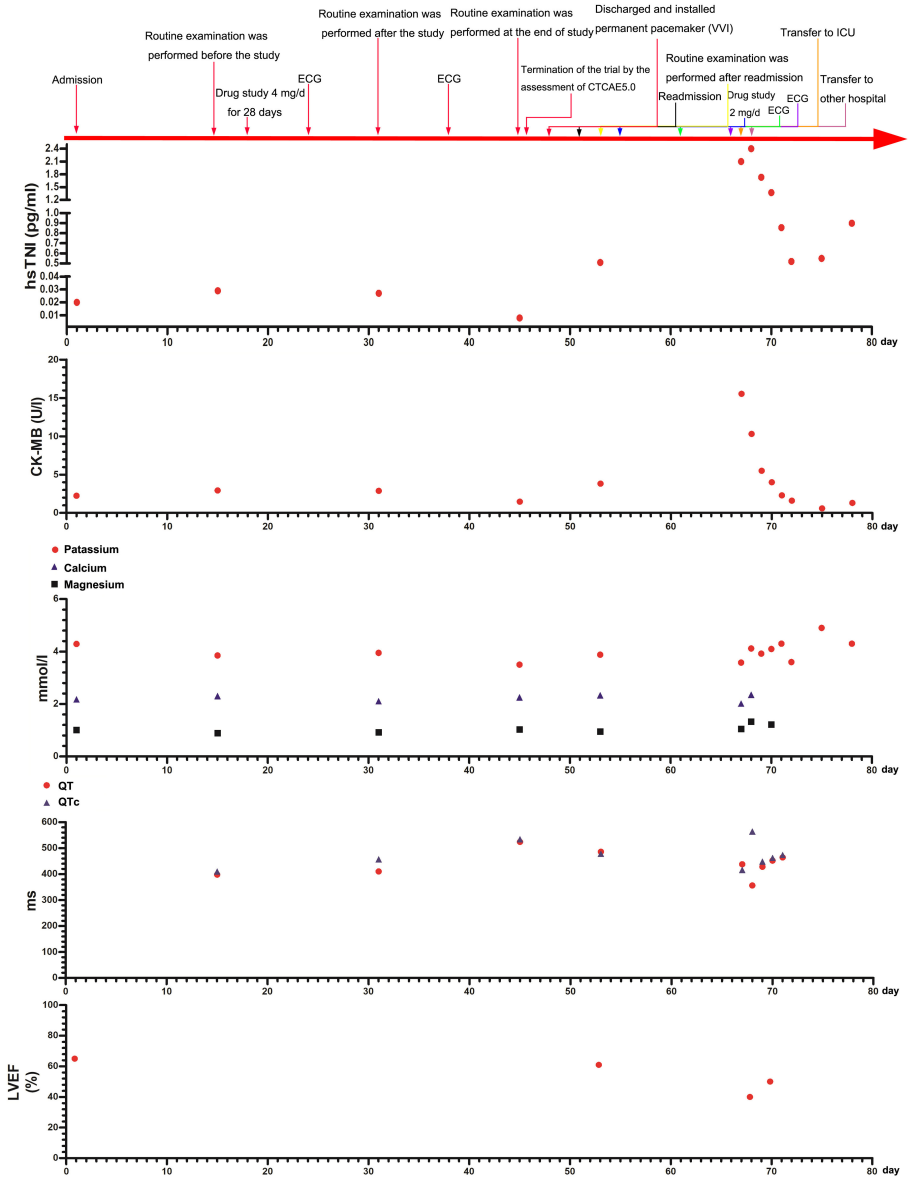

FIGURE 1
Main clinical and laboratory findings and therapeutic interventions from admission on day 0 to discharge from the ICU on day 78 are depicted. The QT interval correction method is after the Bazett formula. hs-TNI, hypersensitive troponin I; CK-MB, creatine kinase-MB; LVEF, left ventricular ejection fraction.

for serum K+ from 4 mEq/L to the upper limit of normal, and serum Ca^{2+} and Mg^{2+} within the normal range was safer (15).

We found a special phenomenon in which both the QT/QTc interval and AV block were gradually exacerbated in this case. We also noticed that the patient had frequent bigeminy before the pacemaker was implanted. There are reports that bigeminy can be another arrhythmia contributing to torsades (16). Although we cannot predict whether a patient will experience sudden cardiac death, the mixed arrhythmias should be noticed as early as possible. Some reports (17, 18) have shown that AV block-induced cardiac electrical and structural remodeling predisposes the heart to TdP in an AV dog model. Bhattad et al. (2023) (19) described that tachycardia usually shortens the QTc interval, but the adjustment is not instantaneous. Bradycardia increases the risk of QTc prolongation and therefore the risk for torsade de point. It is therefore logical that a patient with increasing AV block picture and subsequent bradycardia has an increased risk for torsade de points. Bradycardia and torsade de points are connected. The mechanism by which AV block and PI3K inhibitors induce TdP is that both can lead to prolonged cardiac repolarization and further promote action potential prolongation (18). We observed that the patient still experienced multiple short episodes of TdP when the QTc interval was <500 and <60 ms at baseline. Thus, we believe that the previous standard of discontinuing drugs and continuing drugs no longer seems to be safe.

The report stresses a comprehensive assessment of risk factors for QT prolongation before anticancer therapy. Frequent recording of ECG changes and electrolyte levels is necessary during the treatment. When the QT was gradually prolonged along with this

10.3389/fonc.2024.1331472

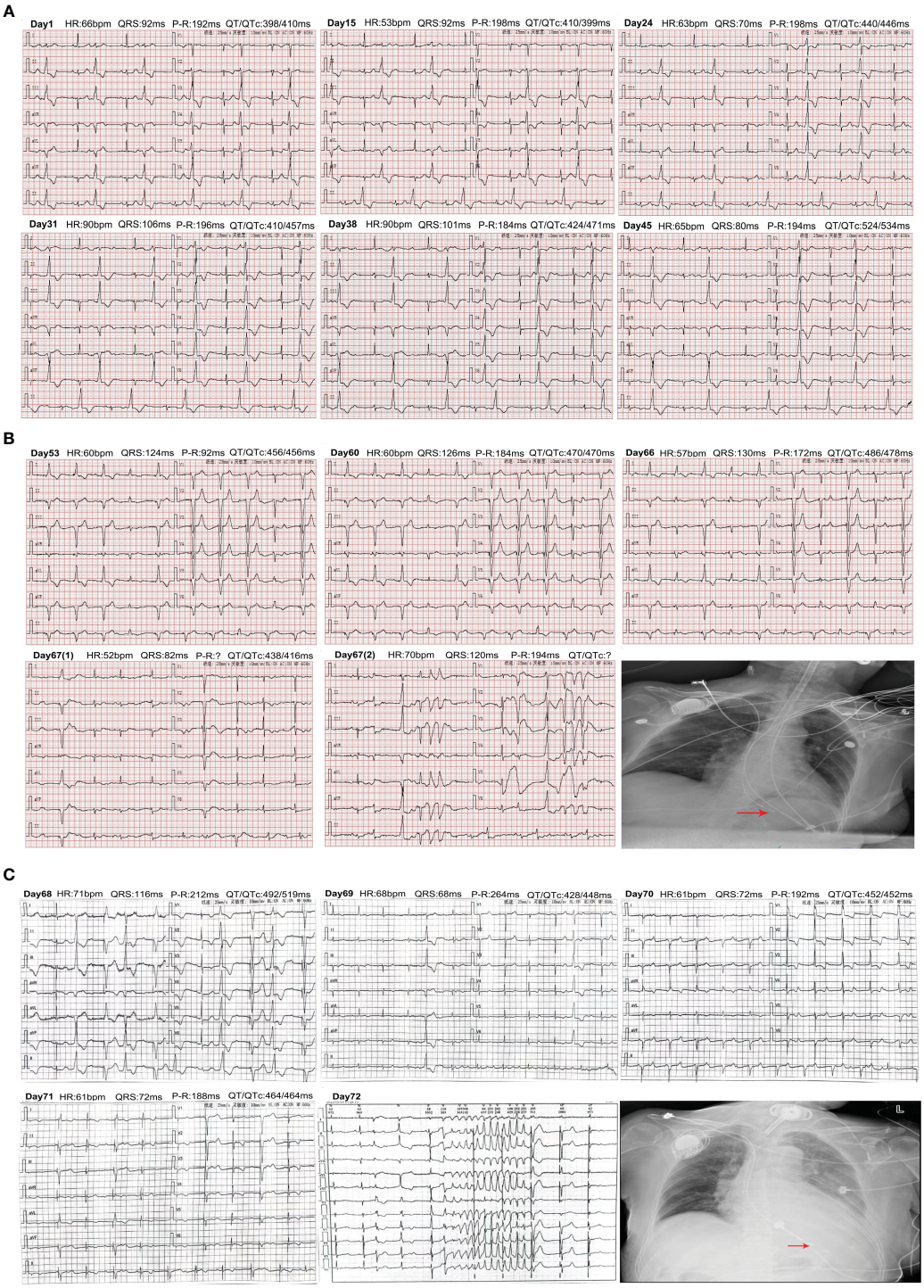

FIGURE 2
Changes of electrocardiogram from admission to discharge. **(A)** Changes in the ECG from admission to before the patient was installed. Days 1–24: ECG showed QT/QTc interval gradually prolongation. Days 31–45: ECG displayed worsening QT/QTc interval and atrioventricular block. **(B)** Changes in the ECG from enrolling in the study again to transfer to our hospital ICU. Days 53–66: ECG showed gradual prolongation of the QT/QTc and worsening of AV block. Day 67: Changes of ECG after being transferred to the ICU. The chest X-ray revealed that the location of the cardiac pacemaker was normal after CPR. **(C)** Changes in the ECG and chest X-ray in the patient after transfer to another hospital's ICU. Days 68–71: ECG changes from days 1 to 4. Day 75: The occurrence of TdP was recorded on the 5th day. The chest X-ray displayed that the location of the cardiac pacemaker was normal.

type, arrhythmias of cardiac repolarization and action potential prolongation appear together. It should be of great concern to healthcare professionals. It is likely to be safer to choose other types of alternative treatment options or downregulate the standard for discontinuing and restarting drugs. No more data were collected from the other patients participating in the trial. We only report this one case, and there was no serum concentration monitoring in this case. We frequently monitored the patients' ECG and found three

kinds of arrhythmias. It seems that it could provide some proof for clinicians to identify early and prevent the occurrence of fatal arrhythmias during anticancer treatment.

Data availability statement

The original contributions presented in the study are included in the article/supplementary material. Further inquires can be directed to the corresponding authors.

Ethics statement

The studies involving humans were approved by the institution of Hubei Cancer Hospital for scientific research paper. The studies were conducted in accordance with the local legislation and institutional requirements. The participants provided their written informed consent to participate in this study. Written informed consent was obtained from the individual(s) for the publication of any potentially identifiable images or data included in this article.

Author contributions

LZ: Conceptualization, Project administration, Supervision, Writing – review & editing. YZ: Data curation, Formal analysis, Investigation, Software, Writing – review & editing. GC: Methodology, Resources, Writing – review & editing. FZ: Validation, Visualization, Writing – original draft. SL: Conceptualization, Supervision, Writing – original draft.

Funding

The author(s) declare that no financial support was received for the research, authorship, and/or publication of this article.

Conflict of interest

The authors declare that the research was conducted in the absence of any commercial or financial relationships that could be construed as a potential conflict of interest.

Publisher's note

References

1. Giraud EL, Ferrier KRM, Lankheet NAG, Desar IME, Steeghs N, Beukema RJ, et al. The QT interval prolongation potential of anticancer and supportive drugs: a comprehensive overview. *Lancet Oncol.* (2022) 23(9):e406–15. doi: 10.1016/S1470–2045(22)00221–2

2. Salem JE, Nguyen LS, Moslehi JJ, Ederhy S, Lebrun-Vignes B, Roden DM, et al. Anticancer drug-induced life-threatening ventricular arrhythmias: a World Health Organization pharmacovigilance study. *Eur Heart J.* (2021) 42:3915–28. doi: 10.1093/eurheartj/ehab362

3. Salvi V, Karnad DR, Panicker GK, Kothari S. Update on the evaluation of a new drug for effects on cardiac repolarization in humans: issues in early drug development. *Br J Pharmacol.* (2010) 159:34–48. doi: 10.1111/j.1476-5381.2009.00427.x

4. Tian X, Wu L, Jiang M, Zhang Z, Wu R, Miao J, et al. Downregulation of GLYAT facilitates tumor growth and metastasis and poor clinical outcomes through the PI3K/AKT/snail pathway in human breast cancer. *Front Oncol.* (2021) 11:641399. doi: 10.3389/fonc.2021.641399

5. Patel VB, Zhabyeyev P, Chen X, Wang F, Paul M, Fan D, et al. PI3Kα-regulated gelsolin activity is a critical determinant of cardiac cytoskeletal remodeling and heart disease. *Nat Commun.* (2018) 9:5390. doi: 10.1038/s41467-018-07812-8

6. Juric D, Janku F, Rodon J, Burris HA, Mayer IA, Schuler M, et al. Alpelisib plus fulvestrant in PIK3CA-altered and PIK3CA-wild-type estrogen receptor-positive advanced breast cancer: A phase 1b clinical trial. *JAMA Oncol.* (2019) 5: e184475. doi: 10.1001/jamaoncol.2018.4475

7. Lu Z, Wu CYW, Jiang YP, Ballou LM, Clausen C, Cohen IS, et al. Suppression of Phosphoinositide 3-Kinase Signaling and Alteration of Multiple Ion currents in drug-induced Long QT syndrome. *Sci Transl Med.* (2012) 4:131ra50. doi: 10.1126/scitranslmed.3003623

8. Cohen IS, Lin RZ, Ballou LM. Acquired long QT syndrome and phosphoinositide 3-kinase. *Trends Cardiovasc Med.* (2017) 27:451–9. doi: 10.1016/j.tcm.2017.05.005

9. André F, Ciruelos E, Rubovszky G, Campone M, Loibl S, Rugo H, et al. Alpelisib for PIK3CA-mutated, hormone receptor-positive advanced breast cancer. *N Engl J Med.* (2019) 380:1929–40. doi: 10.1056/NEJMoa1813904

10. André F, Ciruelos EM, Juric D, Loibl S, Campone M, Mayer IA, et al. Alpelisib plus fulvestrant for PIK3CA-mutated, hormone receptor-positive, human epidermal growth factor receptor-2-negative advanced breast cancer: final overall survival results from SOLAR-1. *Ann Oncol.* (2021) 32:208–17. doi: 10.1016/j.annonc.2020.11.011

11. Novartis Pharmaceuticals Corporation. Highlights of prescribing information, PIQRAY (Alpelisib) tablets, for oral use. Initial U.S.: EB/OL (2022). Available at: https://www.accessdata.fda.gov/drugsatfdadocs/label/2019/212526s000lbl.pdf.

12. Li M, Ramos LG. Drug-induced QT prolongation and torsades de pointes. *P T.* (2017) 42:473–7.

13. European Medicines Agency. ICH Topic E14. The clinical evaluation of QT/QTc interval prolongation and proarrhythmic potential for non-antiarrhythmic drugs (2005). Available at: https://www.ema.europa.eu/en/documents/scientific-guideline/ich-e-14-clinical-evaluation-qt/qts-interval-prolongation-proarrhythmic-potential-non-antiarrhythmic-drugs-step-5_en.pdf (Accessed Nov 12, 2021).

14. United States Food and Drug Administration. E14 Clinical evaluation of QT/QTc interval prolongation and proarrhythmic potential for non-antiarrhythmic drugs (2012). Available at: https://www.fda.gov/regulatory-information/search-fda-guidance-documents/e14-clinical-evaluation-qtqtc-interval-prolongation-and-proarrhythmic-potential-non-antiarrhythmic-0 (Accessed Nov 12, 2021).

15. Herrmann J. Adverse cardiac effects of cancer therapies: cardiotoxicity and arrhythmia. *Nat Rev Cardiol.* (2020) 17:474–502. doi: 10.1038/s41569–020-0348–1

16. Lerma C, Lee CF, Glass L, Goldberger AL. The rule of bigeminy revisited: analysis in sudden cardiac death syndrome. *J Electrocardio.* (2007) 40:78–88. doi: 10.1016/jelectrocard.2006.04.011

17. Van Bavel JJA, Pham C, Beekman HDM, Houtman MJC, Bossu A, Sparidans RW, et al. PI3K/mTOR inhibitor omipalisib prolongs cardiac repolarization along with a mild proarrhythmic outcome in the AV block dog model. *Front Cardiovasc Med.* (2022) 9:956538. doi: 10.3389/fcvm.2022.956538

18. Volders PG, Sipido KR, Vos MA, Spätjens RL, Leunissen JD, Carmeliet E, et al. Downregulation of delayed rectifier K (+) currents in dogs with chronic complete atrioventricular block and acquired torsades de pointes. *Circulation.* (1999) 100:2455–61. doi: 10.1161/01.CIR.100.24.2455

19. Bhattad PB, Jha A, Wholey R. Bradycardia-induced torsades de pointes in atrioventricular block. *Cureus.* (2023) 15:e37507. doi: 10.7759/cureus.37507

frontiers | Frontiers in Cardiovascular Medicine

TYPE Case Report
PUBLISHED 25 June 2024
DOI 10.3389/fcvm.2024.1378333

OPEN ACCESS

EDITED BY
Reto Asmis,
Wake Forest University, United States

REVIEWED BY
Brittany L Siontis,
Mayo Clinic, United States
Shuai Zhang,
China-Japan Friendship Hospital, China
Long Jiang,
First Affiliated Hospital of Guangzhou Medical University, China

*CORRESPONDENCE
Baudouin Bourlond
baudouin-philippe.bourlond@chuv.ch

RECEIVED 29 January 2024
ACCEPTED 20 May 2024
PUBLISHED 25 June 2024

CITATION
Bourlond B, Maurizi N, Antiochos P, Skalidis I, Auf Der Springe K, Royer C, Monney P, Muller O and Kirsch M (2024) Recurrence of an undifferentiated pleomorphic pulmonary artery sarcoma 8 years after initial presentation: a case report.
Front. Cardiovasc. Med. 11:1378333.
doi: 10.3389/fcvm.2024.1378333

Recurrence of an undifferentiated pleomorphic pulmonary artery sarcoma 8 years after initial presentation: a case report

Baudouin Bourlond[1]*, Niccolo Maurizi[1], Panagiotis Antiochos[1], Ioannis Skalidis[1], Katarina Auf Der Springe[2], Claire Royer[3], Pierre Monney[1], Olivier Muller[1] and Mathias Kirsch[3]

[1]Department of Cardiology, Lausanne University Hospital (CHUV), Lausanne, Switzerland, [2]Department of Nuclear Medicine and Molecular Imaging, Lausanne University Hospital and University of Lausanne, Lausanne, Switzerland, [3]Department of Anatomopathology, Lausanne University Hospital (CHUV), Lausanne, Switzerland

Background: Primary cardiac tumors remain exceptionally rare, characterized by a poor prognosis. Among them, sarcomas originating in the pulmonary arteries constitute the most infrequent subgroup within primary cardiac sarcomas.
Case summary: This report presents the case of a 76-year-old female experiencing a recurrence of an undifferentiated pleomorphic intracardiac pulmonary artery sarcoma located in the right ventricular outflow tract, manifesting 8 years after initial remission. Successful outcomes were attained through a combination of surgical resection, state-of-the-art radiotherapy, and chemotherapy. This comprehensive approach proved essential for optimizing both survival and quality of life.
Discussion: The unexpectedly prolonged recurrence-free survival observed in this case underscores the effectiveness of the comprehensive multimodal treatment approach outlined in the existing literature. This highlights the pivotal role of a multidisciplinary strategy in addressing primary cardiac sarcomas, particularly those arising in the pulmonary arteries.

KEYWORDS

cardiac sarcoma, cardiac MRI, pulmonary artery sarcoma, sarcoma, cardio-oncology, case report

Introduction

Primary cardiac tumors are exceptionally rare and associated with a dismal prognosis. Among these, sarcomas originating in the pulmonary arteries constitute the rarest subset of primary cardiac sarcomas. The symptoms are nonspecific and can closely resemble those of various other cardiac diseases. Diagnosing these tumors remains a formidable challenge and is frequently prone to misidentification. Multimodality imaging plays a pivotal role in the diagnostic process, although the definitive diagnosis is ultimately established through anatomopathological examination.

Case report

Patient presentation

We present a case involving a 76-year-old female who experienced a recurrence of undifferentiated pleomorphic pulmonary artery sarcoma, 8 years after achieving remission.

The patient initially presented in 2014, reporting progressive fatigue and exertional dyspnea classified as NYHA II over a 6-month period. During a cardiac examination, a grade 3/6 crescendo-decrescendo systolic murmur was identified. Transthoracic echocardiography (TTE) revealed moderate pulmonary valve stenosis due to a protruding mass in the right ventricular outflow tract (RVOT), further confirmed by transesophageal echocardiography (TOE) (Figures 1A,B). Cardiac computed tomography (CT) and magnetic resonance imaging (MRI) verified a $25 \times 35 \times 24$ mm mass attached to the RVOT, extending into the pulmonary trunk through the pulmonary valve without apparent invasion of the bifurcation (Figures 1C,D). To characterize the nature of the right atrial mass, a whole-body 18-fluorodéoxyglucose positron emission tomography computed tomography (18FDG PET/CT), performed after 24 h of dietary preparation and heparin pre-administration to suppress physiological myocardial FDG uptake (1), revealed low metabolic activity of the tumor (white arrows), comparable to the mediastinal blood pool [maximum standardized uptake value (SUVmax) of the tumor 2.6 vs. 2.4 for the blood pool] (Figure 2), with no signs of metastasis.

The cardiac mass was partially removed through a longitudinal incision in the pulmonary artery. The mass was very large and adherent to the pulmonary infundibulum but also to the right ventricle up to its apex. Only R2 resection was possible under these anatomical conditions. After resection, there was virtually no pulmonary valve or pulmonary artery wall, which means that the continuity of the right outflow tract has to be rebuild using a homograft. Immediate postoperative TOE demonstrated a proper function of the homograft and no complication, particularly on the tricuspid valve.

Anatomopathological analysis indicated a proliferation of poorly differentiated malignant tumor cells within a fibromyxoid stroma (Figures 3A,B). The proliferation included giant cells with clarified, vacuolated, or eosinophilic cytoplasm. The nuclei were large, often multinucleate, with marked pleomorphism. Prominent nucleoli were observed in some cells, along with intranuclear inclusions. Immunohistochemicaly, the cells were positive for CD34 and negative for HMB45, Melan A, S100, pancytokeratin, EMA, desmine, SMA, caldesmon and CD99. MDM2 was not amplified in FISH. A diagnosis of undifferentiated pleomorphic cardiac sarcoma was established.

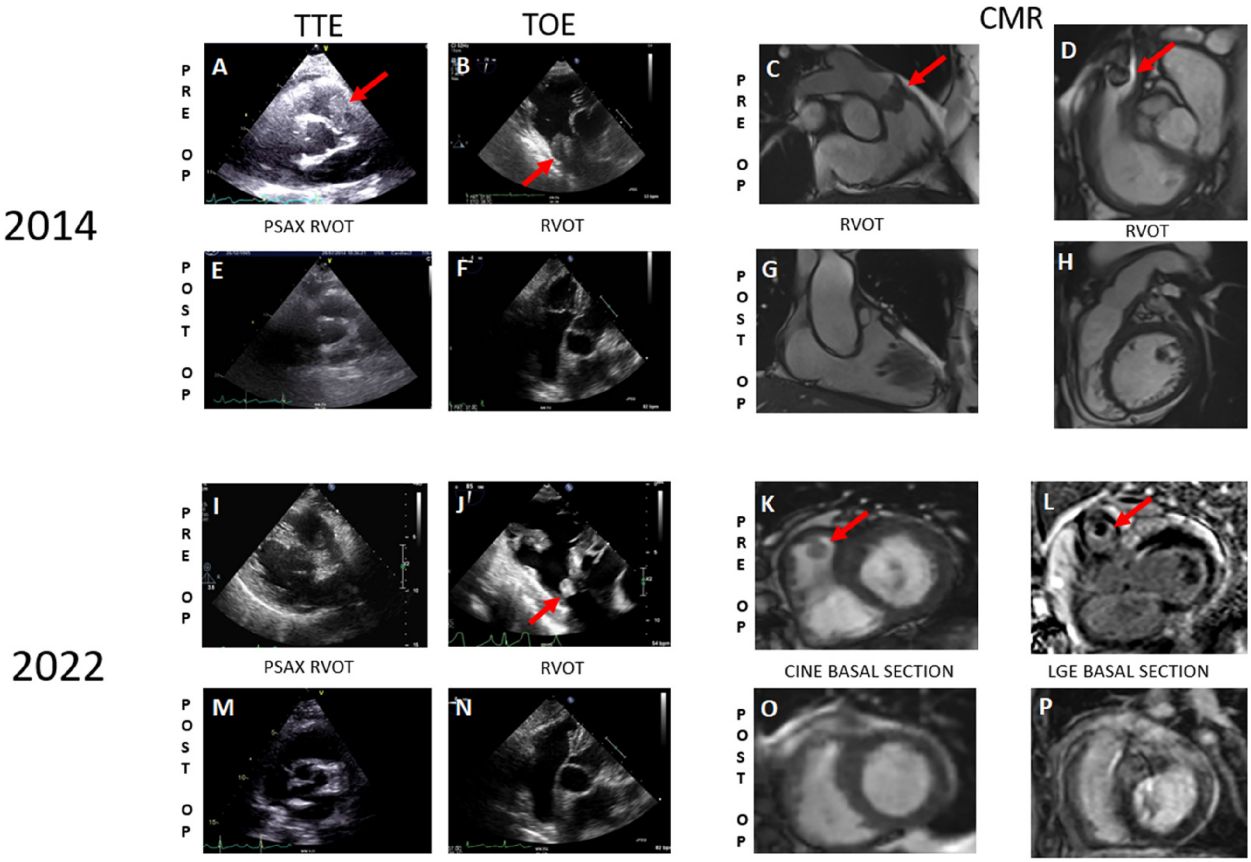

FIGURE 1
Preoperative cardiac imaging from 2014 to 2022 depicts the initial occurrence of pulmonary artery sarcoma and its recurrence, respectively (A–D, I–L) Postoperative imaging from 2014 to 2022 reveals the absence of any lesions (E–H, M–P).

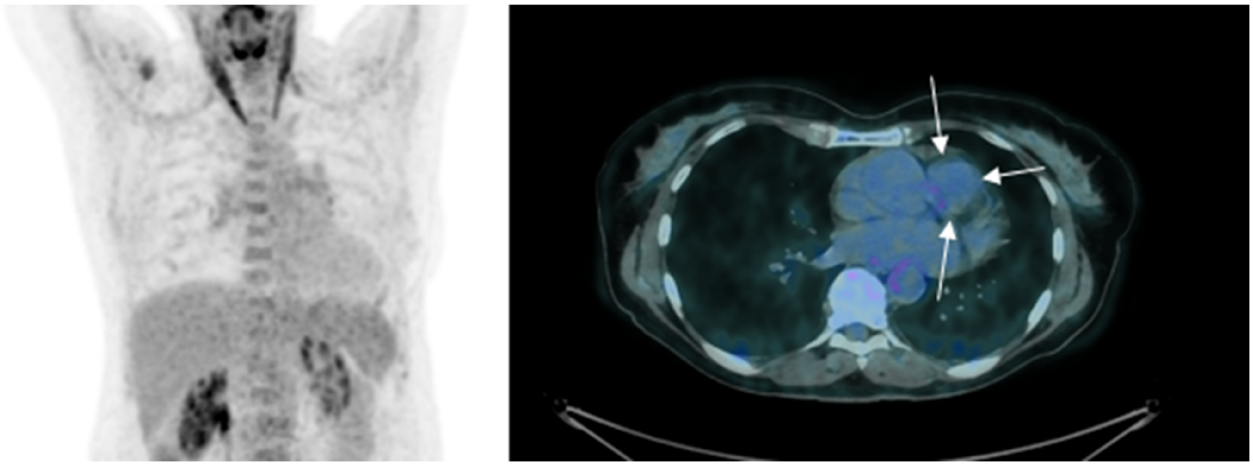

FIGURE 2
18-FDG PET/CT 2014—initial PET imaging reveals a low metabolic activity of the tumor (indicated by white arrows), comparable to that of the mediastinal blood pool [with a maximum standardized uptake value (SUVmax) of 2.6 for the tumor vs. 2.4 for the blood pool]. Please note that myocardial glucose metabolism is suppressed due to a diet low in carbohydrates and high in fats in the days leading up to the examination.

Following radio-chemotherapy with cisplatin (Radiotherapy of 45 Gy—25 fractions of 1.8 Gy—followed by a boost of 12 Gy—6 fractions of 2 Gy—and cisplatin 40 mg/m2, 1×/week for 5 weeks), the patient experienced long-term remission with a good quality of life. Cisplatin therapy was used as a radio-sensibilizing treatment. Subsequent follow-ups with TTE, TOE, and MRI (Figures 1E–H) showed no signs of recurrence.

In 2022, the patient reported a recurrence of progressive dyspnea classified as NYHA II during a follow-up. Upon admission, vital signs included a blood pressure of 144/62 mmHg (mean pressure, 89 mmHg), a resting heart rate of 64 beats per minute, and a transcutaneous oxygen saturation of 97% while breathing ambient air. A systolic pulmonary murmur (3/6) radiating on the carotid arteries was detected during cardiac auscultation. The patient did not exhibit signs of cardiac failure (Killip I), and the neurological examination was normal.

TTE and TOE revealed a resurgence of pulmonary stenosis with a mobile mass measuring 10 × 12 mm in the RVOT (gradient 45/30 mmHg vs. 20/13 mmHg previously) (Figures 1I,J). Cardiac MRI confirmed a T1 isointense, T2 hyperintense pedunculated mass measuring 11 × 11 mm in the RVOT (Figures 1K,L). A differential diagnosis of thrombus was considered, and anticoagulation was initiated. A follow-up MRI after 2 months indicated stability of the mass. Endovascular biopsy attempts were unsuccessful. Multidisciplinary discussions led to the decision for surgical resection of the mass.

The procedure consisted of a transverse incision of the homograft in order to remove the mass which obstructed the pulmonary valve at each systole. The homograft showed signs of degeneration in the form of mild stenosis and insufficiency, but it was decided not to replace the prosthesis, given the complexity of that surgery and the patient's oncological prognosis.

Macroscopically, the mass exhibited a nodular aspect with a smooth surface, brownish with hemorrhagic foci but without obvious necrosis (Figure 3C). Anatomopathological analysis revealed a well-circumscribed tumor encapsulated by fibrous tissue. Tumoral cells exhibited numerous atypia and mitosis, with scattered giant high-grade cells (Figure 3D, arrows) within an eosinophilic stroma (Figure 3D,*). Some cells were multinucleated (arrows). Immunohistochemicaly, the cells were negative for CD31, CD34, ERG, MDM2, Calretinin, MYC, CD68 and CD163. MDM2 was not amplified in FISH as in the previous biopsie. The same morphology and immunohistochemical profile were found in 2014 and in 2022 with high-grade giant cells that were negative for MDM2 (Figure 4). In order to search for a clonal link between the two tumor (2014 and 2022), we performed next-generation sequencing on both tissues and we found the same *TP53* exon 5: mutation c.503A>G (p.His168Arg) in both tumors. Given the very similar localization, morphology, immunohistochemical and genomic profile, a diagnosis of recurrent undifferentiated pleomorphic pulmonary artery sarcoma was confirmed.

Follow-up—patient perspective

After surgical resection, multidisciplinary discussions led to an observational approach, without the implementation of adjuvant treatment. The patient remains asymptomatic, except for NYHA I dyspnea. The cardiac MRI and PET-CT performed at the 3-month follow-up did not reveal signs of new recurrence of the pleomorphic sarcoma (Figures 1M–P).

At the 10-month follow-up, there was evidence of tumoral progression, manifested as a 7 mm thickening of the right pulmonary artery. As the patient's frailty was too important for a third sternotomy, it was decided to perform a pulmonary artery angioplasty to decrease the patient's dyspnea and she received pazopanib treatment (anti-VEGFR). However, this treatment was discontinued due to intolerance a few weeks after initiation. The patient currently declines oncology treatment.

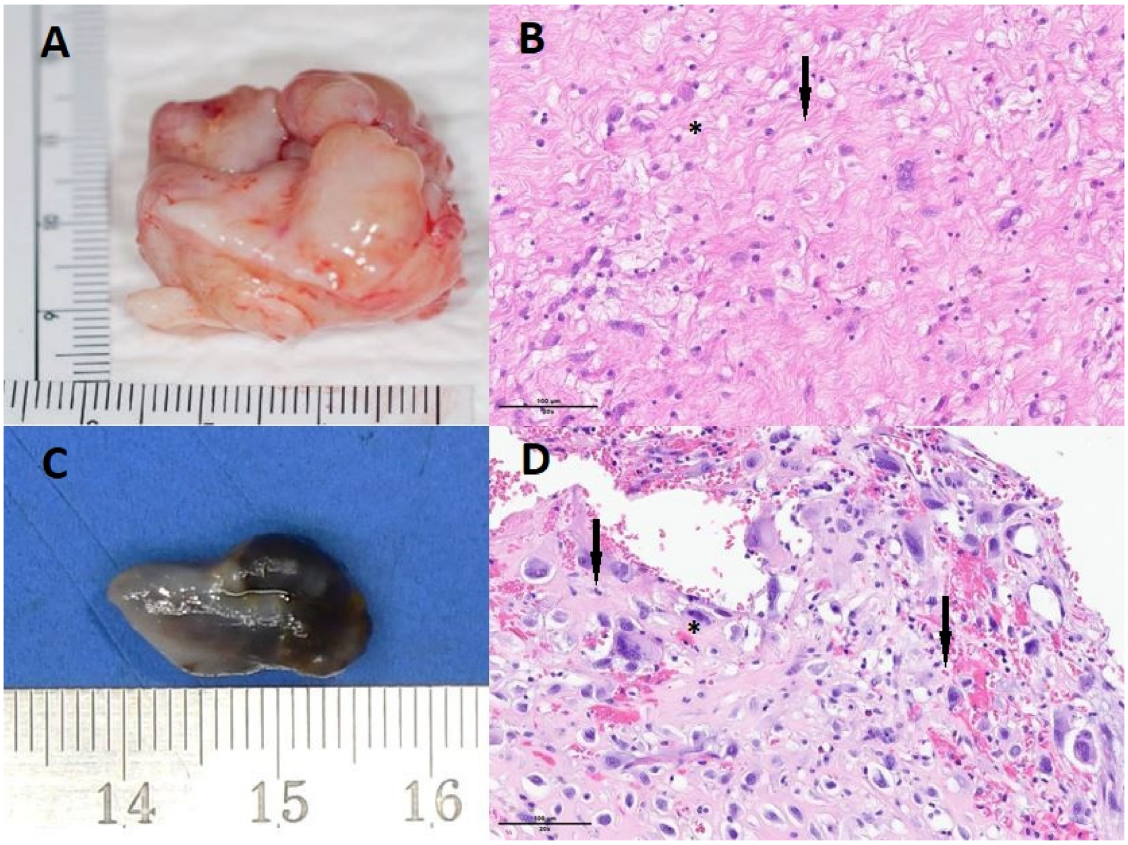

FIGURE 3
Tumoral lesion resected in 2014 (**A**) displaying scattered high-grade giant cells (**B**, indicated by arrows) within an eosinophilic fibromyxoid stroma (**B**, marked with a star), stained with hematoxylin and eosin (HE) at 200× magnification. Immunohistochemicaly, the cells were lightly and focally positive for CD34, and negative for MDM2, HMB45, Melan A, S100, pancytokeratin, EMA, desmine, SMA, caldesmon and CD99. MDM2 was not amplified in FISH. Tumoral lesion resected in 2022 (**C**), measuring approximately 1.5 cm, exhibits a nodular appearance with a smooth surface, appearing brownish with hemorrhagic foci but lacking obvious necrosis. The tumor is well-encapsulated by a fibrous capsule. Anatomopathology with HE staining revealed tumoral cells displaying numerous atypia and mitosis, along with scattered high-grade giant cells (**D**, indicated by arrows) within an eosinophilic stroma (**D**, marked with a star). Some of these cells were multinucleated (**D**, indicated by arrows). Immunohistochemistry did not demonstrate a specific line of differentiation, with a negativity of the following markers: CD31, CD34, ERG, MDM2, Calrétinine, MYC, CD68 et CD163. HE staining at 200× magnification.

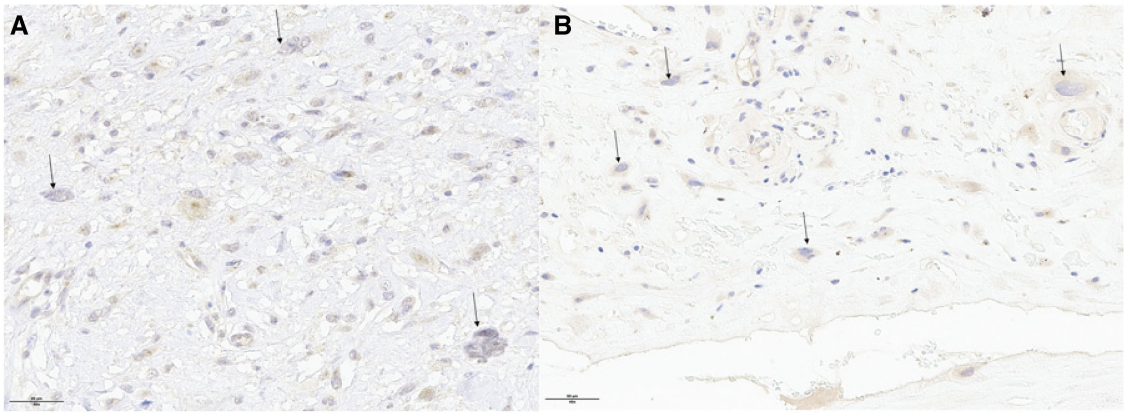

FIGURE 4
The same morphology and immunohistochemical profile were found in 2014 (panel **A**) and in 2022 (panel **B**) with high-grade giant cells that were negative for MDM2.

Discussion

With an incidence ranging from 0.001% to 0.03% in autopsy series, primary cardiac tumors remain exceptionally rare, carrying a poor prognosis (2). Among these, sarcomas represent the most prevalent form of malignant primary cardiac tumors. Notably, sarcomas originating in the pulmonary arteries constitute the rarest subset within primary cardiac sarcomas.

Since its initial description by Mandelstamm in 1923, approximately 300–400 cases of pulmonary arterial sarcoma (PAS) have been reported. Diagnosing PAS remains a challenge as it is frequently misidentified as pulmonary thromboembolism (3). Cardiac sarcomas arise from primitive pluripotent interstitial cells with the capacity for multiple differentiations. The symptoms are nonspecific, resembling those of various other heart diseases, making the diagnosis of cardiac tumors notably challenging.

The diagnosis heavily relies on multimodality imaging, incorporating echocardiography, cardiac computed tomography, and magnetic resonance. However, a definitive diagnosis and treatment hinge on histology, ultimately confirmed through anatomopathology.

The typical onset age for cardiac sarcoma is 45–55 years old, and the female-to-male ratio is 2:1.

The median overall survival for cardiac sarcoma patients is approximately 6 months based on retrospective series (4). Without surgical treatment, the median survival time is a mere 1.5–3 months for pulmonary artery sarcoma (5). However, with "complete" surgical resection, survival improves to 36.5 ± 20.2 months, and with "incomplete" surgical resection, it extends to 11 ± 3 months (6).

Surgical resection remains crucial for the long-term survival of cardiac sarcoma patients, despite the challenges posed by these tumors, such as their location, achieving complete resection, and addressing sarcoma margins. Combining surgical resection with radiotherapy and chemotherapy appears to offer the best prospects for a good quality of life among patients. Recent studies have not demonstrated survival benefits in the last cohorts examined (7). Given the rarity of achieving R0 resection in this type of surgery, active monitoring for disease recurrence is imperative.

Conclusion

To the best of our knowledge, our case represents one of the longest periods of recurrence-free survival documented for a cardiac sarcoma in the current medical literature. Successful outcomes were achieved through surgical resection combined with state-of-the-art radiotherapy and chemotherapy, essential for optimizing both survival and quality of life. This unexpectedly prolonged recurrence-free survival underscores the efficacy of the comprehensive multimodal treatment approach detailed in existing literature, emphasizing the critical role of a multidisciplinary strategy. Given advancements in surgical techniques, personalized radiotherapy protocols, and chemotherapy planning in the contemporary era, it is imperative to reevaluate survival rates for this rare tumor through new studies.

Data availability statement

The original contributions presented in the study are included in the article/Supplementary Material, further inquiries can be directed to the corresponding author.

Ethics statement

Written informed consent was obtained from the individual(s) for the publication of any potentially identifiable images or data included in this article.

Author contributions

BB: Data curation, Investigation, Writing – original draft, Writing – review & editing. NM: Formal Analysis, Writing – review & editing. PA: Writing – review & editing, Formal Analysis, Investigation, Supervision, Validation. IS: Writing – review & editing. KA: Investigation, Writing – review & editing. CR: Investigation, Writing – review & editing. PM: Supervision, Validation, Writing – review & editing. OM: Supervision, Validation, Writing – review & editing. MK: Supervision, Validation, Writing – review & editing.

Funding

The author(s) declare that financial support was received for the research, authorship, and/or publication of this article.

Open access funding by the University of Lausanne.

Acknowledgments

We would like to express our sincere gratitude to S. Rotman, S. Hugelshofer, A. Digklia, S. Papadopoulos and F. Dulguerov for their invaluable assistance in the reviewing and proofreading of this manuscript. Their keen attention to detail, their expertise, and commitment to improving the clarity and accuracy of the content have significantly enhanced the quality of this work.

Conflict of interest

The authors declare that the research was conducted in the absence of any commercial or financial relationships that could be construed as a potential conflict of interest.

Publisher's note

References

1. Osborne MT, Hulten EA, Murthy VL, Skali H, Taqueti VR, Dorbala S, et al. Patient preparation for cardiac fluorine-18 fluorodeoxyglucose positron emission tomography imaging of inflammation. *J Nucl Cardiol*. (2017) 24:86–99. doi: 10.1007/s12350-016-0502-7

2. Burke A, Vermani R. Atlas of tumor pathology. 3rd ed. In: Burke A, Virmani R, editors. *Tumors of the Heart and Great Vessels*. Washington, D.C.: Armed Forces Institute of Pathology (1996). p. 1–11.

3. von Ballmoos M.C. W, Chan EY, Reardon MJ. Imaging and surgical treatment of primary pulmonary artery sarcoma. *Int J Cardiovasc Imaging*. (2019) 35:1429–33. doi: 10.1007/s10554-018-1489-8

4. Hamidi M, Moody JS, Weigel TL, Kozak KR. Primary cardiac sarcoma. *Ann Thorac Surg*. (2010) 90(1):176–81. doi: 10.1016/j.athoracsur.2010.03.065

5. Deng L, Zhu J, Xu J, Guo S, Liu S, Song Y. Clinical presentation and surgical treatment of primary pulmonary artery sarcoma. *Interact Cardiovasc Thorac Surg*. (2018) 26(2):243–7. doi: 10.1093/icvts/ivx318

6. Blackmon SH, Rice DC, Correa AM, Mehran R, Putnam JB, Smythe WR, et al. Management of primary pulmonary artery sarcomas. *Ann Thorac Surg*. (2009) 87(3):977–84. doi: 10.1016/j.athoracsur.2008.08.018

7. Yin K, Luo R, Wei Y, Wang F, Zhang Y, Karlson KJ, et al. Survival outcomes in patients with primary cardiac sarcoma in the United States. *J Thorac Cardiovasc Surg*. (2021) 162(1):107–115.e2. doi: 10.1016/j.jtcvs.2019.12.109

Frontiers in
Cardiovascular Medicine

Innovations and improvements in cardiovascular treatment and practice

Focuses on research that challenges the status quo of cardiovascular care, or facilitates the translation of advances into new therapies and diagnostic tools.

Discover the latest Research Topics

See more →

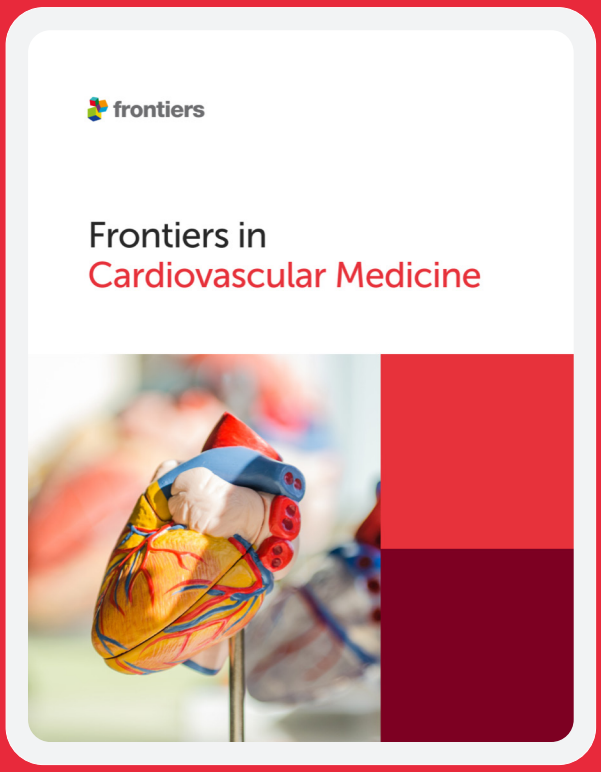

Frontiers

Avenue du Tribunal-Fédéral 34
1005 Lausanne, Switzerland
frontiersin.org

Contact us

+41 (0)21 510 17 00
frontiersin.org/about/contact